



Revision of European Building Code En1991 for Static and Dynamic Roof Loading by

Volcanic Ash

Submitted for the Degree of Doctor of Philosophy

at the University of Northampton

April 2022

Philip Kwame Quainoo

I. DECLARATION

I hereby declare that the work described in this thesis is original work undertaken by me for the degree of Doctor of Philosophy, at the Faculty of Art Science and Technology.

II. DEDICATION

First and foremost, I want to dedicate this achievement to God Almighty for the endless support, good health, strength, sound mind and the direction to have come thus far.

My sincere thanks and gratitude to all the loving and caring images of God that He has placed on my path during this Ph.D. journey; May God bless you! My gratitude goes specifically to the following great individuals.

My special gratitude goes to my supervisory team Professor Nick Petford and Professor Stefan Kaczmarczyk whose mentorship, Support, continuous guidance, and advice have seen me through this special stage of my academic aspirations. Thanks, cannot suffice, but thank you!

III. ACKNOWLEDGMENTS

I am exceedingly appreciative to my supervisor's Professor Nickolas Petford the Vice-chancellor of The University of Northampton and Professor Stefan's Kaczmarczyk of The University of Northampton for their advice, continuous support for giving me detailed patience and feedback during my study. Their enormous experience and abundant knowledge have persuaded me in my academic research and daily life. I cannot stop to thank you again to Professor Nicholas Petford, who had a key interest in the research and help support the software's purchase, the vice-chancellor award. Had it not been for your interest, I would not have completed this study. I want to thank Professor emeritus Janet Wilson, Dr. Masoud Malekzadeh and Dr. Eiman Elbanhawy for their contribution during the study's early stage of the study. Thanks also go to Dr. Mohammed Ghaleeh, Dr. Michael Opoku Agyeman, the postgraduate office, colleagues' students, the IT service, the wonderful members' staff of The Northampton University for all the support given to me during my stay at the university.

Thanks to my brothers and sisters, nice and nephews, especially Professor Albert Kojo Quainoo, Professor George Quainoo, Mr. Patrick Quainoo and Rt. Rev. Moses Owusu-Sekyere Bishop at Word of Faith Mission (House of Faith) in the United Kingdom, for the prayers, support and constantly calling to check on my progress and all the time being there for me when I need them most. I am indebted to my parents, whose constant support and love kept me motivated and confident in my accomplishments and success because they believed in me. Though you are not here, this is for you, mum, and dad. Finally, I could not have completed this thesis without my friend's

Dr. & Mrs. Julius Azasoo, Rev Kojo Acquaaah of Coventry, Mr. Isaac Nkrumah, Dr. Kweku Adams, Mr. & Mrs. Diamond Emmborah, Mr. Lawrence Ekow Arthur, Mr. Kofi Kumi, Dr.

Leila Bendifallah. They supported and provided stimulating discussions and a happy distraction to reset my mind outside of my research. Thanks to individuals who have assisted me in diverse ways, but I have not mentioned your names; this success is all part of your efforts.

IV. ABSTRACT

This thesis presents a numerical procedure for testing the effects of both static and dynamic loading of volcanic ash deposition on concrete roofs. The study aims to propose changes by adding additional action (i.e., volcanic ash loads) to the building regulations to make existing and future European buildings more robust. The investigation uses a Multiphysics simulation approach. A mathematical model is developed to investigate the volcanic ash effects in the context of the EN1991 code. A numerical modelling tool (EDEM software) to implement the Discrete Element Method DEM and a structural analysis tool (ANSYS) for the Finite Element Method (FEM) is used to investigate the scaled models, which are used to subject the pressure loads considering the wind and no-wind effects. The modelling and simulation tests accounted for wind effects, various volcanic ash sizes and the density of the ash material. Still, it can be changed to reflect a range of relevant (measured) eruptive products. The key parameters and the results are illustrated as follows. While using DEM and FEM simulation results, various diameters were used. The modelling technique has been able to interrogate the exploration of the volcanic ash loading effects of various geological and environmental conditions during deposition.

The number of simulated volcanic particles of 160,000, the density of 3000 (kgm^{-3}) for the flat concrete roof and volcanic particle 170,000, and 1000 (kgm^{-3}) density for the 20 degrees pitched concrete tile roof. The variable densities will enable the study to have a different perspective on the effects of stress and the deformation of the volcanic ash particle on the roofs of buildings. The Simulated flat concrete roof for the volcanic ash particles diameter results for wind effects in the horizontal direction of (1 ms^{-1}) are as follows: the volcanic ash particles diameter for 10 mm the DEM maximum Pressures 8581.1 (Pa), the FEM maximum

deformation as 0.081 (mm) and the FEM maximum stress as 4.424 (MPa). The no wind effect (controlled condition) simulations particle variable results are as follows:

- the DEM maximum pressures as 4716.3 (Pa),
- the FEM maximum deformation as 0.040 (mm) and
- the FEM maximum stress as 2.074 (MPa)

The Simulated pitched tile roof for the volcanic ash particles diameter results for wind effects in the horizontal direction of (1 ms^{-1}) are as follows: the volcanic ash particles diameter for 10 mm the DEM maximum Pressures 3472.2 (Pa), the FEM maximum deformation as 0.70084 (mm) and the FEM maximum stress as 11.988 (MPa). The no wind effect (controlled condition) simulations particle variable results are as follows: the DEM maximum Pressures 940.33 (Pa), the FEM maximum deformation as 0.17444 (mm) and the FEM maximum stress as 2.6009 (MPa). As expected, the wind effect resulted in an uneven distribution of the ash on the roof surface, which in turn produced areas of high-pressure load and stress levels. These results will have a possible impact on the designs of buildings on flat roof considerations. The thesis concluded its study by proving the need for the proposition of European building code EN1991-1-1-4 for volcanic ash load arrangement on the roofs of buildings within volcanic prone areas in Europe.

The Implication of the Results

The study aims to investigate the resilience of building roofs against the load due to volcanic ash weight in the volcanic prone area of Europe and propose a revision of the European building code EN1991 (in the current European code regulation) within the volcanic prone areas in Europe. These aims are directly linked to the study's objectives and focus on the gap and

contribution to the research. That is the effect of the volcanic ash on the roofs of buildings within the volcanic prone areas, as this wasn't part of the European building code E1991.

The study could ascertain the effects of the volcanic ash loading using static and dynamic approaches on the roof of the building within the volcanic prone area using the DEM and FEM simulations as illustrated in objective 3. Furthermore, the results of the study have indicated in chapter 5 the effects of the variable volcanic ash densities (1000 kg/m^3 , 2000 kg/m^3 and 3000 kg/m^3) that have led to the collapse of buildings within the volcanic prone areas in Europe as indicated by the study.

This part of the recommendation relates to objective 1, and objective 2 illustrates the research's contribution to the geographical distribution of the regions that will benefit all volcanic-prone areas in Europe from the revision of the building regulation. However, Europe will benefit from this study, but the world at large with countries' experiencing the effect of volcanic ash loadings on the roofs of buildings.

The proposal of the revision of the EN1991 is linked led to objective 4 clearly shows that the results from the various tests indicated the impact of the volcanic ash effects on the roof within the volcanic prone area in Europe. Furthermore, it was clear that the buildings with flat concrete roofs would be more impacted than the pitched roofs within the volcanic prone.

As already indicated, the preliminary simulation test for the tile pitched roof, with the angle of inclination from 35 degrees to 45 degrees, shed most of the volcanic ash on its roof, resulting

in less deformation and stress on the roofs. The study, therefore, recommended the strengthening of all those flat roofs as follows:

- 1) All existing flat roofs should be retrofit or structurally reinforced to increase the roof's resilience against the volcanic ash loading effects.
- 2) Flat roofs should not be encouraged in the design of new buildings within the volcanic prone areas unless buildings designers can increase the strength of buildings with flat roofs within the volcanic prone areas in Europe and the world at large.
- 3) 3) All existing pitched roofs in the volcanic ash-prone areas should be retrofit or structurally reinforced to increase the roof's strength.
- 4) Existing pitched roofs within the range of 20-30 degrees are prone to roof failures. Therefore, they must not be encouraged in volcanic prone areas unless they can be retrofit or structurally reinforced to increase the roof's resilience against the volcanic ash loading effects.
- 5) Pitched roofs buildings with steep roof angles that can flash off the volcanic ash quickly must be recommended within the volcanic prone areas as that helps sheared off the deposition of the volcanic ash loading on the roofs.

This measure means cost implications for owners of buildings within the volcanic-prone areas. This approach will require government support to avert situations where buildings will collapse and kill people in volcanic-prone areas.

Existing pitched roofs with an angle of inclination between 20-30 degrees should be retrofit to increase the strength of the roofs within the volcanic-prone areas. However, this will need

government and political will to undertake such a policy to avert a situation of the hazard of the collapse of the pitched roof within the angle of inclination affected during a volcanic eruption.

The study recommended that newly built buildings should be encouraged to use pitched roofs with steep a steep roofs angle that can flash off the volcanic ash quickly must be recommended within the volcanic prone areas as that will help sheared off the deposition of the volcanic ash loading on the roofs.

Though the designs approach will increase the cost of buildings within the volcanic-prone areas in Europe and the rest of the world, it will help avert the hazard of volcanic ash loading leading to the collapse of roofs of buildings in the volcanic-prone areas and save lives. Every life matters and people who live in the volcanic prone areas in Europe and the rest of the world matter.

This study approach will help make buildings within the volcanic prone areas more resilient against the volcanic ash particle loadings on the roofs and will also contribute to Knowledge.

Talks and Abstracts in Support of Thesis'

Related works with tiles regarding this study are as follows:

- A Revision to European Building Code EN1991 for Static and Dynamic Roof Loading by Volcanic Ash. And presented a Poster presentation VMSM Annual Conference at St Andrew in Scotland from 7th to 10th January 2019.

- Modelling and Simulation of the Effects of Volcanic Ash Loading on Flat Concrete Roof was carried out by The University of Northampton Annual Research Conference: 18 -19 2020.
- Using the Discrete Element Method to Simulate the Effects of Volcanic Ash Particles Falling on a Flat Roof Structure. Which was presented on the 30th of June 2020 Showcasing research, use of EDEM on our website! as “Research Spotlight.
- Modelling and Simulation of Volcanic Ash Particles Falling on Building Roofs to Determine the Stress and Deformation Levels. Manchester 6-9 January 2021.
- EGU GMVP10.1 2021: Ashflow hazard: modelling volcanic ash roof loading and revisions to EU Building Codes. N Petford, P Quainoo, S. Kaczmarczyk, University of Northampton, UK.

TABLE OF CONTENT

	Page
I. DECLARATION	ii
II. DEDICATION	iii
III. ACKNOWLEDGMENTS	iv
IV. ABSTRACT.....	vi
CHAPTER ONE.....	1
1.0. INTRODUCTION	1
1.1 Background.....	1
1.2 Research Problem	6
1.2.1 Scope of the Problem.....	6
1.2.2 Known Problems of Volcanoes.....	7
1.2.3 Establishing the Research Questions	9
1.2.4 Aims and Objectives of the Research	11
CHAPTER TWO	13
2.0. LITERATURE REVIEW	13
2.1 Introduction to Volcanoes.....	13
2.2 Definition of Terms.....	13
2.2.1 Definition of Volcanoes.....	13
2.3 Types of Volcanoes and Characteristics	17
2.4 Pyroclastic Classification Schemes.....	26
2.4.1 Lapilli.....	27
2.5 Definition of Safety and Resilience of the Building Code.....	27
2.5.1 Safety:	28
2.5.2 Resilience:.....	29
2.6 Simulation Time for DEM.....	35
2.7 Bulk Weight Density of Snow	37
2.8 Roof Snow Load Shape Coefficient.....	38
2.9 Reasons Why People Live in Volcanic Prone Areas	38
2.10 Distribution and impacts of Volcanoes in Europe	40
2.11 Volcanic Threat and Impact on Buildings	48
2.11.1 Volcanic Eruption on Canary Island of La Palma, Spain	57
2.12 Current Research Contributions.....	60
2.13 Composition and Properties of Some Roofing Materials	66
2.14 Cases study Areas	77

2.14.1	Mt Etna Volcano Eruption in Italy:.....	80
2.14.1.1	Types of Eruption in Mt Etna Region in Italy.....	81
2.14.1.2	Reasons and Benefits of living in Mt Etna Volcanic Region.....	81
2.14.1.3	Effect of Volcanoes in Mt Etna Region	82
2.14.2	Iceland.....	83
2.15	Material Parameter and Particle Size	86
2.16	Volcanic Ash Loadings.....	87
2.17	Structural Failures.....	87
2.18	Building Regulation	88
2.18.1	Importance of Building Regulations	89
2.19	European Building Codes	92
2.20	Load Arrangements of Volcanic Ash Particles.....	100
2.20.1	Mono-Pitched Roofs	102
2.20.2	Pitched Roofs.....	103
2.21	Finite Element Method (FEM).....	104
2.22	Equation of Motion	106
CHAPTER THREE		108
3.0.	METHODOLOGY	108
3.1	Introduction.....	108
3.2	Computer Simulation Methodology.....	109
3.2.1	Volcanic Ash Material	111
3.2.2	Factors for Concrete Roof Materials.....	115
3.2.2.1	Design Situations	115
3.2.2.2	Design Compressive and Tensile Strengths.....	116
3.2.3	The Equation Governing the Air Phase	119
3.2.4	Equations Governing the Particle	122
3.2.5	The equation governing the coupling.....	123
3.2.6	Particle Collision Model	124
3.2.7	Linear Spring-Dashpot Contact Model.....	127
3.2.8	Two Particle Model.....	128
3.2.9	The Finite Element Method.	129
3.2.10	Size of Volcanic Ash Materials for Simulations.....	131
3.2.11	Simulation Methodology.....	131
3.2.11.1	Particle Numbers and Input Modes.....	133
3.2.11.2	Volcanic Ash Falling on the Roof.....	134
3.2.11.3	Pitched Roof Boundary Conditions for the Simulation	139

CHAPTER FOUR.....	141
4.0. RESULTS	141
4.1 Discrete Element Method DEM and Finite Element Method (FEM) Simulations	141
4.1.1 Preliminary Results.....	141
4.2 Discrete Element Method (DEM) and the Finite Element Method (FEM) modelling simulation approach.....	154
CHAPTER FIVE	184
5.0. DISCUSSIONS AND ANALYSIS	184
5.1 Discussions of Discrete Element Method and Finite Element Method Co-Simulation Results	184
5.2 Discrete Element Method (DEM) and Structural Analysis tool (ANSYS) for the Finite Element Method (FEM) Simulation. (Flat Concrete Roof)	185
5.2.1 Structural Failures Identified from Flat Concrete Roof simulation	189
5.2.2 Discrete Element Method (DEM) and Structural Analysis tool (ANSYS) for the Finite Element Method (FEM) Simulation. (Pitched Concrete Roof).....	199
5.2.3 Structural Failures Identified from Pitched Concrete Roof simulation.....	206
5.2.4 Pitch Roof Simulation Results Discussions	230
5.2.5 FEM simulation for the maximum deformation and the maximum stress results for the tile concrete roof's pitched strength and failure.	232
CHAPTER SIX.....	235
6.0. CONCLUSION AND FUTURE WORK.....	235
6.1 Summary	235
6.2 Recommendation	238
6.2.1 Load Arrangements for Volcanic ash particles.....	240
6.3 Future Work	242
REFERENCES	244
APPENDICES	257

LIST OF TABLES

	Page
Table 2.1: Types of Volcanoes with Examples.....	15
Table 2.2: Types of Volcanoes and Its Effects	17
Table 2.3: Volcanic Explosivity Index VEI. Classification table of the size of volcanic eruption using VEI (Smithsonian database)	19
Table 2.4: Top 5 Volcano Disasters 2000–2010 by Numbers Affected	20
Table 2.5: Top 5 Volcano Disasters 1980–2010 by Numbers Killed	20
Table 2.6: Top 5 Volcano Disasters 2000–2010 by Numbers Killed	20
Table 2.7: Tephra Load-Thickness Equivalencies.....	22
Table 2.8: Damage Distribution of the Pinatubo Sample	22
Table 2.9: Eruption Frequencies for Selected Countries	23
Table 2. 10: Land Coverage and Ash Thickness.....	24
Table 2.11: Characteristics of Standard Cement CEM II/A-V 42,5R.....	25
Table 2.12 Recommended Values Of Coefficients ψ_1 For Different Locations For Building.....	34
Table 2.13: Snow Loads on Roofs.....	34
Table 2.14: Mean Bulk Weight Density of Snow.....	38
Table 2.15: European Cities Near Active or Potentially Active Volcanoes	42
Table 2.16: Death Toll Because of Volcanic Activities.....	44
Table 2.17: Death Tolls as a Result of Volcanic Activities	46
Table 2.18: Density and Load Comparison, 100 m) of Snow and 100 mm (Volcanic Ash)	48
Table 2.19: Chemical Composition	66
Table 2.20: European Cities near Active or Potentially Active Volcanoes	80
Table 2.21: The Comparison For The Two Case Study Areas	86
Table 2.22: Eurocodes	93
Table 2.23: Recommended Values of Coefficients ψ_1 for Different Locations for Building	100
Table 2.24: Imposed Loads on Roofs of Category H.....	101
Table 2.25: Snows Load Shape Coefficients	102
Table 3.1: Various Simulation Values	114
Table 3.2: Partial Factors for Materials for the Ultimate Limit States.....	115
Table 3.3: Strength and Deformation Characteristic for Concrete.	117
Table 3.4: U.K. Decision for Nationally Determined Parameters Described in BS EN 1992-1-2004.....	118
Table 4.1: Result for Discrete Element Method (DEM) Simulations.....	146
Table 4.2: Numerical Modelling Tool (EDEM Software) for Discrete Element Method (DEM) and Structural Tool (ANSYS) with No Wind Effect.....	157

Table 4.3: Numerical Modelling Tool (EDEM software) for Discrete Element Method (DEM) and Structural Tool (ANSYS) with Wind Effect.....	161
Table 4.4: Result of 160,000 Volcanic Ash Particles Simulation with No Wind Effects.....	166
Table 4.5: Result of 160,000 Volcanic Ash Particles Simulation with Wind Effects in The Horizontal	168
Table 4.6: Result of 20 Degrees 170,000 DEM and FEM CO-Simulation for Volcanic Ash Particles with No Wind Effects	170
Table 4.7: Numerical Modelling Tool (EDEM Software) for Discrete Element Method (DEM) and Structural Tool (ANSYS) with Wind Effect.....	175
Table 4.8: Result of 20 Degrees 170,000 DEM and FEM CO-Simulation for Volcanic Ash Particles with No Wind Effects	180
Table 4.9: Result of 20 Degrees 170,000 DEM and FEM CO- Simulation for Volcanic Ash Particles with Wind Effects in The Horizontal Direction.....	182
Table 5.1: Colour Coding for the Volcanic Ash Particles	184
Table 5.2: DEM and (FEM) Simulation Results for The No Wind Effects.....	185
TABLE 5.3: DEM and FEM Simulation Results for the Wind Effects.....	186
TABLE 5.4: DEM and FEM Simulation Results for the No Wind Effects	187
Table 5.5: Result of 80,000 Volcanic Ash Particles Simulation with Wind Effects.....	188
Table 5.6: Structural Failure Colour Coding and Meaning.....	190
Table 5.7: Result of 160,000 Particle Data for No Wind Effects.....	191
Table 5.8: Result of 160,000 Particle Data for Wind Effects	192
Table 5.9: Result of 80,000 Volcanic Ash Particles Results for the No Wind Effects	193
Table 5.10: Result of 80,000 Volcanic Ash Particles Data for The Wind Effects.....	194
Table 5.11: Result of 160,000 Particle Data for No Wind Effects.....	195
Table 5.12: Result of 160,000 Volcanic Ash Particles Data for the Wind Effects	196
Table 5.13: Results for the 80,000 Volcanic Ash Particles Results for the No Wind Effects	197
Table 5.14: Results for the 80,000 Volcanic Ash Particles Data for the Wind Effects	198
Table 5.15: Result of 20 Degrees Concrete Tile Pitched Roof for 170000 Simulations Volcanic Ash DEM and FEM Simulation with No Wind Effects.	200
Table 5.16: Result of 20 Degrees Concrete Tile Pitched Roof for 170000 Simulations Volcanic Ash DEM and FEM Simulation with Wind Effects.....	201
Table 5.17: Result of 25 Degrees Concrete Tile Pitched Roof for 170000 Simulations Volcanic Ash DEM and FEM Simulation with No Wind Effects	202
Table 5.18: Result of 25 Degrees Concrete Tile Pitched Roof for 170000 Simulations Volcanic Ash DEM and FEM Simulation with Wind Effects	203
Table 5.19: Result of 30 Degrees Concrete Tile Pitched Roof for 170, 000 Simulation Volcanic Ash DEM and FEM Simulation with Wind Effects	204

Table 5.20: Result of 30 Degrees Concrete Tile Pitched Roof for 170, 000 Simulation Volcanic Ash DEM and FEM Simulation with Wind No Effects	205
Table 5.21: Result of 20 Degrees Pitched Concrete Tile Pitched Roof for 170 000 Simulation Volcanic Ash DEM and FEM Simulation with No Wind Effects.....	206
Table 5.22: Result of 20 Degrees Pitched Concrete Tile Pitched Roof for 170000 Simulation Volcanic Ash DEM and FEM simulation with wind effects.....	207
Table 5.23: Result of 25 Degrees Pitched Concrete Tile Pitched Roof for 170000 Simulation Volcanic Ash DEM and FEM Simulation with No Wind Effects.....	208
Table 5.24: Result of 25 Degrees Pitched Concrete Tile Pitched Roof for 170000 Simulation Volcanic Ash DEM and FEM Simulation with Wind Effects.....	210
Table 5.25: Result of 30 Degrees Pitched Concrete Tile Pitched Roof for 170000 Simulation Volcanic Ash DEM and FEM Simulation with No Wind Effects.....	211
Table 5.26: Result of 30 Degrees Pitched Concrete Tile Pitched Roof for 170 000 Simulation Volcanic Ash DEM and FEM Simulation with Wind Effects.....	212
Table 5.27: Result of 20 Degrees Pitched Concrete Tile Pitched Roof for 170 000 Simulation Volcanic Ash DEM and FEM Simulation with No Wind Effects_	213
Table 5.28: Result of 20 Degrees Pitched Concrete Tile Pitched Roof for 170000 Simulation Volcanic Ash DEM and FEM simulation with wind effects.....	214
Table 5.29: Result of 25 Degrees Pitched Concrete Tile Pitched Roof for 170000 Simulation Volcanic Ash DEM and FEM Simulation with No Wind Effects.....	215
Table 5.30: Result of 25 Degrees Pitched Concrete Tile Pitched Roof for 170000 Simulation Volcanic Ash DEM and FEM Simulation with Wind Effects.....	217
Table 5.31: Result of 30 Degrees Pitched Concrete Tile Pitched Roof for 170000 Simulation Volcanic Ash DEM and FEM Simulation with No Wind Effects.....	218
Table 5.32: Result of 30 Degrees Pitched Concrete Tile Pitched Roof for 170000 Simulation Volcanic Ash DEM and FEM Simulation with Wind Effects.....	219
Table AP1.1: Results for 80,000 Volcanic Ash Particles Simulation with No Wind Effects.....	257
Table AP1.2:: Set of results for 80,000 Volcanic Ash Particles Simulation with Wind Effects in The Horizontal Direction	261
Table AP1.3: Set of results for the 25 degrees 170,000 DEM and FEM CO- Simulation for Volcanic Ash Particles with No Wind Effects	265
Table AP1.5:: Results for the 30 Degrees 170,000 DEM and FEM co.-Simulation for Volcanic Ash Particles with No Wind Effects.....	273
Table AP1.6: Results for 30 Degrees 170,000 DEM and FEM CO - Simulation for Volcanic Ash Particles with Wind Effects in the Horizontal Direction	276
Table AP2.2: Extracted Table 4.5: Result of 160,000 Volcanic Ash Particles Simulation with Wind Effects in The Horizontal.....	284

LIST OF FIGURES

	Page
Figure 1.1: Consideration of Volcanic Loading on European Building Code/ BS EN 1991	4
Figure 2.1 Classification of polymodal pyroclastic rocks based on the proportions of blocks/bombs, lapilli, and ash. Modified from Le Maitre, 2005.....	26
Figure 2.2: Summary Map of Volcanoes of Europe (Map based on NASA World Wind)	41
Figure 2.3: The Three-Dimension Plate Boundaries Model.....	42
Figure 2.4: Death Tolls as a Result of Volcanic Activities.....	45
Figure 2.5: Death Tolls as a Result of Volcanic Activities.....	47
Figure 2.6: Evolution of Pyroclastic Eruption for image A and image B shows a surge of volcanic ash particles into the atmosphere	50
Figure 2.7: Effect of Volcanic Eruptions on a building	53
Figure 2.8: 2021 Volcanic Ash Eruption in St Vincent	56
Figure 2.9: A house covered by ash from a volcano as it erupts on Canary Island of La Palma, Spain.	57
Figure 2.10: People looking towards an erupting volcano from El Paso on the Canary Island of La Palma	58
Figure 2.11: People cleaning up the ash off a house from the volcano in Las Manchas on the Canary Island of La Palma, Spain	59
Figure 2.12: Effects of Volcanic Deposition on A Roof.....	62
Figure 2.13: Isopach.....	62
Figure 2.14: Effects of volcanic ash deposition on the flanks of the volcano.....	63
Figure 2.15: Variation of Bulk Density with Magma Composition.....	65
Figure 2.16: Two-Dimensional Models	73
Figure 2.17: Three-Dimensional Models	73
Figure 2.18: Model Representation.....	74
Figure 2.19: Mt Etna Location in Italy: Showing Noto and Matera	79
Figure 2.20: A Map of Iceland and its Volcanic Zones with the Locations	85
Figure 2.21: Snow Load Shape Coefficient-Mono-Pitch Roof.....	102
Figure 2.22: Snow Load Shape Coefficients -Pitch Roofs	104
Figure 3.1 Flow Chart for Simulating DEM (Implemented in EDEM) and FEM (Implemented in COMSOL) Tool.....	110
Figure 3.2: Model for Flat Concrete Roof and Tile Concrete Pitched Roof used for the DEM and FEM Simulation Test.	111
Figure 3.3: Deposition of Volcanic Ash Particles on the Flat Concrete.	112

Figure 3.4: Deposition of Volcanic Ash Particles on the Pitch Roof.....	113
Figure 3.5: Differences between the E-E Model and CFD-DEM.....	120
Figure 3.6: Particle Collision Model.....	124
Figure 3.7: Interaction of Two Particles During Simulations	127
Figure 3.8: Deposition of the Volcanic Ash on Top of the Truss Roof	134
Figure 3.9: Contact Shape and Proportionality Relations of Forces for Particle-Particle and Particle– Line Contacts	135
Figure 3.10: Particles Length for a Chain of a Rectangular Particle in Contact with Centroids	135
Figure 3.11: Boundary Condition for the Simulation	139
Figure 4.1: Concrete Roof Model	142
Figure 4.2: Result for Finite Element Method (FEM) Simulations.	144
Figure 4.3: Result for Finite Element Method (FEM) Simulations.	145
Figure 4.4: DEM Results for Finite Element Method (COMSOL) For Stress with No Wind Effects	148
Figure 4.5: DEM Results for Finite Element Method (COMSOL) For Stress with Wind Effects	149
Figure 4.6: DEM Results for Finite Element Method (COMSOL) for Displacement with no Wind Effects	150
Figure 4.7: DEM Results for Finite Element Method (COMSOL) for Displacement with No Wind Effects	151
Figure 4.8 Volcanic Ash Particles Generated from the EDEM	152
Figure 4.9: Sliced Section of the Volcanic Ash Particles' Internal Structure Falling and Settling on the Concrete Roof.	153
Figure 4.10: Volcanic Ash Particles Deposition on the Concrete Roof Plate with the Pressure Load	153
Figure 4.11: DEM and FEM Co-Simulation for the Structural Analysis (ANSYS) Tool	155
Figure:1.12 Coloured coding for the various test results for the FEM simulation test.	156
The colour coding shows the effects of the ash from the lowest level, indicating the blue colour to the red colour coding being the highest loading level on the roof during FEM simulation.	156
Figure 4.13A: DEM Imagery Results showing the Distribution of Pressure Load (Pa).....	158
Figure 4.13B: FEM Imagery Results showing the Distribution of Deformations (mm).	159
Figure 4.13C: FEM Imagery Results showing the Distribution of von Mises Stress (MPa).....	160
Figure 4.14A: FEM Imagery Results showing the Distribution of Pressure Load (Pa).....	162
Figure 4.14B: FEM Imagery Results showing the Distribution of Deformations (mm)	163
.....	164
Figure 4.14C: FEM Imagery Results showing the Distribution of von Mises Stress (MPa).....	164
Figure 4.15A: DEM Imagery Results showing the Distribution of Pressure Load (Pa).....	171
Figure 4.15B: FEM Imagery Results shows the Distribution of Deformations (mm).....	172
Figure 4.15C: DEM Imagery Results showing the Distribution of Pressure load (Pa)	173
Figure 4.15D: DEM Imagery Results showing the distribution of stress Strain (mm/mm).....	174

Figure 4.16A: DEM Imagery Results showing the Distribution of Pressure Load (Pa).....	176
Figure 4.16B: FEM Imagery Results showing the Distribution of Deformations (mm)	177
Figure 4.16C: FEM Imagery Results showing the Distribution of von Mises Stress (MPa).....	178
Figure 4.16D: FEM Imagery Results showing the distribution of stress Strain (mm/mm)	179
Figure 5.1: Maximum Pressure Verse Particle for 80000 Volcanic Ash Particle with No Wind Effects (extracted from Table 4.4).	220
Figure 5.2: Maximum Pressure Verse Particle for 160000 Volcanic Ash Particle with No Wind Effects	222
Figure 5.3: from Table 4.6 for: Maximum Pressure Verse Particle for 160000 Volcanic Ash Particle with No Wind Effects	223
Figure 5.4: from Table 4.6 for Maximum Pressure Verse Particle for 160000 Volcanic Ash Particle with No Wind Effects	224
Table AP1.4:: Results for the 25 Degrees 170,000 DEM and FEM CO-Simulation for Volcanic Ash Particles with Wind Effects in the Horizontal Direction.	269
Figure AP3.1: Pressure exported from the DEM model to the FEM model for the wind effects reading for the maximum pressure as 19497.2 (Pa).....	290
Figure AP3.2: Pressure exported from the DEM model to the FEM model for maximum pressure for the No wind effects reading as 26703 (Pa)	291
Figure AP3.3: Maximum Stress for wind effects reading as 10.769 (MPa).....	291
Figure AP3.4: Maximum Stress for No wind effects reading as 14.39	292
Figure AP3.5: Maximum deformation for wind effects reading as 0.208 (mm)	292
Figure AP3.6: Maximum deformation for No wind effects reading as 0.253(mm).....	293
Figure AP3.7: Model showing DEM simulation of volcanic ash on the concrete roof plate	293
Figure AP3.8: Model without wind effect volcanic ash deposition.....	294
Figure AP3.9: Model with 1 ms ⁻¹ wind effects volcanic ash deposition.....	294
Figure AP3.10: Volcanic Ash Particles Generated from the EDEM	295
Figure AP3.11: Sliced Section of the Volcanic Ash Particles' Internal Structure Falling and Settling on the Concrete Roof.	295
Figure AP3.12: Volcanic Ash Particles Deposition on the Concrete Roof Plate with the Pressure Load	296
Figure AP3.13: Pressure exported from the DEM model to the FEM model for the wind effects reading for the maximum pressure as 19497.2 (Pa).....	297
Figure AP3.14: Pressure exported from the DEM model to the FEM model for maximum pressure for the No wind effects reading as 26703 (Pa)	297
Figure AP3.15: Maximum Stress for wind effects reading as 10.769 (MPa).....	298
Figure AP3.16: Maximum Stress for No wind effects reading as 14.39	298

Figure AP3.17: Maximum deformation for wind effects reading as 0.208 (mm)	299
Figure AP3.17: Maximum deformation for No wind effects reading as 0.253(mm).....	299
Figure AP3.19: Model showing DEM simulation of volcanic ash on the concrete roof plate	300
Figure AP3.20: Model without wind effect volcanic ash deposition.....	300
Figure AP3.21: Model with 1 ms ⁻¹ wind effects volcanic ash deposition.....	301
Figure AP3.22: Volcanic Ash Particles Generated from the EDEM	301
Figure AP3.23: Sliced Section of the Volcanic Ash Particles' Internal Structure Falling and Settling on the Concrete Roof.	302
Figure AP3.24: Volcanic Ash Particles Deposition on the Concrete Roof Plate with the Pressure Load	302
Figure AP3.25: Pressure exported from the DEM model to the FEM model for the wind effects reading for the maximum pressure as 19497.2 (Pa).....	303
Figure AP3.26: Pressure exported from the DEM model to the FEM model for maximum pressure for the No wind effects reading as 26703 (Pa)	304
Figure AP3.27: Maximum Stress for wind effects reading as 10.769 (MPa)	304
Figure AP3.28: Maximum Stress for No wind effects reading as 14.39	305
Figure AP3.29: Maximum deformation for wind effects reading as 0.208 (mm)	305
Figure AP3.30: Maximum deformation for No wind effects reading as 0.253(mm).....	306
Figure AP3.31: Model showing DEM simulation of volcanic ash on the concrete roof plate	306
Figure AP3.32: Model without wind effect volcanic ash deposition.....	307
Figure AP3.33: Model with 1 ms ⁻¹ wind effects volcanic ash deposition.....	307
Figure AP3.34: Volcanic Ash Particles Generated from the EDEM	308
Figure AP3.35: Sliced Section of the Volcanic Ash Particles' Internal Structure Falling and Settling on the Concrete Roof.	308
Figure AP3.36: Volcanic Ash Particles Deposition on the Concrete Roof Plate with the Pressure Load	309
Figure AP3.37: Pressure exported from the DEM model to the FEM model for the wind effects reading for the maximum pressure as 19497.2 (Pa).....	310
Figure AP3.38: Pressure exported from the DEM model to the FEM model for maximum pressure for the No wind effects reading as 26703 (Pa)	310
Figure AP3.39: Maximum Stress for wind effects reading as 10.769 (MPa)	311
Figure AP3.40: Maximum Stress for No wind effects reading as 14.39	311
Figure AP3.41: Maximum deformation for wind effects reading as 0.208 (mm)	312
Figure AP3.41: Maximum deformation for No wind effects reading as 0.253(mm).....	312
Figure AP3.42: Model showing DEM simulation of volcanic ash on the concrete roof plate	313
Figure AP3.43: Model without wind effect volcanic ash deposition.....	313

Figure AP3.44: Model with 1 ms ⁻¹ wind effects volcanic ash deposition.....	314
Figure AP3.45: Volcanic Ash Particles Generated from the EDEM	314
Figure AP3.46: Sliced Section of the Volcanic Ash Particles' Internal Structure Falling and Settling on the Concrete Roof.	315
Figure AP3.47: Volcanic Ash Particles Deposition on the Concrete Roof Plate with the Pressure Load	315

LIST OF APPENDICES

	Page
APPENDIX 1:.....	257
RELATED RESOURCES FOR CHAPTER 4	257
APPENDIX 2:.....	279
EXTRACTION AND EXPANDED TABLE OF RESULTS FROM IN CHAPTER FOUR	279
APPENDIX 3:.....	290
DEM AND FEM SIMULATION ANIMATION RESULTS (IMAGES AND VIDEOS).....	290

LIST OF ABREVIATIONS OR ACRONYMS

Abbreviation	Meaning
A	Area
ANSYS	Structural Analysis Tool
BS	British Standard
CFD	Computational Fluid Dynamics
COMSOL	Software for Multiphysics Simulation
DEM	Discreet Element Method
EDEM	Discrete Element Method
EDEM	Discreet Element Method Software
EJRC	European Joint Research Centre
EU	European Union
FEM	Finite Element Method

LIST OF SYMBOLS

Abbreviation	Meaning
A	Area
Al ₂ O ₃	Aluminum Oxide
Ce	Exposure Coefficient
C _{esl}	The coefficient for Exceptional Snow Loads.
f _{ctd}	Design Tensile Strength of Concrete
f _{ctk}	Tensile Strength of Concrete Roof
Fe ₂ O ₃	Iron (III) Oxide
Ct	Thermal Coefficient
Ff	Frictional Force
Fr	Partial Factor (Safety or Serviceability)
g	Gravitational Acceleration
h	Ash Thickness
K ₂ O	Potassium Oxide
MgO	Magnesium Oxide
Na ₂ O	Sodium Oxide
Pa	Pascal
Qk	Area A
CaO	Calcium Oxide

CHAPTER ONE

1.0. INTRODUCTION

The research focuses on volcanic building codes for the European Regions. The study examines the impact of volcanic ash activities on the roofs of buildings. There is evidence that there are no volcanic building regulations in Europe. Therefore, this study explores the safety and resilience of European buildings. There are building regulations for member states (Bessason et al., 2012). However, there is no clear evidence indicating that they are building regulations for volcanoes. Bessason et al. (2012) explain that "modern buildings are designed and constructed to withstand earthquake".

The essence of this research is that it will propose some standardisation across Europe on volcanic building roofs regulation. Evidence suggests that new volcano sites are being discovered across Europe because of geothermal activity. The volcanic ash effect will investigate the roof of buildings in Europe, within the prone areas, Isopach mapping for dwellings in these volcanic-prone areas and the revision of the EN1991. There will be a visit to these case study areas in Etna in Italy and Iceland for comparative purposes and the applications within Europe.

1.1 Background

Jerram et al. (2017) argue, "Volcanoes holds a fascination that we have from a young age and is something that we like to foster"; they further explain "the interest in some of the most beautiful and charming volcanic feature in the natural world". Contrary to the thoughts of Jerram et al. (2017), this thesis contends that volcanoes do pose a lot of problems, especially concerning buildings. The present work investigates the safety and resilience of building roofs

against volcanic ash in volcanic-prone areas of Europe. It will help with revising the European building code EN1991 within the volcanic-prone areas in Europe. It has been established that volcanoes can have various devastating effects on humans, building settlements along the flanks and within reach of volcanic eruption zones, even to the extent that these natural occurrences can impact countries with no known volcanoes.

Volcanic ash can affect buildings' roofs, as this is just an aspect of a volcanic effect within volcanic prone areas. Moreover, it is not astonishing that there are different types of activities and numerous types of eruptions. This volcanic eruption process and its effects that threaten all aspects of our regular life within and outer the volcanic prone areas cannot be overlooked regarding its associated hazards. (Thomas, 2007).

Volcanic ash can affect larger areas and impact a wide range of assets, even at a relatively small thickness (Blong, 2017). The rigorous lava and rock destruction of an explosive volcanic eruption produced volcanic ash, consisting of less than < 2 mm in average diameter. These fine ash particles consist of $64\mu\text{m}$ in average diameter (Zimanowski et al., 2003). It was acknowledged that the fine ash has a deposition from Plinian (magnetic) eruption. This volume of the fine ash proportion produced due to magnetic eruption can be $> 40\%$ of fine ash.

McIver (2014) claims that the Building Regulations are the statutory instrument that details the base level of performance for buildings' construction and design. Banerjee (2015) argues that building codes are "the primary source for guidance in the design and construction of building structures for many decades." He further explains that "building codes are generally intended to be applied by regulators engineers, architects, and constructors and are also used for various purposes by products and materials, manufacturers of building environmental scientists, real

estate developers, subcontractors, safety inspectors, tenants and others. It has been noted from research that it is the buildings that kill people, not the volcano (Heiken, 2013). That is a valid point from the research view, and as such due consideration must be given to the buildings. It is known that snow on a building roof is heavy when wet and settled; however, the prolonged eruption of debris and hot ashes from volcanic action can settle heavier materials on roofs as compared to that of snow, and it can also have overwhelming consequences, especially in the volcanic prone areas. It can also be deduced that, in a situation where there is a mixed natural occurrence from snow and volcanic ash actions, the question posed by the research is that "can the building roofs in the volcanic prone areas be resilient against the volcanic ash and the snow?"

This research aims to minimise volcanic ash activities that might affect/impact building roofs by proposing a revision of roof building regulations to make existing and future designs of buildings within Europe more resilient.

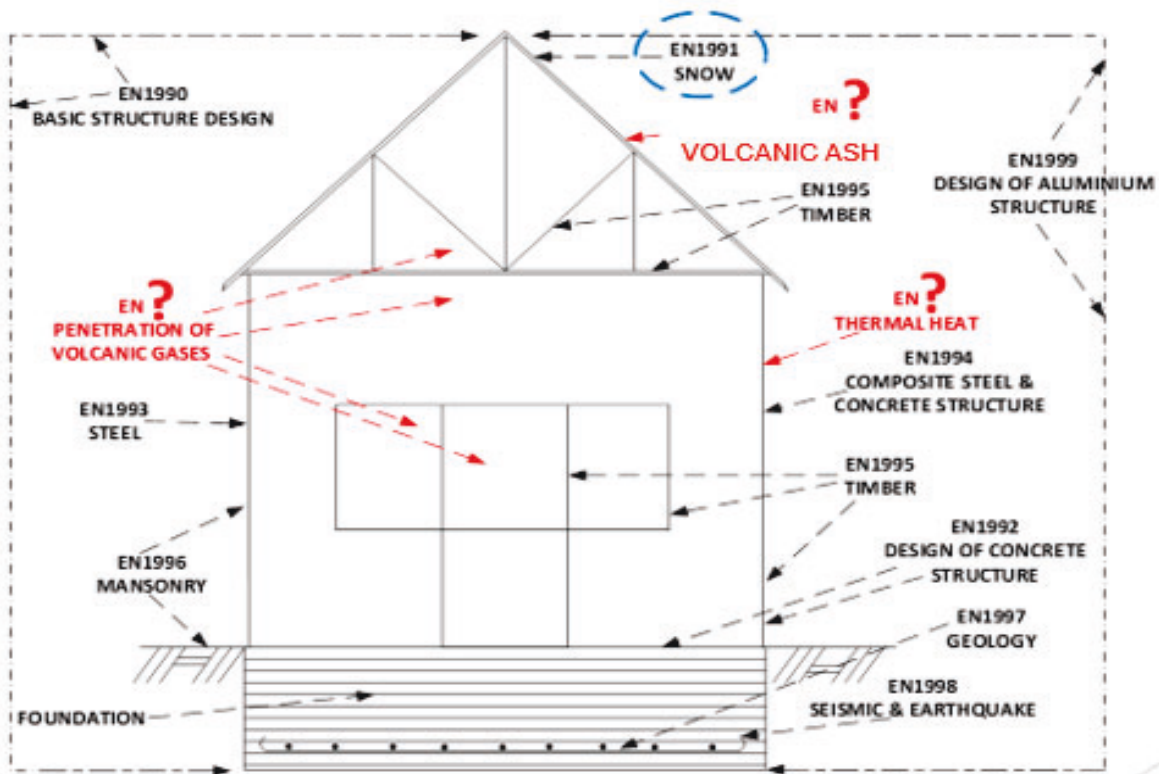


Figure 1.1: Consideration of Volcanic Loading on European Building Code/ BS EN 1991

Figure 1.1 above depicts the various existing building codes within Europe. The red colour indicates where there could be revisions of the building code within the European building regulations. As the problems mentioned above are indicated in red in figure 1.1. This study will focus on the EN1991, which dealt with snow on the roof without considering the effects of volcanic ash activities within Europe. This research focuses on the effects associated with volcanoes when it comes to buildings. Henkin (2013) mentioned that the types of problems, disruptions, upheavals, and damage that buildings may suffer because of volcanic activities include the following:

- Total disruption
- Respiratory problems inside buildings, such as gas penetration into the building
- The building collapsed because of a volcanic earthquake
- Buildings being covered by volcanic ash

- Buildings, roads, airports, etc., are being run over by lava flow
- Falling debris on the roof.
- Roof gutter damage
- Metal corrosion in the building
- Air space problem
- Mudslides
- Temporary evacuation

Building Codes are associated with the different types of volcanic activities by introducing rigorous building codes within the European regions or the volcanic prone countries. They will help reduce the effects on life and properties concerning the EN1991 whilst considering snow and volcanoes.

For example, among other European nations, Iceland and Ireland use European code 8 for seismic design, such as reinforced concrete and steel for their buildings. However, Branca et al., (2015) claim that there are ancient or traditional buildings built without compliance with contemporary building codes designed to minimise risk from earthquakes, which are still in existence and still occupied within volcanic prone areas. These buildings within the volcanic prone areas, which people are occupying, may pose a lot of danger to the occupants, should there be a strong volcanic eruption. The question posed by the research is how Europe cannot have a common standard building regulation for volcanic prone countries across Europe to enforce rigorous implementation of the building code. It will be further elaborated in detail in chapter 3. The proposed revision will help find interventions for both old and existing buildings. The research will explore the measures needed to put in place for remedial action in buildings that may pose a danger to people and their environments within volcanic-prone areas. When revised, the existing building codes will help develop the building codes for volcanic-prone countries and consider the foundations, materials, construction, and maintenance of the

prone area buildings. Laboratory simulation experiments will be conducted on the roof of such buildings to determine the collapse, volcanic ash, and the researcher's knowledge base and shape the building regulations' revision.

The study's rationale is that the revision will enable legislators, policymakers, and governments in Europe to adopt the best practice regarding the impact of volcanic activities, implementing effective and compliant building regulatory regimes to improve building safety and resilience structures within the European regions. The study will compare the findings from the Mt Etna region in Europe will be compared to Iceland. It will enable the study to consider the geographical locations of case study areas, the types of eruptions, the frequencies of eruptions, and the impact of the buildings' volcanic action. It is imperative to consider a second case study area for the research for comparative purposes.

1.2 Research Problem

1.2.1 Scope of the Problem

Indirect hazards include volcanic earthquakes, tsunamis, ground deformation, and structural collapse due to the withdrawal of magma, air shock waves, and lightning. The effect on society of even a moderate volcanic eruption can be significant, as shown by the two moderate Icelandic eruptions of 2010–2011. An unprecedented, large disruption to air traffic, with the cancellation of 108,000 flights, interrupting travel of 10.5 million passengers and costing the airline industry more than \$1.7 billion in lost revenue (Euro control, 2010). Heiken (2013) also reports the loss of \$200 million per day to the International Air Transport Association because of the 2010 Eyjafjallajokull eruption. However, no document was known to directly impact buildings, although the eruption could have impacted communities and countries within the

volcano activities' reach. Had the impact been as severe as it might have been, the cost of losses could have escalated above \$1.7 billion.

Pyle (2017) notes the prediction of the immediate physical consequences such as; an area of up to thousands of kilometers could be buried under volcanic ash, disruption of transportation, disruption of lives and livelihoods, and communication and life's essentials". Pyle identifies life essentials that can be affected such as "freshwater, food, warmth and shelter energy will all be under enormous stress". Forka and Mathew (2011) argue that a toxic chemical gas emitted from Lake Nyos during a volcanic eruption caused the death of some 1,800 people and led to the displacement of many thousands of others like different species of wildlife and livestock also killed in the event, which attracted international and national attention. These known problems are devastating when they do happen, and it is time more studies are channelled into the topic of volcanoes and their behaviour (Pyle, 2017).

1.2.2 Known Problems of Volcanoes

From the preceding discussions, it can be deduced that, while building codes need to be integrated to enhance the supportive function of buildings during the design phase and avoid related concerns during the occupancy phase, the two disciplines such as design and protection are still seen as different processes. The integration of design and protection against hazards remains limited. Most settlements in the Etna region contain large numbers of traditionally constructed houses, public buildings and churches that do not comply with contemporary building codes, which have only been enforced at the community level of administration since 1981 (Branca et al., 2015).

It is similar to Iceland, and the research will explore more about the building codes in Iceland. There are no building regulations for volcanic-prone countries in Europe. Branca et al. (2015) argue that there are some building codes, but, arguable, these are not suitable for volcanic-prone areas in Etna. It will, however, be ascertained during the field trip. It has been identified that, should there be a building code for volcanic prone areas in Etna, that will still be relevant for the research, as that will meet one of the research objectives. Objective 1: To identify the geographic distribution of regions within Europe that will benefit from a revision of building regulations to increase buildings' resilience to volcanic activities.

Italy's most devastating earthquake in almost 30 years, according to Dinmore and Segreti (2009), occurred in Rome and took 260 lives. A magnitude - 6.3 on the Richter scale - would probably not have caused a single death or barely any serious structural damage. The research understanding is that the earthquake of 6.3 on the Richter scale in Rome should not have affected buildings and should not have taken people's lives (the buildings were not resilient to the quake). However, volcanic eruptions can also cause earthquakes or seismic action that could also result in building collapse. Volcanic action is more prominent in Italy and, to be precise, is related to Mt. Etna, one of the world's most active volcanic spots. As a result, Mt Etna is one of the case study areas for the research, while Iceland, where a volcano exploded in 2010, will be the other. At least another case study area within Europe was needed for comparison, considering the time and frequency of eruption; and the local geographical location of Iceland was geography sen because it erupts only once in a while by contrast to the many eruptions of Etna. Dinmore and Segreti (2009) explain that "Construction in Italy is extremely vulnerable due to age and typology." They further added that even a non-frequent earthquake could cause severe devastation.

1.2.3 Establishing the Research Questions

The gap that has been established is that there are no known published works on volcanoes for building regulations in Europe. However, it has been established that some countries like Italy and Iceland have some form of regulations. Buildings, predominantly roofs, are exposed to tephra fall from volcanic eruptions, making the occupants exposed to tephra-induced injury or death. Roof construction type and failure mechanism are the principal factors that determine the tephra load, which damages roofs or causes them to collapse (Spence et al., 2005). Spence et al. (2005) explained that previous field, experimental, and theoretical work suggests that many roofs would collapse under pressure loads in the range of 1–5 KPa. Still, field and other experimental work have shown that some designs can withstand up to 10 KPa. This research will discuss these gaps in theoretical and practical awareness by addressing a central research question. Hence the research aim and objectives were formulated to address these gaps in the research. Several research types have been carried out on the roofs of buildings in Europe, such as covering the roof on the thermal performance of highly insulation roofs in the Mediterranean climate by D'Orezio et al. (2010). A similar experiment has been carried out on roof exposure to tephra around the Vesuvius in Italy (Spence et al., 2005).

Spence et al. (2005) experimented with the Static used load of an ash deposit in the primary hazard intensity measure used to assess the probability of damage or loss when assessing the risk of building damage from ashfall (Spence et al., 2005). Static load from ash accumulation was calculated using the formula below;

$$L_{AF} = \rho gh \tag{2-1}$$

Where

- L_{AF} is ash load in Pascals (Pa; more commonly reported as kPa)

- ρ is the ash density (kgm^{-3})
- g is the gravitational acceleration (9.81 m/s^2)
- h is the ash thickness in meter

The research will consider the revision of the EN1991 regarding the roof building code within the volcanic-prone areas to address these gaps. This study will use the laboratory simulation exploration to unearth the means to make roofs of buildings safe and resilient in volcanic-prone areas. The finite element method COMSOL, which is a commercial software tool implementing the FEM and numerical modelling tool (EDEM software) for the Discrete Element Method (DEM) and structural analysis tool (ANSYS) for the Finite Element Method (FEM) Implemented in EDEM commercial software package. The research will adopt some of the methodology used by some authors (D'Orito et al., 2009; Hampton et al., 2015). The roofing materials considered by these two authors are tiles, copper, and shingle corrugated sheet for the pitched roof. The dry and the wet volcanic ash will be investigated on the pitched roof using variable angles from 20° - 45° .

On the other hand, the static approach will consider the volcanic ash's frictional force on the roof and the roofing materials for both the dry and wet volcanic ash for both static and dynamic approaches. It will help determine the stress on the roof. The investigation outcome will revise the European roofing code (EN1991) within the volcanic-prone areas. This research question or hypothesis addresses these gaps in theoretical and practical knowledge by defining a central research question:

The thesis is to examine how effective is the existing methodology for evaluation of the static and dynamic roof loading to ascertain their effectiveness and put forward strategies for the

revision of building roof regulations against volcanic ash activities to help make them even more effective and workable to reduce or prevent the loss of lives and properties in Europe?

1.2.4 Aims and Objectives of the Research

To pursue the issues raised in the discussions above, this research work seeks to examine and revise the current roof building regulations for volcanic prone countries in Europe and, in comparison, to other codes developed outside Europe hence, this research aims at the following;

1. To investigate the resilience of building roofs against the loads due to volcanic ash's weight in the volcanic prone areas of Europe.
2. To propose a revision of the European building code EN1991 (in the current European code regulation) within the volcanic prone areas in Europe.

The following objectives are identified as key to achieving the aims of the research.

Objective 1: To identify the geographic distribution of regions within Europe that will benefit from revising building regulations to increase buildings' resilience to volcanic activities.

Objective 2: Investigate existing local building roof regulations in Europe and evaluate their effectiveness in preventing the impact of volcanic ash activities compared with the experiences from the two case study areas (Etna and Iceland).

Objective 3: To conduct numerical (finite element modelling (FEM) and the discrete element method (DEM)) modelling tool to assess structural behaviour under loading conditions (static and dynamic).

Objective 4: To propose a revision of the building code EN1991-1-1-3 following the results of objective 3.

These objectives are directly linked to the aims of the research; they will also help develop the revision of EN 1991 building regulations. The next section looks at the expected and anticipated contributions from this research. This research will use the Case Study as a methodology, which focuses on areas with volcanic activities in Etna in Italy and Iceland. The thesis organisation comprises six chapters; this thesis begins with Introductory Chapter 1 and Chapter 2, which present the review of the related literature review should be more comprehensive and will include relevant literature concerning modelling and simulation.

Chapter 3 introduces the research methodology. The diverse approaches to the research, research design and expectations, various methodologies and data collection techniques used for quantitative and qualitative research are all reviewed. This chapter also discusses the research context. Chapter 4 is devoted collapse of the roof using volcanic ash for the collected data results. Chapter 5 provides discussion and analysis. It will include the pilot work for the case study areas (Isopach mapping data, video recordings, architectural location types of new methods and the data analysis process). Chapter 6 involves the Conclusions of the research findings and Future Work.

CHAPTER TWO

2.0. LITERATURE REVIEW

2.1 Introduction to Volcanoes

The essence of this chapter is to gather information on the topic in discussion and identify a gap in the current knowledge. The chapter will be a critical review of the available literature placed in perspective, within the context of how different researchers have approached their research study with regards to what has already been investigated, the areas that have not been investigated, the identification of the gap in the research and how to investigate it. As the thesis's title implies, the focus is more specific, on loading caused by volcanic ash falling on roofs and determining how safe and resilient these buildings are in volcanic-prone areas. That will eventually lead to developing a framework for the European continent and its potential application to other parts of the world. This review will ascertain the relevant literature to analyse how different researchers have approached studying and conceptualising volcanoes and humans' actions. The various sources of information gathered from journals, reference books, news articles, seminars, exhibitions, conference bloggers, etc., will be listed in the bibliography.

2.2 Definition of Terms

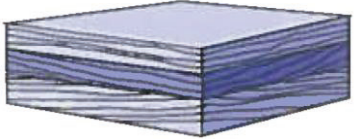



2.2.1 Definition of Volcanoes

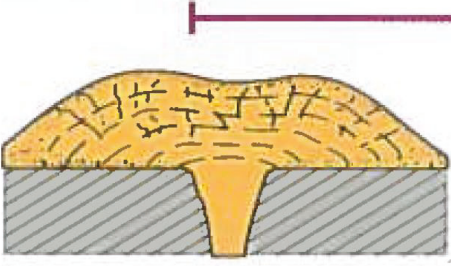

Kereszturi (2014) defines a volcano as “the eruptive subsystem of a volcanic system is extending from, and including, the shallowest magma reservoirs that feed eruptive activity, all magma plumbing pathways and conduits tapping that reservoir, and the volcanic edifice at the surface, and including possible intrusions within such an edifice”. Jerram et al., (2017) in their definition of volcanoes, state that it is more difficult to define volcanoes that are active,

dormant, or extinct. They went on further to explain that; “the expert volcanologist has been puzzled -not to say surprised- when certain volcanoes have suddenly burst into life after a very long period of calmness”.

The type of volcano is very important to the research because it will help illustrate the volcanic ash activities' behaviour in the case study areas in Europe (Etna in Italy and Iceland). Below are the descriptions of volcano's types and effects as per Heiken (2013, front page).

Table 2.1: Types of Volcanoes with Examples

Volcano Type	Characteristics	Examples	Simplified Diagram
Flood or Plateau Basalt	Very liquid lava; flows very widespread; emitted mainly from	North Atlantic Igneous Province, Columbia River, Siberian Traps, Parana-Etendeka	
Shield Volcano	Liquid lava emitted from a central vent; large; sometimes has a collapsed caldera.	Skjaldbreidur, Iceland, Hawaiian volcanoes,	
Cinder cone	Explosive liquid lava; small; emitted from a central vent, if continued long enough.	Chafne des Puys France, Iceland,	
Composite or Stratovolcano	More viscous lavas, much explosive (pyroclastic) debris; large, emitted from	Vesuvius, Italy, Mount Rainier-USA, Colima-Mexico, Dmamavand-Iran Mount Fuji-Japan	

Volcano Type	Characteristics	Examples	Simplified Diagram
Volcanic Dome	Very viscous lava, relatively small; can be explosive; commonly occurs adjacent to/within craters of	Puy de Dome, France Mt. St. Helens dome, Colima central	
Caldera	The very large composite volcano collapsed after an explosive period, frequently associated.	Campi Flegrei, Italy, Crater lake-USA, Long Valley-USA	

Source: (Jerram et al., 2017): Adapted from the USGS

2.3 Types of Volcanoes and Characteristics

This section illustrates the types and characteristics of volcanoes within the different continents in the world. Table 2.1 below shows other types of volcanoes such as Flood or Plateau Basalt Shield Volcano, Cinder Cone, Composite or Stratovolcano, Volcanic Dome and Caldera. Jerram et al. (2017) indicate in Table 2.1 the examples of activities in various parts of the world. This section plays an important role in determining the types of volcanoes.

Table 2.2: Types of Volcanoes and Its Effects

Description of Types of Volcanoes	Effects of Volcanoes in Some Countries Around the World
Pyroclastic flow	A hot mixture of gases, volcanic ash, and pumice that moves downslope at hurricane velocities. That can cover areas ten of square miles; destroys anything in its path. Fatalities are caused by burns and suffocation. (Examples; Manila, Naples, Quito and Montserrat)
Eruption plume	When the eruption column stops rising, high altitude winds carry turbulent eruption clouds downwind, blanketing tens to thousands of square miles.
Volcanic Mudflow (Lahar)	. That involves a rapidly moving slurry of volcanic ash, rocks, and debris. Occurs after the large collapse of the volcano or when heavy rainfall saturates and mobilises ash deposits. The area affected; tens of square miles; Maybe concentrated along river valleys. Fast-moving lahar eliminates or buries everything in its path (e.g., Armero, Shimabara City, Seattle/Tacoma, Manila)
Lava flow	Molten rocks flow downslope from fissures, central vents, and overflowing lava lakes. Flow velocity depends on composition,

Description of Types of Volcanoes	Effects of Volcanoes in Some Countries Around the World
	degassing behaviour, and slope. Areas at risk are usually less than tens of square miles but may be much larger, depending on eruption length, and rate of extrusion. The flow crushes and ignites vegetation and surrounding structures; it can form a lava delta if it reaches the sea. (Examples; Goma, Mexico City, Auckland)
Explosive Eruption from Vent	Gas-thrust-driven, 6 to 25-mile-high, as laden vertical eruption column
Lava fountain	Gas-rich fountain of molten rock from fissure vents; very little threat to the public unless fissure cuts through a town. Fissure vents and lava fountains are a source of lava flows. (Example; Goma)

Source: (Heikin, 2013)

This section illustrates the types and characteristics of volcanoes within the different continents in the world. Table 2.2 above shows other types of volcanoes such as Flood or Plateau Basalt Shield Volcano, Cinder Cone, Composite or Stratovolcano, Volcanic Dome and Caldera. Jerram et al., (2017) indicate in Table 2.3 the examples of activities in various parts of the world. This section plays an important role in determining the types of volcanoes.

Table 2.3: Volcanic Explosivity Index VEI. Classification table of the size of volcanic eruption using VEI (Smithsonian database)

VEI	Ejecta volume	Classification	Description	Plume	Frequency	Some Examples	Occurrences in last 10,000 years*
0	< 10,000 m ³	Hawaiian	non-explosive	< 100 m	constant	Kilauea	many
1	> 10,000 m ³	Hawaiian/ Strombolian	gentle	100–1000 m	daily	Stromboli	many
2	> 1,000,000 m ³	Strombolian/ Vulcanian	explosive	1–5 km	weekly	Tristan da Cunha (1961) Whakaari/White Is. (2019)	< 4250
3	> 10,000,000 m ³	Vulcanian/Peléan	severe	3–15 km	yearly	Surtsey (1963) Soufrière Hills (1995) Ontake (2014) Anak Krakatoa (2018)	989
4	> 0.1 km ³	Peléan/Plinian	cataclysmic	10–25 km	≥ 10 yrs	Mount Pelée (1902) Eyjafjallajökull (2010) Nabro (2011)	461
5	> 1 km ³	Plinian	paroxysmal	> 25 km	≥ 50 yrs	Mount St. Helens (1980) Mount Hudson (1991)	174
6	> 10 km ³	Plinian/Ultra-Plinian	colossal	> 25 km	≥ 100 yrs	Krakatoa (1883) Mount Pinatubo (1991)	52
7	> 100 km ³	Plinian/Ultra-Plinian	super-colossal	> 25 km	≥ 1000 yrs	Tambora (1815)	5 (+2 suspected)
8	> 1,000 km ³	Ultra-Plinian	mega-colossal	> 25 km	≥ 10,000 yrs	Toba (71-72,000 BP)	0

Source: (Jerram et al., 2021)

Table 2.3 explains the level of ejecta volume, classification, description, plume, frequency, and examples. As illustrated, the ejecta volume is in the region between less or equal to 0.1k m³ to greater than 106m³. It confirms why Montserrat was covered within "20 minutes with the Pyroclastic flow", as stated by Heiken (2013) in support of the illustration in Table 2.3. However, he does not mention the amount of ejecta in Montserrat; the level of the explosion is very important for the research because it will help the researcher with the development of the revision for the building code for the roof of buildings in the prone areas, considering the strength and stabilities to be adopted in the volcanic prone areas. The plume level and the frequencies of eruptions will also play a significant role in developing the building codes. That will be deliberated further in the chapter.

Table 2.4: Top 5 Volcano Disasters 2000–2010 by Numbers Affected

Volcano	Country	Year	Deaths	Affected
Tungurahua	Ecuador	2006	5	300,013
Karthala	Comoros	2005	1	245,000
Mt. Merapi	Indonesia	2010	322	137,140
Reventador	Ecuador	2002	0	128,150
Mt. Nyiragongo	Congo Dem Rep.	2002	200	110,400

Source: (EM-DAT, 2014)

Table 2.5: Top 5 Volcano Disasters 1980–2010 by Numbers Killed

Volcano	Country	Year	Deaths	Affected
Nevado Del Ruiz	Colombia	1985	21,800	12,700
Lake Nyos	Cameroon	1986	1,746	10,437
Mt. Pinatubo	Philippines	1991	640	1,036,065
Mt. Merapi	Indonesia	2010	322	137,140
Mt. Nyiragongo	Congo Dem Rep.	2002	200	110,400

Source: (EM-DAT, 2014)

Table 2.6: Top 5 Volcano Disasters 2000–2010 by Numbers Killed

Volcano	Country	Year	Deaths	Affected
Mt. Merapi	Indonesia	2010	322	137,140
Mt. Nyiragongo	Congo Dem Rep.	2002	200	110,400
Nevado del Hila	Colombia	2008	16	8,007

Jabal al-Tair	Yemen	2007	6	15
Mount Arteale	Ethiopia	2007	5	2,000
Tungurahua	Ecuador	2006	5	300,013

Source: (EM-DAT, 2014).

Some recordings seem to vary in some areas, whereas they seem to be the same in other areas. It must be noted that some death tolls were recorded as estimates. From Table 2.5, in Nevada del Ruiz in Columbia, 21,800 deaths in 1985 were recorded, whilst in Table 2.17 in the same year, 1985, 23,942 deaths were recorded.

In Table 2.17 concerning Mt Pinatubo in the Philippines, 320 deaths were recorded in 1991, whilst table 2.5 recorded 640 deaths. The most important aspect is the loss of lives and property, which is not acceptable in any way, but it's very encouraging to note the decline in the death rate. However, there were efforts made to reduce the rate of death in these volcanic-prone areas. There is a clear indication from table 2.5 and table 2.6 that the number of deaths declined even though there were repeated recordings in some areas. From the data, it is also clear that the number of people displaced or affected was generally high. The decline in the number of deaths confirms the researcher's hypothetical views that there has been some good work done regarding research, but there is still a long way to go. Undoubtedly, this research will contribute to developing a volcanic building code, safety, and resilience of building in European volcanic prone areas. That will be compared to other parts of the world when completed.

Table 2.7: Tephra Load-Thickness Equivalencies

Load (KN/m ²)	Thickness (mm)
2	130-150
5	300-550
10	550-650
15	-900

Source (Rabaul, 1994)

The Table illustrates the volume of the Tephra eruption in Rabaul (1994). The load in Table 2.7 shows how the varying loads can have a damaging effect on buildings depending on the type of volcanic eruption.

Table 2.8: Damage Distribution of the Pinatubo Sample

Damage level	Description	Number of buildings	Percentage in damage level	Percentage with damage at or exceeding level
D0	No damage	15	29	100
D1	Light roof dam	3	6	71
D2	Moderate roof damage	8	16	65
D3	Severe roof damage and some damage to vertical structure	8	16	49
D4	Partial roof collapse and moderate damage to rest of building	9	18	33

Source (Spence et al., 2005)

Table 2.8 focuses on volcanic ash's depth regarding the impact on the roofs during and after the eruption. The data shows the number of buildings that have been affected by Tephra

eruption according to Spence et al. (2005,) mentioned 'a building damage survey which was carried out on 29 June 1991, two weeks after the main tephra fall event, by the Field Epidemiology Training Program Team of the Department of Health, Manila, the Philippines. They indicated the impact of the depth of Tephra fall in Olangapo was about (15 cm), and Castellejos, tephra fall depth was about (20 cm). Blong (2003) explained that a house which collapses experienced Tephra loads of ($>7.5 \text{ KN/m}^2$). He went on further to state that some buildings which carried half of the load sustained cosmetic damage. Blong (2003) made another important point because 'residential buildings with less concrete blocks wall experienced less damage than buildings with only timber frame.

Table 2.9: Eruption Frequencies for Selected Countries

Selected countries	Population (2008) a (million)	Number of eruptions		Average eruption frequency	
		VEIb 0–3	VEI 4–7	VEI 0–3	VEI 4–7
Indonesia	239.9	1170	28	6 months	15 years
Iceland	0.3	147	26	6 years 10 months	43 years
Japan	127.7	892	71	7 months	44 years
Guatemala	13.7	105	8	4 years 9 months	53 years
Philippines	90.5	133	11	1 year 4 months	59 Years
Papua New Guinea	6.5	191	23	8 months	81 years
Alaska, Kamchatka, Kuril Islands	1.1	713	115	5 months	100 years
Ecuador	13.8	188	31	2 years 5 months	102 years
Canada, Lower 48 states USA	335.8	147	18	1 year 6 months	143 years
Italy	59.9	242	21	5 years	215 years
Colombia	44.4	5134	15	6 years 6 months	304 years

Mexico	107.7	114	25	7 years 6 months	375 years
New Zealand	4.3	189	17	11 months	394 years
Chile	16.8	339	17	1 year 4 months	554 years
Nicaragua	5.7	130	10	1 year 2 months	806 years
Peru	27.9	39	4	14 years 2 months	832 years

Source: (Jenkins et al., 2014 and Wilson et al., 2010)

Table 2. 10: Land Coverage and Ash Thickness

Ash Thickness (mm)	Land Coverage Area (sqkm)
1–2	236,353
2–4	362,026
4–7	318,945
7–10	178,769
10–20	58,155
20–30	58,042
35–50	14,254
50–70	11,479
70–120	7,918
120–200	6,690
200–350	11,456
350–500	9,738
500–750	3,315
750–1000	961
1000	765

Source: (Blong et al., 2014)

Table 2.10 shows that ash thickness up to (35-50 mm) and more could affect many coverage areas. Anything less than (5-30 mm) could affect large areas but significantly impact the building roofs in the prone areas. With each square kilometer having an equal number of buildings of the same kind for five constructions, it is possible to calculate a vulnerability function that combines Figures. The areas were experiencing each thickness of ashfall in a repeated Tambora 1815 eruption scenario. Areas covered below (10 mm) are given for illustrative purposes as these places would still sustain disruptions as the result of ashfall.

Table 2.11: Characteristics of Standard Cement CEM II/A-V 42,5R

Properties	Values
Compressive strength 2 days	≥ 20 MPa
Compressive strength 28 days	≥ 42.5 and ≤ 62.5 MPa
Setting time (beginning)	≥ 60 min
Expansion	≥ 10 mm
SO ₃	$\geq 4.0\%$
Cl-	$\geq 0.10\%$

Source: (Sánchez et al., 2010)

Cement: The cement used was CEM II/A-V 42.5R, according to European Standard EN 197-1:2000 Standard, with an average content of (80 – 94 %) clinker, (6 – 20 %) siliceous fly ash and additional components up to (5 %), their physical and chemical properties specified are shown. This cement was used in keeping with present procedures at the concrete tile works where the trials were conducted.

2.4 Pyroclastic Classification Schemes

Pyroclasts are defined as fragments generated by disruption as a direct result of volcanic action. The fragments may be individual crystals, or crystal, glass, or rock fragments. Their shapes acquired during disruption or subsequent transport to the primary deposit must not have been altered by later redepositional processes. If the fragments have been altered, they are called "reworked pyroclasts", or "epiclasts" if their pyroclastic origin is uncertain.

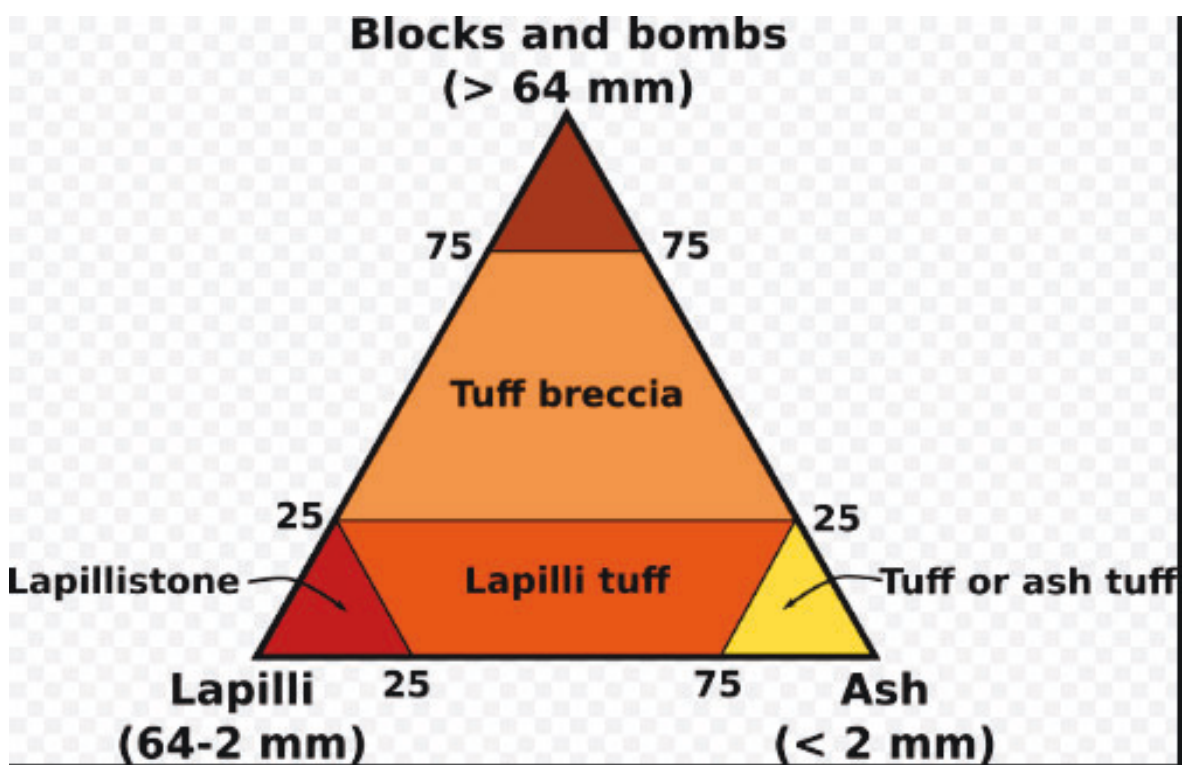


Figure 2.1 Classification of polymodal pyroclastic rocks based on the proportions of blocks/bombs, lapilli, and ash. Modified from Le Maitre, 2005

Bombs: pyroclasts the mean diameter of which exceeds 64 mm and whose shape or surface (e.g. bread-crust surface) indicates that they were in a wholly or partly molten condition during their formation and subsequent transport.

Blocks: pyroclasts the mean diameter of which exceeds 64 mm and whose angular to subangular shape indicates that they were solid during their formation.

Lapilli: pyroclasts of any shape with a mean diameter of 64 mm to 2 mm.

Ash grains: pyroclasts with a mean diameter of less than 2 mm. They may be further divided into coarse ash grains (2 mm to 1/16 mm) and fine ash (or dust) grains (less than 1/16 mm).

2.4.1 Lapilli

Lapilli is spheroid, teardrop, dumbbell, or button-shaped droplets of molten or semi-molten lava ejected from a volcanic eruption that falls to earth while still at least partially molten. Lapilli is a very common form of volcanic rock characteristic of rhyolite, andesite and dacite pyroclastic eruptions. However, thick layers of lapilli can be deposited throughout a basal surge eruption. Most lapilli materials which remain in ancient terrains are formed by the accumulation and welding of semi-molten lapilli into what is known as a welded material.

2.5 Definition of Safety and Resilience of the Building Code.

All these authors' definitions are very significant for the current research. They all make mention how building structures are built and to ensure they are safe for habitation. Since the research will formulate 'A Framework for European Regulations' to assure safety and resilience against volcanic activities in new and existing buildings, there will be a need to establish a framework for the building code for volcanic active prone areas in Europe.

The researcher's view is to review safety and resilience in building regulation in the literature. Concerning this, the researcher will define safety and resilience as follows;

2.5.1 Safety:

According to the Oxford English Dictionary (2017), safety can be defined as the condition to be protected from or unlikely to cause danger, risk, or injury.' The online dictionary also defines safety as the state of being safe, freedom from the occurrence or risk of injury, danger, or loss. Safety involves averting or not causing injury, danger, or loss.

Alhajeri (2011) defines safety as the protection of people from physical injury. He further explained that the borderline between health and safety is ill-defined. The two words are normally used together to indicate concern for the individual's physical and mental well-being at the place of work. '

The International Safety Advisory Group (INSAG), according to Kerstan et al. (2013), defines safety culture as 'the assembly of characteristics and attitudes in people and organisations which establishes that, as a priority, protection and safety issues receive the attention needed by their significance.'

All these authors have similar definitions, and they all go on further to elaborate on two key points. The first phrase is that safety is about 'good safety attitudes or 'good safety management established by organisations. The second descriptive phrase is that good safety culture means assigning the highest priority to safety. (Kerstan, et al.:2013).

2.5.2 Resilience:

This definition builds from the National Research Council (NRC) (2009) statement of resilience as a response to stress and can be considered as a theory that guides the understanding of stress response dynamics; a set of adaptive capacities that call attention to the resources that promote successful adaptation in the face of adversity; and strategy for disaster readiness against unpredictable and difficult to prepare for dangers' (National Research Council 2009). According to Flynn (2016), 'The term resilience refers to the chance to prepare for and adapt to the changing conditions and withstand and recover rapidly from disruptions. Resilience includes the ability to recover and withstand deliberate attacks, accidents, or naturally occurring threats or incidents.'

Resilience is a wide concept with many definitions. Still, most include the ability to:

- contain a shock in a time of
- difficulty: the functional recovery of the building after a disaster or a sudden shock.
- Operate appropriately even if parts of a building fail.

Resilience can be related to the design, construction and operation of building structures that can withstand natural and human-made disasters. Buildings designed for resilience can absorb and rapidly recover from a disruptive event.

Flynn (2016) states further that building resilience necessitates a deep understanding of human factors, the built environment, and the natural environment and how they interact. It also emphasises identifying and validating the attributes, functions, and values whose loss or disruption would be undesirable or harmful. He explained that, too. Often, this knowledge of

what needs to be safeguarded is taken for granted. As a result, efforts to reduce or eliminate risk often overlook trade-offs. They can even compromise the very things that we need to safeguard to assure our way of life and life quality.

Hazard's risk: hazardous events abound. Ettouney (2014). These can be natural hazards such as floods, earthquakes, or human-made hazards such as bomb blasts and hazardous materials spills. They went further to explain that it can include health-related and climatic change.

Operational Risk: Ettouney talked about the uncertainties involved in operations which are linked with all outcomes. They described that some of these uncertainties could yield fewer outcomes and can be described as a risk.

Financial Risk: Ettouney talks about the financial losses related to a project, such as design-build and design-build-maintain with public-private partnerships.

Strategic Risk: Ettouney explains that these risk deals are associated with strategic decisions and depend on the topological scale of interest (such as international, national, local corporate, or network-wide civil infrastructure), e.g., such as national security risk, international risk of health-related issues or risk of civil infrastructure aging in a specific network, etc.

The arguments by Ettouney are valid points, but the researcher's opinions can be linked with the first point raised in 'Hazards risk: hazardous events abound.' The researcher believes that volcanoes are natural occurrences, and they come with associated risks and hazards. On the contrary, the researcher's views on Operational Risk, Financial Risk and Strategic Risk area are important to the research will not be a central focus.

Ettouney describes natural hazards such as floods, earthquakes or human-made hazards such as bomb blasts and hazardous materials spills. They went further to explain that it can include health-related and climatic change.

The European Commission (2013) notes that resilience is the ability of a household, community, individual, country, or region to withstand, adapt, cope, and quickly recover from stresses and shocks such as conflict, drought, violence, and other natural disasters without compromising long-term development. However, the European Commission (2013) argues that building resilience involves the prevention and preparedness of projects such as disaster insurance and early warning systems, which help local communities face the threats caused by hurricanes and violent storms during the rainy season or unpredictable events like volcanoes. The notion of resilience is gaining prominence at the international policy level in Australia, the UK and Canada. Since 2010, resilience has been adopted as one of the Canadian government's key performance indicators (Treasury Board of Canada Secretariat: 2010), although the metrics for measuring resilience are still determined.

From natural disasters to equipment failure and even crime, these risks can damage or destroy critical infrastructure and disrupt the essential services provided by these assets, networks, and supply chains (McClelland: 2010).

The researcher agrees with Flynn and other authors' views regarding building resilience, which goes beyond human factors, the built environment, the natural environment and how they interact. That is why the research incorporates buildings' resilience in volcanic-prone areas when considering the framework for the building regulations. The research intends to explore

the events during the planning stage, including the framework for preparing the building regulation and all the necessary themes during a volcanic eruption. The question posed by the researcher is, how can the buildings (new and existing buildings) in the volcanic prone areas be resilient against volcanic action in the prone areas?

The researcher regards design as an important aspect of building structures' safety and resilience and will explore strategies for improving buildings' design to help make them safe and resilient to volcanoes.

Materials, methods of construction, and regulations enforcement are all key areas the research will consider. The research will examine strict compliance with the prescriptive guidance requirements of the Building Regulations in Europe, which are assumed to provide adequate safety levels to buildings. Consideration will be given to what effect these changes will have on both life and property regarding the safety and resilience of building in volcanic-prone areas. The researcher will be observing the safety of buildings, and the research will look at the safety act to ascertain whether they are regularly implemented and complied with it. The research will investigate how these regulations are monitored and how effective they are. This way, the researcher can incorporate in the framework for the building regulation for volcanic prone areas in Europe; positive recommendations that will help improve the safety and resilience of building against volcanoes.

The research will also establish whether building structures are covered by insurance policies to ensure support for people affected by a natural volcanic disaster.

According to BSEN 1991-1-3, Snow's nature on the plate specifies that Snow can be deposited on a roof in many different patterns. The properties of a roof or other factors causing different patterns include:

- the nature of the roof
- its thermal properties
- the rough nature of the surface
- also, the amount of heat generated under the roof
- the proximity of nearby buildings Regions Ψ_0 Ψ_1 Ψ_2

The snow load on the building roofs is vital to the research because one building was based on the Snow. The study has argued that there were no considerations of the volcanic ash loading effects on the EU roofs. The research sought to adopt some of these considerations for the volcanic ash loading on some of the roof's top with the considered action of the volcanic ash loadings.

According to the BS EN 1991-1-3:2003 code, the snow load on the building roofs is vital to the research because one building was based on the Snow. The study has argued that there were no considerations of the volcanic ash loading effects on the EU roofs. The research sought to adopt some of these considerations for the volcanic ash loading on some of the roof's top with the considered action of the volcanic ash loadings. The building code described the properties of a roof and other factors considerations. The explained concerning different altitude locations with different impact patterns.

Table 2.12 Recommended Values Of Coefficients ψ_1 For Different Locations For Building

Regions	ψ_0	ψ_1	ψ_2
Finland Iceland Norway Sweden	0.70	0.50	0.20
Reminder of other CEN member states, for sites located at altitude H > 1000 m above sea level	0.70	0.50	0,20
Reminder of other CEN member states, for sites located at altitude H 1000 m above sea level	0.50	0.20	0.00

Table 2.13: Snow Loads on Roofs.

Topography	Ce
Windswept a	0.8
Normal b	1.0
Sheltered c	1.2
<p>a) Windswept topography: flat, little shelter afforded by terrain, or unobstructed areas exposed on all sides without, or, higher construction works or trees.</p> <p>b) Normal topography: areas where there is no importance to removing Snow by the wind on the construction worksite because of terrain, other construction works, or trees.</p> <p>c) Sheltered topography: areas in which the construction works sites being considered are considerably lower than the surrounding terrain or surrounded by high trees and surrounded by higher construction works.</p>	

Snow loads on roofs shall be determined as follows:

- for the persistent/transient design situations:
- for the accidental design situations where exceptional snow load is the accidental action.

- For the accidental design situations where exceptional snowdrift is the accidental action, and Annex B applies, the exposure coefficient should determine the roof's snow load.
- The choice should consider future development around the site. It should be taken as 1.0 unless otherwise specified for different topographies. The National Annex may give the values of different topographies. The recommended values are given in Table 5.1 above. The thermal coefficient should be used to reduce snow loads on roofs with high thermal transmittance, particularly for some glass-covered roofs, because of melting caused by heat loss. For all other cases:
- The thermal coefficient C_t should be used to account for reducing snow loads on roofs with high thermal transmittance ($> 1 \text{ W/m}^2\text{K}$), particularly for some glass-covered roofs, because of melting caused by heat loss. For all other cases: $C_t=1.0$

2.6 Simulation Time for DEM

The study's simulation time was set at sec for the accumulation form to reach a stable deposition on the roof. The principle of simulation time related to physical time is the number of volcanic particles located on the roof must be the same. The initial velocity was 0.154, and it has remained unchanged. Modell wind affects volcanic ash deposition. Arrow indicates the direction of the wind flow in the x-axis on the different volcanic particle transportation modes has to be the same for both spherical and non-spherical volcanic particles. The simulation run will help determine the volcanic loading height on the concrete plate and determine the stress and allowable stress. values (max stress). the volcanic drifting will be considered with the wind and non-wind effects.

Further, co-simulation will be conducted using the DEM and FEM analysis to determine the stress, deformation on the concrete roof. That will eventually lead to the determination of the roof's resilience within volcanic-prone areas. Adopting the multi-physics simulation in COMSOL for flat roof models such as the DEM model and FEM was adapted for the research with the same dimension.

The study considered the Concrete flat roof and the pitched tile roof with the following material properties: Density of $2,300 \text{ Kg m}^{-3}$, Young modulus of $25 \times 10^9 \text{ N/m}^2$ and the Poisson ratio of 0.20. The plate's sides will be fixed constraints, and the boundary load pressure will be considered from this DEM simulation pressure results from the data. The load type, as mentioned above, will be user-defined.

The factor of safety of the concrete roof structure is 1.5, according to EN 1992-1-1:2004+A1:2014. According to Seward (1994), the factor of safety for concrete is stated as 1.5 and 1.2 for the partial factor of safety. This study will use the factor of safety of 1.5 for the calculation of the allowable stress. (BS EN 1992-1-1:2004+A1:2014) to determine the allowable stress.

The other flat roof material that will be considered for the research's static and dynamic approach with the modulus of elasticity will be 1200 N/m^2 for the hardwood. In the UK, the basic standard given by the snow loads ranges from 0.3 N/m^2 . However, on the south coast to 1.3 kg m^{-3} in northern Scotland (Seward,1994). This value used within Europe for the roof base's design on the snow effect is very important to this research since these values attached to this research will be related to the volcanic-prone areas in Europe.

Seward (1994) stated that the consideration for the design of roofs loads (BS:6339: part 1998) depends on the following factors:

Geographical location, Height above sea level, slop on the roof and the wind redistribution of the snowdrifts. These considerations were used to design snow loadings on the roofs in European and British standards. These considerations are very important to the research because it's the research's aim that should apply research outcome in Europe and the rest of that; the model considered for this research is the flat concrete roof and that pitched roof with variable angles of inclination such as 20°,25°,30°,35°, and 40°. Seward (1994) explained that Snow would form on steeply pitched roofs in all conditions where there is less. With regards to this research, will be adopted a similar approach for this study concerning the volcanic ash particles for the pitched roof to determine the effect of the volcanic ash on the roof, for the maximum stress and the maximum allowable stress with the variable wind with effect from the y-axis and the situation without wind effect. The allowable loading can be formed from about 0.252 KN/m² for lower buildings in London to 2.0 KN/m² for tall buildings in Edinburgh. This very impact regards the argument made by Seward (1994) that "for the purpose."

2.7 Bulk Weight Density of Snow

According to the BS EN 1991-1-3:2003 (1), The bulk weight density of Snow varies. In general, it increases with the snow cover duration and depends on the site location, climate, and altitude.

(2) Except where specified in Sections 1 to 6, indicative values for the mean bulk weight density of Snow on the ground given in Table E.1 may be used.

Table 2.14: Mean Bulk Weight Density of Snow

Type of snow	Bulk weight density [KN/m ³]
Fresh	1.0
Settled (several hours or days after its fall)	2.0
Old (several weeks or months after its fall)	2.5 – 3.5
Wet	4.0

According to the BS EN 1991-1-3:2003, this section explains snow load shape coefficients for undrifted and drifted snow load arrangements for all types of roofs identified in this standard, except the consideration of exceptional snowdrifts defined in Annex B, where its use is allowed. Special consideration should be given to the snow load shape coefficients to be used. The roof has an external geometry, which may increase snow loads considered significant compared to that of a roof with a linear profile.

2.8 Roof Snow Load Shape Coefficient

The snow load ratio on the roof to the undrifted snow load on the ground, without the influence of exposure and thermal effects. That can be related to the DEM, and FEM simulation study for the tile pitched roof simulation. The study will adopt some of the inclination angles to determine the DEM and FEM results. Below is the various pitched roof information that is relevant to the program.

2.9 Reasons Why People Live in Volcanic Prone Areas

People have various reasons for choosing to live in certain places such as country, town, and community. The reasons could be cultural, economic, political, and social. Pyle (2017) argues that "today more than 500 million people live near volcanoes, and many communities have long coexisted with the volcano in their back yard". However, the researcher is of the view that

in every endeavour, there are bound to be benefits and threats with regard to every natural activity. It is not different from volcanic activities that have taken lives and properties, yet people live near volcanic active prone areas. There are many different reasons why people live or cluster near volcano areas.

Heiken (2013) furthermore explains that, worldwide, 67 large cities with populations greater than 10,000 are located on or near historically active volcanoes, including the three megacities of Tokyo, Manila and Mexico City. The total population at risk in these urban areas exceeded 116 million people by 2006-2007. Heiken (2013) explains that the reason can vary from practical to aesthetic. However, explaining further, he argues that all large communities need a nearby production agriculture economy to sustain them because of the enrichment of the soils in the regions for growing crops. The other point Heiken raises is that some of the volcanic regions' inherent beauty can attract people to the volcanic prone areas. Just as some authors have talked about the damaging effect of volcanic activities in Mount Etna, "Mongibello", there is mention of volcanic activities' positive side.

It could also help us answer the question of why people live near volcanoes. For example, areas surrounding volcanoes like Mt. Vesuvius in Italy are key areas of food production. The fertile land also means that the country does not have to spend so much money importing food to feed its population, which benefits its overall economy (Anon, 2013). Volcanoes are also an important tourist attraction and can draw millions of tourists to an area each year. It can increase after an eruption as people hear about these events on the news and want to see them. Tourism benefits the local and national economy of a country. Iceland attracts millions of tourists due to its volcanic landscape, and 5% of its economy is generated by tourism alone. The volcanoes and plate boundaries generate a lot of heat, which can create geothermal energy production.

That is a renewable energy source, and so is better for the environment and can reduce the amount of non-renewable energy a country must use. Around 90% of Iceland's homes are powered by electricity that is generated from geothermal energy. That can improve a country's energy security as it will be less dependent on energy imports from elsewhere and support its own energy needs. Geothermal areas have enticed industrial developers to provide electrical power and urban heating systems as public baths and other recreational outlets (Heiken, 2013). The nagging question on the mind of the researcher is; "why research the revision of roof building regulation (code) in volcanic prone countries in Europe after all people have lived in these volcanic areas for so long and will continue to live there?"

2.10 Distribution and impacts of Volcanoes in Europe

Concerning the diversity of volcanoes on the European continent, Jerram et al. (2017) state that volcanic activities have been "complicated caused by the collision between Eurasian and the African plate". They further explain that the volcanoes in Europe lie in the margin of "the Mid-Atlantic Ridge, the Canary Islands, southern Italy and the Aegean Sea. Jerram et al. go on to say that the remaining volcanic activity is generally associated with the old system in France and Germany.



Figure 2.2: Summary Map of Volcanoes of Europe (Map based on NASA World Wind)

Source: (Jerram et al., 2017)

The map above illustrates the distribution of some volcanic locations in Europe. Figure 2.1 indicates countries in Europe experiencing volcanic activities such as France, Germany, Italy, Spain, and Iceland, just to mention a few. Some indications suggest the increase of volcanic activities across Europe. Etiope et al. (2007) mention that there are countries in Europe with volcanic activities, such as the Czech Republic, Germany, Greece, Iceland, Italy, and Spain. They argued that the first estimate of methane emission from the geothermal/volcanic component is at the European level. They explain further that, in Europe, 28 countries have geothermal systems and at least ten countries host surface geothermal manifestations (hot springs, mofettes, gas vents). Karátson et al. (2017), stated that "the latest study of eruption is from the Romania region, where the volcano-sedimentary record, is expected from on-going studies". The question asked by the study is whether these countries that are already

experiencing volcanic activity as well as those that Etiope et al. (2007) and Karátson et al. (2017) have suggested are having geothermal activity, have building regulations? It is very relevant for the study to ask this question: Should there be an eruption, how are these buildings going to cope with the impact, especially within countries showing signs of volcanic activities?

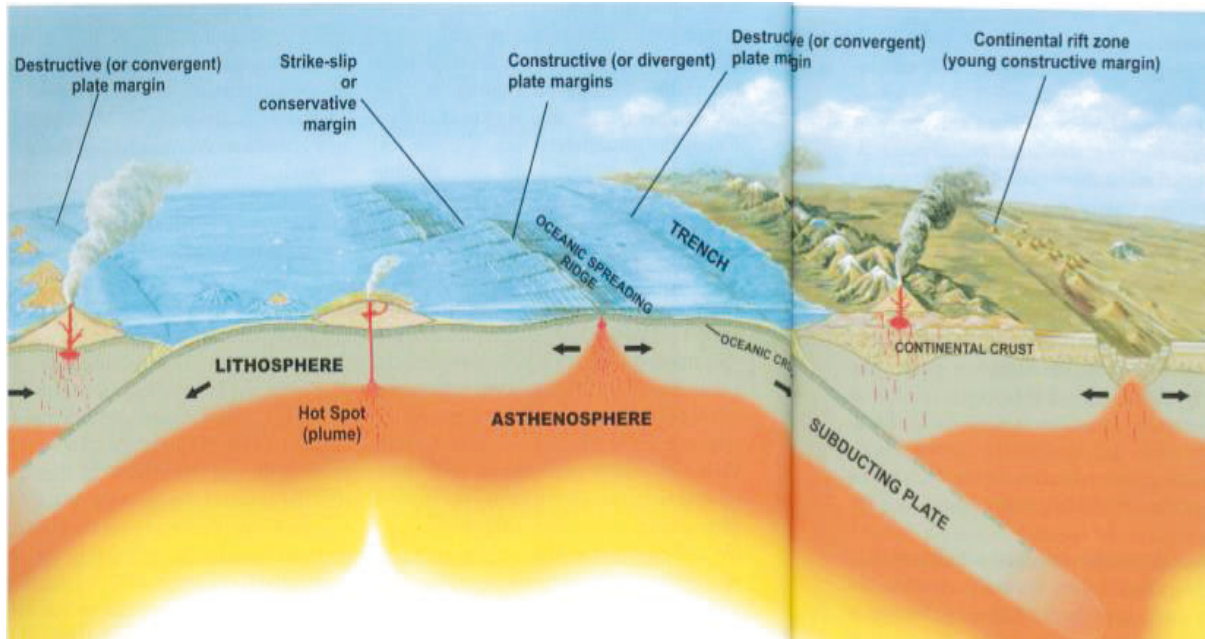


Figure 2.3: The Three-Dimension Plate Boundaries Model.

The three types of plate boundary/margin found on earth are: a constructive (or divergent) plate margin: a strike-slip or conservative margin (USGS). ((Jerram 2021)).

Table 2.15: European Cities Near Active or Potentially Active Volcanoes

City, Country	Population (2006/2007 estimates)	Last Significant Eruptions Nearby Volcanos
Roma, Italy	2,705,603	3,500 years ago,
Catania, Italy	301,564	Active Now
Napoli, Italy	975,139	1944
Torre del Greco	88,918	1944

Source (Heiken, 2013)

Table 2.15 above illustrates European near active or potentially active Volcanoes. It also shows cities in some countries in Europe that are volcanic prone. However, from the study of volcanic hot spots in Europe, the researchers extrapolated the information as stated in the source. As indicated in Table 2.17 (Heiken, 2013), the Catania region can be described as the most active volcanic area in Europe. That is the location of Mt Etna in Italy. The volcanic region's area population is very high because of the volcanic soil's economic benefit, as illustrated on pages 5-7. There is also an indication from Table 2.17 of the high population around the volcanic-prone areas. It is very significant to the research.

These volcanic-prone countries in Europe add impetus to the study because of the prevalence of volcanic activities in the region, as suggested by Karátson et al., (2017), who claim that Romania is one of the most volcanic prone countries. Jerram et al., (2017) argued that Romania is not a known volcanic country in Europe. They suggested some "volcanic activities along with its off-shore territories with subaerial eruption as recent as 1985". They supported their arguments by indicating that there is an on-going hydrothermal activity in an underwater discovery, and this needed attention". Both Jerram et al., (2017) and Karátson et al. (2017) indicated that there could be more volcanic prone countries in Europe that have not yet been discovered or areas that are about to be discovered. In support of their argument, they stated that volcanoes do not always display their present secrets, neither past nor do they always reveal their future intention. These debates affirm the researcher's thoughts and other scientific experts of volcanology about how dangerous these volcanoes can be. As confirmed by Jerram et al. (2017), "nobody can predict the "intent" of the volcanoes. Heiken (2013) describes the volcanic eruption in Montserrat in the Caribbean as "in just 20 minutes, a series pyroclastic flows swept an area of 1.5 square miles and destroyed more than 100 homes, leaving 19 people dead and 9 missing". The Guardian (2015) published about "the shock eruption in 2013 was Japan's

deadliest for almost 90 years, with an estimated 63 people dead, many of their bodies at least partially entombed in volcanic sludge." As confirmed by these authors, the behaviour of volcanic eruption in Montserrat, Japan and many other volcanic prone countries across the world means that the intent of volcanoes cannot be predicted, or, whether they are "Active", "Dormant", or "Extinct". They argued by describing how volcanoes "do not display the secret of their past, nor do they always reveal their future intentions". They also revealed that volcanoes are normally considered active, if they have erupted in the last 10,000 years", and they further explain that "such a value may include volcanoes that are effectively extinct" (Jerram et al., 2017)

Table 2.16: Death Toll Because of Volcanic Activities

Source and Page <i>Pyle:2017)</i>	Location	Years	Death Toll (Estimated)
171	Mt Sufferer Island of St Vincent	1812	56
150	Tambura Japan	1815	10,000
177	Mt Pelee nearby Martingue	1902	1000
159	Anak Krakatoa	1931	1400
164	Montserrat	1997	19

Source: (Pyle, 2017)

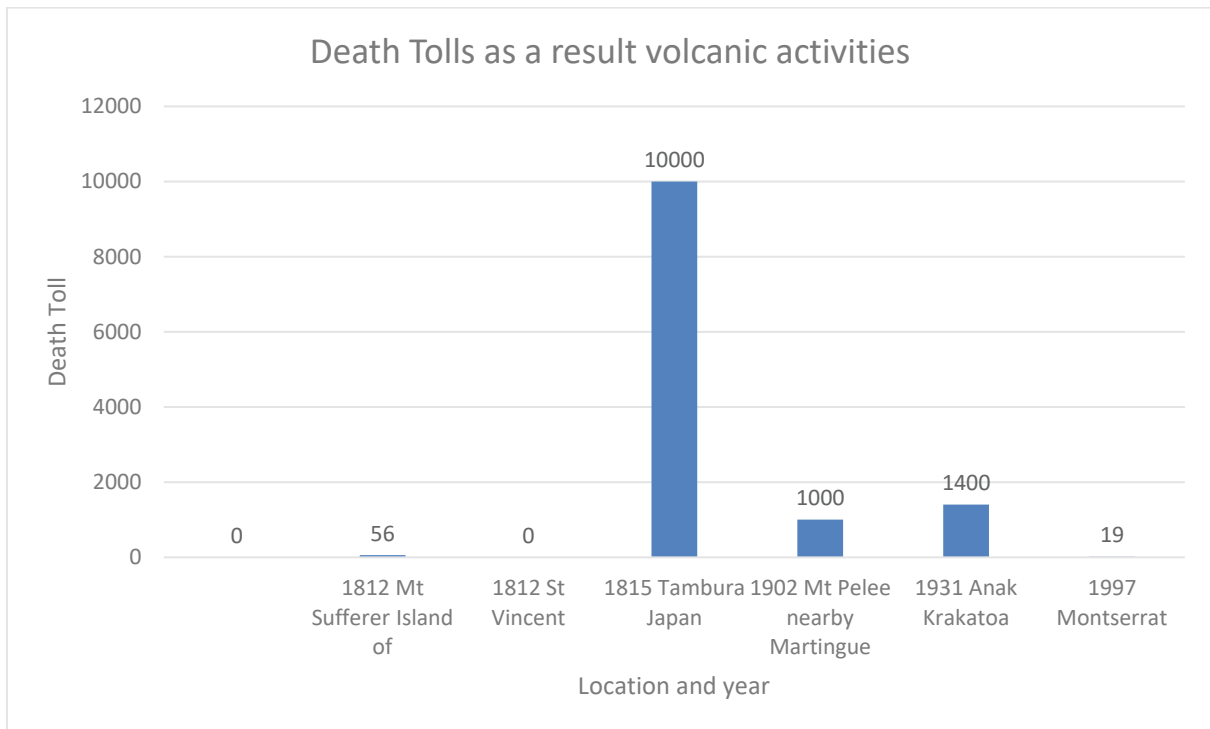


Figure 2.4: Death Tolls as a Result of Volcanic Activities

Source: (Pyle, 2017)

The study intends to use these data for some of the impacts of volcanoes over the past decades. The graph for Figure 2.4 above was plotted using information from Table 2.16. The research intends to carry out a comparative analysis of two sources of information from two authors about the death toll caused by volcanoes over the past year due to their impact. The highest death toll recorded was in 1815, which took the lives of 10,000 people from the graph. The researcher believes there may be an indication that there were no proper systems in place to monitor these volcanic activities' behaviour at the time. The death toll declined to its lowest level in 2000 in Montserrat, which can be attributed to the volcanic observatory station's presence which advised people's immediate evacuation from the active areas.

Table 2.17: Death Tolls as a Result of Volcanic Activities

Source and Page: Henkins (2013)	Location	Years	Death Tolls as a result of volcanic activities.
P94	Shimabara	1637	37000
P24	Vesuvius	1906	216
P175	Volcanic Island, Philippine	1911	1335
P150	Santorini	1956	53
P40	Nyos in Cameroon	1984	1700
P2	Nevada del Ruiz in Columbia	1985	23942
P 90	Mizunashi River	1991	43
P58	Philippine Pinatubo	1991	320
P150	Montserrat	1997	19
P1	Congo, Goma	1997-1998	170
P49	Sarno	1998	150

Source: (Heiken, 2013)

The information in Table 2.17 is taken from Henkins (2013) and summarised. Table 2.17 as indicated, is the names of those volcanoes that have taken people's lives. The death toll is from the lowest to the highest, from the Montserrat eruption in which 19 deaths were recorded to the highest death toll in Shimabara in which 3700 deaths were recorded, according to Heiken (2013). The researcher can argue hypothetically that the low rate of the death toll may be because of interventions to solve the effects of the eruption. Forka and Matthew (2011) suggested that nearly 2,000 deaths resulted from the release of poisonous gas or carbon dioxide in the August 1986 eruption in the Cameroons.

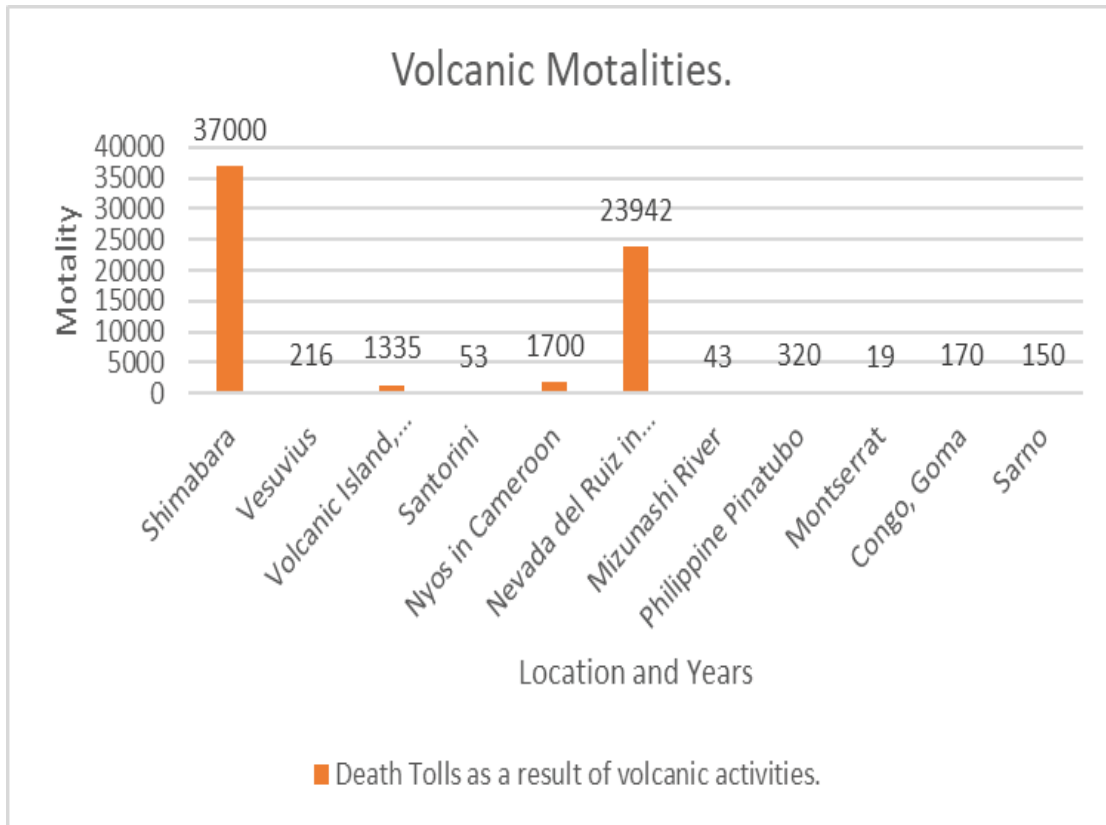


Figure 2.5: Death Tolls as a Result of Volcanic Activities

Source: (Henkins, 2013)

The second data illustrated in Table 2.16 and Table 2.17 compares the two authors as indicated earlier in Heiken (2013). The data was extrapolated and summaries from Henkins (2013).

2.11 Volcanic Threat and Impact on Buildings

Buildings in volcanic prone areas are in constant danger whenever there is an eruption or a seismic action. Bilham (2013) argued it is the buildings that kill people, not the earthquakes.

(1) Flying debris is the major cause of death in tornados. Thomas (2007) also confirms that volcanoes can cause death, as illustrated in (2). Therefore, in earthquakes and tornados, death's major cause is structural damage or collapse. The researcher tends to agree with the argument about the first point, but, on the contrary, buildings should rather save people. The debris can settle on the roof, and if the roof is not strong enough, that will lead to the collapse of the roof. That can lead to serious fatalities, if not deaths of those in the building. The second point expressed by Bilham (2013) is very important because volcanoes can trigger seismic action, and this can affect the foundation of buildings and can lead to structural damage. The research will not discuss tornados even though they are a natural phenomenon that can also influence buildings.

Table 2.18: Density and Load Comparison, 100 m) of Snow and 100 mm (Volcanic Ash)

Description	Density (Kgm ⁻³)	Load (KPa)
New Snow	50 - 70	0.05 - 0.07
Damp new snow	100 - 200	0.1 - 0.2
Settled snow	200 - 300	0.2- 0.3
Dry uncompacted ash	500 - 1,300	0.5 -1.3
Wet compacted ash	1,000 - 2,000	1.0 -2.0

Source: (Johnston,1997)

Table 2.18 shows the comparison of volcanic ash to that of snow. The volcanic ash is heavier than the snow in terms of densities. The loading effects on the roof of buildings, as suggested

by (Johnston 1997), the thought of the study can be affirmed by the comparison of the volcanic ash particle and the snow effects on the roofs of buildings within volcanic prone areas. Tables 2.18 is significant for the study, and it goes further to establish the gap in the study concerning the effects of the volcanic ash particle on volcano-prone areas. A study conducted by the American U.S. Department of the Interior stated that the dry volcanic ash presents a weight ranging from 4 to 7 KN/m³, and rainwater can amplify it by 50% to 100%. They explained that if the ash becomes saturated by rain, it can reach more than 20 KN/m³. So, ash loading may be considered similar to a specific snow load but with some major differences: - being heavier, it is a much more severe loading case (Table 2.18); - ash doesn't melt; these ash loads will have an enormous impact on the roofs of buildings. Wet tephra is known to have a greater load than dry tephra, and various remarks from historical volcanic eruptions in the past 20th Century have shown critical variable thicknesses of tephra under which roofs have collapsed. However, these ashes are dense, abrasive and chemically corrosive (Muzeau et al., 2010).



Figure 2.6: Evolution of Pyroclastic Eruption for image A and image B shows a surge of volcanic ash particles into the atmosphere

Source: (Luck et al., 2002)

The above picture is shown in Figure 2.6 as A and B show the stages of evolution of pyroclastic eruption with its devastating consequences. Eruptions of any volcano may be rare and certainly do not occur on typical political timescales. When they do erupt, volcanoes can obliterate large areas, and there is nothing that humanity can do. However, Volcanoes are the earth's way of cooling down and must release their heat formation and radiogenic isotope within it. The approach to this process is complex, and while a great deal of research is being undertaken concerning volcanic activity, plate tectonics, mantle plumes and the convection of the earth's mantle, relating our current knowledge of these processes to the spatial and temporal likelihood of eruptions is very challenging (Donovan, 2012). The author argues that the timescales of large eruptions are very different from the timescales of governments. They are high-impact but low-probability events. In an increasingly globalised environment, eruptions have transnational impacts and affect both volcano-rich and volcano-free nations. The process of volcanic edifice slope failure threatens all aspects of everyday life for those in the potential hazard zones (Thomas, 2007). Heiken (2013) confirms the argument of Bilham (2013) about the "buildings most heavily damaged during that earthquake were those between 12 to 20 stories high". However, these are indications that volcanoes can react in different ways. Henkins further explains that "a great deal of the destruction was from adjacent buildings of different heights banging into each other, of floors pancaking as buildings collapsed".

Another threat to buildings is that lava flow which has rare low viscosity, moves quickly, according to Henkins (2013), as was the case in Goma. Near the volcano, volcanic eruptions and lahars have destroyed large areas of Montserrat. The capital of Montserrat, Plymouth, has been covered in layers of ash and mud. Many homes and buildings have been destroyed, including the only hospital, the airport and many roads. This lava can overrun humans, and the only way out is to run to safe grounds. Heiken (2013) did confirm this by acknowledging that;

"fallout may be too heavy to keep up with the clearing operation; it is then time to pack some valuables". The research agrees absolutely with the suggestion of Henkins; in such a circumstance, the only way not to endanger ones-self is to leave immediately. Thomas (2007) confirms the opinions of Henkins about the immediate departure, evacuation, or relocation "to avoid any potential confrontation between the volcano and the surrounding population". Thomas describes this action as "the first effort in tackling the problems of volcanoes." Thomas (2007) explains further that, although this would have been the most effective way in preventing loss of life and properties, such action "are not feasible" to a layman, because, even if there are well-documented risk hazards to exist, the tendency for it to be ignored is high. Thomas's argument may be that the occurrence of volcanic hazards is once in a millennium, and apparently, it does not affect most people's daily lives. A typical example given by Heiken (2013) explains how volcanic eruptions and lahars devastated a large part of Montserrat. Plymouth capital was covered in ash and mud, the hospital, the airport, and many roads. The research opinion is that those who died, had they left by being evacuated, may have probably lived.



Figure 2.7: Effect of Volcanic Eruptions on a building

Source: (Luck et al., 2002)

Figure 2.7 shows the collapse of the roof during volcanic activity. It illustrates how devastating volcanoes can impact the roofs of buildings. The Image affirms the importance of the research in the prone areas in Europe. The top of the roof has been burnt down including the structure itself. The blue coloured label indicates the position of the burnt roof by the action of the volcanic eruption.

The volcanic ash can stay in the atmosphere and the environment for a very long, affecting communities far away from the volcano vent. Zhao et al. (2016) carried out a simulation experiment for the snowdrift modelling method by CFD (Computational Fluid Dynamic coupled with DEM (Discrete Element Method)). This paper involves numerical simulation only

(field measurements are mentioned but not carried out with the scope of the work involved) on snowdrift's prediction on tunnel wind test for the field measurement and numerical simulation. Zhao et al., (2016) pointed out the DEM usage because of the limitation of the shape of the roof, which may be attributable to "the change due to the existence of snow, which is, in turn, affects the movement of snowdrift". However, they explained that "the effects have time-varying characteristics". They also pointed out that the DEM usage overcame these limitations by explicit calculation of the particles' contact mechanics which is very important to the current research. DEM has been used for lots of simulations for different materials since it was introduced. (Cundall 197). The Lagrangian solution for granular flows calculation of individual particles addresses engineering problems, granular flows, power machines and rock mechanics with computers' aid. Thus, DEM usage is not different for this current research concerning volcanic ash on the roof of buildings in the prone areas. DEM will help predict volcanic ash's effects on the flat concrete roof and the pitched roof with different roofing materials such as wood cladding, wood shingles, tile, etc.

Figure 2.6 shows the collapse of the roof during volcanic activity. It illustrates how devastating volcanoes can impact the roofs of buildings. The Image affirms the importance of the research in the prone areas in Europe.

The volcanic ash can stay in the atmosphere and the environment for a very long, affecting communities far away from the volcano vent. Zhao et al. (2016) carried out a simulation experiment for the snowdrift modelling method by CFD (Computational Fluid Dynamic coupled with DEM (Discrete Element Method). This paper involves numerical simulation only (field measurements are mentioned but not carried out with the scope of the work involved) on snowdrift's prediction on tunnel wind test for the field measurement and numerical simulation.

Zhao et al. (2016) pointed out the DEM usage because of the limitation of the roof's shape, which may be attributable to "the change due to snow, which is, in turn, affects the movement of snowdrift". However, they explained that "the effects have time-varying characteristics". They also pointed out that the DEM usage overcame these limitations by explicit calculation of the particles' contact mechanics which is very important to the current research. DEM has been used for lots of simulations for different materials since it was introduced in the proposal (Cundall 197). The Lagrangian solution for granular flows calculation of individual particles addresses engineering problems, granular flows, power machines and rock mechanics with computers' aid. Thus, DEM usage is not different for this current research concerning volcanic ash on the roof structures in the prone regions. DEM will help predict volcanic ash's effects on the flat concrete roof and the pitched roof with different roofing materials such as wood cladding, wood shingles, tile, etc.



A



B

Figure 2.8: 2021 Volcanic Ash Eruption in St Vincent

(A) Eruption Cloud Showing Ash Fall-Out and Image

(B) Roof Collapse Under The Weight Of Ash:

Source: http://uwiseismic.com/Downloads/LS_2021_Media%20Fact%20Sheet_Final_15022021.pdf./<https://www.bbc.co.uk/news/world-latin-america-56703409>

The image shows the volcano's eruption, and the image shows the eruption, which has affected buildings within the prone areas and has displaced people in the inhabitants.

The Caribbean Island of St. Vincent erupted layers of ash, bringing major disruption after a volcano erupted on April 9, 2021. (a) Eruption cloud showing ash fall-out and (b) Roof collapse under the weight of the ash. That shows how dangerous it is when there are volcanic eruptions and its devastating impact on building roofs when it is not resilient to withstand the volcanic ash effect., hence, the contribution to knowledge for this research.

2.11.1 Volcanic Eruption on Canary Island of La Palma, Spain



Figure 2.9: A house covered by ash from a volcano as it erupts on Canary Island of La Palma, Spain.

Source: <https://eu.usatoday.com/picture-gallery/news/world/2021/09/20/volcano-spains-canary-island-la-palma-erupts/5788176001/>

Figure 2.9 above shows a house covered by ash from a volcano as it erupts on the Canary Island of La Palma, Spain, on Saturday, Oct. 30, 2021. An erupting volcano on the Spanish island of

La Palma continued to emit vast amounts of magma, gases and ash on Saturday, after days of intense seismic activity and more than five weeks since it erupted. The building is covered in a lot of ash deposition, and it is very dangerous to inhabit. The image may imply that all of the inhabitant's lands and the roofs of buildings within the volcanic prone areas are covered with volcanic ash and some dangers to buildings.



Figure 2.10: People looking towards an erupting volcano from El Paso on the Canary Island of La Palma

Source: <https://eu.usatoday.com/picture-gallery/news/world/2021/09/20/volcano-spains-canary-island-la-palma-erupts/5788176001/>

Figure 2.10 above shows people looking toward an erupting volcano from El Paso on the Canary Island of La Palma, Spain, Saturday, 23rd October, 2021. Lava flows have damaged or

destroyed over 2,100 buildings, mostly houses and farms, and displaced 7,500 residents. Authorities warn that the volcano is showing no signs of stopping.



Figure 2.11: *People cleaning up the ash off a house from the volcano in Las Manchas on the Canary Island of La Palma, Spain*

Source: <https://eu.usatoday.com/picture-gallery/news/world/2021/09/20/volcano-spains-canary-island-la-palma-erupts/5788176001/>

Figure 2.11 above shows people cleaning up the ash off a house from the volcano in Las Manchas on the Canary Island of La Palma, Spain, on Thursday, 14th October, 2021. Hundreds of people in Spain's Canary Islands are fearing for homes and property after a new lava stream

from an erupting volcano threatened to engulf another neighbourhood on the island of La Palma. As seen in Figure 2.11. should there be prolonged loading of the volcanic ash on the roof will mean an increase in the pressure on the roof and its subsequent deformation and stress levels, leading to the roof's collapse. Therefore, the need for the roof of buildings to be consistently cleaned to avoid the collapse of the roofs.

2.12 Current Research Contributions

Several investigations of volcanoes carried out in the past are currently being pursued, as Heiken (2013) points out. He explains that there has been an advance in technology that may have improved the scientists' tools and predictive capabilities. Still, the difficulty of adequately informing the public about a volcano's behaviour and the risks it represents continues to be a major challenge. The research suggested some of these challenges, including buildings' Safety and resilience before and during an eruption. Henkin (2013), since the initial eruption of Mount St. Helens in 1980, volcanologists' capabilities for monitoring eruptions have grown at least one hundred-fold. Developing technology has improved the equipment used to monitor volcanoes. Volcanology is now considered by many to be its discipline, drawing on learning from many research and practice areas (Thomas, 2007; Barclay et al., 2008; Donovan, 2010; Johnston, 2012).

The European Joint research centre (EJRC) for the European Union has the following regulation, as stated below:

- Elaboration of maps for climatic and seismic actions for structural design with the Eurocodes.
- EJRC Scientific and Policy Report: Eurocodes: Background & Applications. Design of Steel Buildings.

- EJRC Scientific and Policy Report: Eurocodes: Structural Fire Design -Scientific and Policy Report:
- Eurocodes 2: Design of Concrete Buildings.
- EJRC Report: Eurocodes 7: Geotechnical Design.
- EJRC Report: Eurocodes 8: Seismic Design of Buildings.

The research agrees with the statement made by these authors, and it is quite intriguing that with all the research on volcanoes, very little progress has been made in developing safety regulations over the years. The researcher believes that there are still several research areas to explore to overcome the impact of volcanoes upon human settlements in these active zones.

It has been established that volcanoes can have various devastating effects on human settlement along the flanks and within reach of volcanic eruption zones, even to the extent that these natural occurrences can impact countries with no volcanoes. Wilson et al., (2011) argued that the world's population of about nine percent lives near a 100 km of a historically active volcano (Horwell and Baxter, 2006).

A vivid effect of the volcanic ash is shown in Figure 2.5. The volcanic ash grain sizes (2015) were more than 100mm, leading to high loading on a building and damage to the building's structural elements. The consideration by these authors was based on the roof and the gutters. Understanding how the volcanic ash fall impact and its behaviour on the roof are very important for the study and will shape the EN 1991, with the thought of the volcanic ash within the volcanic prone areas in Europe, determining the Safety and resilience of roofs. The distribution is very important because this will help the study explore the impact of volcanoes on buildings within the prone areas.



Figure 2.12: Effects of Volcanic Deposition on A Roof

Source: (https://volcanoes.usgs.gov/vsc/images/image_mgr/3200-299/img3254.jpg)

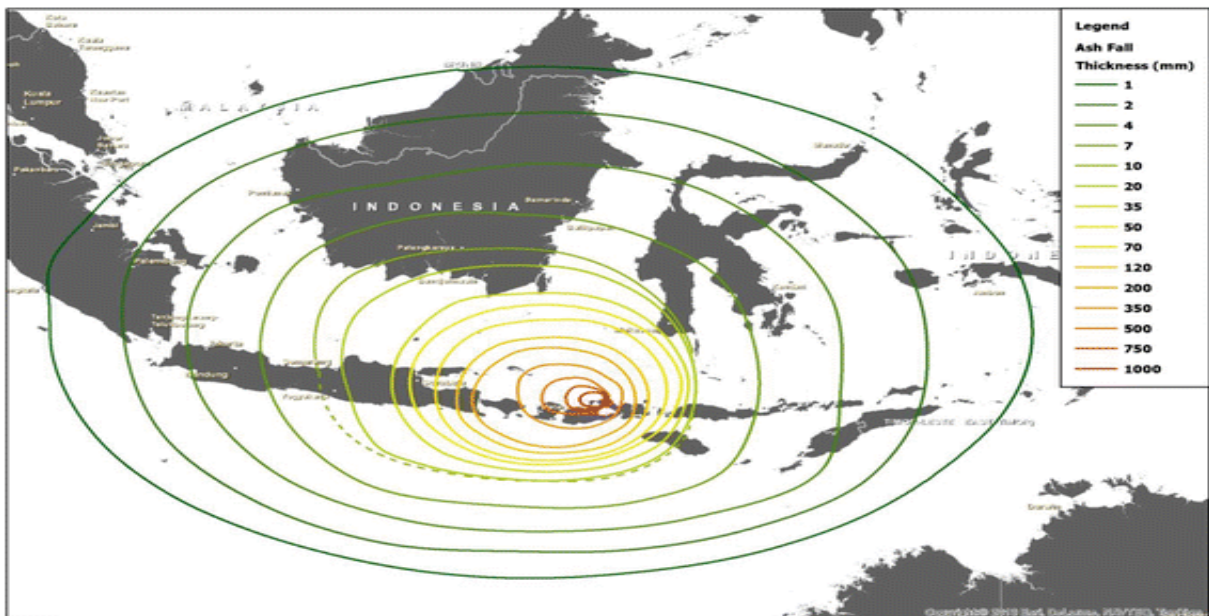


Figure 2.13: Isopach

Source: Blong, et al., 2017.

Ashfall from the 1815 VEI 7 eruption of Tambora is based on Kandlbauer and Sparks (2013) and, to a lesser extent, the Isopach of Self et al. (1984). Additional Isopach and a 2 and 35 mm (inclusive), 70 and 120 mm, 350 mm, beyond the southern portion of the 10 mm Isopach, have been interpolated by eye. For their calculations, a constant thickness of ash is assumed to have fallen between isopachs, equivalent to the bounding Isopach's smallest thickness, showing the total land area between each Isopach pair in the Figure. 2.11. for example, the total number of buildings experiencing each ash fall thickness is five times more than the land area (five buildings per square kilometer).

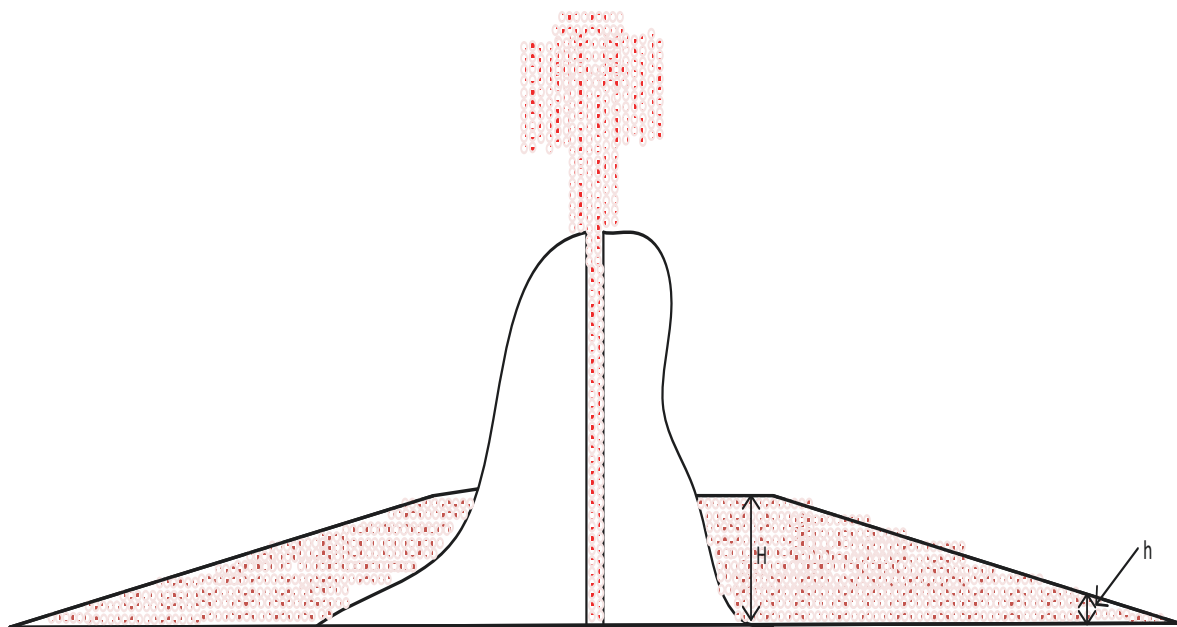


Figure 2.14: Effects of volcanic ash deposition on the flanks of the volcano.

Note: The further away of settlements away from the vent shows the lesser the deposition of the volcanic ash.

It is clear from Figure 2.12 that, buildings further away from the volcanoes' vent will experience less deposition of the ash compared to those buildings nearer to the vent of the volcanic eruption site. Volcanic ash is the material produced by explosive volcanic eruptions (< 2 mm) in diameter. Fine ash is (< 0.063 mm); coarse ash is between (0.063- 2 mm). Volcanic ash comprises various vitric (glassy, non-crystalline), crystalline and lithic (non-magmatic) particles. The density of specific particles may vary between 700- 1200 (kgm^{-3}) for pumice, (2350-2450 kgm^{-3}) for glass shards, (2700-3300 kgm^{-3}) for crystals and 2600-3200 (kgm^{-3}) for lithic particles. Since coarser and denser particles are placed close to the source, fine glass and pumice debris are relatively enriched in ashfall deposits at distal locations (Shiple and Sarna-Wojcicki, 1982). These natural occurrences of volcanoes can have devastating effects on human settlements within the volcanoes' reaches and beyond, with far consequences to buildings within the prone areas and beyond.

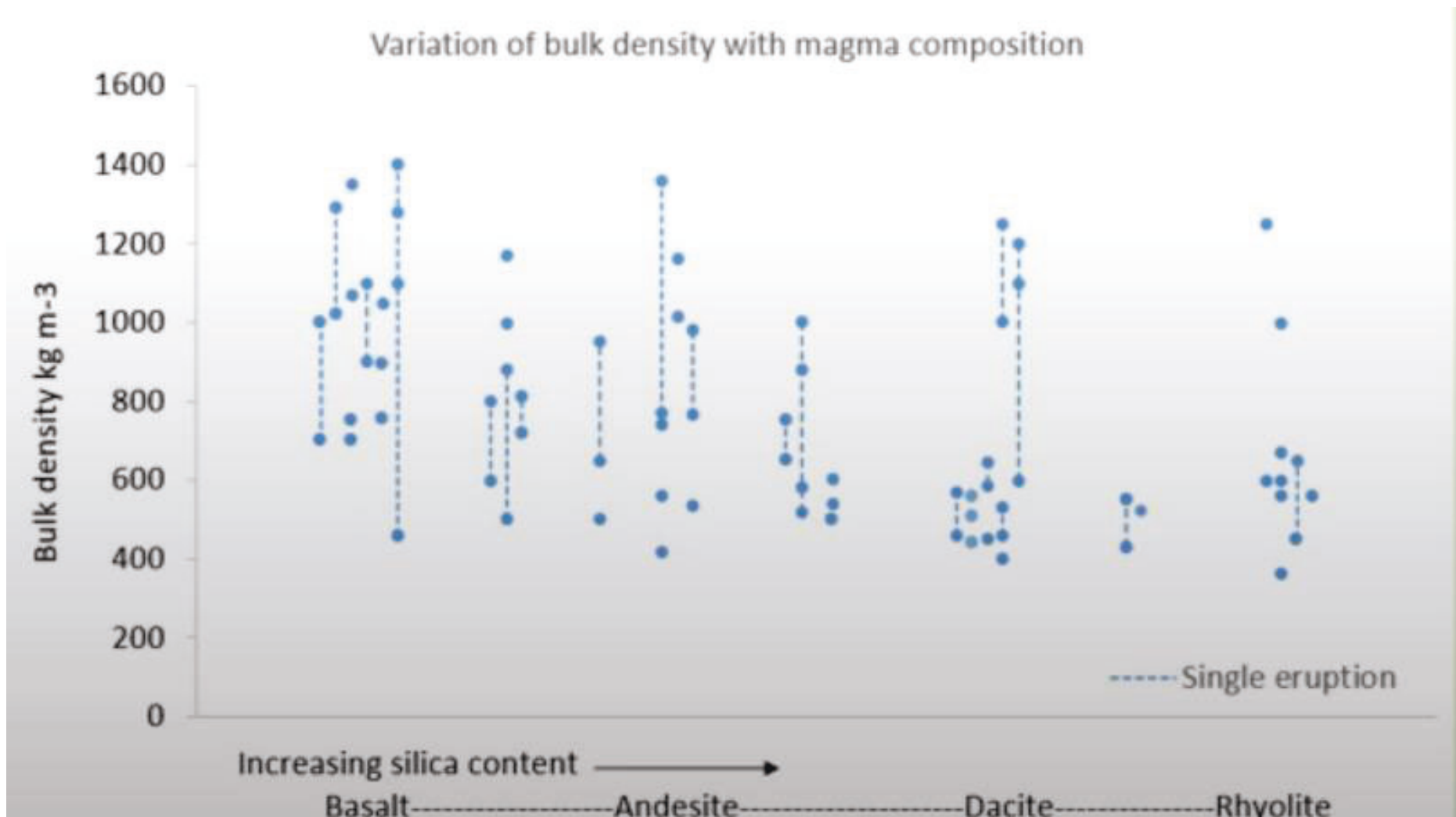


Figure 2.15: Variation of Bulk Density with Magma Composition

Source: Osman et al., @ VMSG21.

The figure illustrates the bulk density (kgm^{-3}) for a single eruption such as Basalt, Andesite, Dacite and Rhyolite for the increasing silica (SiO_2) content during a single eruption. That means that when the silica (SiO_2) level is lower, the magma and magnesium composition's density will be higher, and the weight of the volcanic ash particle (density) be high. However, if the silica (SiO_2) level is high, then the magma and magnesium composition's density will be lower, and the volcanic ash particle (density) will be lower. That is very important because figure 2.9 specifies the various bulk density for a single eruption.

2.13 Composition and Properties of Some Roofing Materials

More than (60–70%) of the building surface is covered by roof covering? Therefore, any action meant to humanising the interface between covering and climate concerning the need for comfort and affordability turns out to be particularly effective (D'Orazio et al., 2010). Across Spain, over 26 million tonnes of clay bricks, roof tiles, blocks, and other such clay building products are manufactured yearly (Sánchez et al., 2010). These discarded clay materials do not affect the clay products' properties (Sánchez et al., 2010). Below are some properties of materials that will be considered for the laboratory experiments.

Table 2.19: Chemical Composition

Majority constituent (%)	Waste Fired Clay Material
SiO_2	67.03
Al_2O_3	19.95
Fe_2O_3	6.29
CaO	0.11
MgO	1.37
Na_2O	0.21
K_2O	3.54
SO_3	0.79
LOI	0.47
$\text{SiO}_2+\text{Al}_2\text{O}_3+\text{Fe}_2\text{O}_3$	93.27

Source: (Sánchez et al., 2010)

Several types of research were carried out on the roofs of buildings in Europe, such as roof covering on the thermal performance of highly insulated roofs in the Mediterranean climate by D'Orezio et al. (2010). Some authors focused on covering insulation on the roof's thermal performance in summer by analysing experimental data from monitoring full-scale mock-ups in Italy (D'Orito et al., 2010).

There has been some investigation done recently by William et al., (2019) for the Tephra cushioning of ballistic impacts on the roof of buildings closer to a volcanic site's vent. They went further to state that, in the 2014 Ontak volcanic eruption, at least 58 people lost their lives due to damage impacted by ballistic to their roofs.

William et al., (2015) studied a practical simulation test where volcano rocks were launched towards clay tiles and reinforced concrete slabs using a pneumatic cannon in laboratory settings. That enables the study to compare the impact of energies and building response. There was a consideration, the target of either directly impacted by rocks or covered with a layer of Tephra before shootings.

The particle size considered was approximately non-spherical thick and, according to William et al. (2017) approximately tripling the penetration threshold of both building materials (reinforce concrete and clay tiles).

The study currently done is different for the sizes from 1(mm), 5 (mm), and 10 (mm) in diameter, which is different from the sizes used by William et al., (2019). The current study's simulation is to get the volcanic ash particles settled on the roof and their behaviour on the roof in terms of its movement, stress, deflection, or deformation. It will achieve through laboratory

simulation using EDEM-Fluent coupling. The particle used for this simulation is less fine than that of William et al. (2019), and this will help with the effect of volcanoes on the building near the vents, which will contribute to knowledge in the field of research.

William et al., (2017) use field data for their studies and explained that “our fragility functions and field studies show that, although unreinforced buildings are highly vulnerable to large ballistic (720 cm diameter) they can still provide shelter on preventing death during eruptions. This statement explains the importance of buildings further away from volcanic vents and the effects of the fine volcanic ash particles that settle on the building, leading to the collapse and death of people living in it. That will help designers make adjustments to buildings' design in volcanic prop areas in Europe and elsewhere.

Though William et al., (2019) used (10-20 cm), thick layers of tephra building material were even more resistant to damage. They did explain that load material on roofs does increase their chance of collapse, but based on previous research, the relatively light load exerted by the 5cm layer of Tephra is likely to have a reliable effect on roof collapse, probably at least for engineered structured in good condition. The question is, are all buildings in the prone areas built with engineering structure conditions?

In their experiment, they did consider two different roofs covering such as copper and tile covering. The type of roof used for the experiment was the pitched roof with the following feature such OSB board (0.05 m), insulation (EPS 0.12 m), fir wood (0.05 m), ventilation duct (0.06 m) (D'Orito et al., 2009). This research approach to computer simulation could be adapted especially for the study.

There was a random categorisation of various injuries and deaths sustained as a result of the Ontak eruption. They explained that sheltered people in unreinforced timber frame buildings were not injured, but those outside were struck and killed by ballet rocks from the eruption (Yamada et al., 2018). However, those sheltered in the timber cladding summit station sustained 19 damaging impacts, 5 of which resulted in penetration of the roof, without death or injuries.

There has been evidence in previous research that suggests that a heavy load of volcanic ash on the building can significantly damage buildings' roofs, leading to injuries to people habiting the buildings. The study's view is to help buildings within the volcanic-prone areas in Europe be more resilient to the effects of volcanoes. The European buildings were designed considering the effects of volcanic ash on buildings' roofs within the prone areas in Europe.

Another concern envisages by these volcanoes' effects ash's impact on buildings within the volcanic areas. During an eruption, most buildings would be exposed to the volcanic ash load will lead cause structure damage (Hampton et al., 2015). However, a prolonged eruption of volcanic ash on a building could have severe detrimental consequences on the building's roof.

Muzeau et al. (2010) stated that “the past 500 years, over 200,000 people have lost their lives due to volcanic eruptions.”Mazzolani, (2019). Talked about the impacts of pyroclastic density currents on buildings during the eruption of the Soufrière Hills volcano, Montserrat. The damage to building within the volcanic prone areas are due to ashfall, which occurs when the ash load exceeds the strength of either the roof supporting structures or material used to cover the structure (Muzeau et al., 2010)

On the other hand, Hampton et al., (2015) stated that ash fall thickness typically decreases exponentially with distance from the eruption source. Williams et al., (2017) experiments provide new insights by quantifying the hazard associated with post-impact shrapnel from building and rock fragments, the effect of impact obliquity on damage and the additional impact resistance buildings possess when claddings are struck in areas directly supported by framing components. That was not well identified in previous work, which may have underestimated building vulnerability to ballistic hazards. The above table illustrates the various researches for Tephra fall for roof gutters in different parts of the world. Previous studies (Johnston, 1997; Spence et al., 1996; Blong, 2003; Spence et al.2005; Macedonio and Costa, 2012; Pomonis et al., 1999) have shown that ash loads of (1–10 KPa) are required to induce structural failure, dependent on building class/type (Jenkins et al., 2014). Theoretical fragility functions for ash-loading roof collapse developed for European roof classes suggest (2–8 KPa) of ash loading is required before the collapse. It is dependent on roof strength (Spence et al., 2005). Spence et al., (2005) experimented with using the Static load of an ash deposit as the primary hazard intensity measure used to assess the probability of damage or loss when assessing the risk of building damage from ashfall (Spence et al., 2005). Static load from ash accumulation was calculated using the formula as;

$$LAF = \rho gh \quad (2-1)$$

Where LAF is ash load in Pascal (Pa; more commonly reported as KPa; referred to as ash load in this paper), ρ is the ash density (kgm^{-3}), g is the gravitational acceleration (9.81 m/s^2), and the ash thickness (Jenkins et al., 2014).

The study will consider the revision of the EN1991 regarding the roof building code within the volcanic-prone areas to address these gaps. This study will use the laboratory simulation exploration to unearth the means to make roofs of buildings in volcanic prone areas safe and resilient, using the finite element (COMSOL) FEM and the discrete element method.

The research will adopt some of the methodology used by some authors (D'Orito et al., 2009; Hampton et al., 2015). The roofing materials considered by these two authors are tiles, copper, and shingle corrugated sheet for the pitched roof. The dry and the wet volcanic ash will be investigated on the pitched roof using variable angles from 15° - 45 °. On the other hand, the research will explore the event where there will be an occurrence of both the snow and the volcanic ash occurring simultaneously.

On the other hand, the static approach will consider the volcanic ash's frictional force on the roof and the roofing materials for both the dry and wet volcanic ash for both static and dynamic approaches. It will help determine the stress on the roof. The investigation outcome will revise the European roofing code (EN1991) within volcanic-prone areas. *Adaption:* Consideration from (D'Orito et al., 2009) includes the building surface area of 80 m² in one level (8 m × 10 m). Two pitches formed the roof, one (10 m long and 6.4 m wide) exposed roof was formed by two pitches, one (10 m long and 6.4 m wide) exposed to the south and the other one (10 m × 3.4 m) to the north, each pitch is divided into 6 types of roofs. And all the buildings were built according to the Italian construction with insulation and ventilation.

Adaption: from Hampton et al., 2015, the challenge for their experiment was the volcanic ash's adaption with similar properties because of the real volcanic ash. Though this may not impact the real result, on the other hand, it would have been better to use real volcanic ash throughout

the study. The consideration from Hampton et al., 2015 will be the variation of the roof pitch from 15° - 45 ° with the different roofing materials. This roof was constructed regarding New Zealand (NZ) building code standard (NZ 3604). They used the design and construction of timber-framed building up to three-story high; the roof materials used were galvanised corrugated roofing Iron (metal sheet) (Hampton et al.,2015).

Modelling: The model for the flat concrete roof will and the pitched roof with a variable angle of inclination will illustrate below. Figure 2.10 illustrates the modelling part in more detail, carried out in both 2D and 3D. Simulations will involve a roof building of varying inclination angles with different roofing materials (structural integrity) to be adopted for the experimental simulations.

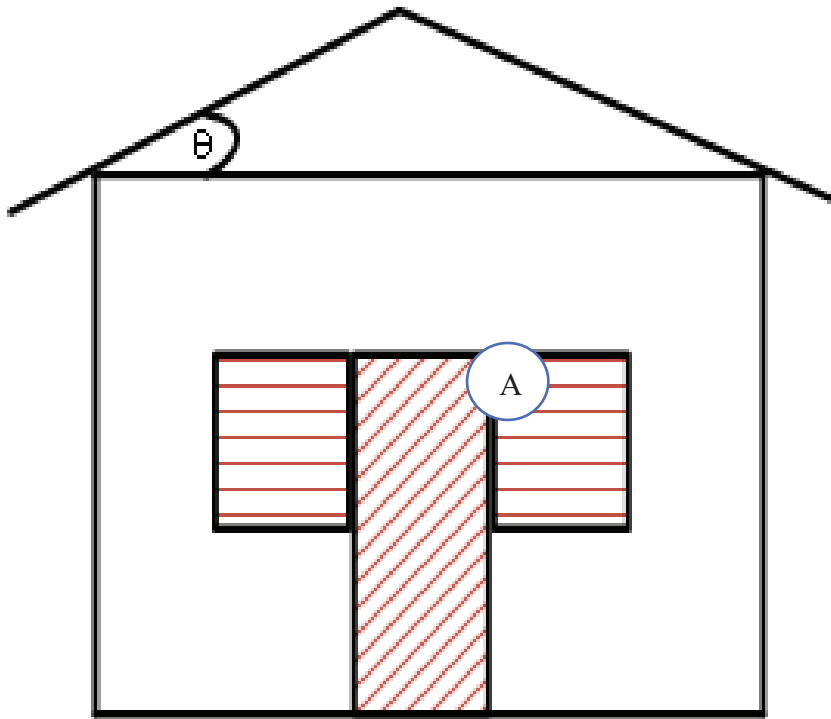


Figure 2.16: Two-Dimensional Models

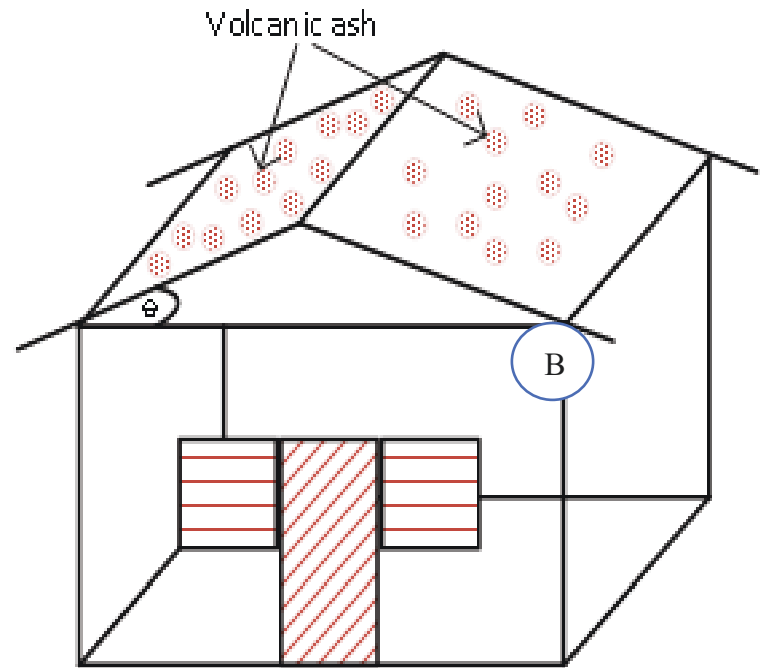


Figure 2.17: Three-Dimensional Models

Figure 2.16: two (A) and Figure 2.17 two (B): are two and three-dimensional models (B) of the roof loading problem to be investigated for different types of roof buildings of varying sizes with different roofing materials to assess the resilience of the roof against volcanic ash. The derived formula below from Static load ash accumulation was calculated using the formula as $L_{AF} = \rho gh$, (Spence et al., 2005) Where L_{AF} is ash load in Pascals (Pa; more commonly reported as $\text{Pa} / \text{N/m}^2$; referred to as ash load in this paper), ρ is the ash density (kgm^{-3}), g is the gravitational acceleration (9.81 m/s^2), and the ash thickness (Jenkins et al., 2014). Figure 2.16 shows the derivation of pressure exerted upon an inclined roof. $L_{AF} = \rho gh$, (Spence et al., 2005)

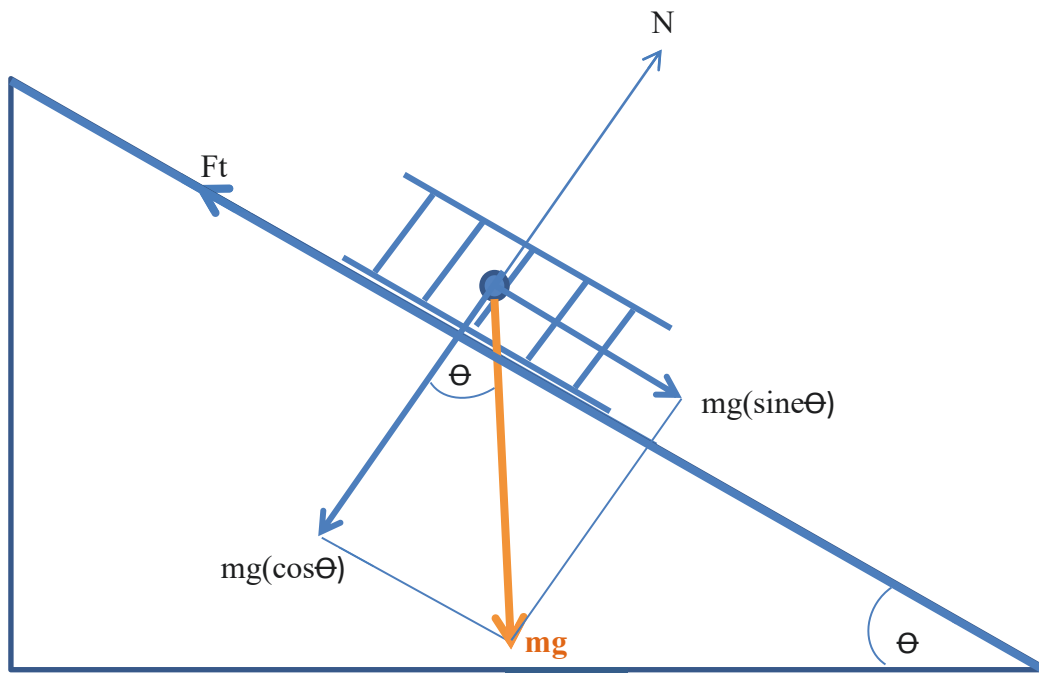


Figure 2.18: Model Representation

$$F_{\text{net}} = ma \tag{2-2}$$

Note:

$$\rho = m/V$$

$$V = Ah$$

$$F_t = \mu N \quad (2-3)$$

$$N = mg \cos \theta$$

This implies that

$$F_t = \mu mg \cos \theta = \mu \rho g V \cos \theta$$

Equation of motion:

$$F_{\text{net}} = \rho g V \sin \theta - F_t \quad (2-4)$$

$$= \rho g Ah \sin \theta - F_t$$

$$ma = \rho g Ah [\sin \theta - \mu \cos \theta]$$

For static equilibrium (or motion at constant speed)

$$0 = \rho g Ah [\sin \theta - \mu \cos \theta] \quad (2-5)$$

For dynamic motion

$$ma = \rho g Ah [\sin \theta - \mu \cos \theta] \quad (2-6)$$

$$\rho A ha = \rho Ahg [\sin \theta - \mu \cos \theta]$$

$$a = g [\sin \theta - \mu \cos \theta] \quad (2-7)$$

$$\text{Pressure} = F/A = \{\rho g Ah [\sin \theta - \mu \cos \theta]\}/A$$

$$\text{Pressure} = \rho g Ah \cos \theta / A = \rho gh \cos \theta \quad (2-8)$$

Where:

μ - is-coefficient friction

ρ - is the ash density (kg/m^3)

g - is the gravitational acceleration (9.81 m/s^2)

h - is the ash thickness (m)

v - is the volume of ash

A - is the Area

F_t - is the frictional force

N - is the normal force

m - is the mass of ash.

Θ - is the angle of the plane

Figure 2.17 shows the weight management's resolution in the normal direction to the roof surface and parallel direction to the roof surface. The above formula was from previous research will help with the numerical simulations that will be used to quantify the effect of volcanic ash on the building roof with a focus on key structural variables including pitch and variable angle of inclination to determine the frictional force of the volcanic ash, in both static and dynamic modes. Results will allow quantification of the resilience of roof design against volcanic ash deposition.

That will help the researcher to determine stress. Similarly, the European code EN 1991 did consider the snow load effects on building roofs, and the research intends to propose including the ash load in the code. There are references in the literature that suggest most of the death tolls are because of the roof's collapse during a volcanic eruption. Please refer to appendix A. Spence et al. (2005) explain that new studies undertook the roof strengths in the area around Mt. Vesuvius in southern Italy. Also, undertook field surveys in other European volcanic

locations to assess building vulnerability tephra fall. Spencer's statement may suggest that some work has been done recently in Vesuvius in southern Italy to assess building vulnerability to Tephra fall. The research will explore knowledge that will help shape the current research on the European regulation for volcanic prone areas.

Volcanic ash will be considered; impacts on the roof will help formulate roof building regulation revision. It will take into consideration the effects as shown in figure 2.10 and figure 2.11 showing volcanic ash fall accumulation and pitched roofs from empirical laboratory experiments: The research expectations to develop an argument that the roof is not the only cause of failure within the fabric of the building within the volcanic prone areas. The type of eruption will determine the type of effects on building in the volcanic-prone areas. This study's aspect is the current edition of the Objectives and will require more instigation in the knowledge base in other literature.

According to damage resulting from the impact of pyroclastic flows on buildings, several factors are combined: the duration of the phenomenon, the temperature of the flow, and the pressure produced by the impact (Zuccaro, 2010 ad). Wet tephra is known to have a greater load than dry tephra, and various observations from historical volcanic eruptions in the 20th Century have shown critical variable thicknesses of tephra under which roofs have collapsed.

2.14 Cases study Areas

As revealed above, volcanoes' problems can be addressed and solved, resulting in improvements that can be observed globally. Therefore, adopting solutions to building codes and health and safety problems in one country may be adapted to other countries to improve their building codes further. The research will investigate buildings' roofs' safety and resilience

in the two case study areas within Europe in Etna, Italy, and the second in Iceland. These are among the volcanic hotspots in the world. The study will investigate the building types in Italy and Iceland, especially within the case study areas.

It is clear that the research's focus is based in Europe; however, it is essential to make a comparative exploration to ascertain whether the findings for Etna in Italy concerning volcanoes Safety can apply resilience to another European country. The first case study will investigate the types of building in Italy, especially within the case study areas in Etna. The study needs to elaborate on the history of volcanic activities within the case study area. It will expound on the knowledge of volcanic activities within the regions of the case study areas. It will throw light on how the eruption impacted people living within the volcanic regions in Etna, how they behave during and after an eruption etc. That will have a positive impact on the research. In the research of Heap et al., (2013), Mt, Etna (Italy), the largest volcanic edifice in Europe (40 km wide and standing 3.3 km above sea level), was a case study. Their main reason was that the Mt. Etna volcano represents an ideal candidate for study. Firstly, Mt. Etna is one of the most intensively monitored volcanoes on earth (Heap et al., 2013). However, over the last 20 years, new technological developments and denser monitoring networks at Mt. Etna have provided one of the highest quality logical, geophysical, and geochemical datasets available for any volcano in the world (Bonaccorso, 2004; Acocella and Puglisi, 2012). Figure 2.17 below is the Location of Mt Etna in Italy: Sketch map of southern Italy showing Noto and Matera two plates (i.e. the Eurasian plate and the African plate) the eruption of volcanoes most appropriate for this research. The volcano Mt Etna sits on the radio telescopes location (triangle) and their baseline (continuous line) east coast of Sicily, Italy. It is set between Messina and Catania's cities and lies between the convergent plate margin between the African Plate and the Eurasian Plate.

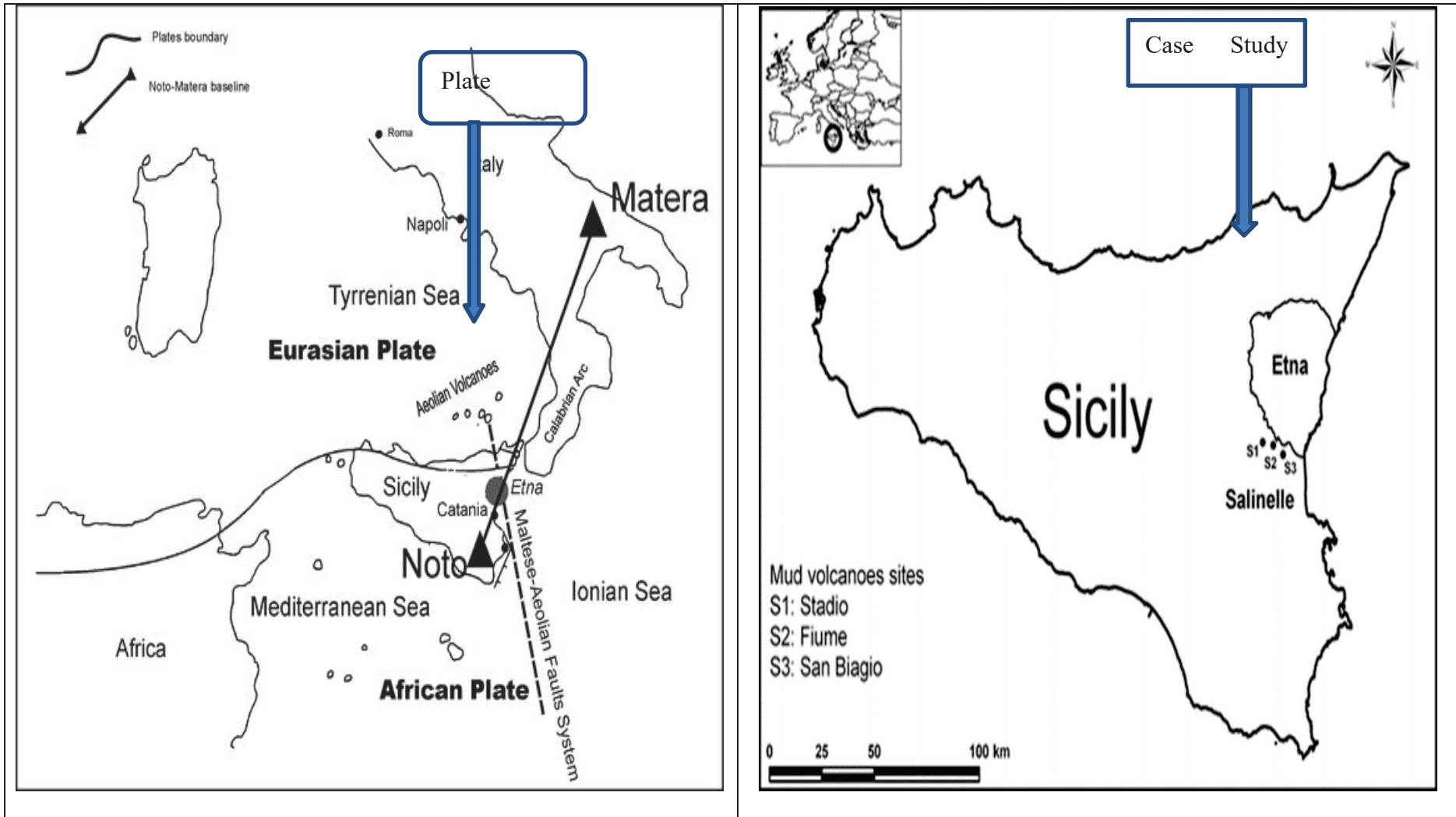


Figure 2.19: Mt Etna Location in Italy: Showing Noto and Matera

2.14.1 Mt Etna Volcano Eruption in Italy:

Table 2.20: European Cities near Active or Potentially Active Volcanoes

<i>Note:</i> There has been a lot of volcanic eruptions in Mt. Etna since it is among the world's most active volcanic prone spots and in Europe.		
City, Country	Population (2006/2007 estimates)	LASR Significant Eruptions By Nearby Volcano(s)
Roma, Italy	2,705,603	3,500years ago
Catania, Italy	301,564	Active Now+Historic
Napoli, Italy	975,139	1944+Historic
Torre del Greco	88,918	1944+Historic

Source: (Heiken, 2013)

Heiken (2013) listed the volcanic regions in the world, as indicated above, but for this research, the researchers extrapolated the data related to Italy to debate the importance of the region of Etna. As mentioned earlier, Etna is among one of the most active volcanoes in the world, and different authors have proved this. It is very important to note the population as 2006/2007, according to Heiken (2013), will have increased by 2017 to more than 301,564, which is a significant indicator for the research.

By contrast, Gino et al. (2010) further explain that Etna in Sicily is continuously active. Frequently, its eruptions affect populated areas or cultivated land, and the chances of one or more highly disruptive events are important in the next few years or decades. Many authors suggest that Mt Etna is among the world's most active volcanic spots in the world. Other authors such as Corsaro et al. (2009) argue that Mount Etna, the most active volcano in Europe, is a large (40 km wide and 3.3 km high) basaltic stratovolcano that has been built since 0.5 Ma in

eastern Sicily, at the junction of tensional tectonic fractures that cut the locally 20 km thick African continental margin. La Delfa et al. (2012) describe the located Mt. Etna as a volcano in eastern Sicily, in a zone in which the African and Eurasian plates converge (McKenzie, 1972; Argus et al., 1989).

2.14.1.1 Types of Eruption in Mt Etna Region in Italy

There are different types of volcanic eruptions in the Mt Etna region and exploring these eruptions will be very important for the research. The study will investigate the impact of volcanic activities on buildings in the Etna region and how best these can help shape the revision of the European building roofs Regulation. It will help the research probe into how the type of eruption may impact buildings and how safe and resilient the buildings are in the Mt Etna region.

2.14.1.2 Reasons and Benefits of living in Mt Etna Volcanic Region

In every endeavour, there are bound to be the benefit and threats of every natural activity. That will not be different from volcanic activities that have taken lives and properties, yet people live near volcanic active prone areas. Branca et al. (2013) argued that "today most settlements in the Etna region contain large numbers of traditionally constructed houses, public buildings and churches that do not comply with contemporary building codes, which have only been enforced at the community level of administration since 1981". There are various reasons people live near volcanic prone areas, and these reasons are not different from other parts of the world. The Benefits Later employment diversity occurred in the region. Much of the stone used in re-building came from quarries located on the 1669 lava. Farmers found alternative employment in pastoralism as wage labourers and working plots of land located outside the worst affected area (Chester et al., 2010).

2.14.1.3 Effect of Volcanoes in Mt Etna Region

Mt Etna poses a significant challenge to the inhabitants of Sicily, Messina and the Catania region along the base and flanks of the volcanic mountain regarding a variety of volcanic hazards.

Scollo et al. (2012) explained that reducing hazards may be accomplished using remote sensing techniques to evaluate volcanic plumes' important features. Gino et al. (2010) the major hazard related to Etna's eruptions is from lava flows and effecting land and property (Behncke et al., 2005; Bisson et al., 2009)

Gino et al. (2010) argue that the major hazard related to Etnas eruptions is lava movement invading and destroying land and property (Behncke et al., 2005; Bisson et al., 2009). Andronico et al., (2015) argue that hazard from tephra fallout mainly impacts aviation operations and road traffic, while minor damage affects crops and roofing (Barnard, 2004; Scollo et al., 2013). Fortunately, serious injuries are not common (Branca et al., 2015). Apart from Nicolosi, effectively masked, much of the damage attributed to buildings by volcanic earthquakes was because lava flows quickly covered most of the settlements affected. Vulnerability to volcanic earthquakes of traditional buildings, which are often constructed of rubblestone, remains a serious concern.

Per Bonanno et al., (2012) stated the type of flow trace element effect was assessed using mosses in a densely local d area affected by mud volcanoes. Such volcanoes, locally called Salinelle, are phenomena that occur around Mt. Etna (Sicily, Italy) and are interpreted as the surface outflow of a hydrothermal system located below Mt. Etna, releasing sedimentary fluids (hydrocarbons and NaCl brines) along with magmatic gases (mainly CO₂ and He). To date,

scarce data are available about the presence of trace elements, and no biomonitoring campaigns are reported about the cumulative effects of such emissions. Bonanno et al., (2012) showed that natural phenomena such as mud volcanoes might release emissions with significant trace elements concentrations, potentially hazardous in densely inhabited areas.

To develop a revision by incorporating volcanic ash activity into European, regional and local building roof regulations in volcanic prone areas.

2.14.2 Iceland

Volcanism in Iceland is remarkably assorted for an oceanic island because of special geological and climatological conditions. It structures nearly all volcano types and outbreak styles known on Earth (Thordarson and Larsen, 2007). There are many volcano spots in Iceland, and some are Eyjafjallajökull (Iceland) is located on (63.63°N, 19.62°W), and (1666 m a.s.l). In 2010 Eyjafjallajökull volcano erupted to a height of 8km maximum, releasing ash plumes of heights exceeding 8 km above sea level. That was thought to be a moderate eruption; however, it had a great deal of impact on aviation and countries such as Great Britain, Scandinavia and Central Europe, forcing the closure of most of the European airspace. The wind direction helped release fine volcanic ash diameter of less than about ($5.3 \cdot 10^{-3}$ cm) (Langmann et al., 2012). The Askja central volcano located in the North Volcanic Zone of Iceland, a zone which is extending at ~ 2 (cm) /year in a $\sim N 105^\circ$ direction, belongs to the Askja volcanic system (Thordarson and Larsen, 2007; Perlt et al., 2008; DeMets et al., 2010). The Askja volcano has produced more than 175 eruptions (both effusive and explosive) during the last (7 KPa), more than (50 KPa), of which occurred in historical times (Hartley et al., 2016) Trippanera et al., (2018) stated that “bout half (24) happened inside the Askja caldera, with most of the remainder located on the flanks of the central volcano or the fissure swarm at the foot of the massif.”

Furthermore, they explained that “Small basaltic eruptions, associated with the formation of scoria cones and emplacement of lava flows, took place between 1921 and 1929 along the rim of the Öskjuvatn caldera” (Trippanera et al., 2018). Figure 2.1., as abstracted by Trippanera et al. (2018), shows some of Iceland's various volcanic spots.

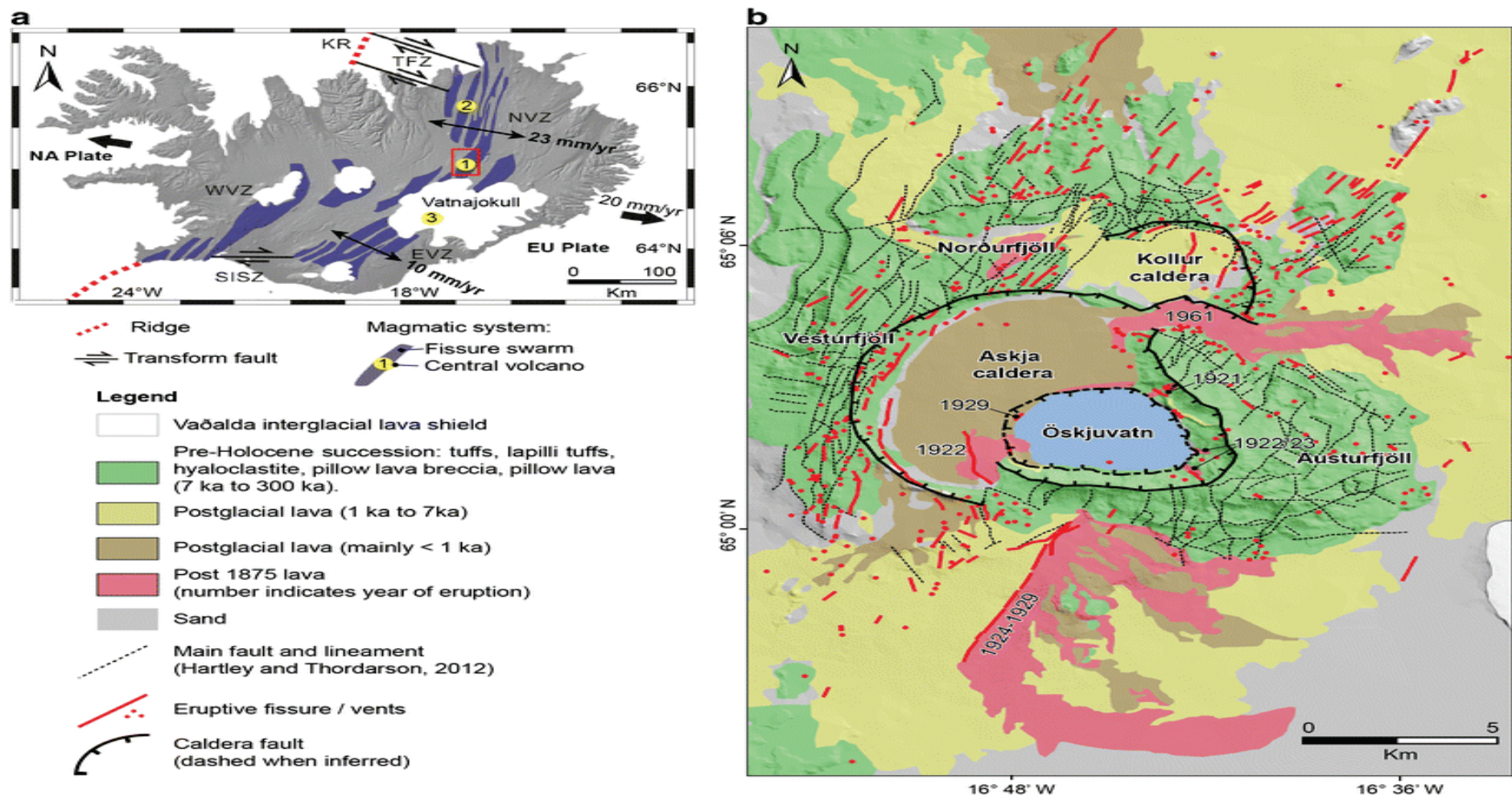


Figure 2.20: A Map of Iceland and its Volcanic Zones with the Locations

Note: The case for the choice of Mt. Etna in Italy and Iceland is presented in Table 2.8 below.

Table 2.21: The Comparison For The Two Case Study Areas

Comparison	Mt. Etna in Italy	Iceland
Geographical Location	Europe	Europe
Setting	Urban Volcanic Observatory station	Urban Volcanic Observatory station
Types of Volcanic Eruption	Tephra fall deposits, both summit and flank eruptions	pyroclastic flows, lahars magma
Ash	Much ash	Less ash
Viscosity	High viscosity	Low viscosity
Volcanic Activity	Frequent Active	Active

2.15 Material Parameter and Particle Size

Zhoe et al. (2016) set the simulation ton that involved DEM/FEM co-simulation for the snow methodology experiment for the density at 30 (kgm^{-3}). The approach will guide the study for the research Poisson ratio of the snow particle was set at 0.25. This study will consider the volcanic ash particles' various density at 1000 (kgm^{-3}), 2000 (kgm^{-3}), 3000 (kgm^{-3}), respectively. The poison ratio of the volcanic ash particles will be set at 0.15. Hobbs et al. (1991) assumed the volcanic ash particle to be 2300 (kgm^{-3}) (which is suitable for the Rhyolite glass) depending on the ash's size. The variable density will help to study the compare the results will be variable ash size particles. The variable volcanic ash particles suggested for the study are 1 (mm), 5 (mm), and 10 (mm) size particles. Saxby et al. (2018) described "the vertical air velocity is mostly on the order of ± 0.001 to $\pm 0.1\text{ms}^{-1}$ with extremes around ± 1 (where \pm refers to up/ down). They explained that the vertical velocities at altitude miss leading to considering the root change concerning the ground level. They explained that the coordinate

system would give a false impression of the terrain effects, considering the vertical velocities by considering the sea level.

2.16 Volcanic Ash Loadings

The importance of the study is to get the volcanic ash on the roof. The loading of the volcanic ash load will help determine the maximum stress and deformation on the roof. According to Dacre et al. (2013), the volcanic eruption mass deposition will be about 95%. London VAACS PSD default described larger Particles $d=100\mu\text{m}$ could travel very far when the shape is non-spherical (Maryonet et al.,1999). Thus, this researcher was not particular on the distance of the particle travel distance but only considered the volcanic ash's initial velocity in the range of ± 0.001 to $0.1(\text{ms}^{-1})$ as suggested by the vertical air velocity (Saxb2012 et al., 2018). The volcanic ash shape is for spherical and non-spherical sizes such as 1mm, 5mm and 10mm. In their experiment, Bell et al., (2017) used a constant density of $2600(\text{kgm}^{-3})$; the DEM approach for the friction coefficient is of order 0.1- 0.5 will not be suitable for the atom. They explained that there is no smooth transition between atoms macroscopic particles adequately.

2.17 Structural Failures

Studies have been carried out (Spence et al., 2005, Costa 2012) suggested that ash loads of (1- 10 kPa) are required to induce structural failure depending on the ash loading roof's fragility collapsed developed by the European Union roof design. They suggested that (2 -8 kPa) can be required to cause roof collapse. That is dependent on the strength of the roof, according to (Spence et al., 2005, Hampton et al.,2005).

Spence et al., 1996.5 explained that the roof damage in Pinatubo with 150-200(mm) thick of ashfall, only 3 of the 51 buildings (6%) were assessed as light damage meaning only gutter damage with 15 buildings showed no damage (29%) and the remaining 33 buildings showed structure damage (65%). However, the analysis did not include measured actual ash loading on the damaged building. The number of damaged buildings, then the number of damaged roof buildings was very high. Tribilco (1997) stated that the (1995-199) eruption discharged about 5mm thick ash particles that affected thousands of residential homes exposed to less than <5 (mm) of ashfall over 123 homes registered for the claims (90%) related to ash damage to the roofs, 26 had damage caused by ash and 9 which may have been caused by ash. Due to rusting the galvanised sheet (roof flashing or gutters), most claims were very high above the roof. A height great enough for the individual ash particles Hampton et al. (2015) used a sieve hopper for their experiment with the dimension of (0.8 m × 3.0 m) positioned 1.5 (m) above the roof height, great enough for individual ash particles ≤ 1 (mm) to reach the terminal setting velocities. This research adopts this method to incorporate the 1.5 (m) height for the volcanic ash particle's distance to travel from the EDEM simulation factory to settle on the Model plate in the simulation box. (Wilson et al., 2012a: Wilson et al., 2012a: Armienti et al.,1998.

2.18 Building Regulation

There are various kinds of definitions for different Regulations. This research intends to concentrate on Building Regulations.

According to Pilkington (2016), Building Regulations are defined as how a new building or alteration is to be built to be structurally safe, protected from the risk of fire, energy-efficient and has adequate ventilation for its purpose. Pilkington (2016) further states that building

regulation has three purposes; to ensure people's health and safety in and around buildings, to ensure the conservation of energy, and ensure access and facilities for disabled people.

The building portal (2016) defines Building Regulations as minimum standards for design, construction and alterations to virtually every building. They are developed by the government and approved by Parliament. McIver (2014) states that the Building Regulations are the statutory instrument that details the base level of performance for buildings' construction and design. The Building Regulations are supported by Approved Documents, which guide how to achieve compliance. However, the local government and the Department for Communities also state that Building Regulations are set nationally as broad statements of requirements that enable building control bodies to adopt a flexible approach to determining compliance. Wirral (2017) states that Building Regulations set performance standards in designing and constructing buildings, ensuring people's health and safety in and around those buildings. They also incorporate measures to conserve fuel and power and ensure the provision of facilities for disabled people. Appendix A defines the safety and resilience of buildings.

2.18.1 Importance of Building Regulations

Building regulation is a very important mechanism within the built environment. It tends to control the way people must build.

- 1) Flying debris is the major cause of death in tornados. Though the research will not be focusing on tornadoes, volcanoes tend to cause a lot of debris during an eruption, which affects people and leads to the loss of life and properties.
- 2) Therefore, in earthquakes and tornados, death's major cause is structural damage or collapse. On the other hand, in floods, people seek refuge on rooftops of surviving

homes and buildings. Buildings that survive and remain intact during a disaster can preserve lives. This statement reinforces the essence of this research regarding building codes within the volcanic active prone areas. If the building code is not in place, people will build without reference and conformity to safety standards.

The researcher supports the statement by Natalia et al. (2013) that building regulations under the Building Act 1984' are, however, intended to ensure the safety of people in and around buildings; to conserve fuel and power; to reduce carbon emissions; and to ensure the provision of access and facilities for the disabled. The authors also state that it is important that the developers, builders and homeowners fully understand the regulations' implications. Omissions and errors due to non-compliance with the regulations can be unsafe, environmentally damaging and costly. The researcher believes that ensuring people's Safety around buildings must assure the building's resilience against volcanic eruption.

Roger Bilham (2013) further explained that building codes could save lives and reduce structural damage in natural disasters. Bilham continues that 'Man has developed and continues to improve materials and building design features that can withstand many of the forces of natural disasters. Building codes specify the use of these materials and design features to create structures that have resilience to the forces of natural disasters. However, having a building code that incorporates resilient features to disaster forces is only the first of the three steps required for effective building codes. The research agrees with Roger Balham's (2013) statement and reiterates the importance of this research. Bilham (2013) again explains the other two steps as authorities in geographic regions impacted by certain types of natural disasters must adopt building codes that provide resilience to those disaster types as step two. Then, the final step is for the regional authorities to assure enforcement of the codes.

The researcher agrees with these authors (Bilham 2013; Natalia et al., 2013) about building regulations' imperative and importance. This assessment underpins the research's importance with the 'A framework for European regulations to assure Safety and resilience against volcanic activities in new and existing buildings.

The first objective is to identify the geographic distribution of regions within Europe that will benefit from a revision of building regulations to increase buildings resilience against volcanic activities. This objective is very important to the study because it will allow the researcher to investigate the European region countries susceptible to volcanic activities. Concerning section 2.7, both authors (Grant Heiken 2013., Etiope et al., 2007 and Karátson et al.,2017) all spoke about volcanic prone and newly formed volcanic and dead volcanic regions in Europe.

Stefano Branca et al. (2015) argued that settlements in the Etna region contain large numbers of traditionally constructed houses, public buildings and churches that do not comply with contemporary building codes, which have only been enforced by community-level administration since 1981. the researcher is, however, of the view that the statement by Branca et al. (2015) will not be different from the rest of the volcanic-prone countries in the European region. The researcher's question is: what are we going to do regarding traditional traditionally constructed houses, public buildings, and churches that do not comply with contemporary building codes that have only been enforced at the community level of administration since 1981? As part of the research's originality, the research will contribute to this area to explore the framework for building regulation in both the new and existing buildings. The framework will investigate how these traditional buildings in volcanic-prone areas are maintained and remedied to be safe and resilient in these volcanic-prone areas.

Only recently, new regulations to prevent buildings' construction and strike of seismically active faults have been put in place (Azzaro et al., 2010). However, there was not any mention of volcanic code for building in general in the volcanic region. The researcher believes that even if building codes volcanic prone countries, it would be worthwhile to revise the building code for the volcanic-prone region in Europe. This revision would help increase the safety and resilience of buildings within volcanic-prone regions. The new regulation in reference is to (Azzaro et al. 2010) is to prevent the buildings along strike of seismically active faults, and not building code for safety and resilience in the construction of building in the volcanic prone.

2.19 European Building Codes

For the research, the researcher will summarise the various segments of the European building codes and compared them with other buildings codes from other parts of the world. That will help Shape the framework for the building regulation. Below are the various segments of the codes as follows

Table 2.22: Eurocodes

European Codes	Parts of Codes		Description of codes
EN 1990: Basis of structural design	EN:1990 to EN:2002	Eurocode -Basis of structural design	<p>EN 1990 is required to be used in line with EN 1991 to EN 1999 for the structural design regarding buildings and other civil engineering works, including structure fire design, execution and temporary structure geotechnical aspects,</p> <p>EN 1990 explains the applicability for designing structures where materials or other actions that are not within the range of EN 1991 to EN 1999 are considered.</p> <p>EN 1990 are used for the appraisal of existing construction structure, in alteration, developing the design of repairs and or in assessing changes</p> <p>EN 1990 as a guidance document for the design of structures outside the scope of the EN Eurocodes EN 1991 to EN 1999, for:</p> <ul style="list-style-type: none"> ▪ focusing on the assessing of other actions and their combinations; ▪ for the modelling material and structural behaviour. ▪ focussing on assessing the numerical values of the reliability format.
	EN:1990 to EN:2002/ A1:2005	Eurocode -Basis of structural design	
EN 1991: Actions on structures	EN 1991-1-1:2002	Eurocode 1: Actions on structures -Part 1-1: General actions - Densities, self-weight, imposed loads for building	<p>EN 1991 Eurocode 1: this section provides complete information on all actions that should normally consider in designing buildings and other civil engineering works.</p> <p>It comes in four parts, according to the EN1991-1-1:2002: the four main parts; the first part is divided into sub-parts that cover densities, self-weight and imposed loads; Snow; wind; thermal actions, loads during execution and accidental actions. This section, especially the densities, self-weight, imposed and snow, directly impacts the current study that can be adopted.</p>
	EN 1991-1-2:2002	Eurocode 1: Actions on structures - Part 1-2: General actions - Actions on structures exposed to fire	

European Codes	Parts of Codes		Description of codes
	EN 1991-1-3:2003	Eurocode 1: Actions on structures - Part 1-3: General actions - Snow loads	
	EN 1991-1-4:2005	Eurocode 1: Actions on structures - Part 1-4: General actions - Wind actions	
	EN 1991-1-5:2003	Eurocode 1: Actions on structures - Part 1-5: General actions - Thermal actions	
	EN 1991-1-6:2005	Eurocode 1: Actions on structures - Part 1-6: General actions - Actions during execution	
	EN 199		
		2: Design of concrete structures	
	EN 1992-1-1:2004	Eurocode	

European Codes	Parts of Codes		Description of codes
Concrete		design for structures -Part 1-1: General rules and rules for buildings	<p>according to the EN 1992 Eurocode 2, buildings' design and other civil engineering works in plain, prestressed concrete and reinforced concrete. That means the state and requirements for the serviceability of structures and Safety; the basis of their design and verification are given in EN 1990: Basis of the design structure. EN Eurocode 2 is related to the requirements for serviceability resistance, and durability etc.</p> <p>Part 1.1 gives general basic rules for the structure's design in prestressed concrete and reinforced concrete, while Part 2 gives a general basis for the design and detailing of bridges in reinforced and prestressed concrete.</p> <p>EN Eurocode 2 is supposed to be used in line with:</p> <ul style="list-style-type: none"> ▪ EN 1990: Eurocode - design of structure; ▪ EN 1991: Eurocode 1 - Actions on structures;

Extracted from: Structural Eurocodes (2003), Structural Eurocodes (2009), The European Union Per Regulation (2011) and Thomas (2007)

The above codes for European member states illustrate the various types of building regulations within the European Union. Concerning the building code that deals with most aspects of building regulations, the researcher will explore the differences and similarities of the European codes? Other volcanic prone building codes. That will help the researcher to draw/identify strategies for the framework.

The structural Eurocode programme comprises the following standards generally consisting of several Parts:

- EN 1990 Eurocode: Basis of structural design
- EN 1991 Eurocode 1: Actions on structures
- EN 1992 Eurocode 2: Design of concrete structures
- EN 1993 Eurocode 3: Design of steel structures
- EN 1994 Eurocode 4: composite steel and concrete structures design
- EN 1995 Eurocode 5: Timber structures design
- EN 1996 Eurocode 6: masonry structures design
- EN 1997 Eurocode 7: Design of the Geotechnical
- EN 1998 Eurocode 8: Earthquake resistance structural design.
- EN 1999 Eurocode 9: Aluminium structures design Eurocode standards recognise regulatory authorities' responsibility in each Member State.

These have been illustrated in Table: 2.22; the researcher's observation suggests that per Eurocode,' all of the EN 9191 code relating materials have a Part 1-1 which relate to the design

of buildings and other civil engineering structures, etc. Parts 1-2 focuses on steel, composite steel and concrete, etc.

Except for the foundation for the volcanic prone areas, the EN 1998 seismic or earthquakes measure will need some level revision for its suitability within the volcanic prone areas. The roof of the building, which is taken care of by the EN 1991 considered the snow elements 'This is a valid point in the researcher's view, and as such, due consideration must be given to the roof. The prolonged eruption of debris and hot ash from volcanic action can settle heavy materials on the roof compared to the snow and can have devastating consequences, especially in volcanic-prone areas.

Considering the building materials which are taken care of by the Eurocode EN 1994, EN 1995 and EN 1996, the research must identify the materials that are best suited for these volcanic prone areas. As it is clear, the recent fire raging in Grenfell Tower in London killed an estimated 78 people worse by the cladding material, which was very susceptible to fire. According to Loughlin et al. (2002), a pyroclastic surge traveled along the Paradise River and impacted the lower part of Harris village. They further explain how a wooden rum shop at the edge of the surge zone burned to the ground, and bottles within it melted to form a contorted shape and took one-person life. '

There was a report of wooden roofs of large concrete homes near the margins of the surge being damaged, only on the side impacted by the pyroclastic surge (Loughlin et al.,2002:). It is worth mentioning that, according to Loughlin et al. (2002), 'concrete walls inevitably or invariably survived the impact. They argued that, while such walls, when impacted by block-and-ash flows or the main part of a surge, they remained standing, but the roofs, windows and interiors

were generally destroyed. Loughlin et al. (2002:) also report an eyewitness account that there was one house at the end where he witnessed the paint just started to cake up, blistering and the shingles just singed, they started melting while he was watching.' These conditions of pyroclastic eruption prove the extent of heat this type of volcanic eruption carries along with it, should there be an eruption. The researcher views that building materials should be safe and resilient to fire during a volcanic eruption. However, there were indications that there were survivors of people near the margins zones who stayed inside the building (Loughlin et al., 2002).

In considering Safety and resilience, in the researcher's view, every aspect of the building fabric must function to its optimal level. That brings into focus the contribution of this research to address some of these issues related to buildings in volcanic prone areas.

This section is vital to the study because it helps the study determine the allowable stress by indicating the tensile strength of the concrete roof and the factor of Safety from the EN code 1992-1-1:2004(E). The coefficient value is determined from the National Standard BSEN 1992-1-1:2004. The study will use these values to calculate the allowable stress in chapter 3 for the DEM and the FEM co-simulations.

According to the EN1992-1-1-3.1(2)P. The design tensile strength F_{ctd} is determined from the formula in the equation.

The design tensile strength f_{ctd} for concrete is determined according to EN1992-1-1 §3.1.6(2)P:

$$f_{ctd} = \alpha_{ct} f_{ctk,0.05} / \gamma_C \quad (2-9)$$

where design state, as specified in EN1992-1-1-3 and the National Annex.

The coefficient α_{ct} considers long-term effects on the tensile strength and unfavourable effects, resulting from how the load is applied. It is specified in, and the National Annex see also EN1992-2 §3.1.6(102)P and the National Annex).

There are two considerations for concrete strength; however, since the tensile strength has impacted concrete, there is no consideration regarding the compressive strength as it is not required at this stage. The concrete's coefficient α_{ct} will be considered from the EN1992-1-1 from the national annex code; the study will use the EU values and the UK values from table 3.4 The factor of Safety for concrete according to the BS EN 1992-1-1:2004 EN 1992-1-1:2004 (E) is 1.5 for concrete.

Table 2.1N of the BSEN1992-1-1:2004 explains the factors for materials for ultimate limit states, Design situations γ_C for concrete γ_S for γ_S for prestressing steel, etc., the values for the Persistent & Transient 1.5 1.15 1.15

The values for factors for materials for serviceability limit state verification should be 1.5 factor of safety for concrete, for persistent and transient design situations 1.2 for accidental design situations. The EN 1992 -code refers to the partial factor of safety for concrete in the limit states as 1.5. However, this research will consider the 1.5 for the concrete roof. The snow loading information adopted by the study is presented in Appendix A

Table 2.23: Recommended Values of Coefficients ψ_1 for Different Locations for Building

Regions	ψ_0	ψ_1	ψ_2
Finland Iceland Norway Sweden	0.70	0.50	0.20
Reminder of other CEN member states, for sites located at altitude H > 1000 m above sea level	0.70	0.50	0,20
Reminder of other CEN member states, for sites located at altitude H 1000 m above sea level	0.50	0.20	0.00

2.20 Load Arrangements of Volcanic Ash Particles

The study thus considers the load arrangement with regards to the snow arrangement. The study will be guided by a similar approach to the proposition regarding the volcanic ash particles consideration.

1) P the EN1991 code considers the following two primary load arrangements on the roof:

- undrifted snow load on roofs
- drifted snow load on roofs

2) The arrangements of load should be determined using the specified code.

3) P loads of snow on roofs shall be determined as follows:

a) for the persistent/transient design situations

$$S = \mu_i \cdot C_e \cdot C_t \cdot S_k \quad (2-10)$$

b) the accidental design situations where exceptional the loading of the snow is the accidental action (except for the cases covered in 5.2 (3) P c)

$$S = \mu_i \cdot C_e \cdot C_t \cdot S_{AD} \quad (2-11)$$

- c) for the accidental design situations where exceptional snowdrift is the accidental action and

$$S = \mu_i S_k \quad (2-12)$$

where:

- μ_i is the snow load shape coefficient
- S_k is the characteristic value of snow loading of the snow on the ground
- S_{Ad} is the design value of exceptional loading of snow on the ground for a given location
- c_e is the exposure coefficient
- C_t is the thermal coefficient

Table 2.24: Imposed Loads on Roofs of Category H

Roof	q_k [kN/m ²]	Q_k [kN]
Category H	q_k	Q_k
<p>For category H, q_k may be selected within the range 0.00 kN/m² to 1.0 kN/m², and Q_k may be selected within the range 0.9 kN to 1.5 kN.</p> <p>Where a range is given, the values may be set by the National Annex. The recommended values are:</p> <p>$q_k = 0.4$ kN/m², $Q_k = 1.0$ kN /m² q_k may be varied by the National Annex dependent upon the roof slope.</p> <p>q_k may be assumed to act on area A, which the National Annex may set. The recommended value for A is 10 m², within the range of zero to the roof's whole area.</p>		

Table 2.11 shows the minimum values given do not consider uncontrolled accumulations of construction materials that may occur during maintenance.

2.20.1 Mono-Pitched Roofs

According to BS EN 1991-1-3:2003, the snow load shape coefficient used for mono-pitched roofs is given in Table 2.25.

Table 2.25: Snows Load Shape Coefficients

Angle of pitch of roof α :	$0^\circ < \alpha < 30^\circ$	$30^\circ < \alpha < 60^\circ$	$\alpha > 60^\circ$
μ_1	0.8	$0.8 \cdot (60 - \alpha) / 30$	0.0
μ_2	$0.8 + 0.8 \cdot \alpha / 30$	1.6	-

Table 2. 25 shows Snow's load shape coefficients. According to BS EN 1991-1-3:2003, the values given in table 2.25 above apply when the snow is not prevented from sliding off the roof. Where snow fences or other obstructions exist or where the roof's lower edge is terminated with a parapet, then should not reduce the shape should not reduce the snow load shape coefficient below 0.8. The coefficient will be adapted from the EN code to determine the allowable stress of the concrete roof.

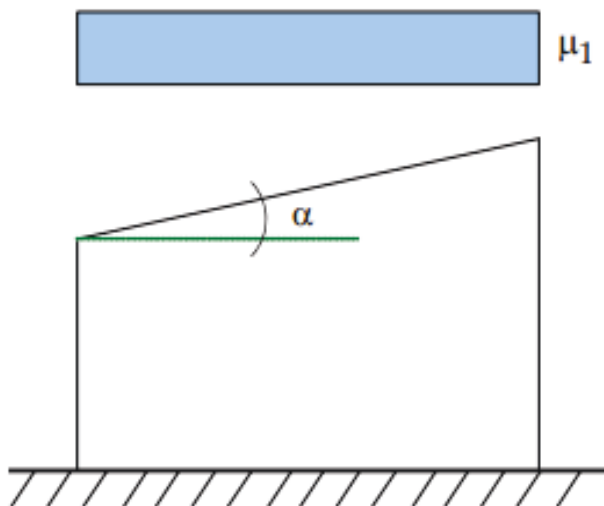


Figure 2.21: Snow Load Shape Coefficient-Mono-Pitch Roof

Figure 2.15 shows the Snow load shape coefficient-mono-pitch roof. BS EN 1991-1-3:2003 According to BS EN 1991-1-3:2003, there is research evidence that for larger roofs (e.g. square or almost square roofs with a length of about 40 m), the snow layer may be a non-uniform maximum value of the ratio between the roof and the ground snow loads reaches unity. The mono section can be related to the DEM and FEM modelled for the simulation test.

2.20.2 Pitched Roofs

The study will conduct DEM and FEM simulation tests for the pitched roof for the variable angles of inclination for 20 degrees, 25 degrees, 30 degrees 35 degrees 40 degrees and 45 degrees respectively. The study will most consider the BSEN 1991-1-1-3:2003 and will be adopted for the simulation test results.

The EN code in this section does explain the snow load shape coefficients that should be used for pitched roofs given in Figure 2.21, where the values are given apply when snow is not prevented from sliding off the roof. Where snow fences or other obstructions exist or where the roof's lower edge is terminated with a parapet, that should not reduce the concrete coefficient value below 0.8.

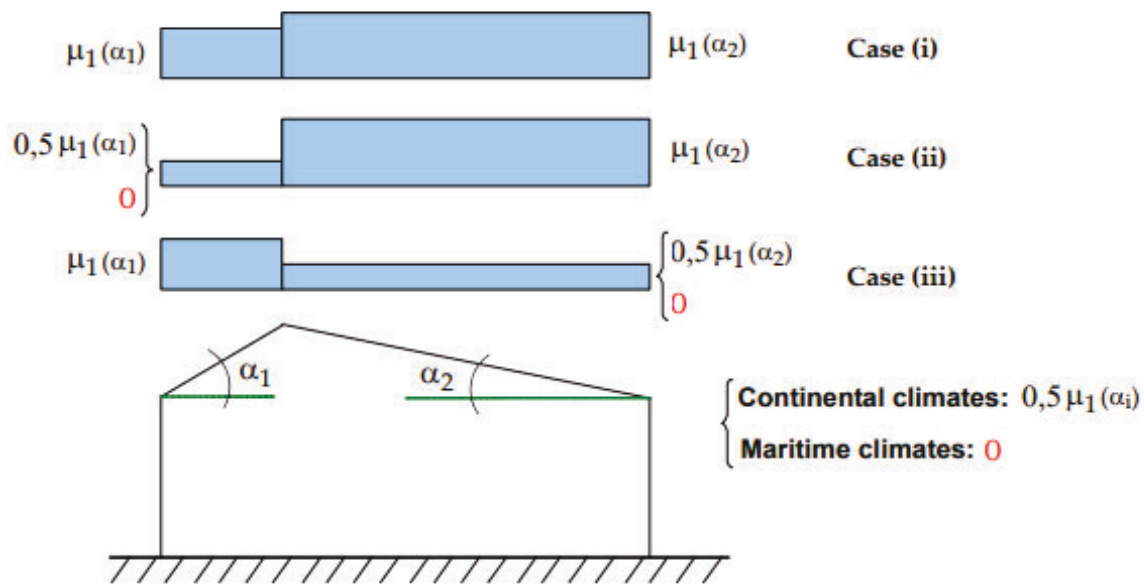


Figure 2.22: Snow Load Shape Coefficients -Pitch Roofs

Since the patch plays a significant part of the research objective 3: that is to conduct numerical (finite element modelling (FEM) and the discrete element method DEM modelling tool to assess structural tolerance under loading conditions (static and dynamic). This section's imperative has necessitated the modelling of the variable angles for pitched tile concrete roofs for the DEM and FEM simulation to determine the DEM maximum pressure. The FEM maximum deformation, the maximum stress and the maximum strain effect on the roof.

2.21 Finite Element Method (FEM)

According to Rao (2017), the finite element method simulates a complicated problem by replacing it with a simpler solution. The finite element method is the numerical method for an accurate solution for complex engineering problems that can also use it solving a wide range of practical problems, especially in engineering research and applied mathematics.

RAO (2017) further stated that the finite element method could be employed to the various boundaries and initiate value conditions on the dependent variables or derivatives. He argued that the finite element method has three categories, namely.

1. Equilibrium or steady-state or time-independent problems value
2. Eigenvalue problems
3. Propagation or transient problems.

These three categories directly link to the study as the equilibrium or steady-state can be referred to the research, which determines the stress distribution and deformation values from the building roof's volcanic ash pressure loading, a mechanical problem. The eigenvalue is also related to this study, according to Rao (2017), it may be considered an extension of the equilibrium problem with critical values of a certain parameter. It is determined in addition to the steady-state configurations this links to the mode shapes if its solid mechanic or structure problem. That has a direct link to the study because of the structure mechanic approach the study adopts.

The third category is the propagation of the transient approach, which depends on a related problem. The FEM simulation has determined a time-dependent problem during the cause of simulation. Rao (2017) argued about the six step-step orderly processes to be considered when carrying out a simulation are as follows;

- Divide the structure into discrete elements (discretisation)

Rao (2017) described the finite element method's applicability as a beneficial and versatile tool for a wide range of problems. He argued that FEM is linked to many software packages for

various structural and solid mechanics problems. This study uses the finite element method for the study's methodology with the Ansys software, which will help determine the stress deformation and strain value of the volcanic ash on the roof of buildings for the flat concrete roof and the pitched roof. Rao (2017) went further to explain that's ANSYS general-purpose finite element analysis software. He explained how that could be used for Ansys mechanical, structural, and Ansys Multiphysics for field problems. This study aims to use the discrete element method simulation with the finite element method with Ansys mechanical tool for the co-simulation as part of the study's methodology.

2.22 Equation of Motion

Rao (2017) explained the equation of motion, which can be derived by applying Newton's second law of motion to a differential volume (dx, dy, dz) mass dm. The motion equations can be derived by applying Newton's second law to a differential volume (dx, dy, dz) of a fixed mass dm eq [17.1] when the body forces acting on the fluid per unit mass are given by the vector,

$$\vec{B} = B_x \vec{i} + B_y \vec{j} + B_z \vec{k} \quad (2-13)$$

the application of Newton's law in x-direction gives

$$dF_x = dm a_x = (\rho dx dy dz) a_x$$

dF_x is the differential force acting in the x-direction, and a_x is the acceleration of the fluid in the x-direction. Using a figure like that of Eq. (17.38) can be rewritten as

$$dF_x$$

$$\begin{aligned}
dF_x = & (\rho dx dy dz) B_x - \sigma_{xx} dy dz + \left(\sigma_{xx} + \frac{\partial \sigma_{xx}}{\partial x} dx \right) dy dz - \sigma_{yx} dx dz \\
& + \left(\sigma_{yx} + \frac{\partial \sigma_{yx}}{\partial y} dy \right) dx dz - \sigma_{zx} dx dy + \left(\sigma_{zx} + \frac{\partial \sigma_{zx}}{\partial z} dz \right) dx dy
\end{aligned} \tag{2-14}$$

Dividing this equation throughout by the volume of the element gives

$$\rho B_x + \frac{\partial \sigma_{xx}}{\partial x} + \frac{\partial \sigma_{yx}}{\partial y} + \frac{\partial \sigma_{zx}}{\partial z} = \rho a_x \tag{2-15}$$

Similarly, we can obtain the y and z directions;

$$\rho B_y + \frac{\partial \sigma_{xy}}{\partial x} + \frac{\partial \sigma_{yy}}{\partial y} + \frac{\partial \sigma_{zy}}{\partial z} = \rho a_y \tag{2-16}$$

The above processes can be applied to the study using the FEM simulations. Rao (2011) generally stated that, for an equilibrium difficulty, the element equations in a local coordinate system can be stated in the standard form as shown below:

$$[k^{(e)}] \vec{\phi}^{(e)} = \vec{p}^{(e)} \tag{2-17}$$

$[K^{(e)}]$ $\vec{p}^{(e)}$ and are the element characteristic matrix and vector, respectively, $\vec{\phi}^{(e)}$ and is the vector of nodal unknowns of element e. Suppose the field variable is a directional quantity such as displacement, velocity, or force. In that case, a coordinate transformation exists between the local and global degrees of freedom (unknowns) of the element e.

CHAPTER THREE

3.0. METHODOLOGY

3.1 Introduction

This section would define the approach adopted to obtain the data specified in the full description of the research approach. The focus will be based on the modelling of the pitched roof and the flat concrete roof for the simulation of the FEM and DEM. The research will be done using finite element analysis and discrete element method) based on the COMSOL Multiphysics, numerical modelling tool (EDEM software) for the Discrete Element Method (DEM), structural analysis tool (ANSYS) for the Finite Element Method (FEM) tool to calculate and validate the impact of volcanic ash loading on roofs. The DEM model will simulate volcanic ash particles' behaviour and how they move and determine how the load acting upon the roof is distributed.

Simulations would involve a roof of varying inclination angles with concrete roofing materials (structural integrity) to be adopted for the experimental simulations. Figure 2.10 and figure 2.11: On page 48 are One (a) and three-dimensional models (b) of the roof loading. These (a) and three-dimensional models (b) of the roof loading problem be investigated for different roof buildings of varying sizes with different roofing materials to assess the roof's resilience against volcanic ash. A roof model was developed and numerically simulated to predict volcanic ash's effects, focusing on key structural variables, including pitch and variable angle, to determine the stress and deformation level of the volcanic ash, the ash's movement on the inclined roof in both static and dynamic modes. Results would allow quantification of the resilience of roof design against volcanic ash deposition.

This research will focus on volcanic ash's impact on the roofs of buildings within volcanic-prone areas. Zhao et al. (2016) investigated the impact of Snowdrift formation on roofs, especially on long-span lightweight roofs, a major problem in snowy and windy areas. They pointed out that news about structural damages due to snowdrifts was reported frequently in recent years with global warming. This assertion is not different from volcanic ash's impact on buildings' roofs within the volcanic prone areas and beyond. Therefore, this research will adopt some of the methodology and approach of Zhao et al. (2016) regarding snowdrift drift.

That was important to study the effects of volcanic ash on the roof of buildings with the design consideration of flat roofs, pitch roofs and truss roof structures, which will lead to the prediction for the revision of the European building code EN1991.

3.2 Computer Simulation Methodology

There will be a Multiphysics approach for the simulation methodology, which includes the finite element method (FEM), using the COMSOL software, the discrete element method (DEM) using the EDEM software, the co-simulation for the DEM. The co-simulation for FEM and the DEM. The finite element method (FEM) will help solve deflection and stress the volcanic ash load on the building's roof using console software. The research will introduce a coupled multi-engineering finite element method (FEM) implemented in the COMSOL Multiphysics approach for detailed and accurate calculation of the stress, and deformation of the roof's volcanic ash pressure plate (Nguyen, D N, and V.O., D.J.,2020).

The finite element method, which is numbered, has been used in many past experiments to solve various problems. Huises and Chao (1983) used the finite element method for structured stress analysis in engineering mechanics. Comsol (2012) explained that "modelling and

simulation are becoming indispensable tools in design is finite that can be used for all fields engineering". Nicholas M.B(1987) explained that it comprises a tailed modelling solution for structured Mechanical, Chemical Engineering. Comsol AB (2014) stated that "it is used when hand calculation cannot provide accurate results". That can use be used for modelling all physical phenomena (linear non-linear dependent). It can apply to geometry or the process in question and is very complex. However, the key results obtained from EDEM and Ansys for the study are in Figure 4.3. Below is the Figure showing the DEM and FEM (COMSOL) simulation test. The DEM is on the left side, and the FEM (COMSOL) is on the right side, as shown. That doesn't form the main key simulation approach for the data.

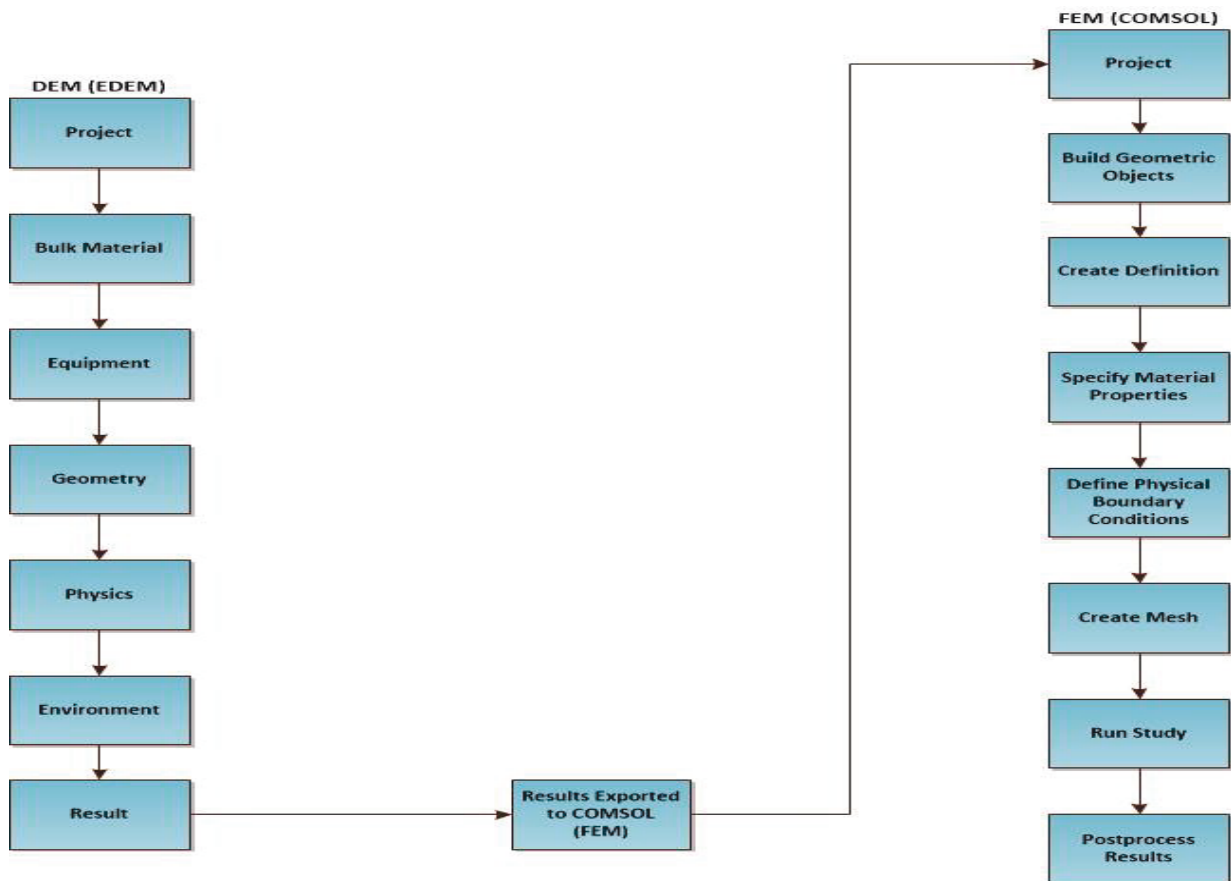


Figure 3.1 Flow Chart for Simulating DEM (Implemented in EDEM) and FEM (Implemented in COMSOL) Tool.

It is not the key main simulation approach to the study. However, used it for the preliminary study for the early stage of the study. The diagram shows that the left side is the DEM simulation process from the project stage to the result stage. The results are then exported to the FEM (COMSOL), where the simulation process takes place till the stress and the deformation results are attained.

3.2.1 Volcanic Ash Material

A model is created to help with Multiphysics computer-aided software such as the DEM and FEM co-simulation for the structural analysis (ANSYS) tool Analysis software for the study. This software can create 3D models such as a $10\text{ m} \times 10\text{ m} \times 0.154\text{ m}$ model for a concrete roof with an angle of 2 degrees and the tile pitched concrete roof. This model will be scaled to 1:10 to create a unit per meter square of the simulation model. The scaled roof models are as follows: $1\text{ m} \times 1\text{ m} \times 0.0154\text{ m}$ flat roofs, and the $1\text{ m} \times 1\text{ m} \times 0.0055\text{ m}$ tiled concrete pitched roof will emerge. It will enable the study to know the volcanic ash's impact within the roof's square meter. according to R. J. S. Spence (2005) stated that the Design ash loads is common in northern Europe, such as in the U.K., are between 0.5 and 1.0 kPa.

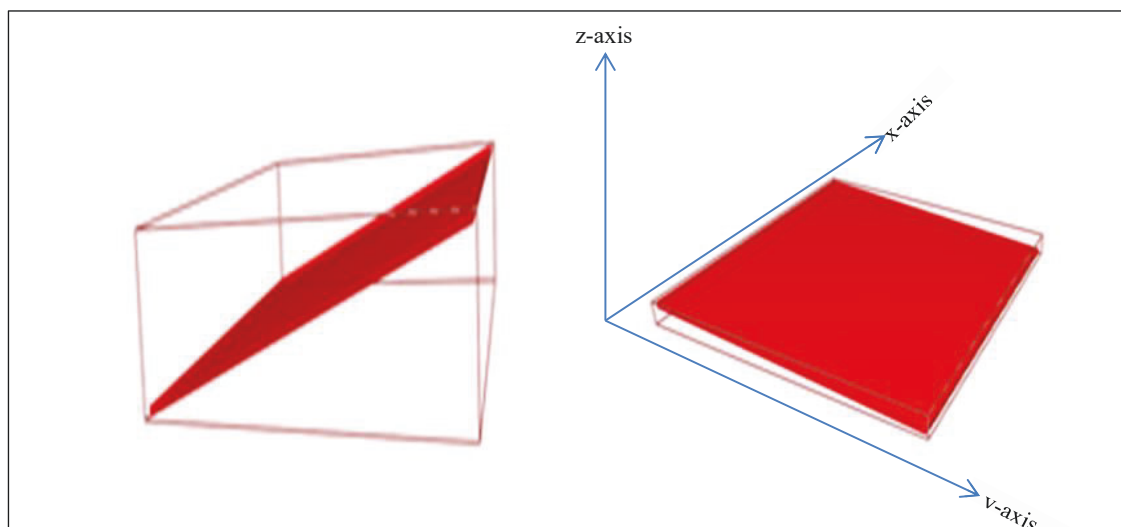


Figure 3.2: Model for Flat Concrete Roof and Tile Concrete Pitched Roof used for the DEM and FEM Simulation Test.

The model for the pitched roof and the flat concrete roof with an inclination angle will determine the model for the deposition of the volcanic ash particles on the roof.

Key Assumptions:

- The model was a flat plate scaled to 1:10 (1 m × 1 m × 0.0154 m.)
- The material was homogenous in the x-axis and y-axis.
- The vertical fall of the volcanic ash is constant in the z-axis
- On the x-axis, the material fall intensity is different from the point load.
- The load varies per every inclination on the axis applying the multiple loads.

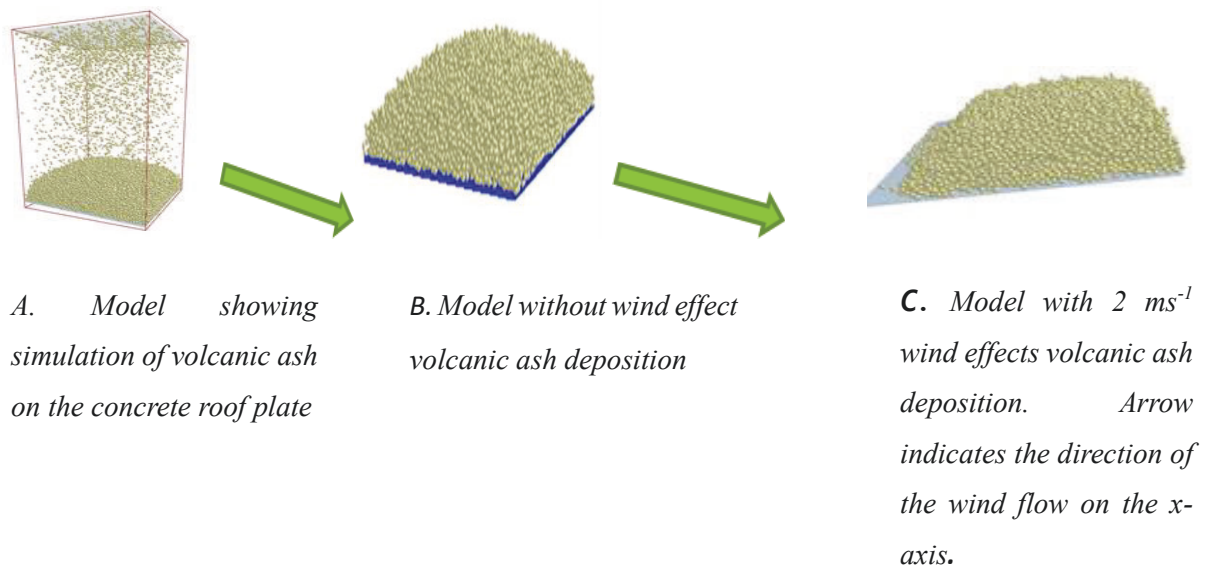


Figure 3.3: Deposition of Volcanic Ash Particles on the Flat Concrete.

Figure 3.4 shows (1 m × 1 m × 0.0154 m) deposition of the 10 mm volcanic ash particles on the flat concrete. Model for concrete flat roof with 2° angle inclination to determine the height of the roof. Figure 3.3 shows (1m × 1m × 0.0154 m) deposition of the 10mm volcanic ash particles on the flat concrete.

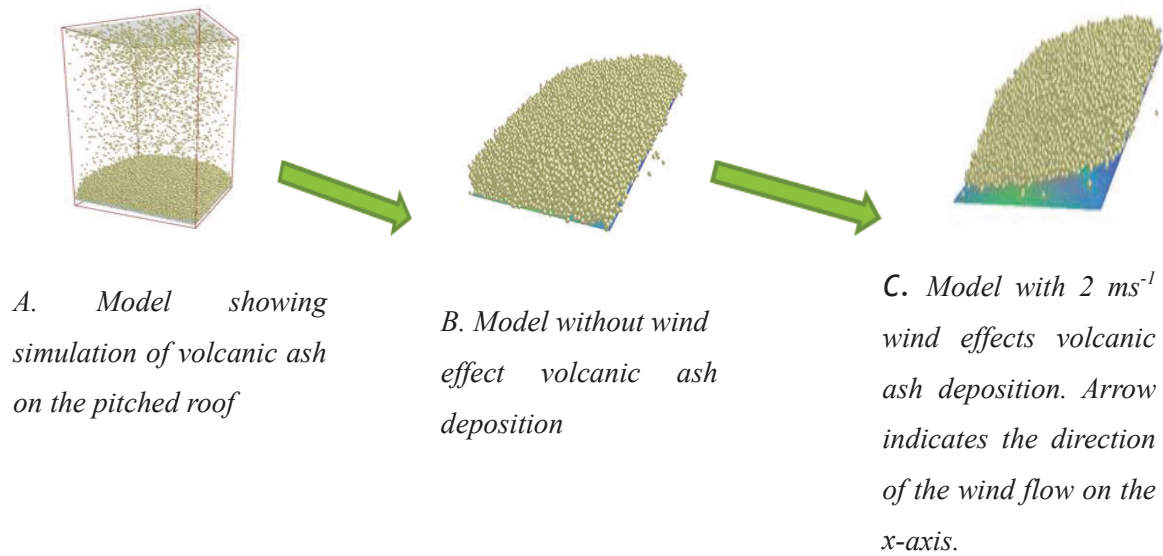


Figure 3.4: Deposition of Volcanic Ash Particles on the Pitch Roof

This model was used to simulate the discrete element method DEM with the various volcanic ash particle for the simulation. that the particles are modelled as spherical objects of diameters as per above with 80,000, 160,000, and 170,000 volcanic ash particles deposition on the flat roof for 2 kinds of simulation will deplore as:

- 1) Simulation without wind effects and the later simulation with wind effect.
- 2) Simulation with wind effects and the later simulation with wind effect.

The other model to be created will be the pitched Roof $10 \text{ m} \times 10 \text{ m} \times 0.154 \text{ m}$ which will be scaled to 1:10 to determine by the angle of $20^\circ, 25^\circ, 30^\circ, 35^\circ, 40^\circ$ and 45° . Modelling tool (EDEM software) for the Discrete Element Method (DEM) and structural analysis tool (ANSYS) for the Finite Element Method (FEM) use the following parameter d for the DEM simulation.

Table 3.1: Various Simulation Values

Type of Roof Model Plate	The model angle of inclination (degs)	Particle Variable loadings (Numbers)	Volcanic Particles size (mm)	Particles Variable Densities (kgm ⁻³)	Coefficient of Restitution	Coefficient of Static Friction	Coefficient of Rolling Friction	Poison Ratio EN1992-	Initial velocity (ms ⁻¹)
flat concrete roof	2	80,000, 160,000	1, 5 and 10	2300	0.145	1.1	0.9	0.2	
Pitch Tiles roof	20°,25°,30°,35°, 40°and 45°.	160,000 and 170,000	1, 5 and 10	2300	0.145	1.1	0.9	0.2	
Volcanic ash Particles			1, 5 and 10	1000,2000 and 3000	0.145	1.1	0.9	0.15	0.0134

The same approach used by Zhoe et al., (2016) for the Zhoe involved DEM/CFD co-simulation can be adopted for the study for the current study.

3.2.2 Factors for Concrete Roof Materials

According to the EN 1992-1-2 factors for ultimate limit states, γ_C and γ_S should be used.

Table .3.2: Partial Factors for Materials for the Ultimate Limit States

Design situations	γ_C for concrete	γ_S for reinforcing steel	γ_S for prestressing steel
Persistent & Transient	1.5	1.15	1.15
Accidental	1.2	1.0	1.0

3.2.2.1 Design Situations

1) The EN code explains that,

- γ_C for concrete
- γ_S for reinforcing steel
- γ_S for prestressing steel Persistent & Transient 1.5 1.15 1.15 Accidental 1.2 1.0 1.0

2) Should take the values for partial factors for materials for serviceability limit state verification should be taken as those given in the sections of this Eurocode.

The values of γ_C and γ_S in the serviceability limit stated for use may be found in its National Annex. The recommended value for situations not covered by sections of this Eurocode is 1.0.

3) Lower values of γ_C and γ_S may be used if justified by reducing the calculated resistance uncertainty.

3.2.2.2 Design Compressive and Tensile Strengths

The value of the design compressive strength is defined as

$$f_{cd} = \alpha_{cc} f_{ck} / \gamma_C \quad (3-1)$$

γ_C is the safety factor for concrete, and α_{cc} is the coefficient taking account of long-term effects on the compressive strength and unfavourable effects resulting from the way the load is applied. The value of α_{cc} for use in a Country should lie between 0.8 and 1.0 and may be found in its National Annex. The recommended value is 1.0. The value of the design tensile strength, f_{ctd} , is defined as;

$$f_{ctd} = \alpha_{ct} f_{ctk,0.05} / \gamma_C \quad (3-2)$$

where γ_C is the safety factor for concrete, and α_{ct} is a coefficient taking account of long-term effects on the tensile strength and unfavourable effects resulting from the way the load is applied. The recommended value is 1.0.

Table 3.3: Strength and Deformation Characteristic for Concrete.

Strength classes for concrete															Analytical relation / Explanation
f_{ck} (MPa)	12	16	20	25	30	35	40	45	50	55	60	70	80	90	
$f_{ck,cube}$ (MPa)	15	20	25	30	37	45	50	55	60	67	75	85	95	105	2.8
f_{cm} (MPa)	20	24	28	33	38	43	48	53	58	63	68	78	88	98	$f_{cm} = f_{ck} + 8$ (MPa)
f_{ctm} (MPa)	1.6	1.9	2.2	2.6	2.9	3.2	3.5	3.8	4.1	4.2	4.4	4.6	4.8	5.0	$f_{ctm} = 0.30 \times f_{ck}^{2/3} \leq C50/60$ $f_{ctm} = 2.12 \ln(1 + (\frac{f_{cm}}{10})) > C50/60$
$f_{ctk,0.05}$ (MPa)	1.1	1.3	1.5	1.8	2.0	2.2	2.5	2.7	2.9	3.0	3.1	3.2	3.4	3.5	$f_{ctk,0.05} = 0.7 \times f_{ctm}$ 5% fractile
$f_{ctk,0.95}$ (MPa)	2.0	2.5	2.9	3.3	3.8	4.2	4.6	4.9	5.3	5.5	5.7	6.0	6.3	6.6	$f_{ctk,0.95} = 1.3 \times f_{ctm}$ 95% fractile
E_{cm} (GPa)	27	29	30	31	33	34	35	36	37	38	39	41	42	44	$E_{cm} = 22 \left[\left(\frac{f_{cm}}{10} \right)^{0.3} \right] (f_{cm} \text{ in MPa})$
ϵ_{c1} (‰)	1.8	1.9	2.0	2.1	2.2	2.25	2.3	2.4	2.45	2.5	2.6	2.7	2.8	2.8	See Figure 3.2 $\epsilon_{c1}(‰) = 0.7 f_{ck}^{0.2} \leq 2.8$
ϵ_{cu1} (‰)	3.5									3.2	3.0	2.8	2.8	2.8	See Figure 3.2 for $f_{ck} \geq 50$ MPa $\epsilon_{cu1}(‰) = 2.8 + 27 \left[\frac{98 - f_{ck}}{100} \right]$
ϵ_{c2} (‰)	2.0									2.2	2.3	2.4	2.5	2.6	See Figure 3.2 for $f_{ck} \geq 50$ MPa $\epsilon_{c2}(‰) = 2.0 + 0.085(f_{ck} - 50)^{0.22}$
ϵ_{cu2} (‰)	3.5									3.1	2.9	2.7	2.6	6.6	See Figure 3.2 for $f_{ck} \geq 50$ MPa $\epsilon_{cu2}(‰) = 2.6 + 35[(90 - f_{ck})/100]^4$
n	2.0									1.75	1.6	1.45	1.4	1.4	for $f_{ck} \geq 50$ MPa $n = 1.4 + 23.4[(90 - f_{ck})/100]^4$
ϵ_{c3} (‰)	1.75									1.8	1.9	2.0	2.2	2.3	See Figure 3.4 for $f_{ck} \geq 50$ MPa $\epsilon_{c3}(‰) = 1.75 + 0.55[(f_{ck} - 50)/40]$
ϵ_{cu3} (‰)	3.5									3.1	2.9	2.7	2.6	2.6	See Figure 3.4 for $f_{ck} \geq 50$ MPa $\epsilon_{cu3}(‰) = 2.0 + 35[(90 - f_{ck})/100]^4$

Table 3.4: U.K. Decision for Nationally Determined Parameters Described in BS EN 1992-1-2004

Subclause	Nationally Determined Parameter	Eurocode ⁵ recommendation	UK decision
11.3.7 (1)	Value of k	$k = 1,1$ for lightweight aggregate concrete with sand as fine aggregate $k = 1,0$ for lightweight aggregate (both fine and coarse aggregate) concrete	Use the recommended value
11.6.1 (1)	Values of $C_{IRd,c}$, $v_{l,min}$ and k_1	$C_{IRd,c} = 0,15/\gamma_c$ $v_{l,min} = 0,28k^{3/2}f_{lck}^{-1/2}$ $k_1 = 0,15$	Use the recommended values $\langle \eta \rangle$
11.6.2 (1)	Value of v_1	$v_1 = 0,5\eta_1[1 - f_{lck}/250]$	$\langle \eta \rangle v_1 = 0,5\eta_1[1 - f_{lck}/250]$ generally for lightweight concrete, except in Expression (11.6.5), when the recommended value may be used. For lightweight concrete, v_1 should not be modified in accordance with Note 2 of 6.2.3 (3). $\langle \eta \rangle$
11.6.4.1 (1)	Value of k_2	0,08	Use the recommended value
12.3.1 (1)	Values of $\alpha_{cc,pl}$ and $\alpha_{ct,pl}$ (plain concrete)	$\alpha_{cc,pl} = 0,8$ $\alpha_{ct,pl} = 0,8$	$\alpha_{cc,pl} = 0,6$ $\langle \eta \rangle \alpha_{ct,pl} = 0,8 \langle \eta \rangle$
12.6.3 (2)	Value of k	1,5	Use the recommended value
A.2.1 (1)	Value of $\gamma_{s,red1}$	1,1	Use the recommended value
A.2.1 (2)	Value of $\gamma_{c,red1}$	1,4	Use the recommended value
A.2.2 (1)	Value of $\gamma_{s,red2}$ and $\gamma_{c,red2}$	$\gamma_{s,red2} = 1,05$ $\gamma_{c,red2} = 1,45$	Use the recommended values
A.2.2 (2)	Value of $\gamma_{c,red3}$	1,35	Use the recommended value
A.2.3 (1)	Value of η and $\gamma_{c,red4}$	$\eta = 0,85$ $\gamma_{c,red4} = 1,3$	Use the recommended values
C.1 (1)	Values for fatigue stress range, minimum relative rib area and β	Table C.2N $\beta = 0,6$	Use the recommended values
C.1 (3)	Values of a , f_{yk} , k , ϵ_{uk}	For $f_{yk} a = 10$ MPa For k and $\epsilon_{uk} a = 0$ Minimum and maximum values for f_{yk} , k , ϵ_{uk} in accordance with Table C.3N	Use the recommended values

The values used $f_{ctk,0.05}$ (Tensile strength of concrete roof) will be used from Table 3.3 according to the BSEN1992-1-1:2004:EN 1992 1 – 1: 2004 (E) and e coefficient value α_t of the concrete roof will be used from Table 3.3 shows the UK decisions for Nationally determined parameters described in N.A. to BSEN 1992-1-1:2004. The factor of safety to calculate the allowable stress is taken from table 3.4 factors safety for materials for ultimate limit states as 1.5 for the calculations. However, the code states two values are 0.8 for the United Kingdom (U.K.) and that of the European Union (E.U.) to be 1.0. Based on these two values, the research will consider both values and calculate the allowable stress and compare both data analyses.

However, this implies that f_{ctd} (design tensile strength) = $0.8 \times 2.7 / 1.5 = 1.44$ MPa

Therefore,

$$f_{ctd} \text{ (design tensile strength)} = 1.0 \times 2.7 / 1.5 = 1.8 \text{ MPa}$$

These values will be used to compare the results from the result simulation from the numerical modelling tool (EDEM software) for the Discrete Element Method DEM and structural analysis tool (ANSYS) for the Finite Element Method (FEM) to determine which of the roofs will be resilient to the volcanic ash loadings.

3.2.3 The Equation Governing the Air Phase

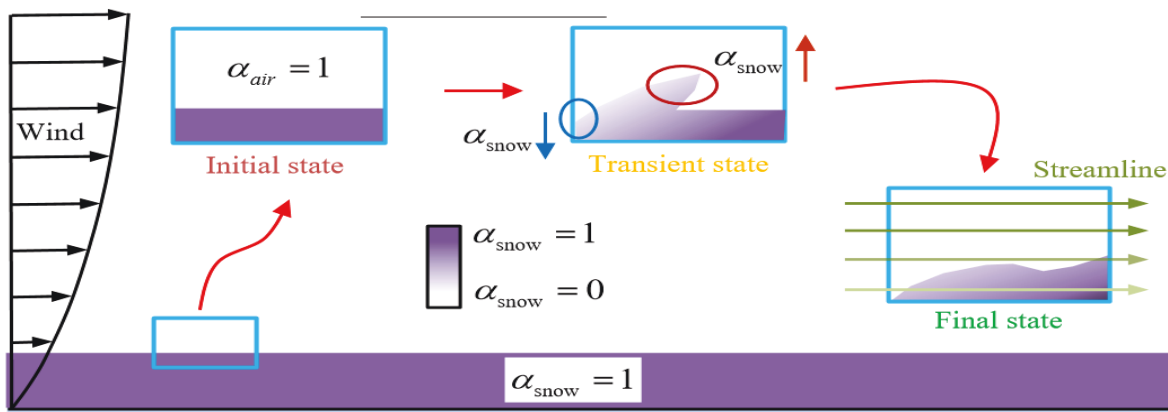
This section of the simulation of volcanic ash includes the continuous phase (air) movement and spread phase (volcanic ash) on the roof. The flow field characteristics are solved by adding the transport equation of volcanic ash attention, an empirical formula under the condition of fully developing volcanic ash, to the Navier-Stokes equation of air.

When the Energy transfer is disregarded, meaning the mass and momentum need to be covered.

The continuity equation for the airflow is given by;

$$\frac{\partial}{\partial t}(a_z \rho_z) + \nabla \cdot (a_z \rho_z v_z) = \frac{\partial}{\partial t}(m_p) \quad (3-3)$$

The subscript z refers to air, and p refers to volcanic ash particles particle, α is the volume fraction, ρ is the density, v is the velocity, and m is the mass



(a) E-E model

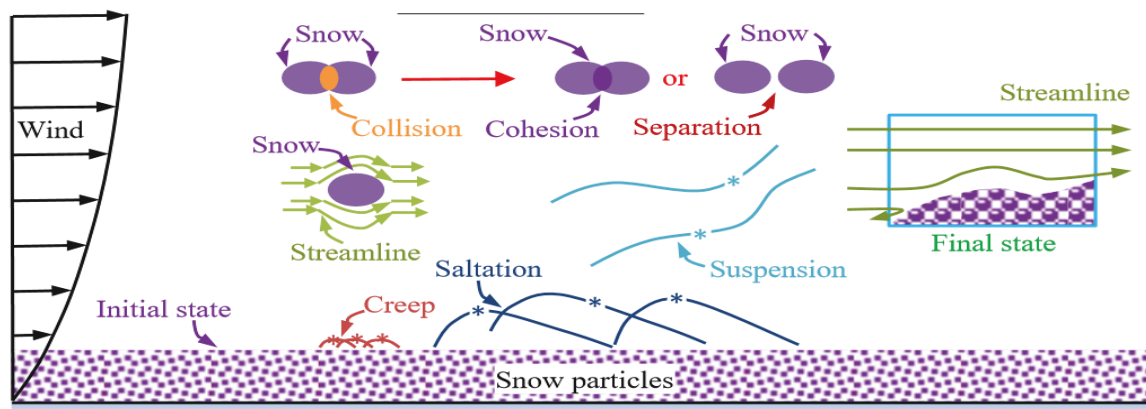


Figure 3.5: Differences between the E-E Model and CFD-DEM

Source: (Zhao et al., 2016)

Zhao et al., 2016 used the differences between the E-E model and CFD-DEM as shown in figure 3.5 to illustrate the effect of the wind direction and the effects of the traditional Eulerian–Eulerian (E-E) model and CFD-DEM. α_{snow} refers to the volume fraction of snow in cells. This study intends to use the Discrete Element Method (DEM) - Computational Fluid Dynamics (CFD) co- simulation. This approach has not been used to simulate volcanic ash particles on the concrete roof and the tiles concrete pitched roof. The process is tested by relating the simulation results to the volcanic ash depth distribution of the flat concrete roof, and the tiles pitched roof. The rate of change of the volcanic ash particle’s mass in any grid cell is given by;

$$\frac{\partial m_z}{\partial t}(t) = m_z(t) - m_p(t - \tau) \quad (3-4)$$

Where τ is the time step of CFD. A similar equation exists for the conservation of momentum is given by;

$$\frac{\partial}{\partial t}(\alpha_z \rho_z v_z) \cdot \nabla + (\alpha_z \rho_z v_z v_z) = -\alpha_z \nabla_z + \nabla \cdot \tau_z + \alpha_z \rho_z g_z - f_{\text{drag}} \quad (3-5)$$

Where τ_z is the stress tensor and ρ is the pressure shared by air and volcanic ash particles, g_z is the gravitational acceleration, and F_{drag} is the average drag force.

$$\tau_z = -\frac{2}{3}(\mu_{\text{pff}} \nabla \cdot v_z)I + \mu_{\text{pff}}[\nabla \cdot v_z + (\nabla \cdot v_z)^T] \quad (3-6)$$

$$f_{\text{drag}} = \frac{1}{\Delta V} \sum_{i=1}^{n_p} F_{\text{drag},i} \quad (3-7)$$

Where μ_{aff} is the effective viscosity of air, I is the unit tensor, and n_p is the number of volcanic ash particles. The drag force of particle i named $F_{\text{drag},i}$, g is given by Eq (5)

$$f_{drag,i} = 0.5 C_Z \rho_z A_p (v_z - v_p) |v_z - v_p| \quad (3-8)$$

Where A_p is the projected area of the particle and C_Z is drag coefficient depending on the

$$Re = \frac{\rho_z v_z d_p |v_z - v_p|}{\mu_f} \quad (3-9)$$

$$C_Z = \begin{cases} 24/R_e & R_e \leq 0.5 \\ 24(1.0 + 0.15R_e^{0.687})/R_e & 0.5 < R_e \leq 1000 \\ 0.44 & R_e > 1000 \end{cases} \quad (3-10)$$

where d_p implies the diameter of the particle, μ_f denotes the viscosity coefficient to air.

3.2.4 Equations Governing the Particle

The translation and rotational motion equation (3-11) and equation (3-11) of volcanic ash particles are governed, considering the gravity, the collision, and the drag force.

$$m_p \frac{dv_{p,i}}{dt} = m_p g + f_{drag} + \sum_{j=1}^{n_c} (F_{nij} + F_{tij}) \quad (3-11)$$

$$I_p \frac{d\omega_a}{dt} = \sum_{j=1}^{n_c} T_{ij} \quad (3-12)$$

Where m_p , $v_{p,i}$ and ω_p are the mass, the linear velocity and the angular velocity of particle p, respectively; F_{nij} , F_{tij} and T_{ij} are the normal contact force, the tangential contact force and the moment between particle i and particle j, respectively; I_p is the moment of inertia of the particle, n_c is the total number of particles that impact particle p at the same time. T_{ij} and I_p is given and respectively.

$$m_p \frac{dv_{p,i}}{dt} = m_p g + f_{drag} + \sum_{j=1}^{n_c} (F_{nij} + F_{tij}) \quad (3-11)$$

$$I_p \frac{d\omega_a}{dt} = \sum_{j=1}^{n_c} T_{ij}. \quad (3-12)$$

Where m_p , $v_{p,i}$ and ω_p are the mass, the linear velocity and the angular velocity of particle p, respectively; F_{nij} , F_{tij} and T_{ij} are the normal contact force, the tangential contact force and the moment between particle i and particle j, respectively; I_p is the moment of inertia of the particle, n_c is the total number of particles that impact particle p at the same time. T_{ij} and I_p is given and respectively.

$$T_{ij} = D_i \times (F_{tij} + F_{nij}) \quad (3-13)$$

$$I_p = \frac{1}{10} m_p d_p^2 \quad (3-14)$$

Where D_i is the distance vector between the centre mass of particle a to the contact point. (Zhao et al.,2016).

3.2.5 The equation governing the coupling

This section deals with the coupling and interaction between volcanic ash particles. The air is simulated by volume fraction denoted as u when using DEM for the volcanic ash on the building's roof. The volume fraction of volcanic ash particles denoted α_p and the volume fraction of air denoted as α_e in mesh, cells are given and, respectively.

$$\alpha_p = \sum_{k=1}^{n_p} \frac{V_{Pk}}{\Delta V} \quad (3-15)$$

$$\alpha_e = 1 - \alpha_p \quad (3-16)$$

Where n_p is the total number of particles in the mesh cell, V_{Pk} and ΔV is the volume of particle k and the mesh cell, respectively.

3.2.6 Particle Collision Model

The mathematical model's derivation in the section follows closely Zhao et al.,2016 and is adapted to the problem involving volcanic ash. Crowe et al., (1998) augured with regards to the linear spring-damper contact model; however, this research will use the same approach for the standard contact between volcanic ash particles is simulated by spring and damper, the tangential contact between volcanic ash particles is simulated by spring damper, as contact force is calculated according to the standard amount of overleaping and the tangential displacement between volcanic ash particles, where surface deformation of volcanic ash particles and contact force loading history are ignored (Zhao et al.,2016).

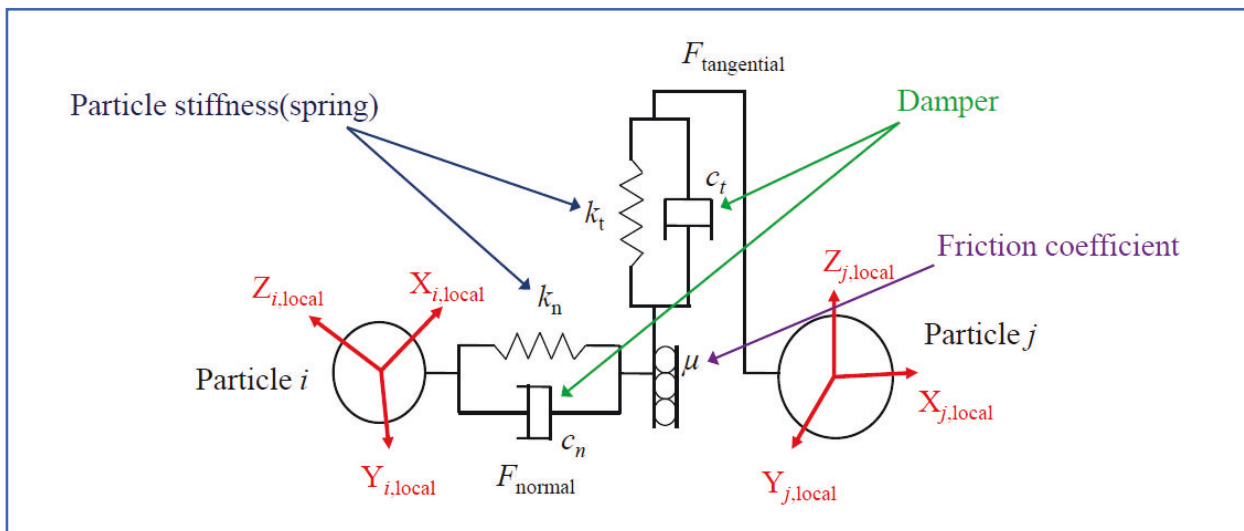


Figure 3.6: Particle Collision Model

Source: (Zhao et al.,2016), Rowe (1998)

F_{nijq} denoting the standard contact force is given by:

$$F_{nij}=(-k_n\alpha^{1.5} - c_n\mathbf{Gn})n \quad (3-17)$$

Where k_n is the standard spring coefficient and c_n is the standard damping coefficient, α is the standard amount of overleaping, and G is the relative velocity between volcanic ash particle i and volcanic ash particle j , given and n is the normal unit vector from the centre of particle i to the centre of particle j .

$$G = v_i - v_j \quad (3-18)$$

F_{tij} denoting the normal contact force is given

$$F_{tij} = \begin{cases} -k_t\delta - c_t G_{ct} & |F_{tij}| \leq \mu|F_{nij}| \\ -\mu|F_{nij}|t & |F_{tij}| > \mu|F_{nij}| \end{cases} \quad (3-19)$$

Where k_t is the divergent spring coefficient and c_t is the tangential damping coefficient, δ is the divergent displacement of the contract point, μ is the friction coefficient between volcanic ash particles, G_{ct} the slip velocity on the contact point and t is the unit tangential vector.(Zhao et al.,2016).

$$G_{ct} = G - (Gn \cdot n) + d_i\Omega_i \times n + d_j\Omega_j \times n \quad (3-20)$$

Where d_i and d_j , Ω_i and Ω_j are the diameter and the pointed velocity of particle i and particle j , n is the unit standard vector from the centre of particle i to the center of particle j . The stiffness kn can be given by using the Hertzian contact theory (Johnson 1985).

$$K_n = \frac{4}{3} \left(\frac{1-V_i^2}{E_i} + \frac{1-V_j^2}{E_j} \right)^{-1} \left(\frac{d_i-d_j}{d_i d_j} \right)^{-1/2} \quad (3-21)$$

Where V_i , V_j , E_i , E_j , d_i and d_j are the Poisson ratio, young's modulus, and the diameter of particle i and particle j respectively. The stiffness k_t can be given using Mindlin's theory (Mindlin 1949).

$$K_t = 8\delta^{1/2} \left(\frac{1-V_i^2}{G_i} + \frac{1-V_j^2}{G_j} \right)^{-1} \left(\frac{d_i+d_j}{d_i d_j} \right)^{-1/2} \quad (3-22)$$

Where a is the standard amount of overlap, V_i and V_j , G_i and G_j , d_i and d_j are the Poisson ratio, shear modulus and the diameter of particle i and particle j respectively. The standard damping coefficient denoted C_n and the tangential damping coefficient meant C_t can be given according to Cundall and Strack (1979) by;

$$C_n = \sqrt{mK_n} \quad (3-23)$$

$$C_t = \sqrt{mK_t} \quad (3-24)$$

Where m is the mass, K_n and K_t are the standard spring coefficient and the lateral spring coefficient respectively. Interconnections are considered by adding standard cohesion force to the above spring-damper contact model, and the standard cohesion force mean as F_c is given by;

$$F_c = KA$$

Where K is the energy density; and A is the contact area.

3.2.7 Linear Spring-Dashpot Contact Model

Rao, S.S., (2005) uses the linear spring - dashpot contact model to explain the analytical solution and numerical simulation in MATLAB. He explained the particle's behaviour when they come into contact, as illustrated in the Figure below.

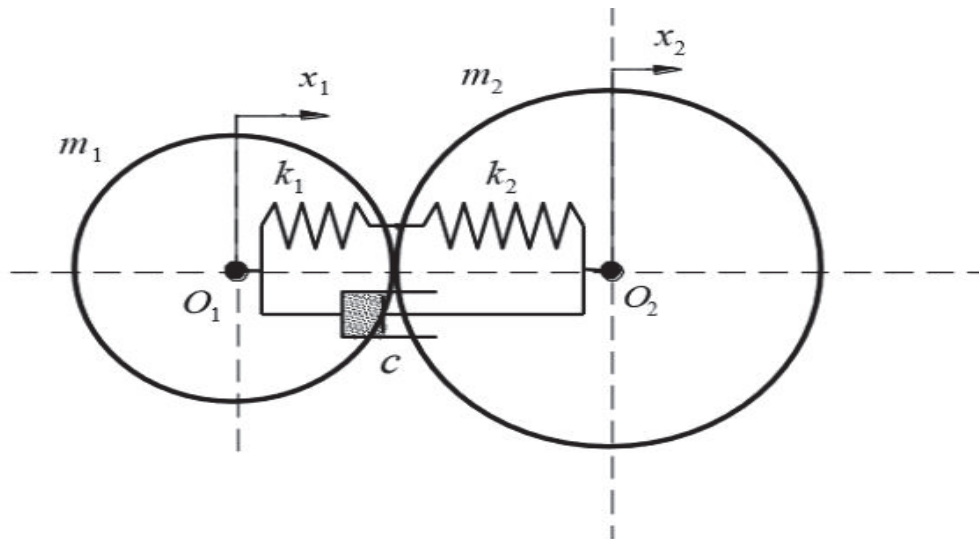


Figure 3.7: Interaction of Two Particles During Simulations

Source: Rao, S.S., (2005)

Figure 3.7 shows the interaction between two particles during simulations (Rao, S.S., (2005). Rao (2005) elaborated on the following about the two-particle model (1) description from the Figure shown below: The two particles of mass m_1 and m_2 respectively, are in contact. As stated below for the interaction for the two-particle model (1).

- Their stiffness properties are represented by linear springs of constants k_1 and k_2 , respectively.
- Damping properties in the contact area are represented by a dashpot of the coefficient of viscous damping c .

3.2.8 Two Particle Model

Rao (2005) did explain that if the particle displacements along the lines O_1 , O_2 are x_1 and x_2 , respectively, then the equations of motion can be derived using Newton's 2nd law motion as follows:

$$M_1 \ddot{x}_1 = -c(\dot{x}_1 - \dot{x}_2) - K(x_1 - x_2) \quad (3- 24)$$

$$M_2 \ddot{x}_2 = -c(\dot{x}_1 - \dot{x}_2) + K(x_1 - x_2) \quad (3- 25)$$

where k is the effective stiffness determined from;

$$\frac{1}{K} = \frac{1}{K_1 + K_2} \quad (3- 26)$$

$$K = \frac{K_1 K_2}{K_1 + K_2} \quad (3- 27)$$

The system described by Eqns (1) represents a 2 degree-of-freedom (DoF) model, which can be reduced to a single DoF (SDoF) model by multiplying the 1st equation by m_2 , the 2nd equation by m_1 and then subtracting the side of the equation by the side. This yield

$$m_1 m_2 = (\ddot{x}_1 - \ddot{x}_2) + (m_1 + m_2) + (\dot{x}_1 + \dot{x}_2) + (m_1 + m_2)K (X_1 - X_2) = 0 \quad (3 - 28)$$

Using in (2) the effective mass is defined as:

$$M = \frac{m_1 + m_2}{m_1 + m_2} \quad (3- 29)$$

and denoting $x = x_1 - x_2$ yields the following equation

$$\ddot{x} + \frac{c}{m} \dot{x} + \frac{K}{m} x = 0 \quad (3- 30)$$

Rao (2005) Mechanical vibrations (si edition).

The linear 2nd order ordinary differential equation (ODE) has the following general solution:

$$x(t) = C_1 \left\{ -\frac{c}{2m} + \sqrt{\left(\frac{c}{2m}\right)^2 - \frac{K}{m}} \right\} t + C_2 \left\{ -\frac{c}{2m} + \sqrt{\left(\frac{c}{2m}\right)^2 - \frac{K}{m}} \right\} \quad (3-31)$$

where C_1 and C_2 are arbitrary constants to be determined from the initial conditions of the system given as $x(0) = x_0$, $\dot{x}(0) = \dot{x}_0$

They noted that the Eqn. (3) can then be presented in the following (more compact) form

$$\ddot{x} + 2\zeta\omega \dot{x} + \omega^2 x = 0 \quad (3-32)$$

$$\text{Where } \omega = \sqrt{\frac{K}{m}}, \zeta = \frac{c}{2m\omega} \quad (3-33)$$

3.2.9 The Finite Element Method.

The derivation of the finite element equation for the two-dimensional problem as follows.

- Divide the structure into discrete elements (discretisation).
- Select a proper interpolation or displacement model.
- Derive element stiffness matrices and load vectors

From the assumed displacement model, the stiffness matrix and the load vector of an element are to be derived by using a suitable variational principle, a weighted residual approach (such as the Galerkin method) or equilibrium conditions

According to Rao (2011), Step 4 deals with Compiling element equations to obtain the overall balance equations. Since the structure is made of several finite elements, the individual element stiffness matrices and load vectors are to be assembled, and the overall balancing equations must be devised as:

$$[K]\vec{\Phi} = \vec{P} \quad (3-34)$$

[K] Is the assembled stiffness $\vec{\Phi}$ matrix, the vector of nodal \vec{P} displacements, and the vector of nodal forces for the complete structure.

Step 5: Explain the process to solve for the unknown nodal displacements. The overall equilibrium equations must be changed to accommodate the boundary conditions of the problem. therefore, with the incorporation of the boundary conditions, the equilibrium equations can be expressed as

$$[K]\vec{\Phi} = \vec{P} \quad (3-35)$$

Rao (2011) mentioned that linear problems $\vec{\Phi}$ can be solved very easily. However, for non-linear problems, the solution must be obtained in a sequence of steps, with each *step* including the modification of the stiffness matrix [K] and the load vector \vec{P} .

These 6: Compute element strains and stresses. If required, the known nodal displacements $\vec{\Phi}$ can compute strains and stresses by using the necessary equations of solid or structural mechanics.

According to Rao (2011), they modify the previous six steps' terminology to extend the concept to other fields. For instance, the term continuum or domain in place of structure, field variable in place of displacement, the characteristic matrix in place of stiffness matrix, and element

resultants in place of element strains. It is the reason why the process can apply to this current study.

3.2.10 Size of Volcanic Ash Materials for Simulations

This study will focus on variable volcanic ash sizes for a distance close to the vent and the distance away from the vent with different volcanic ash mixes. Again, the research tends to compare the roof in relation to the ash sizes. That will have a direct bearing on the methodology of the DEM simulation. Claire J. Horwell (2007) explained that "GSD results for health-pertinent fractions for a suite of 63 ash samples show that the fraction of respirable (04 mm) material ranges from 0 –17 vol%, with the variation reflecting factors such as the style of the eruption and the distance from the source". However, they drew a strong correlation between the amount of 04 mm – 010 mm material observed for all ash types. As pointed out by Claire J. Horwell (2007), this relationship is stable at all distances from the volcano and, with all eruption styles, can be applied to volcanic plume and ash fallout models. The prediction of the revision of the European code EN1991 of volcanic ash on roofs currently relies on computer simulations. The development of computational mechanics, especially the Finite Element Method (FEM) and Discrete element method DEM for numerical simulations have advantages on low cost. The short cycle can easily carry out the parametric analysis. Appendix B presents information on the amount of volcanic - size material distribution and cumulative volume.

3.2.11 Simulation Methodology

Study on volcanic ash about this study centre on the roof covered by volcanic ash's uniform distribution with a certain depth. Ash falls from the 1815 VEI 7 eruption of Tambora based on Kandlbauer and Sparks (2013) and, to a lesser extent, the Isopach of Self et al. (1984). Additional Isopach between 2 and 35 mm (inclusive), between 70 and 120 mm and those 350

mm and greater, as well as the southern portion of the 10 mm (dashed line) Isopach, have been interpolated by eye. For their calculations, a constant thickness of ash is assumed to have fallen between Isopach, equivalent to the bounding Isopach's smallest thickness, showing the total land area between each Isopach pair. The focus will be on the deposition roofs of the volcanic ash particles on the roof.

The volcanic ash particles density is variable, relating to its falling and sedimentation condition closely. (Shiple and Sarna-Wojcicki, (1982); Polacci, M., 2012. and Siddique, R., 2008) consider that this kind of density for individual particles varies with different eruptions.

- 700–1200 (kgm^{-3}) for pumice
- 2350–2450 (kgm^{-3}) for glass shards
- 2700–3300 (kgm^{-3}) for crystals
- 2600–3200 (kgm^{-3}) for lithic particles
- 1000 - 2000 (kgm^{-3}) for Lapilli

The size of volcanic ash particles changes a lot simultaneously, but the diameter is usually less than 4mm. Volcanic ash refers to pyroclasts with $D < 2$ mm; volcanic ash particles ash is distinguished into coarse Ash when $D > 64$ μm and < 2 mm and fine ash when $D < 64$ μm ;(Rose and Durant 2009) distinguish fine ash when $D < 1000$ μm and very fine ash when $D < 30$ μm ; the classical spherical model in DEM simulates volcanic ash particles, and the complex physical phenomena of volcanic ash particles such as sublimation and thawing are ignored. The size of volcanic ash particles is simulated as Gaussian distribution, the average value is 3 mm, and the standard deviation is 0.05 according to measure results. The density of volcanic

ash particles on the roof with a certain depth should be initialised in DEM to accelerate the computation.

3.2.11.1 Particle Numbers and Input Modes

The number of volcanic ash particles mainly be committed by the total volume of volcanic ash particles on the roof and the size of volcanic ash particles; when the openings between particles are ignored, the number of particles is given by;

$$P_z = \frac{Q_v}{B_w} \quad (3-26)$$

P_z is the total number of particles in simulation; Q_v is the total volume of volcanic ash particles on the roof in nature; B_w is the average volcanic ash particles volume. (Zhao et al.,2016) equivalent conversion of simulation time with physical time. Supposing that, the number of volcanic ash particles on the roof in simulation and environment is equal;

$$P_z = a_l \quad (3-27)$$

Where a_l is the total number of volcanic ash particles on the roof in nature. Physical time denoted as Z_s is given by;

$$Z_s = \frac{a_l}{a_u A} \quad (3-28)$$

Where $a_u A$ is the number of volcanic ash particles located on the roof per unit of time in nature. Simulations time denoted as T_c is given by;

$$Z_c = \frac{P_z}{a_u T} \quad (3-29)$$

Where auT is the number of volcanic ash particles inlet in the computational domain per unit time in the simulation. The ratio of volcanic ash particles particle inlet in nature and simulation is designated as En ;

$$En = \frac{auA}{auT} \quad (3-30)$$

Considering some particles may run out of the computation domain in the form of a suspension in simulation, an inequality (28) is required.

$$Zc \geq EnZs. \quad (3-31)$$

3.2.11.2 Volcanic Ash Falling on the Roof

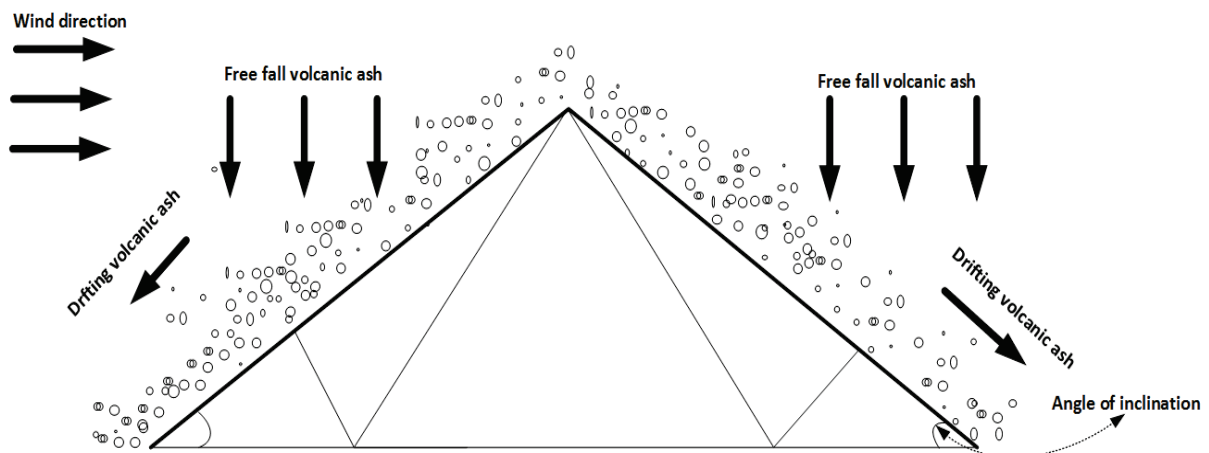


Figure 3.8: Deposition of the Volcanic Ash on Top of the Truss Roof

Figure 3.8 The Figure shows the deposition of the volcanic ash on top of the truss roof. It is known that the elastic force acting between rectangular ('linear'), spherical ('Hertzian') and wedge-shaped contacts should vary with the deformation δ (or the depth of the overlap in our discrete element approach) as δ^1 , $\delta^{3/2}$ and δ^2 , respectively; For symmetry reasons, the

exponent is the same for contacts between equal shapes as between such shapes and planes. The force law based on the area overlap of DEM particles that we explain here will indeed reproduce such dependencies. Even though experiments have been performed with ideally spherical particles. They pointed out that even on technical surfaces, many continuum-mechanical assumptions (such as that the following equations will determine the free fall and damping of the volcanic ash particle on the roof of the building).

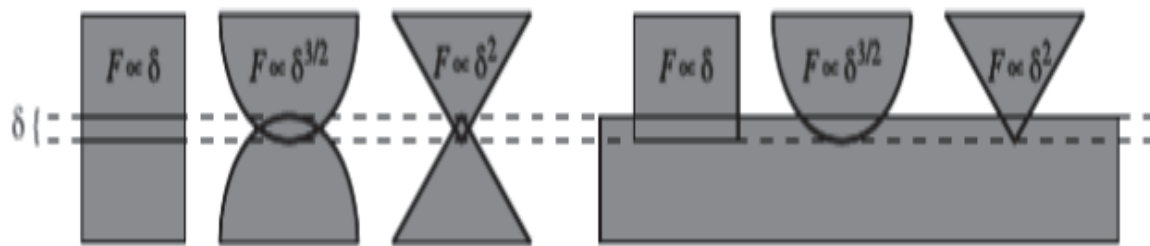


Figure 3.9: Contact Shape and Proportionality Relations of Forces for Particle-Particle and Particle-Line Contacts

Source: Matuttis and Chen (2014).

Figure 3.9 shows contact shape and proportionality relations of forces for particle-particle and particle-line contacts. Matuttis and Chen (2014).

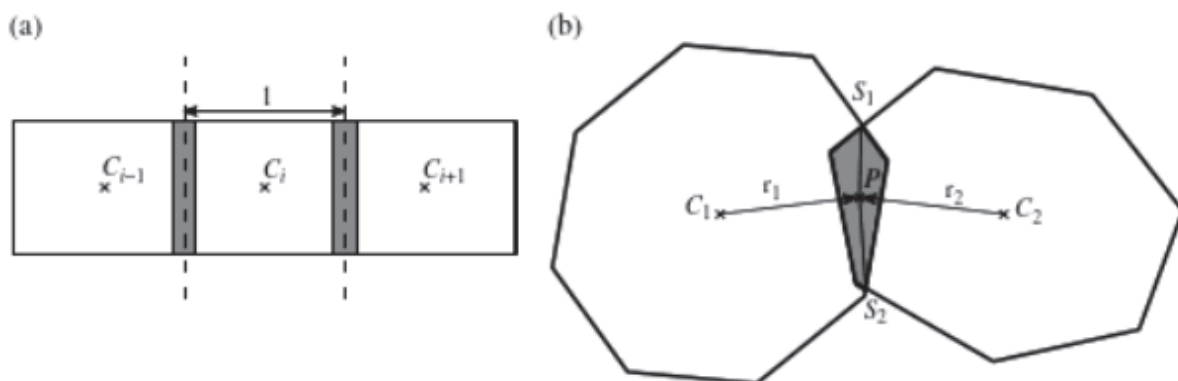


Figure 3.10: Particles Length for a Chain of a Rectangular Particle in Contact with Centroids

Figure 3.10 (a) particles length for a chain of a rectangular particle in contact with centroids at C_{i-1} , C_i , C_{i+1} .(b) variables for the force computation for two interacting polygons: the force point P is the centroid of the overlap polygon S_1 , S_2 are the intersection points of the outlines of the polygons and r_1 Matuttis and Chen (2014).

According to Matuttis and Chen (2014), the relative normal velocity $V \frac{1}{vel}$ is the normal damping can be computed. The equation is the elastic force law.

$$|f^{el}| = Z_{zD} A |l| \quad (3-32)$$

$$T_1 = r_1 \times f$$

$$T_2 = r_2 \times -f$$

Where r_1 and r_2 are the vectors from the centers of mass C_1 and C_2 of the two polygons to the force P. and the total force F acts on the point P.

Where Y_{2D} A Young modulus of which has units [N/m] by the area. A is the magnitude of the force which will be proportioned to the Area A. of overlap between the two-particle. Particle length. The length factor l needed to normalize the sound velocity is obtained from $r_1 = r_1$ and

$$r_2 = r_2 \text{ as } l = \frac{4r_1 r_2}{r_1 + r_2} \quad (3-33)$$

which has the same mathematical form as the reduced mass. (for round particles of equal diameter, this would be practically equal to the particle radius; for squares, it would be the Matuttis, and Chen (2014): Singer, (1992). augured that “Quantitatively, the Poisson ratio would have to be included, but as explained, the relationship between the Poisson ratio, the bulk modulus and Young’s modulus is not as simple as predicted by conventional continuum

theory. Moreover, on particle surfaces, the quantities are not necessarily the same as for the bulk

$$\omega = \sqrt{\frac{Y_2 D}{M^*}} \quad (3-34)$$

$$M^* = \frac{m_1 + m_2}{\frac{1}{m_1} + \frac{1}{m_2}} \quad (3-35)$$

Is the reduced mass of the two particles $m_1 = m_2$ is constant? Can the relation of normal velocity damping be computed according to (Matuttis and Chen 2014)? They explained the area-dependent force law equation. The normal damping should be as follow;

$$\omega = -D \sqrt{\frac{A}{l}} \cdot m^* \cdot v_{1.2} \quad (3-36)$$

l is the characteristics length, and m^* is the reduced mass with the same mathematic form as the reduced mass (Matuttis and Chen 2014). With $m_1 = m_2$

m^* being individual masses of contacting particles. For the collision between a particle of mass m and m_z and a wall (which can be viewed as a particle that will not be moving according to Newton Law of motion), the mass m_2 of the wall would be a very large value. So that m_i is virtually the same as m_i . eq (32) according to (Matuttis and Chen 2014). Matuttis and Chen explained further that the time evaluation of the kinetic energy in a system of 295 particles which were related from a certain height to settle on the floor. As the particles fall, the kinetic energy grows to a maximum. When all particles are deposited on the floor, the energy is dissipated by normal damping and friction (with friction coefficient $\mu=0.3$). If the damping is

truncated, the kinetic energy decays on the kinetic energy is much slower and practically saturated at a constant value.

$$F_{da} = \frac{-D\sqrt{A}}{iM^*} - V \frac{1}{1.2} \quad (3-37)$$

Where i is the characteristic length from the equation and M^* is the reduced mass

$$M^* = \frac{m_1 + m_2}{m_1 + m_2} \quad (3-38)$$

where c_1 and c_2 are the individual masses of contacting volcanic ash particles. The collision between a particle of mass c_1 and a wall and the mass c_2 of the wall would be a very large value so that M^* is virtually the same as the c_1 . According to (Matuttis and Chen 2014). The DEM simulation function is perfectly in a physically meaningful way, one or the other's character. The same approach relates to other descriptions of the mathematical concept regarding models (Matuttis and Chen 2014).

This research will consider both the round and polygonal shape of volcanic ash particles for different sizes particles such as ($< 2 \mu\text{m}$, $< 4 \mu\text{m}$, $< 6 \mu\text{m}$ $< 8 \mu\text{m}$ and, $< 410\mu\text{m}$). There will be simulation interrogation for each size of the volcanic ash. The effects of these on the roof surface, on the other hand, will also be simulated for some mixed-size particles to interrogate the impact of the roof further. That will enhance the knowledge base of the research. There will be a consideration for two dimensions for the volcanic ash.

3.2.11.3 Pitched Roof Boundary Conditions for the Simulation

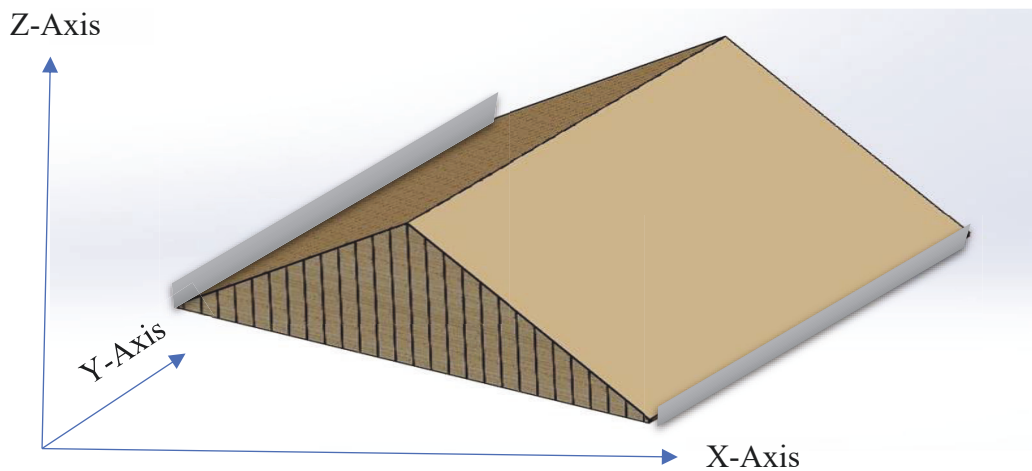


Figure 3.11: Boundary Condition for the Simulation

The pitched roof's boundary condition will be at the front elevation and the roof's back elevation section. The study structure model was based on a scientific approach for the design of the model. It involved an appropriate structure model involving relevant variables. The $1\text{ m} \times 1\text{ m} \times 0.0154\text{ m}$ scaled from $10\text{ m} \times 10\text{ m} \times 0.154\text{ m}$ is appropriate to allow the study to predict the volcanic ash particles' structural behaviour on the flat concrete roof's surface. The tile pitched roof will constrain the model at the roof's edges for both the pitched roof and the flat concrete roof models. It will enable the roof modelling for the DEM and FEM simulations based on static actions appropriate for the pressure load for deformation, stress and strain relationships of the members and their connections and between members of the roof. (EN 1991 to EN 1999). The DEM and FEM model simulation will determine the action effects to establish the interpretations of relevant structural members, their masses, strength, stiffness and damping characteristic, and all relevant non-structural members with their properties. The process may involve the dynamic actions as quasi-static; may consider dynamic parts either by including them in the static values or applying equivalent dynamic amplification factors to the static

actions according to the BS EN 1990:2002+A1:2005 EN 1990:2002+A1:2005 (E). Please, refer to Appendix B for further information on the boundary conditions.

CHAPTER FOUR

4.0. RESULTS

This section will compile the DEM (implementing the EDEM) and the FEM (Implementing the COMSOL) software for the preliminary investigation's simulation data. However, it is not the key approach for the study. Therefore, the section will also compile the Discrete Element Method DEM and Finite Element Method (FEM) Simulations, the main key simulation approach for the study.

4.1 Discrete Element Method DEM and Finite Element Method (FEM) Simulations

4.1.1 Preliminary Results

A simulation test with a volcanic ash layer pressure on a flat concrete roof shows deflection is inversely proportional to the roof's thickness and its moment of inertia. The research was an ongoing study, and further work was required; and the study will assess the volcanic ash effects of changing density on various roofing materials to determine the stress impact, maximum deflection, and the roof's collapse failure due to volcanic ash pressure. The test's concrete model was ($10\text{ m} \times 10\text{ m} \times 0.154\text{ m}$) with volcanic ash deposition on the roof, as this model is scaled to 1:10 to create a unit per meter square of the simulation model. In addition, the following assumption was considered as stated in Chapter 3.

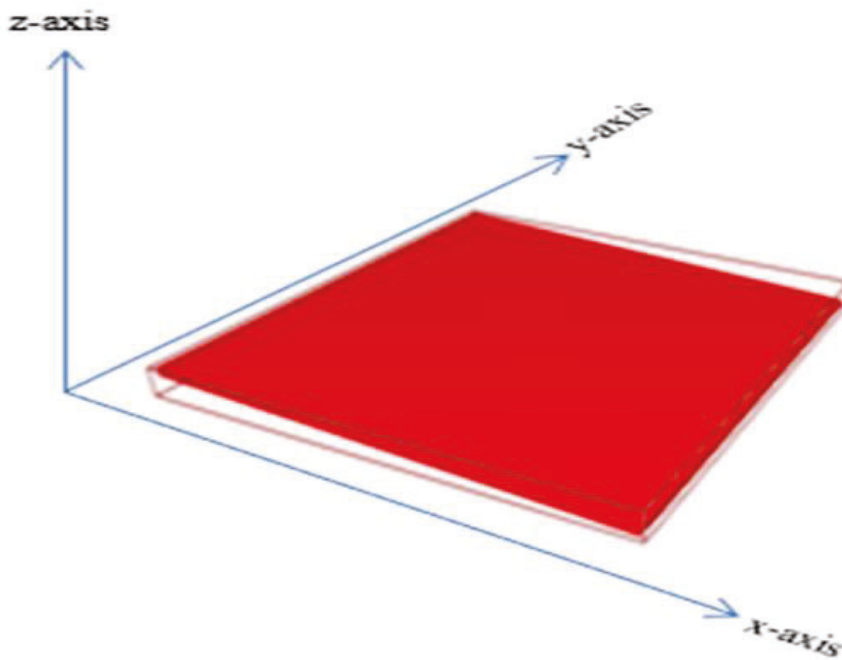


Figure 4.1: Concrete Roof Model

A DEM numerical modelling is implemented in (EDEM software) to investigate ($1\text{m} \times 1\text{m} \times 0.0154$) m concrete slabs with 10 mm size volcanic ash deposition particle loadings on the flat concrete roof. The research follows a multi-method approach. First, numerical modelling for the Discrete Element Method DEM modelling and the Finite Element Method (COMSOL) simulation tool is deployed to interrogate the volcanic ash effects loadings on a flat concrete roof within the roof within the current EN1991 code. O'Sullivan (2015) stated that COMSOL (FEM) Multiphysics is a commercial finite element engine that can solve a large variety of pre-programmed partial differential equations (PDEs) instantaneously. He further states that COMSOL(FEM) has two main interfaces for geoscience and geotechnical applications: subsurface movement and geomechanics modules. The phenomena that can model include stress-strain behaviour, etc. Can custom partial differential equations (PDEs), ordinary differential equations (ODEs), and initial value problems be quantified without programming through a graphical user interface? The study also used this approach to determine the roof's

stress and deformation effects to determine the simulation process. COMSOL Multiphysics (FEM) is a multipurpose interface that allows data to be swapped between continuum models based on the particle scale model. The discrete element method DEM can shape COMSOL models through a graphical user interface. Each model is described by a model tree which includes a series of nodes that describe the model geometry, material properties, boundary conditions, PDE, solutions, etc. The information associated with these nodes can be accessed and modified by JAVA classes or MATLAB scripts.

The results obtained below in figure 4.2 and figure 4.3 use the Finite Element Method (COMSOL) simulation by applying a pressure of 500 N/m^2 (due to the ash load) combined with the roof self-weight

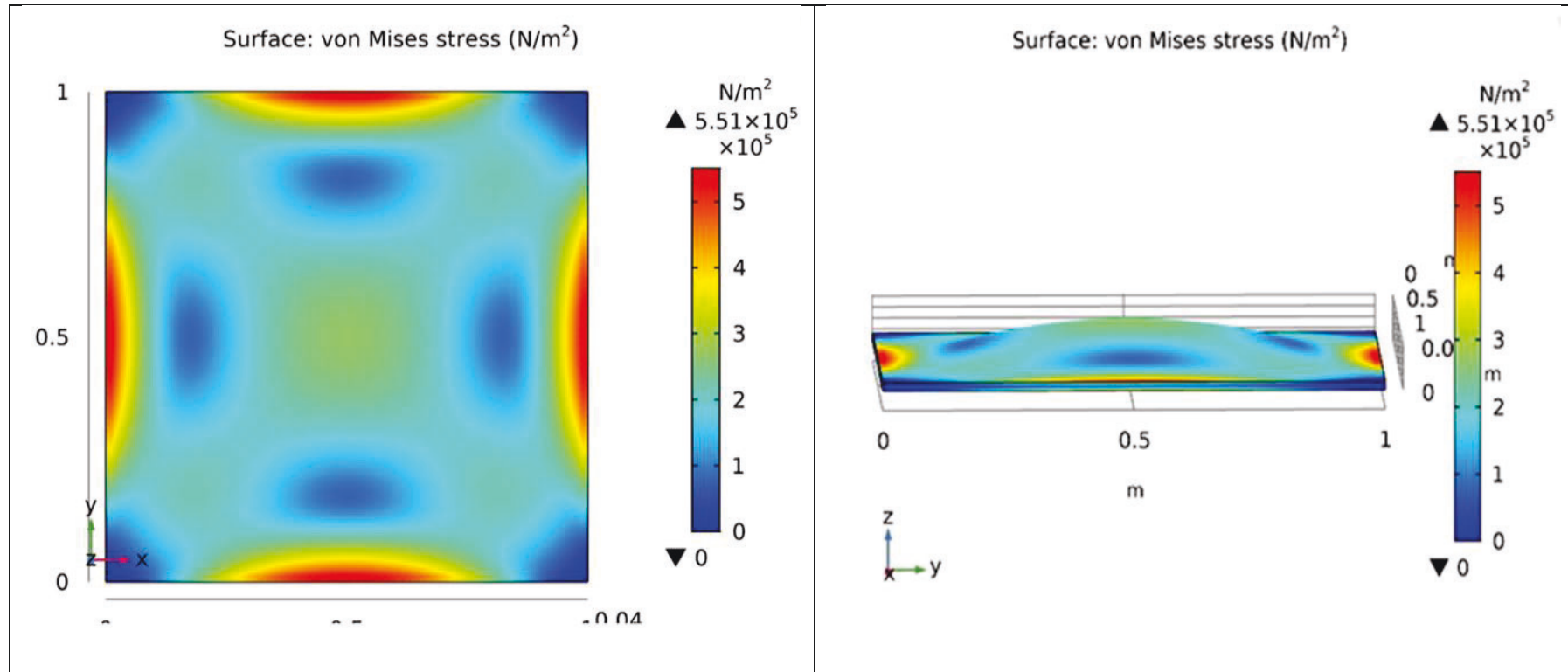


Figure 4.2: Result for Finite Element Method (FEM) Simulations.

Figure 4.2 shows the Finite Element Method (COMSOL) simulation results by applying a pressure of 500 N/m² (due to the ash load) combined with the roof self-weight. The red spots show where the stress is acting, and a parabolic shape indicates the stress acting on the flat concrete roof plate. The stress results are 5.51×10^5 (N/m²).

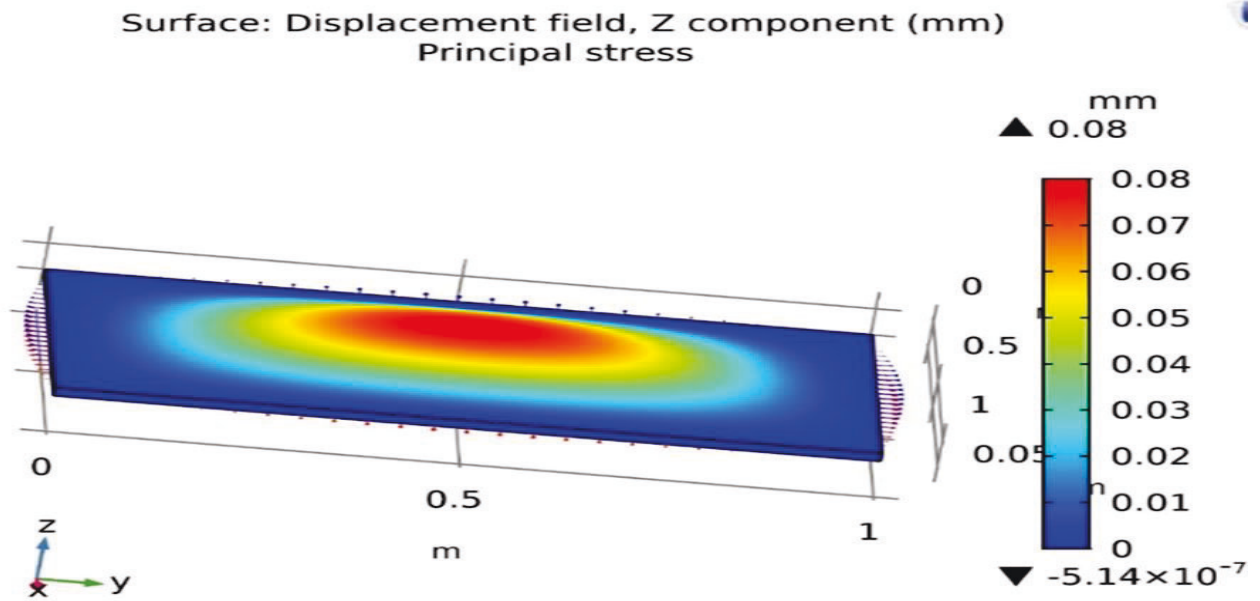
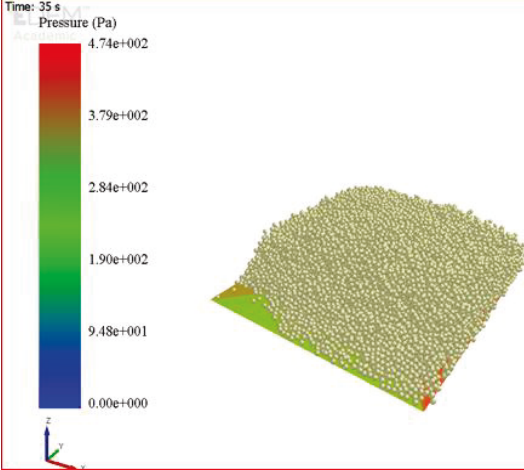
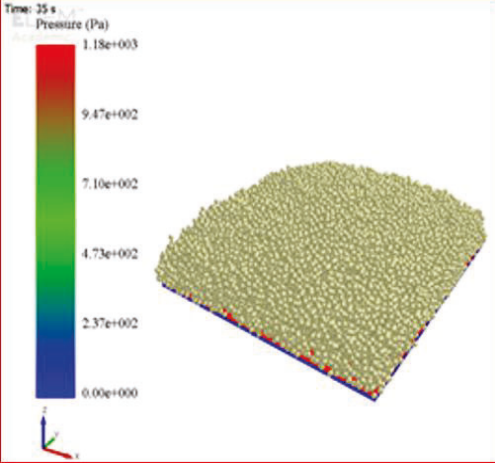


Figure 4.3: Result for Finite Element Method (FEM) Simulations.

Figure 4.3 shows the Finite Element Method (COMSOL) simulation results by applying a pressure of 500 N/m^2 (due to the ash load) combined with the roof self-weight. The red spots show where the displacement area on the flat concrete roof plates. The arrows indicate the stretching of the pressure loadings on the roof. The displacement results are 0.08 mm impact which on the vies of the study will have a significant impact on the roof.

Table 4.1: Result for Discrete Element Method (DEM) Simulations

Type of roof model plate	Model angle of inclination (degrees)	Volcanic Particle size (mm)	Particle loading (Number)	Particle Densities (kg/m ³)	Simulation with wind effects results	Simulation without wind effects results	DEM Simulation with wind effects pressure (Pa) Recorded.	Simulation without wind effects pressure (Pa) Recorded.
Flat concrete roof	2 degrees	10	170,000	1000			9.48e+001, 1.90e+002, 2.84e+002, 3.79e+002, 4.74e+002.	2..37e+002, 4.73e+002, 7.10e+002, 9.47e+002, 1.18e+003.

3

Table 4.1 shows the results from figure 4.1. The first column is the type of roof (Flat concrete roof). The second is the angle of inclination of the flat concrete roof, and the third vertical column is 10 mm size diameter of the volcanic ash particles. The fourth vertical column is the 170,000 volcanic ash particles simulated. The fifth vertical column is the DEM simulation rest for the wind effects, and the sixth column is the DEM image results for the wind effect, and the sixth vertical column is the DEM image results for the no wind effect. The seventh column is the DEM simulation with wind effect pressure(Pa). Finally, the eighth vertical column is the DEM simulation with no wind effect pressure (Pa) maximum pressure loading of the 10 mm volcanic ash particles values, was used to uniformly distributed on the z-axis on the flat concrete plate to determine the maximum stress and the maximum displacement values as shown in figure 4. 5 to figure 4.8 below.

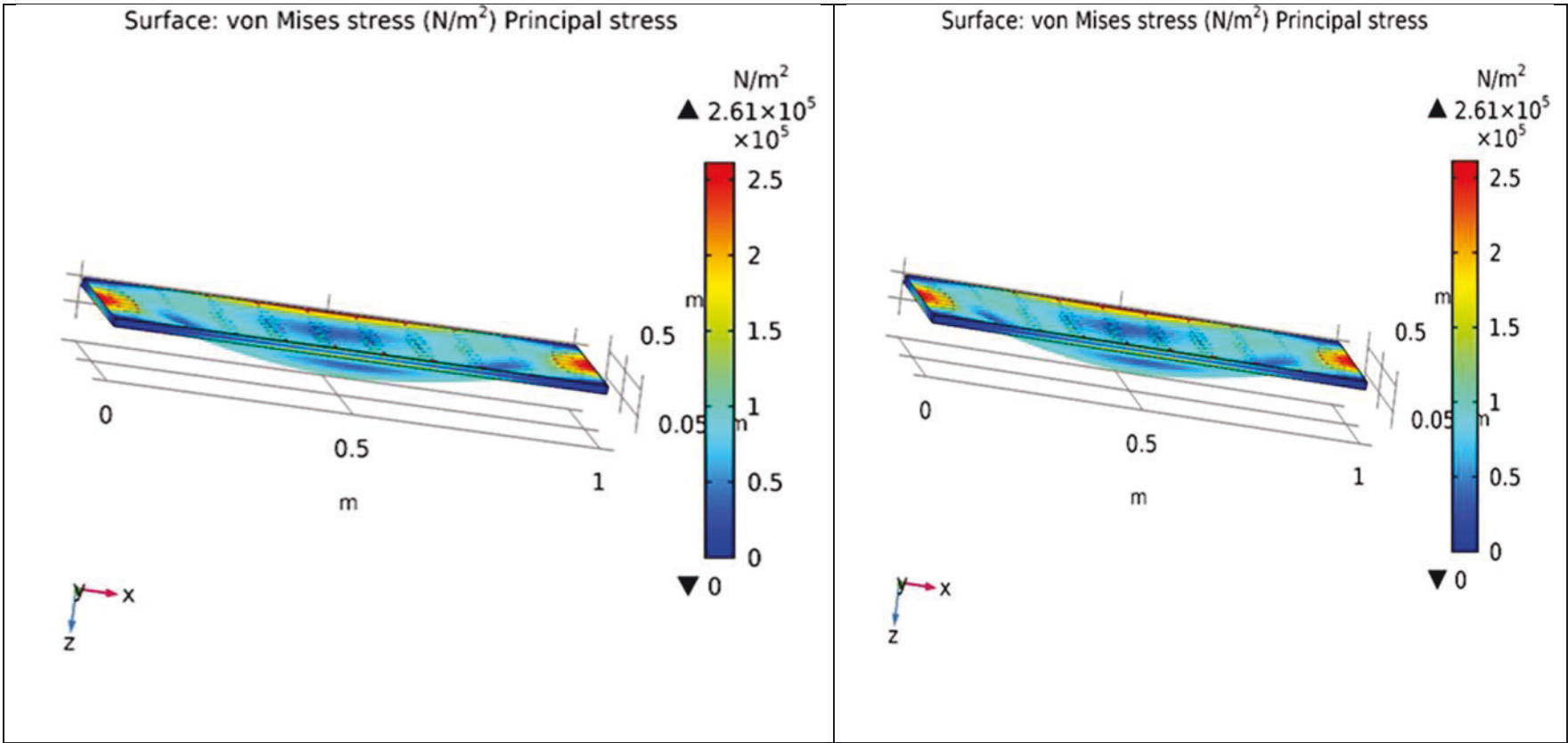


Figure 4.4: DEM Results for Finite Element Method (COMSOL) For Stress with No Wind Effects

Figure 4.5: DEM Results used for the Finite Element Method (COMSOL) tool simulation to determine stress with no wind effects. Figure. 4.4: shows the results using the finite element method (COMSOL) tool simulation to determine the stress and the displacement with wind effects. The image on the left side shows the concave nature of the volcanic ash loading effect on the roof, while the right-side image shows the red spots where the stress is acting on the roof. The results indicate the maximum stress reading as $2.61 \times 10^5 \text{ N/m}^2$ for the no wind effect

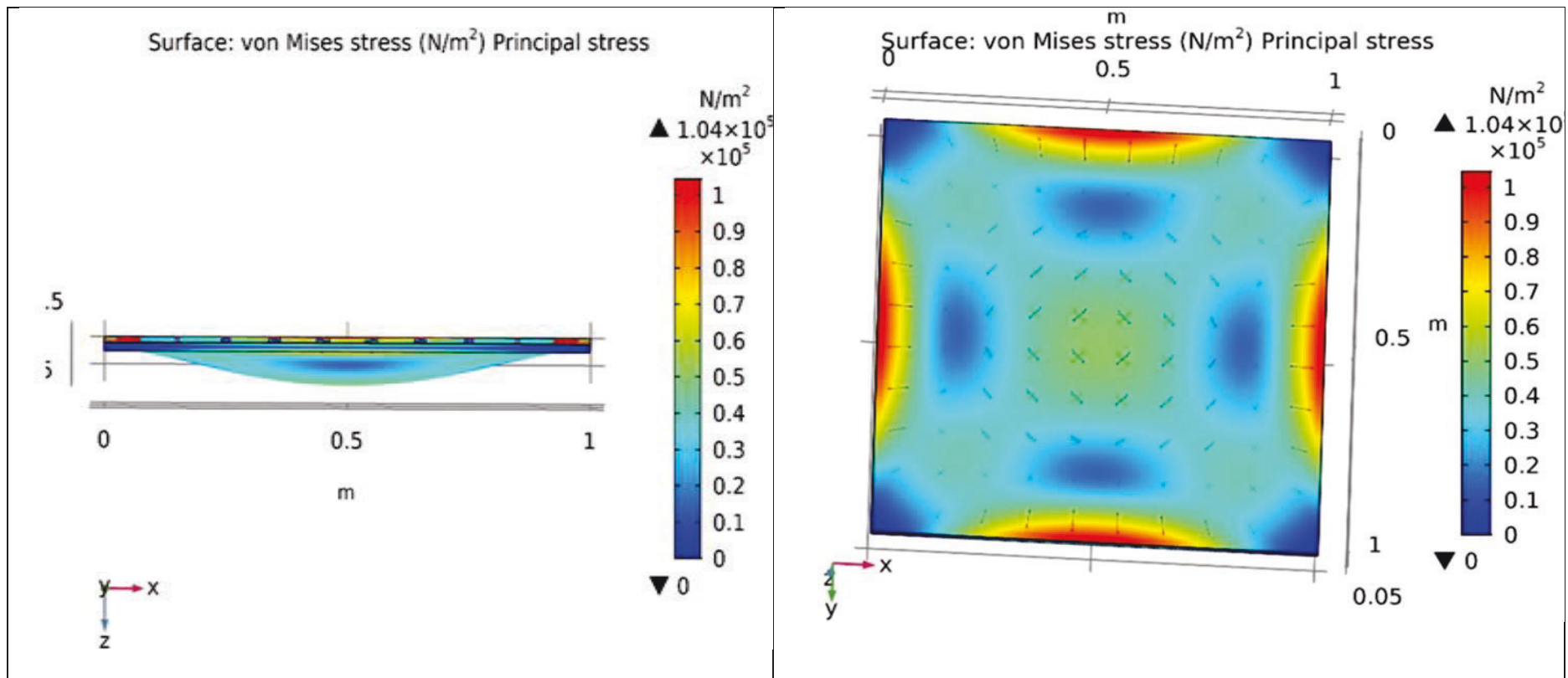


Figure 4.5: DEM Results for Finite Element Method (COMSOL) For Stress with Wind Effects

Figure 4.5: DEM results used for the Finite Element Method (COMSOL) tool simulation to determine stress with wind effects. Figure. 4.5 shows the Finite Element Method (Comsol) tool simulation results to determine the stress and displacement with wind effects. The image on the left side shows the concave nature of the volcanic ash loading effect on the roof, while the right-side image shows the red spots where the stress is acting on the roof. The results indicate the maximum stress reading as $1.04 \times 10^5 \text{ N/m}^2$ for the no wind effect.

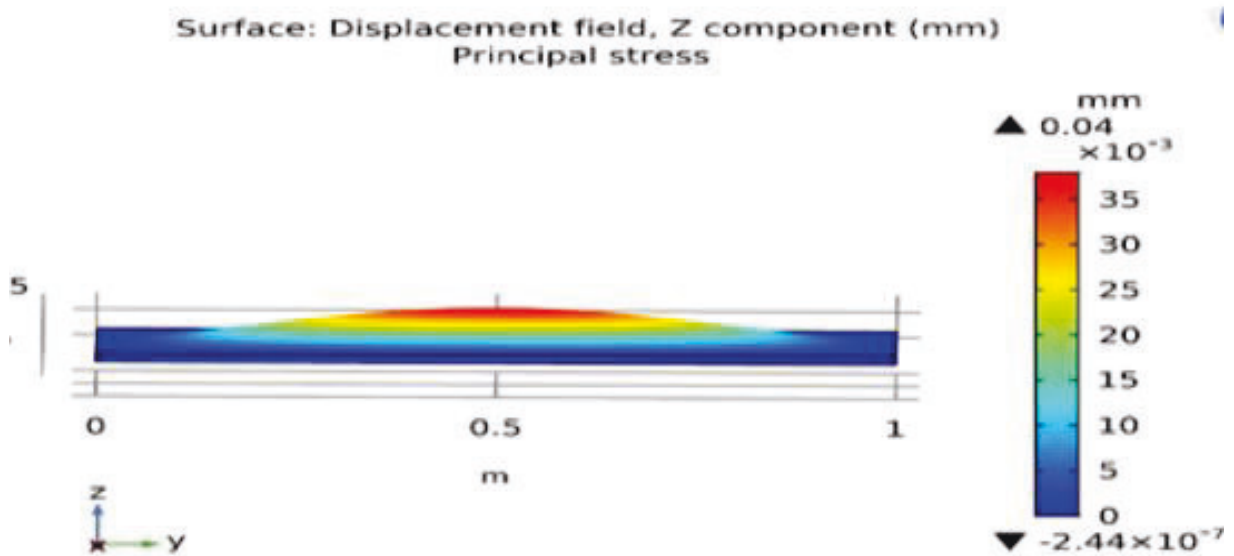


Figure 4.6: DEM Results for Finite Element Method (COMSOL) for Displacement with no Wind Effects

Figure. 4.6 results using the Finite Element Method (Comsol) to determine the Displacement with No wind effects. Figure. 4.7 shows the Finite Element Method (Comsol) tool simulation results to determine wind effects stress. The image shows the parabolic displacement effect of the volcanic ash loading on the roof, and the results indicate the maximum displacement reading as 0.04 mm.

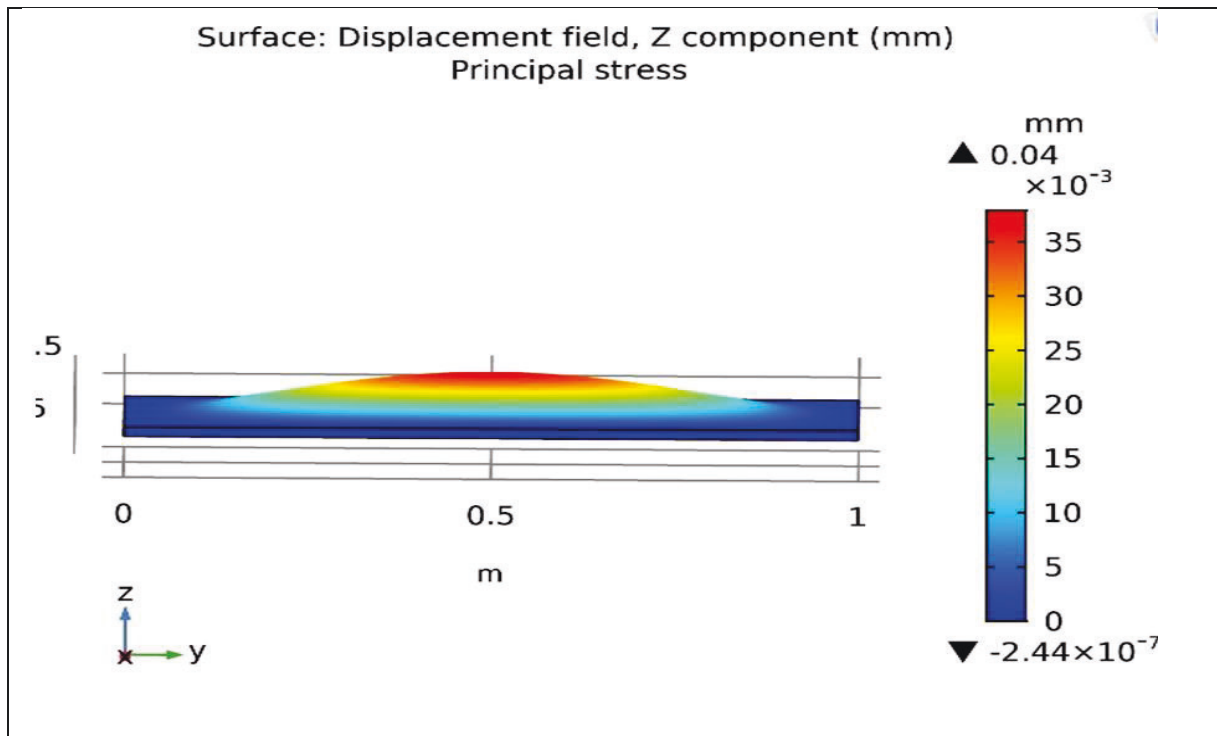


Figure 4.7: DEM Results for Finite Element Method (COMSOL) for Displacement with No Wind Effects

Figure 4.7 shows results using the Finite Element Method (Comsol) to determine the wind effects. The Finite Element Method (Comsol) tool simulation results to determine the stress with wind effects; the image shows the concave displacement nature effect of the volcanic ash loading on the roof. The results indicate the maximum displacement reading at 0.02 mm.

The section shows the DEM results are used to predict the uneven distribution of the volcanic ash loads on the roof surface, which are then transferred onto the FEM to determine stress and deformation levels. The results of the study will have a potential impact on the designs of buildings and flat roofs.

Time: 0.990014 s
EDEM™
Academic

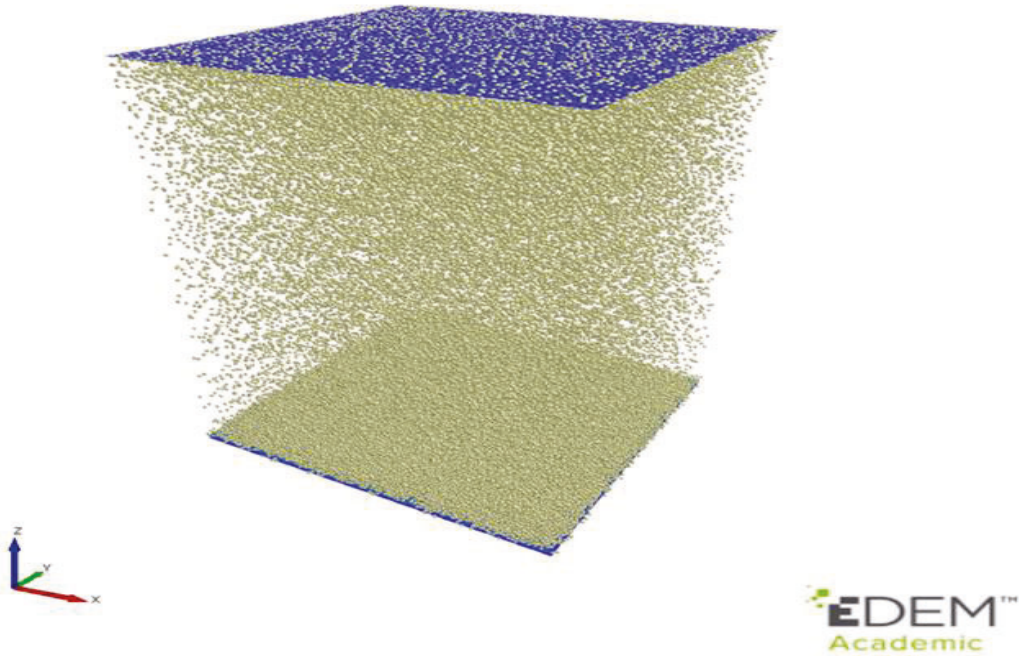
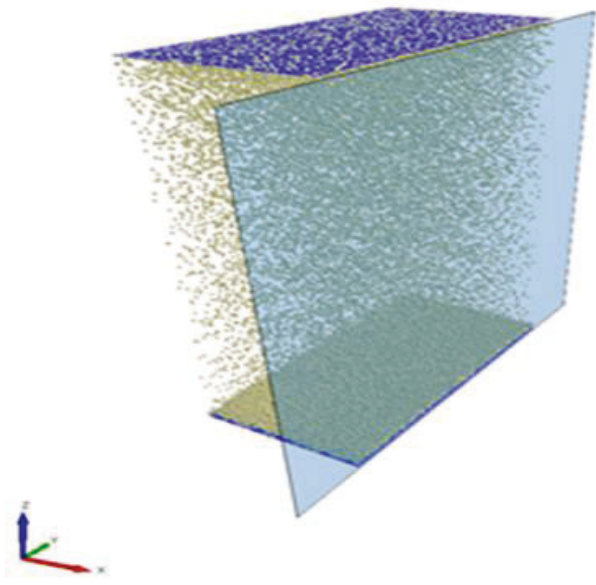


Figure 4.8 Volcanic Ash Particles Generated from the EDEM

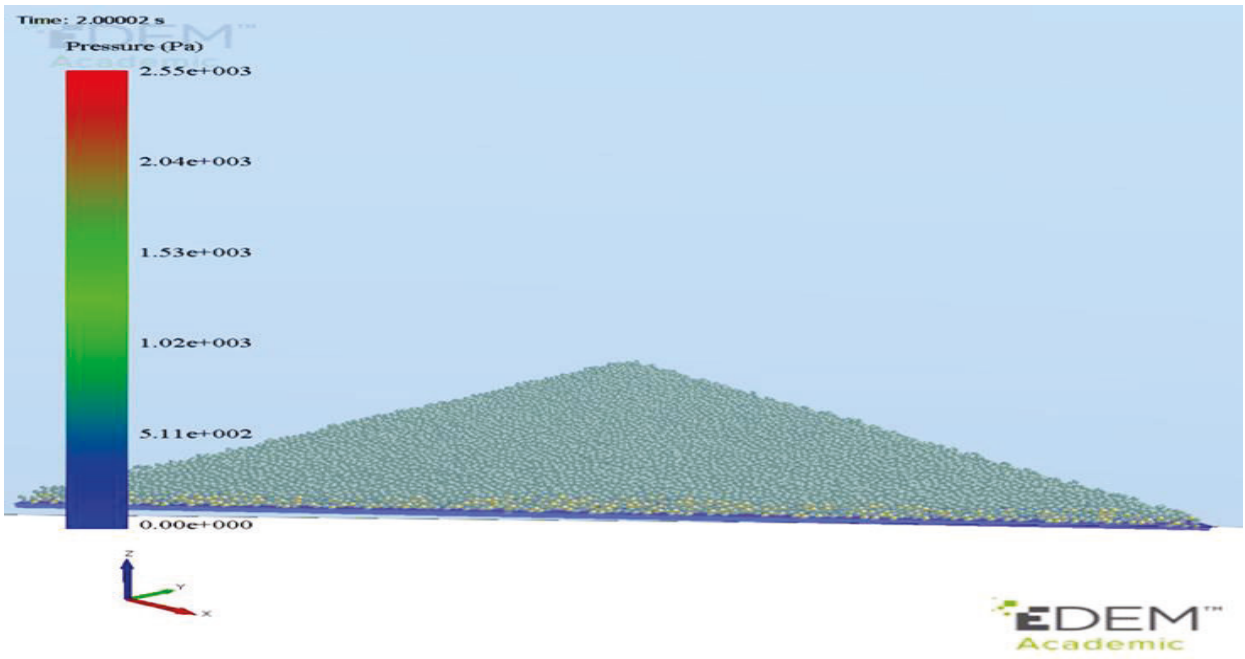
Figure 4.8 Volcanic ash particles generated from the EDEM volcanic ash particle factory falling and settling on the concrete roof during the simulation.

Time: 0.990014 s
EDEM™
Academic



EDEM™
Academic

Figure 4.9: Sliced Section of the Volcanic Ash Particles' Internal Structure Falling and Settling on the Concrete Roof.



EDEM™
Academic

Figure 4.10: Volcanic Ash Particles Deposition on the Concrete Roof Plate with the Pressure Load

Figure 4.10 The image shows a symmetrical section of the roof plate volcanic ash particle deposition on the flat concrete roof plate with the pressure load for the DEM simulation test result.

4.2 Discrete Element Method (DEM) and the Finite Element Method (FEM) modelling simulation approach.

The study usage of the EDEM Add-in for the ANSYS workbench. The study is wearing to carry out the simulation that allows the volcanic ash particle to fall onto the roof models. However, it also allows data transfer to be exported to some compatible software for further simulations. An example of such compactable software is the ANSYS for the finite element simulation. The process of carrying out the research using the DEM and the FEM is illustrated the figure 4.11A as follows:

Flow Chart for Simulation of (EDEM Software) DEM and FEM for the Structural Analysis (ANSYS) Tool

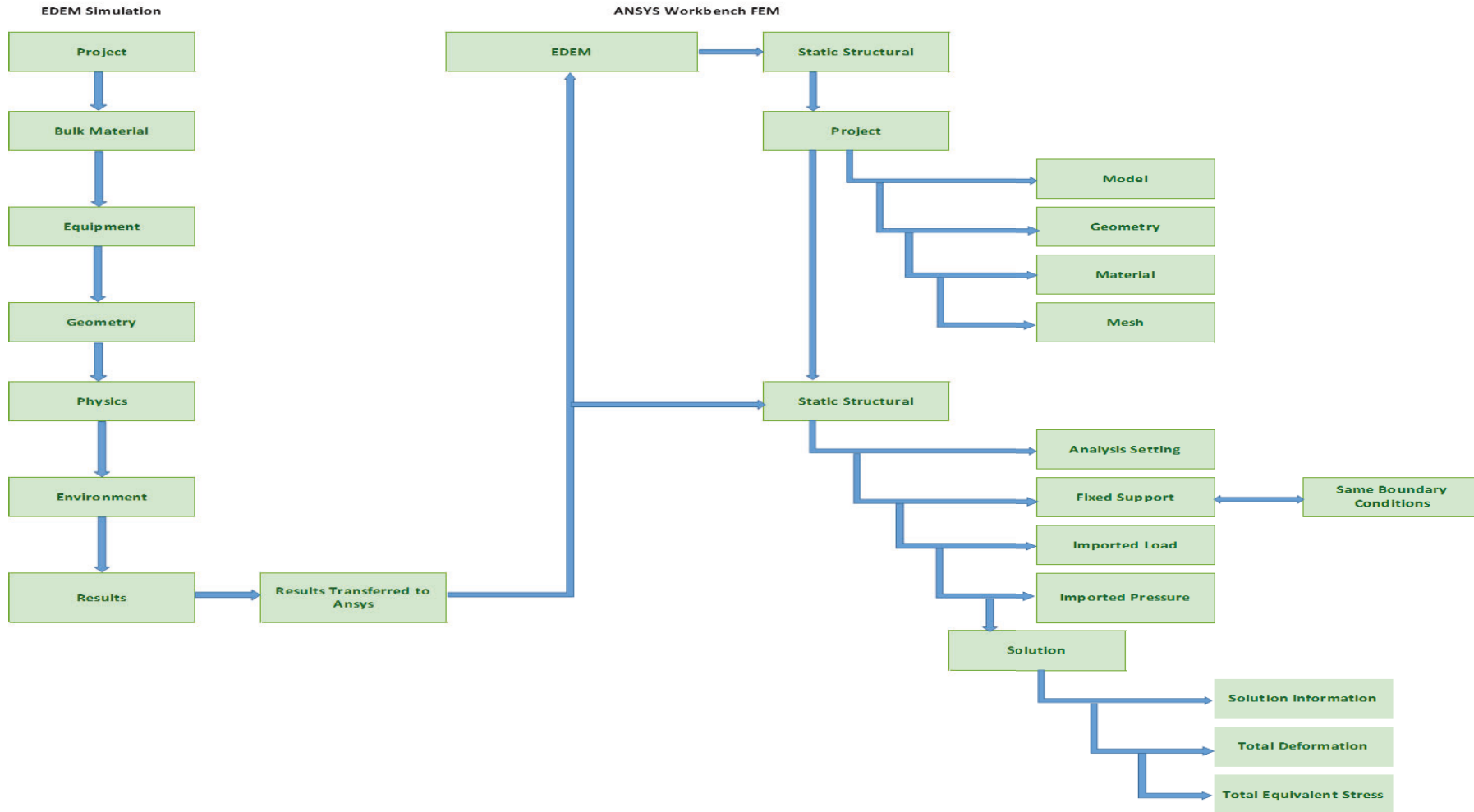


Figure 4.11: DEM and FEM Co-Simulation for the Structural Analysis (ANSYS) Tool

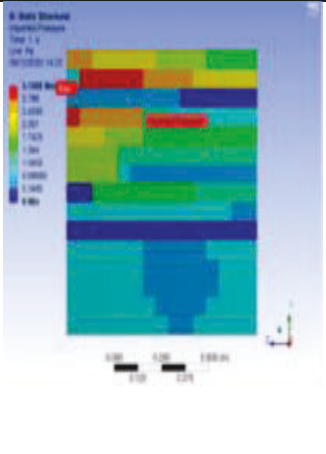
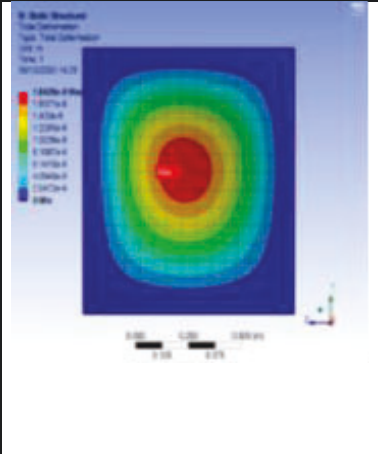
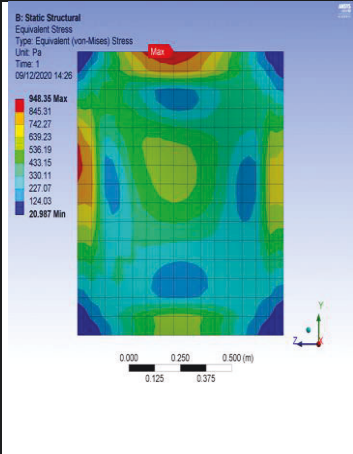
Figure 4.11 illustrates the study's summary approach for the systematic steps method used for the DEM and FEM co-simulation for the structural analysis (ANSYS) tool. The model created in solid works for the pitched roof and the flat concrete roof is exported to the structural analysis (ANSYS) tool. The steps include the DEM simulation test to get the maximum pressure of the volcanic ash particles. The maximum pressure result is imported to the structural analysis (ANSYS) tool to determine the maximum pressure. The FEM structural analysis (ANSYS) tool constrains the model to determine the maximum deformation simulation results, the maximum von Mises stress, and the maximum strain of the modelling roofs. The colures below indicate the various recordings from the lowest level from the blue colure and the highest (maximum) recordings for the FEM simulations results as shown in the figure below.



Figure:1.12 Coloured coding for the various test results for the FEM simulation test.

The colour coding shows the effects of the ash from the lowest level, indicating the blue colour to the red colour coding being the highest loading level on the roof during FEM simulation.

Table 4.2: Numerical Modelling Tool (EDEM Software) for Discrete Element Method (DEM) and Structural Tool (ANSYS) with No Wind Effect.

Volcanic Ash Particle Size in Diameter (mm)	Volcanic Ash Particle densities (Kg/m ³)	DEM Maximum Pressure (Pa)	FEM Maximum Deformation (mm)	FEM Maximum von Mises stress (MPa)	FEM Imagery Results shows the distribution of pressure load (Pa)	FEM Imagery Results shows the distribution of deformations (mm)	FEM Imagery Results shows the distribution of von Mises stress (MPa)
1	1000	3.13646	1.842e-5	0.0094835			

Note: Table 4.2 above illustrates the No Wind Effect imagery results showing the distribution of pressure load, deformations, and von Mises stress.

Table 4.2: shows the results below that were tabulated from the numerical modelling tool (EDEM software) for the Discrete Element Method (DEM) and structural analysis tool (ANSYS) for the Finite Element Method (FEM) simulation. The first column is the volcanic ash particle size in diameter (mm). The second is the volcanic ash particle densities (Kgm³).

The third column is the DEM maximum pressure Loadings (Pa). The fourth column is the FEM maximum deformation (mm). The fifth column is the DEM simulation stress for the wind effects, and the sixth column is the DEM image results FEM maximum stress (MPa), and the sixth column is the DEM image results. Finally, the seventh column is FEM image results for maximum deformation (mm), and the eight-column FEM image results in maximum Stress (MPa). This section is linked to table 4.4 result and table 5.1 results data for the 160,000 volcanic ash particles for the no wind effects simulation.

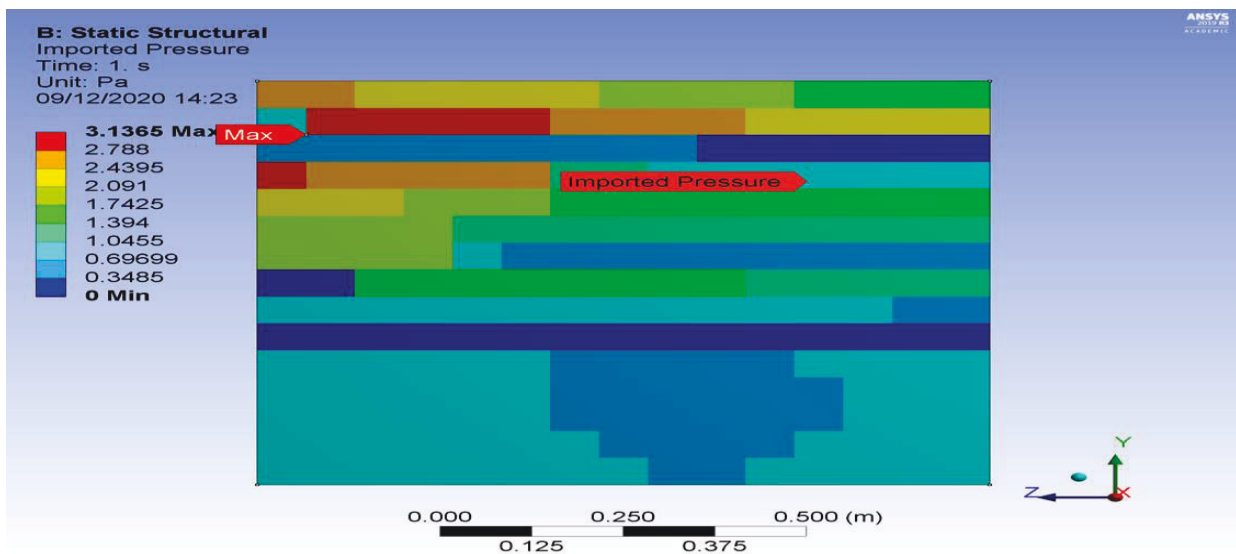


Figure 4.13A: DEM Imagery Results showing the Distribution of Pressure Load (Pa)

Note: Figure 4.13A is an extract from Table 4.2 and it shows a set of results No Wind Effect imagery results show the distribution of pressure load (Pa), the distribution of deformations (mm) and the distribution of stress (MPa).

As indicated, the various colours show the various effects of the pressures on the roof. As indicated in Figure 12, the blue colours show the lowest effect of the pressure on the and the corresponding increase of the volcanic ash pressure load effect on the roof to the red colours, which is the higher (maximum) pressure effects as a result of the volcanic ash loading on the roof. This colour coding relates to the FEM simulation test results for all tests. The value pressure is 3.1365 Pa as the highest. Therefore, the red spot of the roof shows the maximum pressure loading effects on the roof, whereas the blue colours show the lowest pressure on the roof.

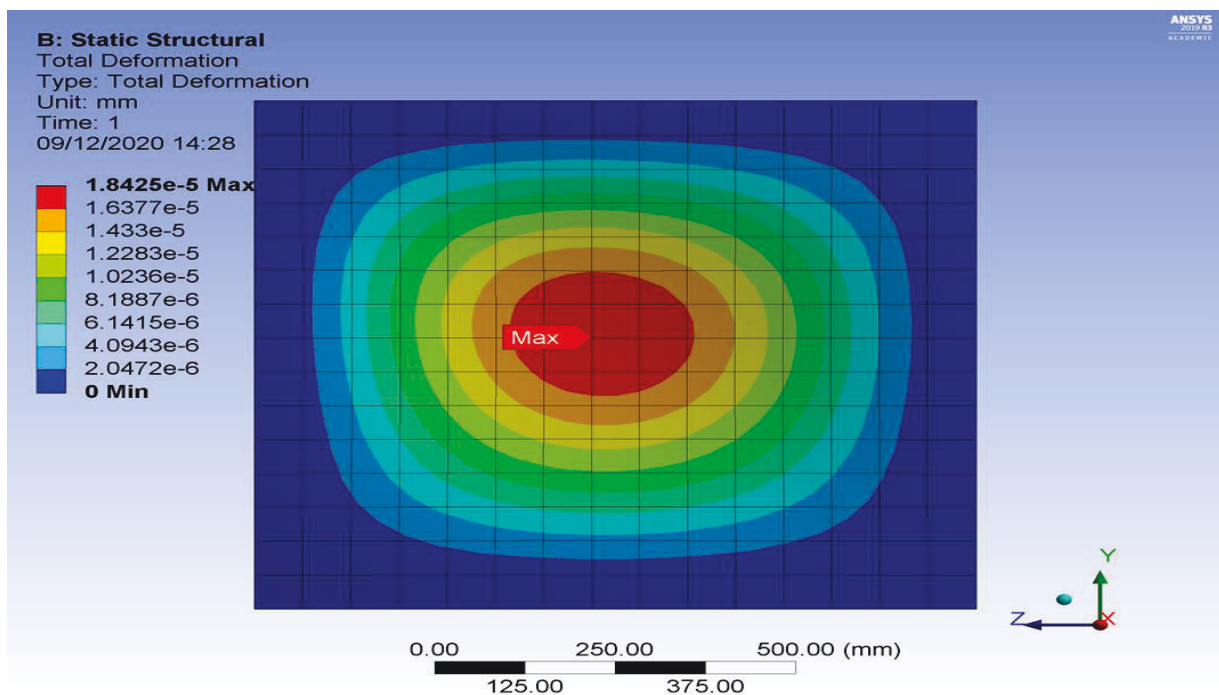


Figure 4.13B: FEM Imagery Results showing the Distribution of Deformations (mm).

Note: Figure 4.13B: Extracted from Table 4.2: shows a set of results No Wind Effect imagery results show the distribution of pressure load (Pa), the distribution of deformations (mm), and the distribution of stress (MPa).

The figure shows the various colour coding for the total deformation, as shown in the figure. The red spot shows the maximum deformation on the roof, which can have many effects. The deformation occurs in the centre of the roof, and it causes the expansion of the roof. The rest of the colour coding will not have a detrimental effect on the roof compared to red. The highest value is 1.8425×10^{-5} mm maximum.

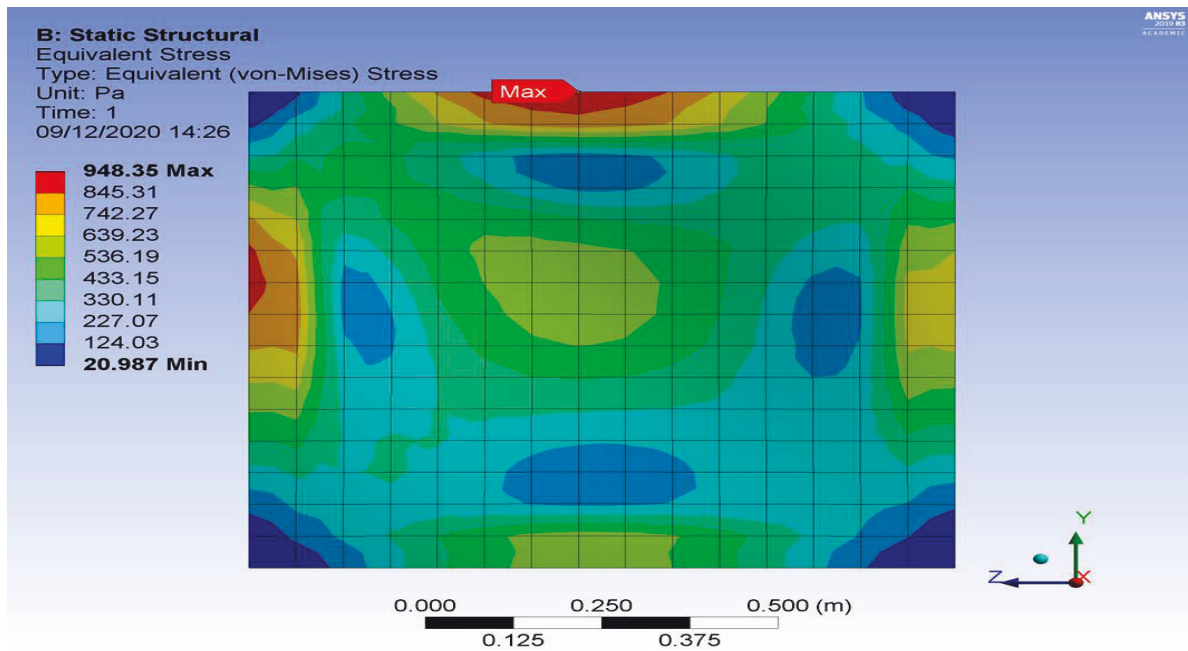
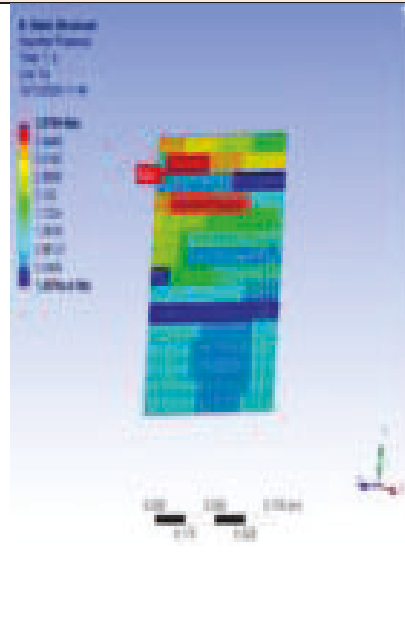
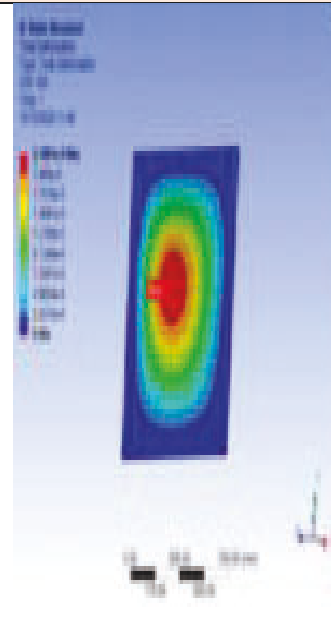
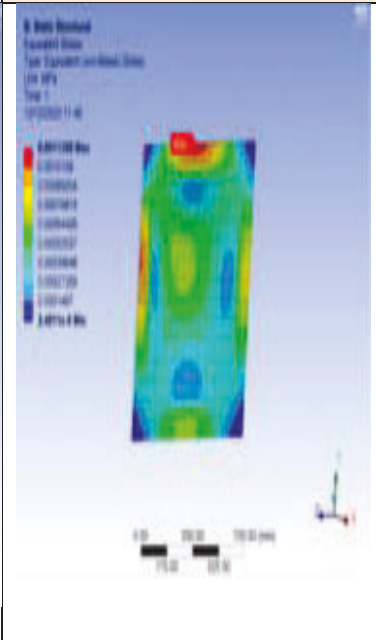


Figure 4.13C: FEM Imagery Results showing the Distribution of von Mises Stress (MPa)

Note: Figure 4.13C is an extract from Table 4.2 and it shows a set of results No Wind Effect imagery results show the distribution of pressure load (Pa), the distribution of deformations (mm), and distribution of stress (MPa).

The static structured equivalent stress is indicated in the image results; the red spots show the highest stress value of 948.35 (MPa) maximum compared to the lowest stress values on the roof. Therefore, the other colours will not have many such devastating effects on the roof compared to the red spots.

Table 4.3: Numerical Modelling Tool (EDEM software) for Discrete Element Method (DEM) and Structural Tool (ANSYS) with Wind Effect

Volcanic Ash Particle Size in Diameter (mm)	Volcanic Ash Particle densities (Kg/m ³)	Horizontal direction (ms ⁻¹)	Maximum Pressure (Pa)	Maximum deformation (mm)	FEM Maximum von Mises stress (MPa)	FEM Imagery Results shows the distribution of pressure load (Pa)	FEM Imagery Results shows the distribution of deformations (mm)	FEM Imagery Results shows the distribution of von Mises stress (MPa)
	1000	0.1	3.8754	2.1881e-5	0.0011398			

Note: Table 4.3.: was extracted from Table 4.4: and it shows a set of results No Wind Effect Imagery Results shows the distribution of pressure load (Pa), the distribution of deformations (mm), and the distribution of von Mises stress (MPa).

The first column is the volcanic ash particle size in diameter (mm), and the second is the volcanic ash particle densities (Kg m^{-3}). The third column is the Horizontal direction (ms^{-1}). The fourth column is the Maximum Pressure (Pa). The fifth column is the Maximum Deformation (mm), and the sixth column is the DEM Maximum Stress (MPa), the seventh column is FEM Imagery Results that show the distribution of pressure load (Pa). The eighth column is FEM Imagery Results shows the distribution of deformations (mm), and the ninth - FEM Imagery Results show the stress distribution (MPa).

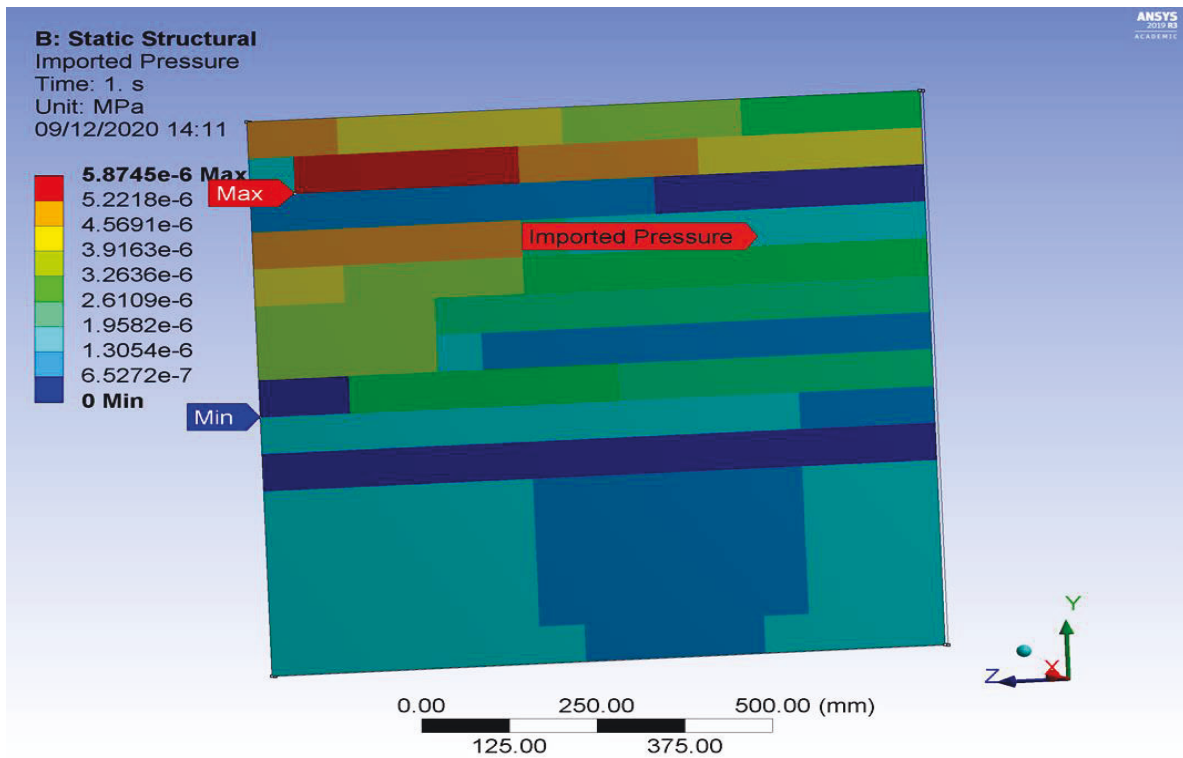


Figure 4.14A: FEM Imagery Results showing the Distribution of Pressure Load (Pa)

Note: Figure 4.14A is an extract from Table 4.3 and it shows a set of results No wind effect imagery results show the distribution of pressure load (Pa), the distribution of deformations (mm), and distribution of stress (MPa).

As shown in the image, the red spot is the highest volcanic ash loading pressure point on the roof, with the record values as 5.8745×10^{-6} Pa maximum and the lowest volcanic ash loading pressure recorded as 0 Pa for the blue colour did. Therefore, the rest of the colour coding with the corresponding values will not have any devastating effects on the roof.

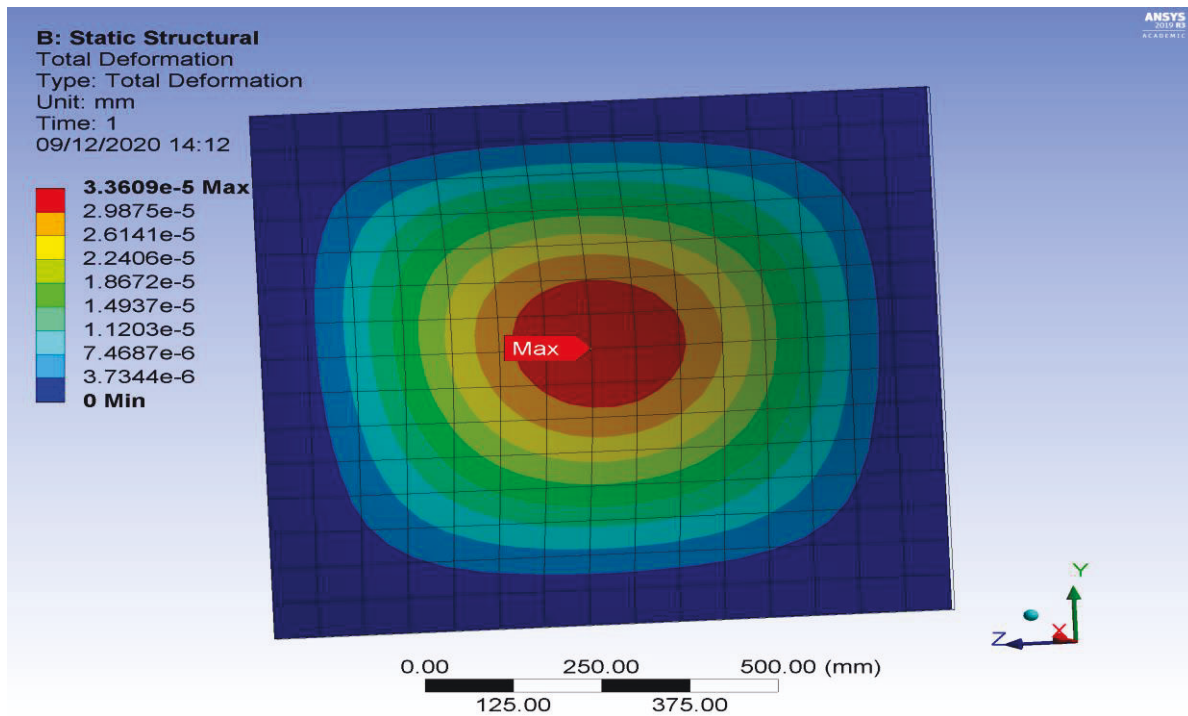


Figure 4.14B: FEM Imagery Results showing the Distribution of Deformations (mm)

Note: Figure 4.14B is an extract from Table 4.3 and it shows a set of results No Wind Effect imagery results show the distribution of pressure load (Pa), the distribution of deformations (mm), and distribution of stress (MPa).

The static structured total deformation image shows that the roof's deformation occurred in the middle of the roof, which could have a devastating effect. The deformation value on the roof as shown is 3.3609×10^{-5} mm as shown. The rest of the colour coding will not have much on the roof.

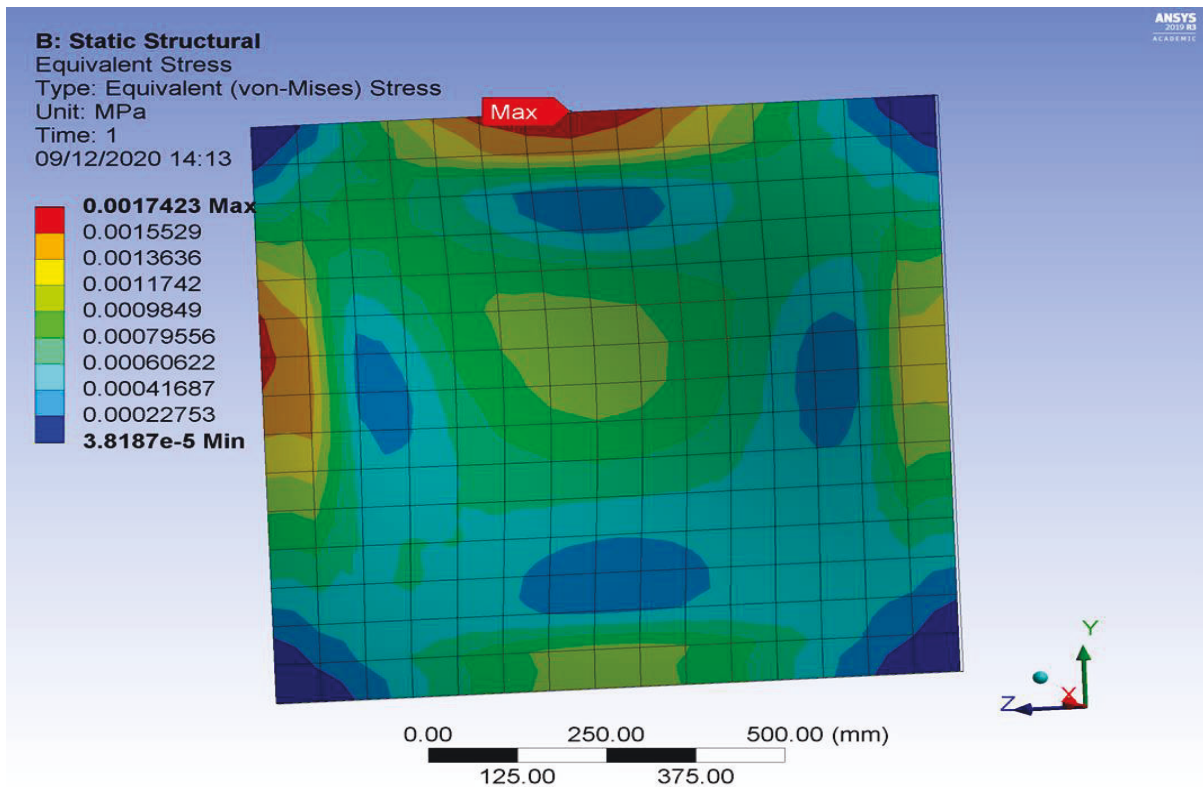


Figure 4.14C: FEM Imagery Results showing the Distribution of von Mises Stress (MPa)

Note: Figure 4.14C is an extract from Table 4.3 and it shows a set of results No Wind Effect Imagery Results show the distribution of pressure load (Pa), the distribution of deformations (mm), and the distribution of stress (MPa).

The static structured equivalent stress indicates that the red colour coding is the highest recorded value recorded as 0.001423 MPa compared to the lowest stress value recorded as 3.8187×10^{-5} mm MPa. Therefore, apart from the red colour, coding will not have many effects on the roof.

Table 4.3: shows the results below were tabulated from the numerical modelling tool (EDEM software) for the Discrete Element Method DEM and structural analysis tool (ANSYS) for the Finite Element Method (FEM) simulation. The first column is the volcanic ash particle size in diameter (mm), and the second vertical is the volcanic ash particle densities (Kgm^{-3}). The third column is the Horizontal wind direction of $0.1 \text{ (ms}^{-1}\text{)}$. Finally, the fourth column is the DEM maximum pressure Loadings (Pa).

The fifth column is the FEM maximum deformation (mm). The sixth column is the DEM simulation rest for the wind effects. The seventh column is the DEM image results FEM Maximum Stress (MPa), and the eighth vertical columns are the DEM image results. The ninth vertical column is the FEM Image Results for Maximum Deformation (mm), and the eighth column FEM image results for Maximum Stress (MPa). This section is linked to table 4.5 and table 5.2 results data for the 160,000 volcanic ash particles for the wind effects simulation. Figure 4.14 shows DEM Imagery Results shows the distribution of pressure load (Pa), FEM Imagery Results shows the distribution of deformations (mm), and the FEM Imagery Results show the distribution of stress (MPa). The results below were tabulated from the numerical modelling tool (EDEM software) for the Discrete Element Method DEM and structural analysis tool (ANSYS) for the Finite Element Method (FEM) simulation.

The results below were tabulated from the numerical modelling tool (EDEM software) for the Discrete Element Method (DEM) and structural analysis tool (ANSYS) for the Finite Element Method (FEM) simulation.

Table 4.4: Result of 160,000 Volcanic Ash Particles Simulation with No Wind Effects

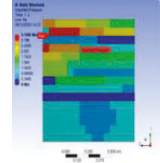
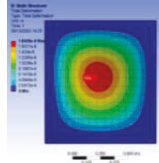
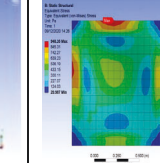
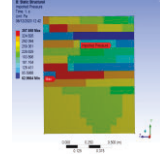
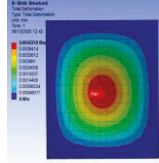
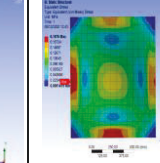
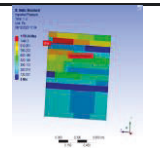
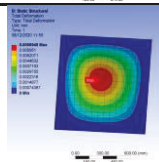
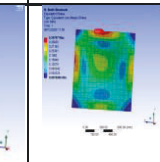
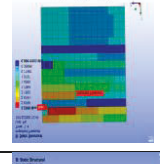
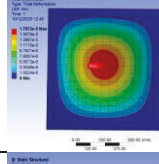
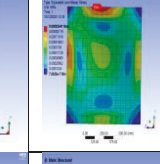
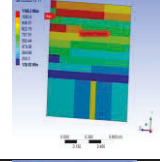
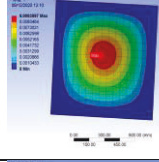
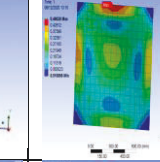
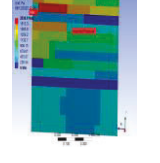
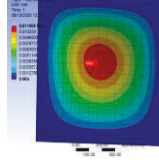
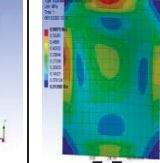
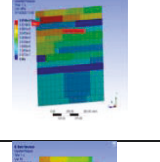
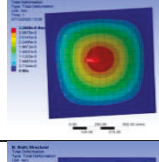
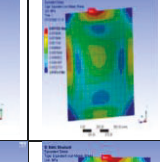
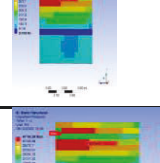
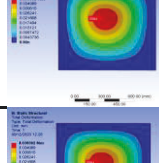
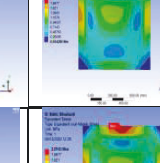

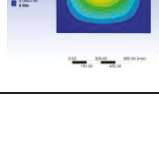
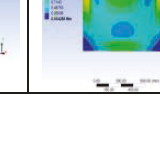
Volcanic Ash Particle Size in Diameter (mm)	Volcanic Ash Particle densities (Kg/m ³)	Maximum Pressure (Pa)	Maximum Deformation (mm)	FEM Maximum von Mises stress (MPa)	FEM Imagery Results shows the distribution of pressure load (Pa)	FEM Imagery Results shows the distribution of deformations (mm)	FEM Imagery Results shows the distribution of von Mises stress (MPa)
1	1000	3.13646	1.8425e-5	0.00094835			
5	1000	357.6	0.004	0.188			
10	1000	1170.4	0.007	0.347			
1	2000	3.2388	1.7572e-5	0.00092441			
5	2000	1165.33	0.0093897	0.48028			
10	2000	2038.83	0.011508	0.59875			
1	3000	5.97452	3.3609e-5	0.0017423			
5	3000	737.77	0.0042	0.216			
10	3000	4716.3	0.040	2.074			

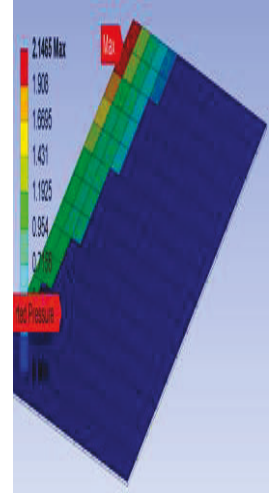
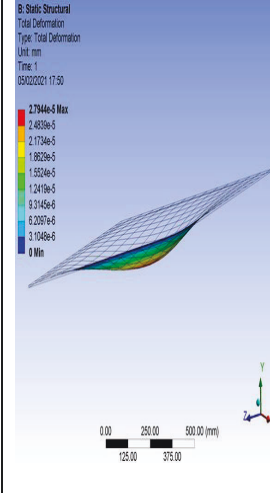
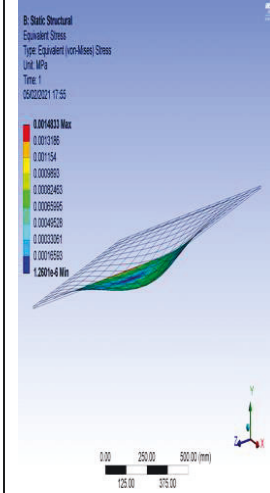
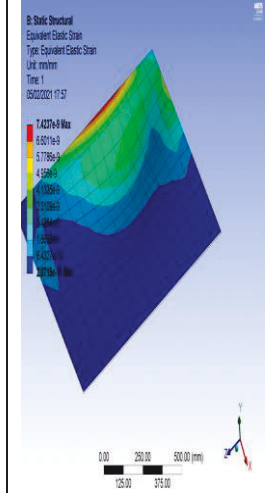
Table 4.4 shows the simulated results for 160,000 volcanic ash particles above from the numerical modelling tool (EDEM software) for the Discrete Element Method DEM and structural analysis tool (ANSYS) for the Finite Element Method (FEM) simulation parameters with No wind effects. This section is linked to table 5.3 results data for the 160,000 volcanic ash particles for the no wind effects simulation. The results for the 1000 (Kgm^{-3}) density show that an increase in the pressure results from the 1 mm diameter volcanic ash particles to the diameter volcanic ash particles with the density of 2000 (Kgm^{-3}) from 3.13646 (Pa) to the 3.2838 (Pa) the 5 mm diameter volcanic particles also show an increase in the pressure values from 357.6 (Pa) to 1165.53 (Pa) and 737.77 (Pa) respectively.

Table 4.5: Result of 160,000 Volcanic Ash Particles Simulation with Wind Effects in The Horizontal

Volcanic Ash Particle Size in Diameter (mm)	Volcanic Particle densities (Kg/m ³)	Ash densities (ms ⁻¹)	Horizontal direction (ms ⁻¹)	Maximum Pressure (Pa)	Maximum Deformation (mm)	FEM Maximum von Mises stress (MPa)	FEM Imagery Results show the distribution of pressure load (Pa)	FEM Imagery Results shows the distribution of deformations (mm)	FEM Imagery Results shows the distribution of von Mises stress (MPa)
1	1000	0.1	3.8754	2.1881e-5	0.0011398				
5	1000	0.5	370.73	0.053	0.244				
10	1000	1.0	2274.54	0.021	1.128				
1	2000	0.1	3.09309	1.8016e-5	0.00092997				
5	2000	0.5	1338.42	0.013	0.633				
10	2000	1.0	19497.2	0.208	10.769				
1	3000	0.1	3.397008	1.7599e-5	0.0093599				
5	3000	0.5	819.58	0.006	0.298				
10	3000	1.0	8581.1	0.081	4.424				

Table 4.5: shows the simulated results for 160,000 volcanic ash particles above from the numerical modelling tool (EDEM software) for the Discrete Element Method (DEM) and structural analysis tool (ANSYS) for the Finite Element Method (FEM) simulation tool with wind effects. This section is linked to table 5.4 results data. The figure also shows a pattern of the variable densities for the $0.1 \text{ (ms}^{-1}\text{)}$ and $1.0 \text{ (ms}^{-1}\text{)}$ reflects the increase in the maximum pressure effects on the roofs. The 10mm diameters for the volcanic ash particles have the highest impact on the simulations' stress values, followed by the 5mm diameter volcanic ash particles and the least 1 mm particles. The images show the distribution of the pressure deformation and the stress on the roofs for data collection in Chapter 4.

Table 4.6: Result of 20 Degrees 170,000 DEM and FEM CO-Simulation for Volcanic Ash Particles with No Wind Effects

Volcanic Ash Particle Size in Diameter (mm)	Volcanic Ash Particle densities (Kg/m ³)	DEM Maximum Pressure (Pa)	FEM Maximum Deformation Results (mm)	FEM Maximum von Mises stress (MPa)	FEM Maximum Strain Results (mm/m)	DEM Imagery Results shows the distribution of pressure load (Pa)	FEM Imagery Results shows the distribution of deformations (mm)	FEM Imagery Results shows the distribution of von Mises stress (MPa)	FEM Imagery Results shows the distribution of stress Strain (mm/mm)
1	1000	2.1465	2.7944e-5	0.0014833	7.4237e-9				

Note: Table 4.6 shows a set of results for the 20 Degrees 170,000 DEM and FEM CO-Simulation for Volcanic Ash Particles with No wind effects.

The first column is the volcanic ash particle size in diameter (mm), and the second is the volcanic ash particle densities (Kgm³). The third column is the DEM maximum pressure Loadings (Pa), and the fourth column is the FEM maximum deformation (mm). The fifth column is the FEM simulation stress for the NO wind effects. The sixth column is the FEM maximum strain results (mm/ (MPa), and the seventh column is DEM imagery results showing the distribution of pressure load (Pa). The eight-column is FEM imagery results showing the distribution of deformations (mm)), the ninth column is FEM Imagery Results shows the distribution of stress (MPa) and the column is the FEM imagery results shows the distribution of stress and strain. Table 4.9 is taken from Table 4.1. This section shows the introduction of the 20 degrees DEM and FEM simulation results indicated for the 170,000 volcanic ash particles with effects of 0.1ms⁻¹ was introduced. That impacted the roof, with an even distribution of volcanic ash on the roof. The 5 mm size particle had an immense effect on the roof for the DEM pressure loading on the roof 61578.66 (Pa) compared with the simulation results with the no wind effects in Table 2.1465 (Pa). Table 4.9 shows the enlarged imagery results from Table 4.9, showing different imagery results for the simulation.

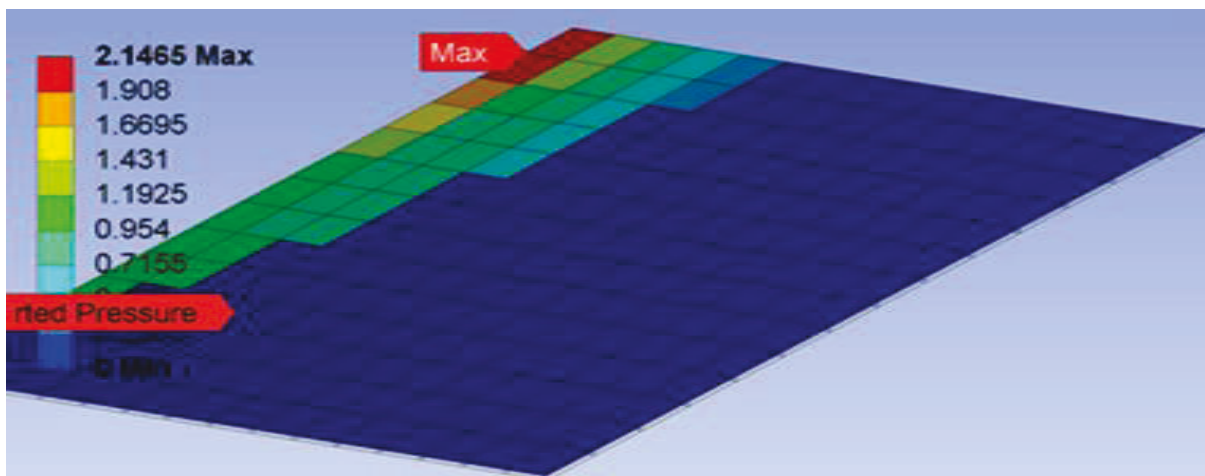


Figure 4.15A: DEM Imagery Results showing the Distribution of Pressure Load (Pa)

Note: Figure 4.15A is an extract from Table 4.6 and it shows a set of results for the 20 Degrees 170,000 DEM and FEM CO-Simulation for Volcanic Ash Particles with No Wind Effects

Figure 4:15A as shown in the DEM imagery results, the red spot indicates where the pressure is acting most with the highest recordings of 2.1465Pa and the lowest recording of 0Pa with

the colour coding. Thus, the red colour shows the pressure acting at the top of the pitched roof, affecting the roof.

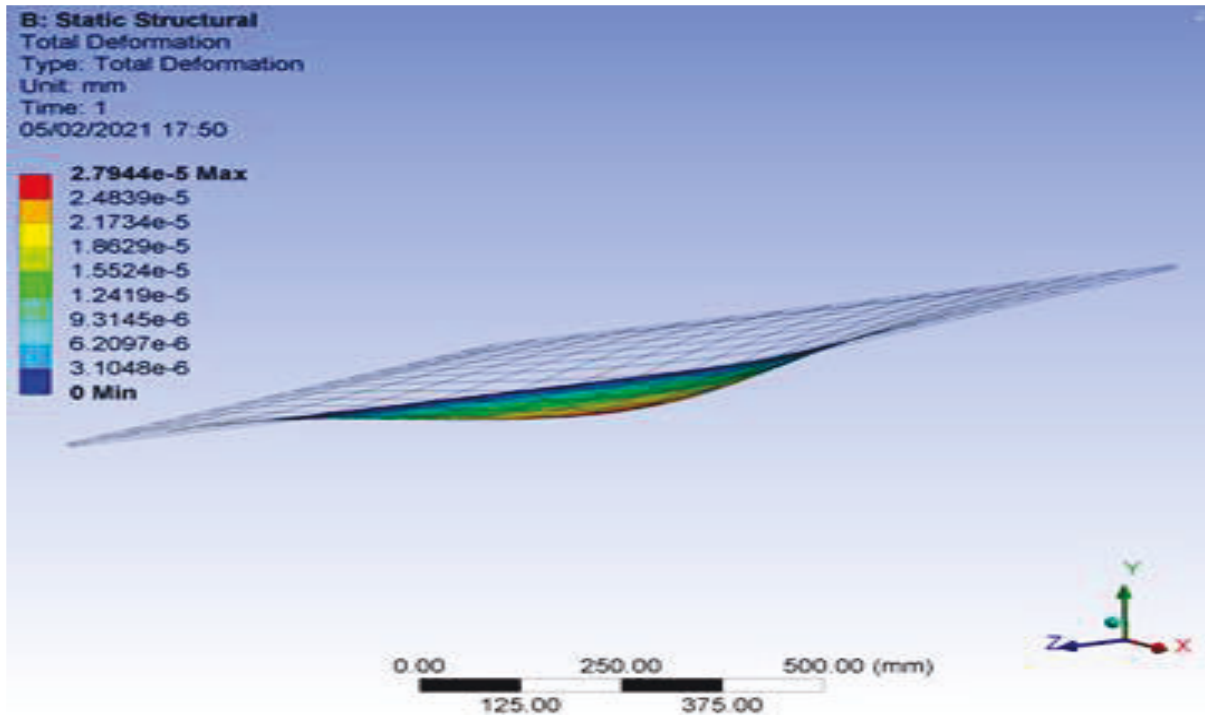


Figure 4.15B: FEM Imagery Results shows the Distribution of Deformations (mm)

Note: Figure 4.15B is an extract from Table 4.6 and it shows a set of results for the 20 Degrees 170,000 DEM and FEM CO-Simulation for Volcanic Ash Particles with No Wind Effects

Figure 4:15B shows the deformation of the volcanic ash on the roof. The static structural total deformation shows the slant view of the effects of the ash on the roof, and the bottom part indicates the maximum value of 2.7944e5 mm of the deformation. The lowest value with the blue colour coding indicates a recording of 0mm. That means the rest of the colour coding will not have any devastating effect on the roof.

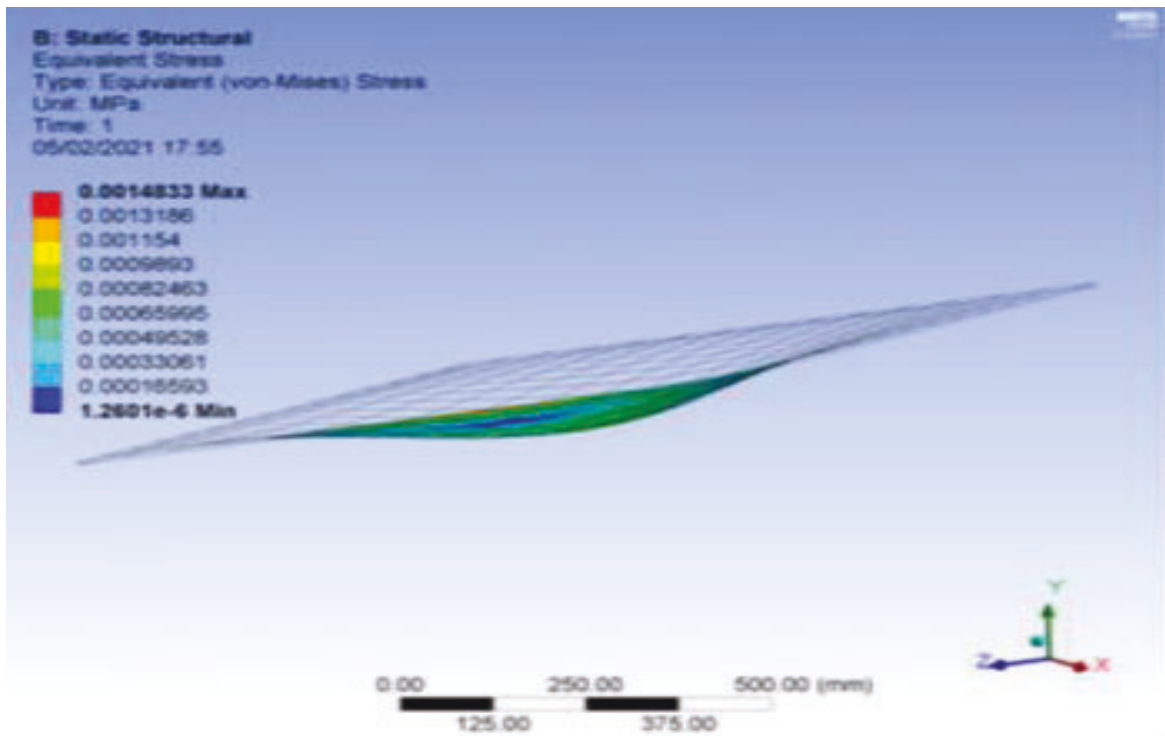


Figure 4.15C: DEM Imagery Results showing the Distribution of Pressure load (Pa)

Note: Figure 4.15C is an extract from Table 4.6 and it shows a set of results for the 20 Degrees 170,000 DEM and FEM CO-Simulation for Volcanic Ash Particles with No Wind.

The images indicate the maximum stress values of 0.0014833 MPa as indicated on the roof. The slant image shows that the bottom part indicates the red colour coding as the maximum stress levels on the pitched roof. The blue colour coding indicates the lowest part of the stress levels on the roof. However, the rest of the colour coding will not have devastating effects on the roof.

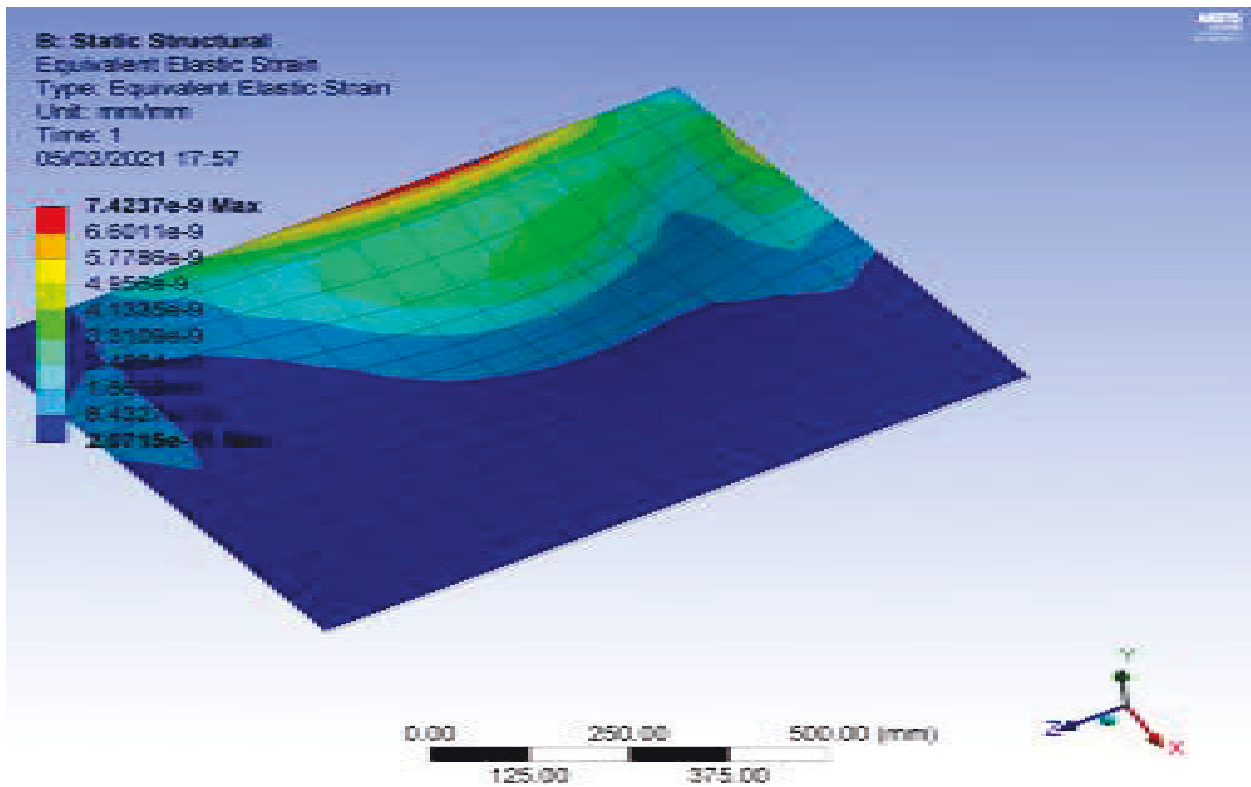
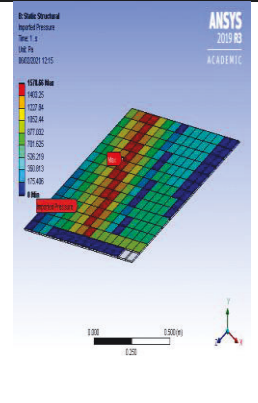
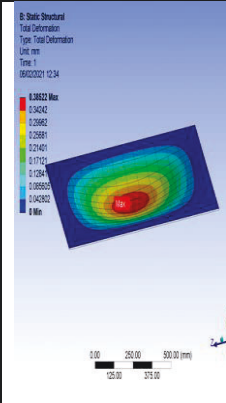
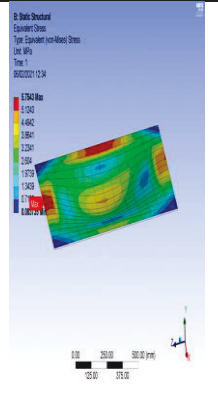
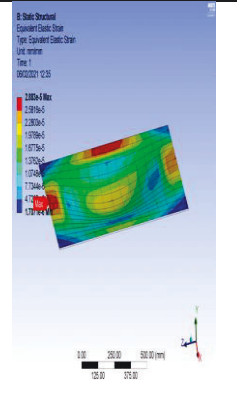


Figure 4.15D: DEM Imagery Results showing the distribution of stress Strain (mm/mm)

Note: Figure 4.15D is an extract from Table 4.6 and it shows the distribution of stress Strain (mm/mm).

The red colour at the edge of the roof indicates the strain value of $7.4238e^{-9}$ as the highest value recordings and the lowest indicating the lowest value of $2.0715e^{-11}$. The rest of the colour coding and the recordings doesn't affect the roof.

Table 4.7: Numerical Modelling Tool (EDEM Software) for Discrete Element Method (DEM) and Structural Tool (ANSYS) with Wind Effect

Volcanic Ash Particle Size in Diameter (mm)	Volcanic Ash Particle densities (Kg/m ³)	Horizontal direction (ms ⁻¹)	DEM Maximum Pressure (Pa)	FEM Maximum Deformation Results (mm)	FEM Maximum von Mises stress (MPa)	FEM Maximum Strain Results (mm/m)	DEM Imagery Results shows the distribution of pressure load (Pa)	FEM Imagery Results shows the distribution of deformations (mm)	FEM Imagery Results shows the distribution of von Mises stress (MPa)	FEM Imagery Results shows the distribution of stress Strain (mm/mm)
5	1000	0.5	1578.66	0.38522	5.7543	2.883e-5				

Note: The FEM Imagery Results show the distribution of stress Strain (mm/mm) Figure 4.15A, B, C, D below were Extracted from Table 4.9 showing the DEM and FEM Imagery Results: shows the results below were tabulated from the numerical modelling tool (EDEM software) for the Discrete Element Method (DEM) and structural analysis tool (ANSYS) for the Finite Element Method (FEM) simulation. The first column is the FEM Imagery Results shows the distribution of pressure load (Pa), and the second column is the FEM Imagery Results shows the distribution of deformations (mm). The third column is FEM Imagery Results shows the distribution of stress (MPa). The fourth column is FEM Imagery Results shows the distribution of stress, and strain (mm/mm). The fifth column is the FEM maximum deformation (mm). Finally, the sixth column is the DEM simulation rest for the wind effects.

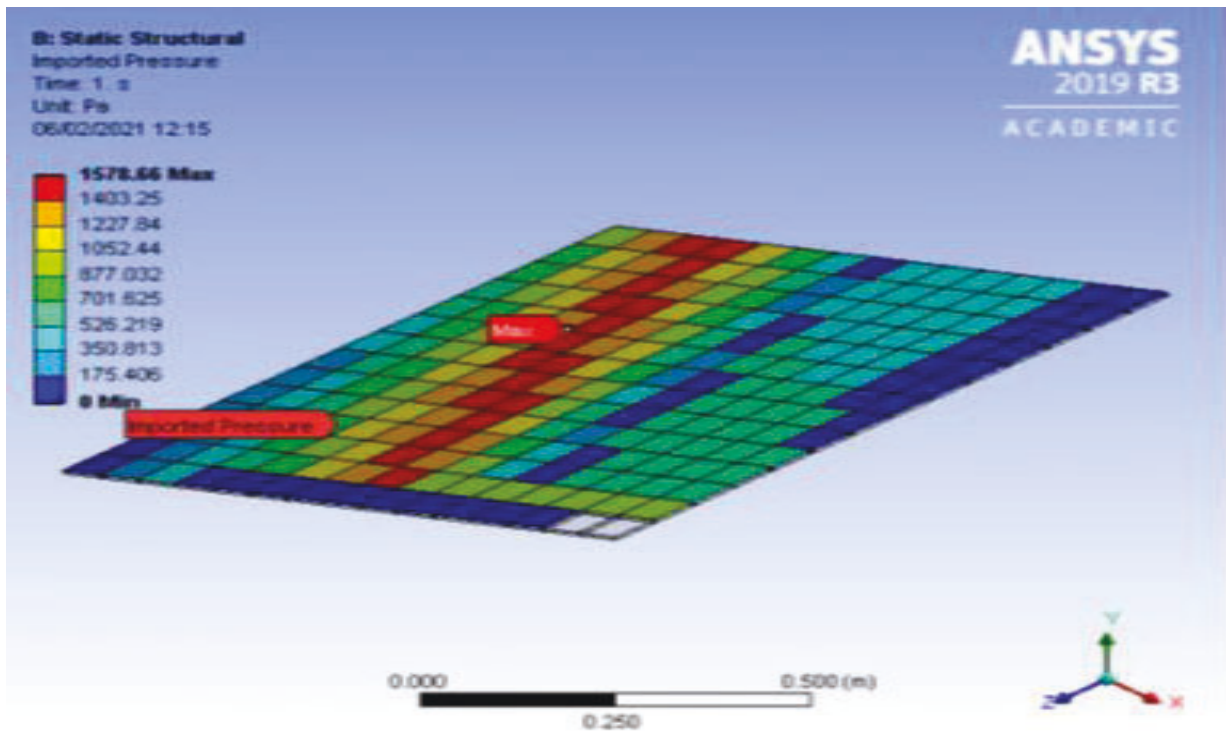


Figure 4.16A: DEM Imagery Results showing the Distribution of Pressure Load (Pa)

Note: Figure 4.16A is an extract from Table 4.7 and it shows the numerical modelling tool (EDEM software) for the Discrete Element Method.

The image shows the red colour coding as the position on the roof with the static structured imported pressure values of 1578.66 Pa. As shown, the blue colour coding and the rest of the volcanic ash pressure loading on the roof have no effect on the pitched roof.

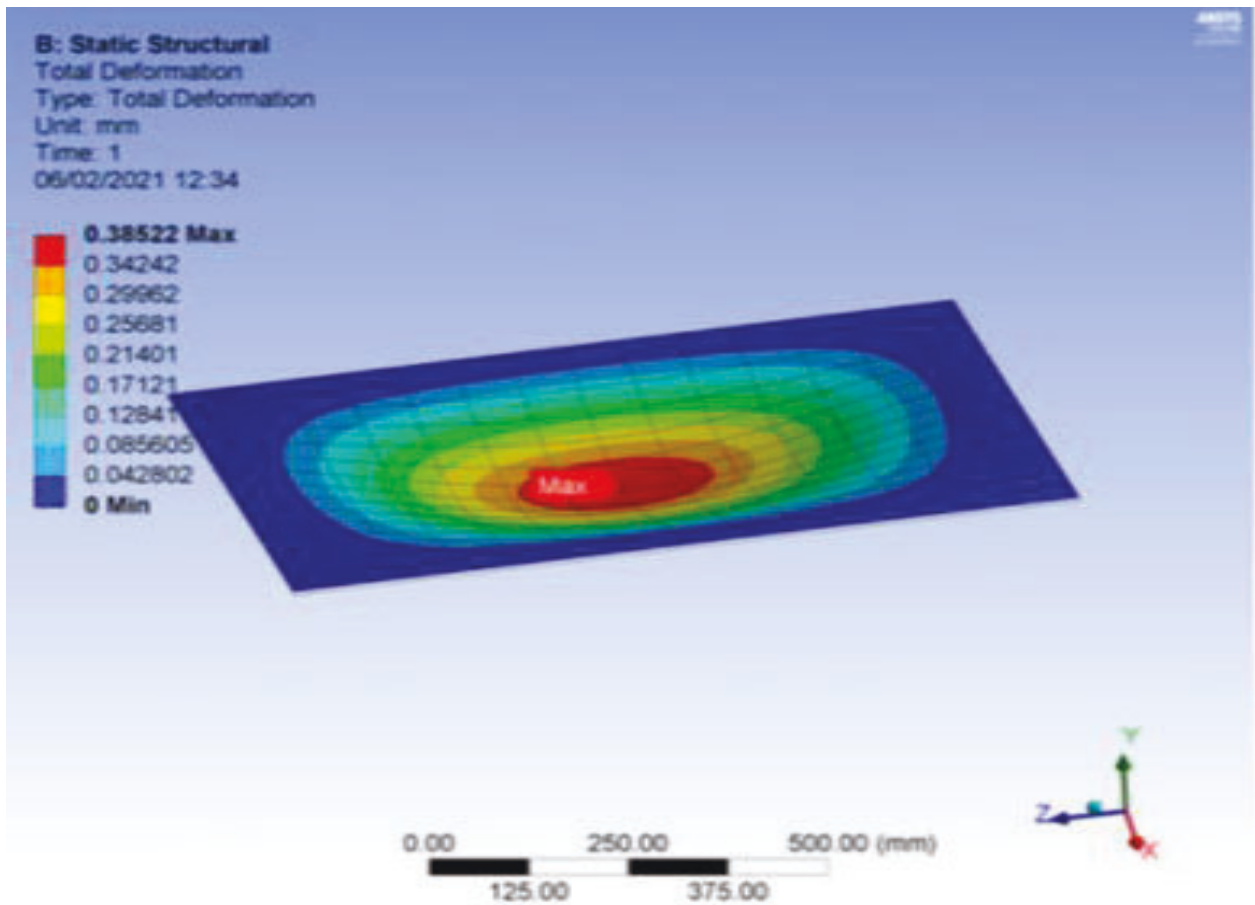


Figure 4.16B: FEM Imagery Results showing the Distribution of Deformations (mm)

Note: Figure 4.16B is an extract from Table 4.7 and it shows the numerical modelling tool (EDEM software) for the Discrete Element Method.

The image shows the static structural total deformation on the pitched roof. The concave nature indicates the red spot in the centre of the roof for the depression. The value for the maximum depression is 0.38522 mm. The rest of the concave coding doesn't have effects on the rest of the depression. So, the depression shows the extent of deformation on the pitch, which must be discussed very seriously.

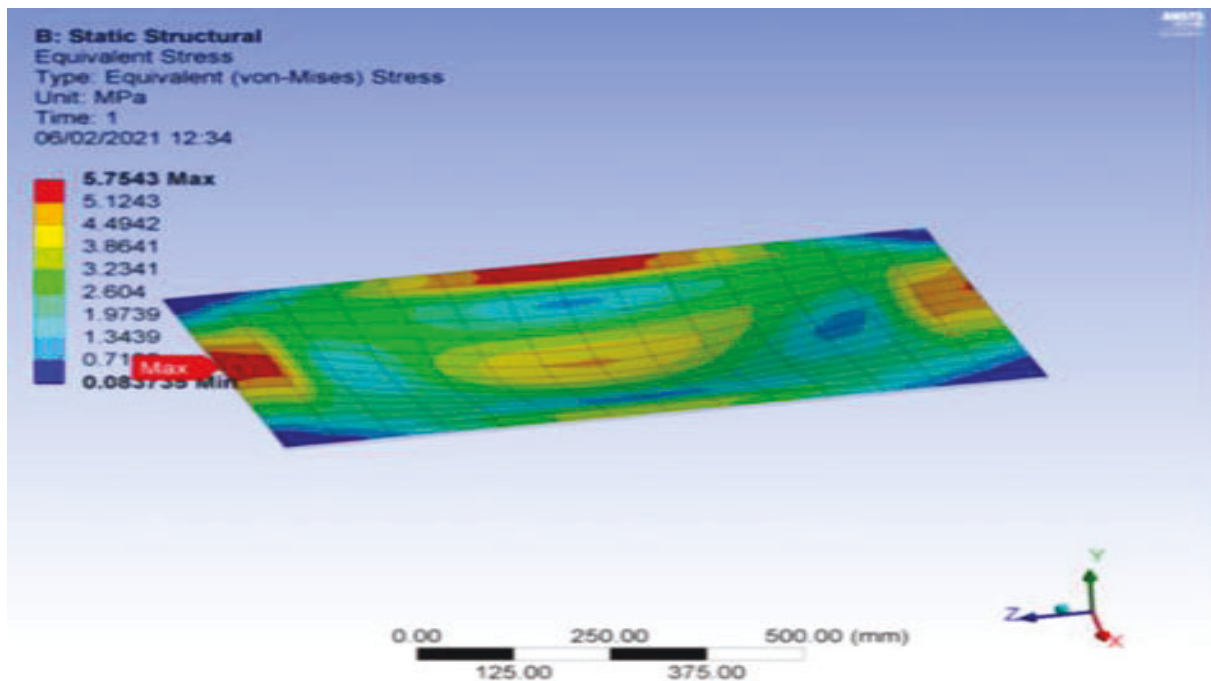


Figure 4.16C: FEM Imagery Results showing the Distribution of von Mises Stress (MPa)

Note: Figure 4.16C is an extract from Table 4.7 and it shows the numerical modelling tool (EDEM software) for the Discrete Element Method.

The image shows the static structure equivalent stress for the FEM simulation test results. The red colour coding indicated that the stress put on the figure indicates the red colour value of 5.7543 MPa. The rest of the colour indicates the lowest spot for the stress value on the roof. Therefore, the rest of the colour coding has no impact on the roof, as shown in the image.

FEM Imagery Results show the distribution of Strain (mm/mm)

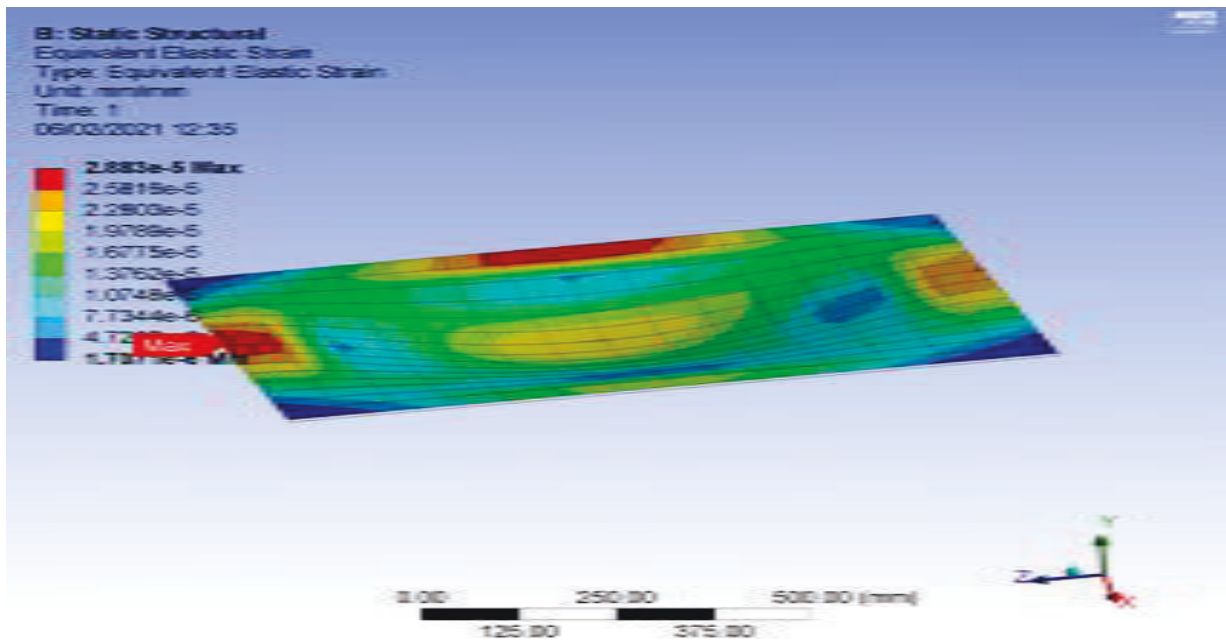
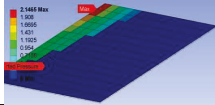
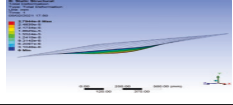
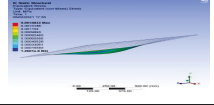
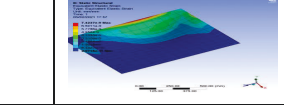
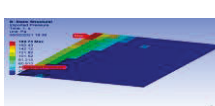
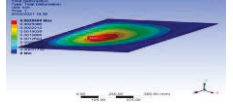
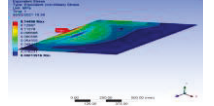
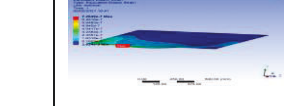
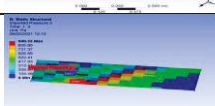
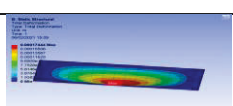
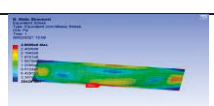
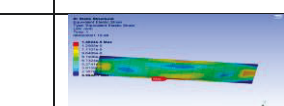
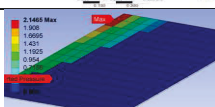
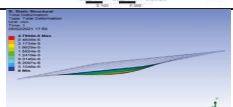
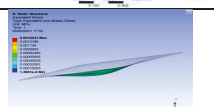
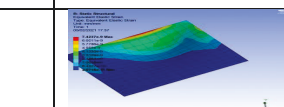
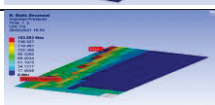
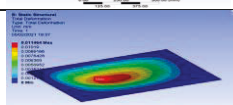
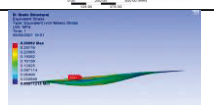
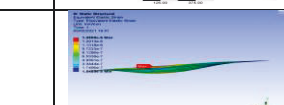
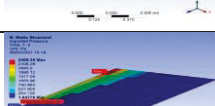
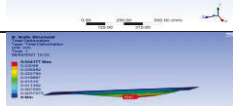
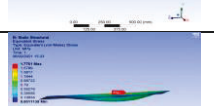
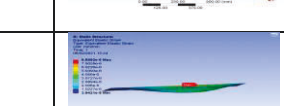
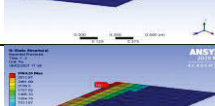
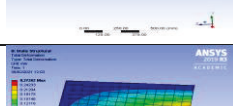
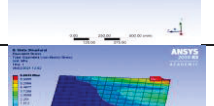
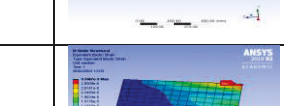

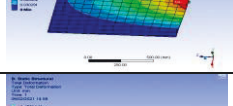
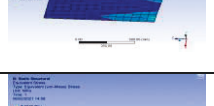
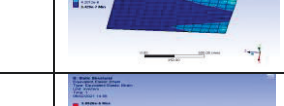


Figure 4.16D: FEM Imagery Results showing the distribution of stress Strain (mm/mm)

Note: Figure 4.16D is an extract from Table 4.7 and it shows the numerical modelling tool (EDEM software) for the Discrete Element Method.

The image shows the static structure equivalent strain for the FEM's simulation test results. The red colour coding indicates the stress effect on the pitched roof. The strain position on the roof has indicated the strain value of $2.883e^{-5}$. The rest of the colour coding does not significantly affect the roof compared to the other colour coding.

Table 4.8: Result of 20 Degrees 170,000 DEM and FEM CO-Simulation for Volcanic Ash Particles with No Wind Effects

Volcanic Ash Particle Size in Diameter (mm)	Volcanic Ash Particle densities (Kg/m ³)	DEM Maximum Pressure (Pa)	FEM Maximum Deformation Results (mm)	FEM Maximum von Mises stress (MPa)	FEM Maximum Strain Results (mm/m)	DEM Imagery Results shows the distribution of pressure load (Pa)	FEM Imagery Results shows the distribution of deformations (mm)	FEM Imagery Results shows the distribution of von Mises stress (MPa)	FEM Imagery Results shows the distribution of stress Strain (mm/mm)
1	1000	2.1465	2.7944e ⁻⁵	0.14833	7.4237e ⁻⁹				
5	1000	182.73	0.0028559	0.14496	7.2549e ⁻⁷				
10	1000	940.33	0.17444	2.6009	1.4024e ⁻⁵				
1	1000	2.1465	2.7944e ⁻⁵	0.14833	7.4237e ⁻⁹				
5	2000	153.593	0.011464	0.289921	1.4508e ⁻⁶				
10	2000	2369.35	0.043177	1.7761	8.8892e ⁻⁶				
5	3000	3164.25	0.27262	6.6844	3.3467				
10	3000	2556.8	0.47581	7.6946	3.8526e ⁻⁵				

The set of results for the 25 Degrees and 30 Degrees 170,000 DEM and FEM CO-Simulation for Volcanic Ash Particles with wind and No Wind Effects is presented. Table 4.8 shows the results for 170,000 volcanic ash particles below were tabulated from the simulation data sorting for the various numerical results flat roof from the numerical modelling tool (EDEM software) for the discrete element method DEM. The structural analysis tool (ANSYS) for the finite element method (FEM) simulation results for the variable pitch concrete tile roof for 20-degree.

Table 4.8 the simulation was carried out using volcanic ash particles size in diameter of 1mm,5mm and 10mm with variable volcanic ash particles densities for 1000 (Kgm^{-3}) 2000 (Kgm^{-3}) and 3000 (Kgm^{-3}), respectively. Table 4.9 shows the DEM pressure results, the FEM deformation results, FEM stress results and the FEM strain results. The imagery distribution for the various categories is indicated for the DEM and FEM results.

Table 4.9: Result of 20 Degrees 170,000 DEM and FEM CO- Simulation for Volcanic Ash Particles with Wind Effects in The Horizontal Direction

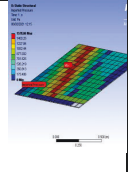
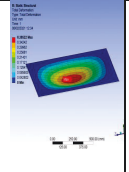
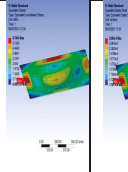
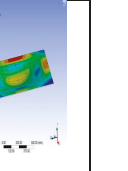
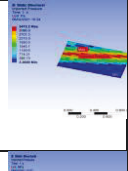
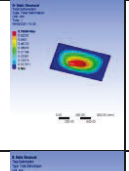
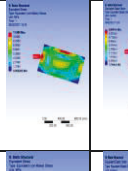
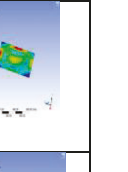
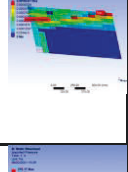
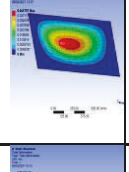
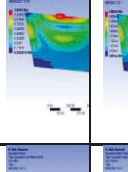
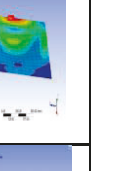
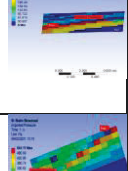
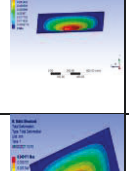
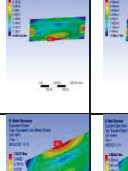
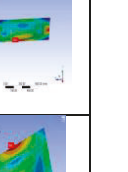
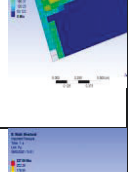
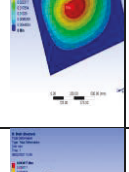
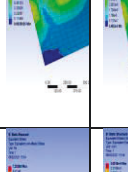
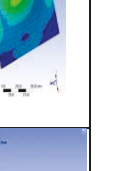
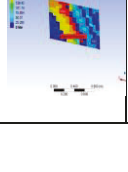
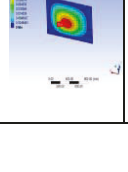
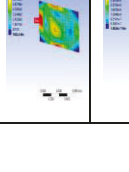
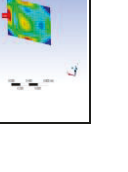
Volcanic Ash Particle Size in Diameter (mm)	Volcanic Ash Particle densities (Kg/m ³)	Horizontal direction (ms-1)	DEM Maximum Pressure (Pa)	FEM Maximum Deformation Results (mm)	FEM Maximum von Mises stress (MPa)	FEM Maximum Strain Results (mm/m)	DEM Imagery Results shows the distribution of pressure load (Pa)	FEM Imagery Results shows the distribution of deformations (mm)	FEM Imagery Results shows the distribution of von Mises stress (MPa)	FEM Imagery Results shows the distribution of stress Strain (mm/mm)
5	1000	0.5	1578.66	0.38522	5.7543	2.883e-5				
10	1000	1.0	3472.2	0.70084	11.988	6.0047e-5				
5	2000	0.5	562.81	0.041757	1.0516	5.2623e-6				
10	2000	1.0	278.17	0.053258	0.87847	4.393e-6				
5	3000	0.5	541.111	0.040171	1.0121	5.0648e-6				
10	3000	1.0	227.56	0.043617	0.72025	3.6018e-6				

Table 4.9 shows the results for 170,000 volcanic ash particles below were tabulated from the simulation data sorting were carried out for the various numerical results flat roof from the numerical modelling tool (EDEM software) for the discrete element method (DEM). In addition, the structural analysis tool (ANSYS) for the finite element method (FEM) simulation results for the variable pitch concrete tile roof for 20 degree).

Table 4:9 shows the DEM and FEM simulation results for the 170,000 particles with wind effects; the simulation test was carried out for the 1mm,5 mm and 10 mm volcanic ash diameter sizes without the 1mm volcanic ash diameter size. As a result, the 10 mm and 5mm volcanic ash particles show higher DEM pressure results.

CHAPTER FIVE

5.0. DISCUSSIONS AND ANALYSIS

5.1 Discussions of Discrete Element Method and Finite Element Method Co-Simulation Results

This section will discuss and analyse the data from chapter 4. To determine the ranges for data results from the input variables from the simulation test using the modelling tool (EDEM software) for the Discrete Element Method DEM and structural analysis tool (ANSYS) for the Finite Element Method (FEM) as expected, the literature review's theoretical analyses will be related to the envisaged simulation test results for the flat concrete roof and the pitch roof model. The modelling tool (EDEM software) for the Discrete Element Method DEM and structural analysis tool (ANSYS) for the Finite Element Method (FEM) simulations effects of the volcanic ash simulation on the flat concrete roof and the pitch tile roof will help determine whether failures may occur. As a result of the volcanic ash particle's deposition on the building's roofs within the volcanic prone areas. These results will set the tone for the discussions of the various test for the Discrete Element Method DEM and Structural Analysis tool (ANSYS) for the Finite Element Method (FEM) simulation for the Flat Concrete Roof and Pitched Concrete Roof.

Table 5.1: Colour Coding for the Volcanic Ash Particles

Volcanic Ash Particle Size in Diameter (mm)	Colour	Colure coding
1	Blue	
5	Green	
10	Gold	

5.2 Discrete Element Method (DEM) and Structural Analysis tool (ANSYS) for the Finite Element Method (FEM) Simulation. (Flat Concrete Roof)

Table 5.2: shows the simulation data extracted from the results in Table 4.4 for the 160,000 volcanic ash particles simulation with No wind effects. The first column shows the variable volcanic ash particles diameter for 1 mm, 5 mm, and 10 mm. The second column shows the variable volcanic ash particle densities for 1,000 (Kgm⁻³), 2,000 (Kgm⁻³) and 3,000 (Kgm⁻³).

Table 5.2: DEM and (FEM) Simulation Results for The No Wind Effects

Volcanic Ash Particle Size in Diameter (mm)	Volcanic Ash Particle densities (Kgm ⁻³)	DEM Maximum Pressure (Pa)	FEM Maximum Deformation Results (mm)	FEM Maximum von Mises stress (MPa)	Maximum volcanic ash layer thickness on the roof. (mm)
1	1000	3.13646	1.8425e ⁻⁵	0.00094835	359.17
5	1000	357.6	0.004	0.188	271.94
10	1000	1170.4	0.007	0.347	540.50
1	2000	3.2388	1.7572e ⁻⁵	0.00092441	603.38
5	2000	1165.33	0.0093897	0.48028	374.86
10	2000	2038.83	0.011508	0.59875	627.06
1	3000	5.97452	3.3609e-5	0.0017423	414.99
5	3000	737.77	0.0042	0.216	389.03
10	3000	4716.3	0.040	2.074	681.17

The third column shows the DEM simulation result for the maximum pressure loading on the flat concrete roof (Pa). The fourth column shows the simulation results from the FEM maximum deformation results (mm), and the fifth column shows the FEM maximum stress results (MPa). The sixth column shows the maximum height of the volcanic ash deposition on

the concrete roof after the DEM simulation. Table 5.2 the values for the 1 mm volcanic ash particles are lesser than the 5 mm volcanic ash particle. The 10 mm volcanic ash particles have the highest values, as shown in table 5.2. That means the stress levels will impact the roofs.

TABLE 5.3: DEM and FEM Simulation Results for the Wind Effects

Volcanic Ash Particle Size in Diameter (mm)	Volcanic Ash Particle densities (Kgm ⁻³)	Horizontal wind direction (ms ⁻¹)	DEM Maximum Pressure (Pa)	FEM Maximum Deformation Results (mm)	FEM Maximum von Mises stress (MPa)	Maximum volcanic ash layer thickness on the roof. (mm)
1	1000	0.1	3.8754	2.1881e ⁻⁵	0.0011398	376.38
5	1000	0.5	370.73	0.053	0.244	763.87
10	1000	1.0	2274.54	0.021	1.128	
1	2000	0.1	3.09309	1.8016e ⁻⁵	0.00092997	459.24
5	2000	0.5	1338.42	0.013	0.633	396.18
10	2000	1.0	19497.2	0.208	10.769	
1	3000	0.1	3.397008	1.7599e ⁻⁵	0.0093599	529.59
5	3000	0.5	819.58	0.006	0.298	492.72
10	3000	1.0	8581.1	0.081	4.424	

Table 5.3 shows the results from the simulation data extracted from Table 4.5 for the 160,000 volcanic ash (ms⁻¹) particles simulation with No wind effects. The first column shows the variable volcanic ash particles diameter for 1 mm, 5 mm, and 10 mm. The second column shows the variable volcanic ash particle densities for 1,000 (kgm⁻³), 2,000 (kgm⁻³) and 3,000 (kgm⁻³). The third column shows the DEM simulation result for the horizontal wind velocity direction (ms⁻¹). The fourth column shows the DEM simulation result for the maximum pressure loading on the flat concrete roof (Pa). The fifth column shows the DEM simulation

result for the maximum pressure loading on the flat concrete roof (Pa). The sixth column shows the results for FEM maximum stress results (MPa). The seventh column shows the maximum height of the volcanic ash deposition on the concrete roof after the DEM simulation.

Table 5.3 the simulation with the wind effects has high values for the 1mm DEM particle results have 3.8754 (Pa) with 1000 (Kgm^{-3}) density 1mm DEM particle results have 3.09309 (Pa) with 2000 (Kgm^{-3}) 1 mm DEM particle results have 3.397008 (Pa) with 3000 (Kgm^{-3}) these results may have an impact on the roof. Table 5.5: DEM and (FEM) Simulation Results for the Wind Effects.

TABLE 5.4: DEM and FEM Simulation Results for the No Wind Effects

Volcanic Ash Particle Size in Diameter (mm)	Volcanic Ash Particle densities (Kgm^{-3})	DEM Maximum Pressure (Pa)	FEM Maximum Deformation Results (mm)	FEM Maximum von Mises stress (MPa)	Maximum volcanic ash layer thickness on the roof. (mm)
1	1000	17.5146	0.00016594	0.0083915	762.47
5	1000	708.139	0.0039647	0.20675	649.35
10	1000	2756.85	0.022562	1.1593	746.30
1	2000	3.23877	1.7572-5	0.00092441	
5	2000	698.26	0.00338012	0.19978	313.72
10	2000	4252.68	0.027465	1.655	231.37
1	3000	1.58896	9.1727e ⁻⁶	0.00047463	
5	3000	659.918	0.0039246	0.20135	572.19
10	3000	26703	0.25235	14.39	460.45

Table 5.4 shows the simulation data extracted from Table 4.6 for the 80,000 volcanic ash particles simulation with No wind effects. The first column shows the variable volcanic ash particles diameter for 1mm, 5 mm and 10 mm. The second column shows the variable volcanic ash particle densities for 1,000 (Kgm^{-3}), 2,000 (Kgm^{-3}) and 3,000 (Kgm^{-3}). The third column

shows the DEM simulation result for the maximum pressure loading on the flat concrete roof (Pa). The fourth column shows the simulation results from the FEM maximum deformation results (mm), and the fifth column shows the FEM maximum stress results (MPa). The sixth column shows the maximum height of the volcanic ash deposition on the concrete roof after the DEM simulation. Table 5.4 shows that the 10 mm volcanic ash will have the highest impact on the roof compared to the 1mm volcanic ash particles. The 3000 (Kgm^{-3}) volcanic particles have the stress values ash shown in table 5.4.

Table 5.5: Result of 80,000 Volcanic Ash Particles Simulation with Wind Effects

Volcanic Ash Particle Size in Diameter (mm)	Volcanic Ash Particle densities (Kgm^{-3})	Horizontal wind direction (ms^{-1})	DEM Maximum Pressure (Pa)	FEM Maximum Deformation Results (mm)	FEM Maximum von Mises stress (MPa)	Maximum volcanic ash layer thickness on the roof. (mm)
1	1000	0.1	1.1817	6.8103e^{-6}	0.00035234	419.28
5	1000	0.5	480.428	0.006538	0.17653	677.40
10	1000	1.0	7174.4	0.071698	3.789	720.74
1	2000	0.1	48.557	0.0004906	0.025401	567.53
5	2000	0.5	452.69	0.004	0.168	380.54
10	2000	1.0	4772.1	0.0475731	2.4913	417.40
1	3000	0.1	4.43208	3.1389e^{-5}	0.001448	981.59
5	3000	0.5	437.51	0.003	0.162	463.34
10	3000	1.0	1385.3	0.012318	0.63573	493.69

Table 5.5 shows the results from the simulation extracted from the results in table 4.7 for the 80,000-volcanic ash (m/s^{-1}) particles simulation with No wind effects. The first column shows the variable volcanic ash particles diameter for 1 mm, 5 mm, and 10 mm. The second column shows the variable volcanic ash particle densities for 1,000 (Kgm^{-3}), 2,000 (Kgm^{-3}) and 3000 (Kgm^{-3}). The third column shows the DEM simulation result for the horizontal wind velocity

direction (ms^{-1}). The fourth column shows the DEM simulation result for the maximum pressure loading on the flat concrete roof (Pa), and the fifth column shows the DEM simulation result for the maximum pressure loading on the flat concrete roof (Pa). the sixth column shows the results for FEM maximum stress results (MPa). Finally, the seventh column shows the maximum height of the volcanic ash deposition on the concrete roof after the DEM simulation Data results from the discussion for the failure of structure using Stress results from the numerical modelling tool (EDEM software) for the Discrete Element Method (DEM) and structural analysis tool (ANSYS) for the Finite Element Method (FEM) simulation. Table 5.5 the simulation with the wind effects has the following effects have the following results for 2000 (Kgm^{-3}) density. For example, 1 mm ash particles DEM pressure results of 1.181 7 (Pa) with 1000 (Kgm^{-3}) density 5 mm ash particle DEM pressure DEM results is 480.428 (Pa) with 2000 (Kgm^{-3}) 10 mm ash particles DEM pressure results of 7.174.4(Pa) with the 3000 Kgm^{-3} . That shows an increment of the DEM pressure density results for the simulation.

5.2.1 Structural Failures Identified from Flat Concrete Roof simulation

This subsection describes how the allowable stress was related to the maximum stress regarding the EU and the UK regions.

The $\sigma_{\max} \leq \sigma_a = \text{Ultimate Tensile strength of concrete material} / \text{factor of safety}$.

The criterion is that the maximum stress is less than the permissible (allowable) stress.

- $\sigma_{\max} \leq \sigma_a = 1.8 \text{ MPa}$ (EU Values)
- $\sigma_{\max} \leq \sigma_a = 1.44 \text{ MPa}$ (UK values)

Table 5.7 indicates 160,000 Particles data for the failure of roof structure using stress results from the modelling tool (EDEM software) for the Discrete Element Method DEM and structural analysis tool (ANSYS) for the Finite Element Method (FEM) simulation in relation to the allowable stress (EU Code values). Table (5.7) shows the simulation results in Chapter 5 (Table 5.2 and Table 4.4), for the 160,000 volcanic ash particles simulation with No wind effects. The meaning of the colours highlighted as yellow and red in the colour coding is presented in Table 5.6.

Table 5.6: Structural Failure Colour Coding and Meaning

Maximum stress \leq Allowable Stress is satisfied (MPa)	
Maximum stress \leq Allowable stress' is not satisfied (MPa)	

The colures for the structural failures coding for the allowable stress was related to the maximum stress regarding the EU and the UK regions.

Table 5.7: Result of 160,000 Particle Data for No Wind Effects

Volcanic Ash Particles Size(mm)	Volcanic Particles Density(Kgm ⁻³)	FEM Maximum von Mises stress (MPa)	FEM Maximum Strain Results (mm/mm)	≤ Allowable Stress (MPa)	Maximum stress ≤ Allowable Stress is satisfied (MPa)	Maximum stress ≤ Allowable stress' is not satisfied (MPa)
1	1000	0.00094835	4.7422e ⁻⁹	1.8		
5	1000	0.188	9.3761e ⁻⁷	1.8		
10	1000	0.34707	1.7355e ⁻⁶	1.8		
1	2000	0.00092441	4.6224e ⁻⁹	1.8		
5	2000	0.48028	2.4016e ⁻⁶	1.8		
10	2000	0.59875	2.9946e ⁻⁶	1.8		
1	3000	0.0017423	V	1.8		
5	3000	0.216	1.0812e ⁻⁶	1.8		
10	3000	2.074	1.0373e ⁻⁵	1.8		

The first column shows the variable volcanic ash particles diameter for (1 mm, 5 mm, and 10 mm), the second column shows the variable volcanic ash particle densities for 1000 (Kgm⁻³), 2,000 (Kgm⁻³) and 3,000 (Kgm⁻³). The third column shows the FEM maximum stress results (MPa). The fourth column shows the FEM maximum strain results, and the fifth shows $\sigma_{\max} \leq \sigma_a$ Allowable Stress (MPa). The sixth column shows the nature of assessing the results used for the criterion $\sigma_{\max} \leq \sigma_a$ allowable and the seventh column shows $\sigma_{\max} \leq \sigma_a$ allowable is not satisfied (MPa) for flat concrete roof structure. Table 5.7 shows that the 10 mm volcanic ash particles size (m) for the volcanic particle density of 3000 (Kgm⁻³) indicates that the text doesn't satisfy the condition for column four from table 5.7. The rest of the test certifies the condition, which means the structure will be safe.

Table 5.8: Result of 160,000 Particle Data for Wind Effects

Volcanic Ash Particles Size (mm)	Volcanic Particles Density (Kgm ⁻³)	Horizontal wind direction (ms ⁻¹)	FEM Maximum von Mises stress (MPa)	FEM Maximum Strain Results (mm/m)	≤ Allowable Stress (MPa)	Maximum stress ≤ Allowable Stress is satisfied (MPa)	Maximum stress ≤ Allowable stress' is not satisfied (MPa)
1	1000	0.1	0.0011398	5.6995e ⁻⁹	1.8	Low	
5	1000	0.5	0.244	1.2182e ⁻⁶	1.8	Low	
10	1000	1.0	1.128	5.6386e ⁻⁶	1.8	Low	
1	2000	0.1	0.00092997	4.6502e ⁻⁹	1.8	Low	
5	2000	0.5	0.633	3.165e ⁻⁶	1.8	Low	
10	2000	1.0	10.769	5.3851e ⁻⁵	1.8	Low	
1	3000	0.1	0.0093599	4.5803e ⁻⁹	1.8	Low	
5	3000	0.5	0.298	1.4873e ⁻⁶	1.8	Low	
10	3000	1.0	4.424	2.2123e ⁻⁵	1.8		

Table 5.8 shows 160,000 particle data for the failure of roof structure using stress results from the modelling tool (EDEM software) for the Discrete Element Method DEM and structural analysis tool (ANSYS) for the Finite Element Method (FEM) simulation in relation to the allowable stress (EU Code values). In addition, table 5.8 shows the simulation results in (table 5.3 and table 4.5) for the 160,000 volcanic ash particles simulations with No wind effects.

The first column shows the variable volcanic ash particles diameter for 1mm, 5 mm and 10 mm. The second column shows the variable volcanic ash particle densities for 1,000 (kgm⁻³) 2,000 (kgm⁻³), and 3,000 (kgm⁻³) The third column shows the horizontal wind direction (ms⁻¹). The fourth column shows the FEM maximum stress results (MPa). The fifth column shows the FEM maximum strain results, and the sixth shows the $\sigma_{\max} \leq \sigma_a$ Allowable Stress (MPa). The seventh column shows the nature of assessing the results used for the criterion $\sigma_{\max} \leq \sigma$ allowable, and the eight-column shows $\sigma_{\max} \leq \sigma_a$ allowable is not satisfied (MPa) for flat

concrete roof structure. Table 5.8 the result shows that 10mm volcanic ash particles for the densities of 2000 (Kgm⁻³) and 3000 (Kgm⁻³) did not certify the criterion for column six the rest of the test did certify the condition for the column, which means that these two densities of 2000 (Kgm⁻³) and 3000 (Kgm⁻³) are not safe the stress value will impact on the roofs.

Table 5.9: Result of 80,000 Volcanic Ash Particles Results for the No Wind Effects

Volcanic Ash Particles Size(mm)	Volcanic Particles Density (Kgm ⁻³)	FEM Maximum von Mises stress (MPa)	FEM Maximum Strain Results (mm/m)	≤ Allowable Stress (MPa)	Maximum stress ≤ Allowable Stress (MPa) is satisfied	Maximum stress ≤ Allowable stress' is not satisfied (MPa)
1	1000	0.0083915	4.1962e ⁻⁸	1.8	Low	
5	1000	0.20675	1.338e ⁻⁶	1.8	Low	
10	1000	1.1593	5.7937e ⁻⁷	1.8	Low	
1	2000	0.00092441	2.5058e ⁻⁹	1.8	Low	
5	2000	0.19978	9.9896e ⁻⁷	1.8	Low	
10	2000	1.655	8.2754e ⁻⁶	1.8	Low	
1	3000	0.00047463	2.3733e ⁻⁹	1.8	Low	
5	3000	0.20135	1.0068e ⁻⁶	1.8	Low	
10	3000	14.39	7.1957e ⁻⁵	1.8		

Table 5.9 shows 80,000 Particle data for the failure of roof structure using stress results from the modelling tool (EDEM software) for the Discrete Element Method DEM and structural analysis tool (ANSYS) for the Finite Element Method (FEM) simulation in relation to the allowable stress (EU Code values). Table (5.9) shows the simulation results in (Table 5. 3 and Table 4. 5) Table 4.5 for the 16,000 volcanic ash particles simulation with No wind effects. The first column shows the variable volcanic ash particles diameter for 1 mm, 5 mm, and 10 mm. The second column shows the variable volcanic ash particle densities for 1,000 (Kgm⁻³), 2,000 (Kgm⁻³) and 3,000 (Kgm⁻³). The third column shows the FEM maximum stress results (MPa). The fourth column shows the FEM maximum strain, the fifth shows the $\sigma_{max} \leq \sigma_a$ Allowable

Stress (MPa). The sixth column shows the nature of assessing the results used for the criterion $\sigma_{\max} \leq \sigma_a$ allowable, and the seventh column shows $\sigma_{\max} \leq \sigma_a$ allowable is not satisfied (MPa) for flat concrete roof structure. Table 5.9, the result indicates a similar pattern to table 5.5 with 10mm volcanic ash particle size, and the 3000 (Kgm⁻³) did not certify the criterion for column five. It means the test will have an impact on the roof. The rest of the test will be safe.

Table 5.10: Result of 80,000 Volcanic Ash Particles Data for The Wind Effects

Volcanic Ash Particles Size(mm)	Volcanic Particles Density (Kgm ⁻³)	Horizontal direction (ms ⁻¹)	FEM Maximum von Mises stress (MPa)	FEM Maximum Strain Results (mm/m)	≤ Allowable Stress (MPa)	Maximum stress ≤ Allowable Stress is satisfied (MPa)	Maximum stress ≤ Allowable stress' is not satisfied (MPa)
1	1000	0.1	0.00035234	1.7618e ⁻⁹	1.8	Low	
5	1000	0.5	0.17653	8.8274e ⁻⁷	1.8	Low	
10	1000	1.0	3.789	1.8947e-5	1.8		
1	2000	0.1	0.025401	1.2702e ⁻⁷	1.8	Low	
5	2000	0.5	0.168	8.3821e ⁻⁷	1.8	Low	
10	2000	1.0	2.4913	1.2458e-5	1.8		
1	3000	0.1	0.001448	7.2407e ⁻⁹	1.8	Low	
5	3000	0.5	0.162	8.1084e ⁻⁷	1.	Low	
10	3000	1.0	0.63573	3.1789e ⁻⁶	1.8	Low	

Table 5.10 shows 80,000 Particle data for the failure of roof structure using stress results from the modelling tool (EDEM software) for the Discrete Element Method (DEM) and structural analysis tool (ANSYS) for the Finite Element Method (FEM)simulation in relation with the allowable stress (EU Code values). Table 5.10 shows the simulation results in chapter 5, table 5.5 and 4.7 for the 80,000 volcanic ash particles simulation with No wind effects. The first column shows the variable volcanic ash particles diameter for 1 mm,5 mm and 10 mm. The second column shows the variable volcanic ash particle densities for 1,000 (Kgm⁻³), 2,000

(Kgm⁻³) and 3,000 (Kgm⁻³). The third column shows the horizontal wind direction (ms⁻¹). The fourth column shows the FEM maximum stress results (MPa). The fifth column shows the FEM maximum strain results, from the sixth shows the \leq Allowable Stress (MPa). The seventh column shows the nature of assessing the results used for the criterion $\sigma_{\max} \leq \sigma_a$ allowable and the eight-column shows $\sigma_{\max} \leq \sigma_a$ allowable is not satisfied (MPa) for flat concrete roof structures. Table 5.10 the reset shows that the 10 mm volcanic ash particles for 1000 (Kgm⁻³) density and the 2000 (Kgm⁻³) density did not certify the criterion for column six. The column six criteria on the roof are due to the stress impact.

Table 5.11: Result of 160,000 Particle Data for No Wind Effects

Volcanic Ash Particles Size(mm)	Volcanic Particles Density (Kgm ⁻³)	FEM Maximum von Mises stress (MPa)	FEM Maximum Strain Results (mm/m)	\leq Allowable Stress (MPa)	Maximum stress \leq Allowable Stress is satisfied (MPa)	Maximum stress \leq Allowable stress' is not satisfied (MPa)
1	1000	0.00094835	4.7422e ⁻⁹	1.44	Low	
5	1000	0.188	9.3761e ⁻⁷	1.44	Low	
10	1000	0.347	1.7355e ⁻⁶	1.44	Low	
1	2000	0.00092441	4.6224e ⁻⁹	1.44	Low	
5	2000	0.48028	2.4016e ⁻⁶	1.44	Low	
10	2000	0.59875	2.9946e ⁻⁶	1.44	Low	
1	3000	0.0017423	8.7121e ⁻⁹	1.44	Low	
5	3000	0.216	1.0812e ⁻⁶	1.44	Low	
10	3000	2.074	1.0373e ⁻⁵	1.44		

Table 5.11 shows the 16,000 Particle data for the failure of flat concrete roof structure using stress results from the modelling tool (EDEM software) for the Discrete Element Method DEM and structural analysis tool (ANSYS) for the Finite Element Method (FEM) simulation in relations with the allowable stress (UK Code values). Table 5.11 shows the results from the

simulation data in table 5.5 and table 4.7 for the 160,000 volcanic ash particles simulation with No wind effects. The first column shows the variable volcanic ash particles diameter for 1mm, 5 mm and 10 mm. The second column shows the variable volcanic ash particle densities for 1,000 (Kgm⁻³), 2,000 (Kgm⁻³) and 3,000 (Kgm⁻³). The third column shows the FEM maximum stress results (MPa). The fourth column shows the FEM maximum strain results, the fifth shows the $\sigma_{\max} \leq \sigma_a$ Allowable Stress (MPa). The sixth column shows the nature of assessing the results used for the criterion $\sigma_{\max} \leq \sigma_a$ allowable, and the seventh column shows $\sigma_{\max} \leq \sigma_a$ allowable is not satisfied (MPa) for flat concrete roof structure. Table 5.10, the 10 mm volcanic ash particles for the 3000Kgm⁻³ density that did not certify the criterion for column five. The rest of the results certified the criterion, which means the roof will be safe and won't impact the roof.

Table 5.12: Result of 160,000 Volcanic Ash Particles Data for the Wind Effects

Volcanic Ash Particles Size(mm)	Volcanic Particles Density(Kgm ⁻³)	Horizontal direction (ms ⁻¹)	FEM Maximum Stress Results (MPa)	FEM Maximum Strain Results (mm/m)	≤ Allowable Stress (MPa)	Maximum stress ≤ Allowable Stress is satisfied (MPa)	Maximum stress ≤ Allowable stress' is not satisfied (MPa)
1	1000	0.1	0.0011398	5.6995e ⁻⁹	1.44	Low	
5	1000	0.5	0.244	1.2182e ⁻⁶	1.44	Low	
10	1000	1.0	1.128	5.6386e ⁻⁶	1.44	Low	
1	2000	0.1	0.00092997	4.6502e ⁻⁹	1.44	Low	
5	2000	0.5	0.633	3.165e ⁻⁶	1.44	Low	
10	2000	1.0	10.769	5.3851e ⁻⁵	1.44		
1	3000	0.1	0.0093599	4.5803e ⁻⁹	1.44	Low	
5	3000	0.5	0.298	1.4873e ⁻⁶	1.44	Low	
10	3000	1.0	4.424	2.2123e ⁻⁵	1.44		

Table 5.12 shows the 160,000 Particle data for the failure of roof structure using stress results from the modelling tool (EDEM software) for the Discrete Element Method DEM and

structural analysis tool (ANSYS) for the Finite Element Method (FEM) simulation in relation to the allowable stress (UK Code values). Table 5.12 shows the results from the simulation data in Table 5.4 And Table 4.6 for the 160,000 volcanic ash particles simulation with No wind effects. The first column shows the variable volcanic ash particles diameter for 1mm, 5 mm and 10 mm. The second column shows the variable volcanic ash particle densities for 1,000 (Kgm⁻³), 2,000 (Kgm⁻³) and 3,000 (Kgm⁻³). The third column shows the horizontal wind direction (ms⁻¹). The fourth column shows the FEM maximum stress results (MPa). The fifth column shows the FEM maximum strain the sixth shows the \leq Allowable Stress (MPa). The seventh column shows the nature of assessing the results used for the criterion $\sigma_{max} \leq \sigma_{allowable}$ and the eight-column shows $\sigma_{max} \leq \sigma_a$ is allowable is not satisfied (MPa) for flat concrete roof structure. Table 5.12, the test result indicates that the 10 mm volcanic ash particles with the volcanic ash densities of 2000 (Kgm⁻³) and 3000 (Kgm⁻³) did not certify the column's criterion six as dictated in column eight. It means the volcano will impact the roof; however, the rest of the test will be safe by certifying the criterion for column six.

Table 5.13: Results for the 80,000 Volcanic Ash Particles Results for the No Wind Effects

Volcanic Ash Particles Size (mm)	Volcanic Particles Density (Kgm ⁻³)	FEM Maximum von Mises stress (MPa)	FEM Maximum Strain Results (mm/m)	\leq Allowable Stress (MPa)	Maximum stress \leq Allowable Stress is satisfied (MPa)	Maximum stress \leq Allowable stress' is not satisfied (MPa)
1	1000	0.0083915	4.1962e ⁻⁸	1.44	Low	
5	1000	0.20675	1.338e ⁻⁶	1.44	Low	
10	1000	1.1593	5.7937e ⁻⁷	1.44	Low	
1	2000	0.00092441	2.5058e ⁻⁹	1.44	Low	
5	2000	0.19978	9.9896e ⁻⁷	1.44	Low	
10	2000	1.655	8.2754e ⁻⁶	1.44	Low	
1	3000	0.00047463	2.3733e ⁻⁹	1.44	Low	
5	3000	0.20135	1.0068e ⁻⁶	1.44	Low	
10	3000	14.39	7.1957e ⁻⁵	1.44		

Table 5.13 shows the 80,000 Particle data for the failure of roof structure using stress results from the modelling tool (EDEM software) for the Discrete Element Method DEM and structural analysis tool (ANSYS) for the Finite Element Method (FEM) simulation in relation to the allowable stress (EU Code values). (Table 5.12) shows the simulation results in (Table 5.5 and Table 4.7 for the 160,000 volcanic ash particles simulation with No wind effects. The first column shows the variable volcanic ash particles diameter for 1mm,5 mm and 10 mm. The second column shows the variable Volcanic Ash Particle densities for 1,000 (Kgm⁻³), 2,000 (Kgm⁻³) and 3,000 (Kgm⁻³). The third column shows the FEM maximum stress results (MPa). The fourth column shows the FEM maximum strain results (mm/m), and the fifth shows the $\sigma_{\max} \leq \sigma_a$ Allowable Stress (MPa). The sixth column shows the nature of assessing the results used for the criterion $\sigma_{\max} \leq \sigma_a$ allowable, and the seventh column shows $\sigma_{\max} \leq \sigma_a$ allowable is not satisfied (MPa) for flat concrete roof structure. Table 5.13, the test results indicate that the 10mm volcanic ash particle for the volcanic ash density of 3000 (Kgm⁻³) did not certify the column five criterion indicated in column eight. The rest of the results certified the criterion for column six; thus, the volcanic ash loading will not impact the roof.

Table 5.14: Results for the 80,000 Volcanic Ash Particles Data for the Wind Effects

Volcanic Ash Particles Size(mm)	Volcanic Particles Density (Kgm ⁻³)	Horizontal direction (ms ⁻¹)	FEM Maximum von Mises stress (MPa)	FEM Maximum Strain Results (mm/m)	\leq Allowable Stress (MPa)	Maximum stress \leq Allowable Stress is satisfied (MPa)	Maximum stress \leq Allowable stress' is not satisfied (MPa)
1	1000	0.1	0.00035234	1.7618e ⁻⁹	1.44	Low	
5	1000	0.5	0.17653	8.8274e ⁻⁷	1.44	Low	
10	1000	1.0	3.789	1.8947e ⁻⁵	1.44		
1	2000	0.1	0.025401	1.2702e ⁻⁷	1.44	Low	
5	2000	0.5	0.168	8.3821e ⁻⁷	1.44	Low	
10	2000	1.0	2.4913	1.2458e ⁻⁵	1.44		
1	3000	0.1	0.001448	7.2407e ⁻⁹	1.44	Low	
5	3000	0.5	0.162	8.1084e ⁻⁷	1.44	Low	
10	3000	1.0	0.63573	3.1789e ⁻⁶	1.44	Low	

Table 5.14 shows the 80,000 Particle data for the failure of roof structure using stress results from the modelling tool (EDEM software) for the Discrete Element Method DEM and structural analysis tool (ANSYS) for the Finite Element Method (FEM) simulation in relation to the allowable stress (UK Code values). Table 5.14 shows the results from the simulation data in table 5.4 and Table 4.6 for the 80,000 volcanic ash particles simulation with No wind effects, and the first column shows the variable volcanic ash particles diameter for 1mm,5 mm and 10 mm. The second column shows the variable Volcanic Ash Particle densities for 1000 (Kgm^{-3}), 2000 (Kgm^{-3}) and 3000 (Kgm^{-3}), and the third column shows the Horizontal wind direction (ms^{-1}). The fourth column shows the FEM maximum stress results (MPa). The fifth column shows the FEM maximum strain the sixth shows the \leq Allowable Stress (MPa). The seventh column shows the nature of assessing the results used for the criterion $\sigma_{\max} \leq \sigma_a$ allowable, and the eighth column shows $\sigma_{\max} \leq \sigma_a$ allowable is not satisfied (MPa) for flat concrete roof structure. In Table 5.14, the results show that the 10mm volcanic ash particles size for the volcanic ash densities of 1000 (Kgm^{-3}) and 2000 (Kgm^{-3}) did not certify the criterion for column six. It means FEM stress results will have an impact on the roof. However, the rest of the FEM simulation tests are safe.

5.2.2 Discrete Element Method (DEM) and Structural Analysis tool (ANSYS) for the Finite Element Method (FEM) Simulation. (Pitched Concrete Roof)

Table 5.15 shows the 20 degrees pitched concrete roof simulation data from Table 4.8 for the 170,000 volcanic ash particles simulation with No wind effects. The first column shows the variable volcanic ash particles diameter for 1 mm, 5 mm, and 10 mm. The second column shows the variable volcanic ash particle densities for 1000 (Kgm^{-3}), 2000 (Kgm^{-3}) and 3000 (Kgm^{-3}). The third column shows the DEM simulation result for the maximum pressure loading

on the flat concrete roof (Pa). The fourth column shows the simulation results from the FEM maximum deformation results (mm).

Table 5.15: Result of 20 Degrees Concrete Tile Pitched Roof for 170000 Simulations Volcanic Ash DEM and FEM Simulation with No Wind Effects.

Volcanic Ash Particle Size in Diameter (mm)	Volcanic Ash Particle densities (Kgm^{-3})	DEM Maximum Pressure (Pa)	FEM Maximum Deformation Results (mm)	FEM Maximum von Mises stress (MPa)	FEM Maximum Strain Results (mm/mm)
1	1000	2.1465	2.7944e^{-5}	0.14833	7.4237e^{-9}
5	1000	182.73	0.0028559	0.14496	7.2549e^{-7}
10	1000	940.33	0.17444	2.6009	1.4024e^{-5}
1	2000	2.1465	2.7944e^{-5}	0.14833	7.4237e^{-9}
5	2000	153.593	0.011464	0.289921	1.4508e^{-6}
10	2000	2369.35	0.043177	1.7761	8.8892e^{-6}
1	3000	3164.25	0.27262	6.6844	3.3467
5	3000	2556.8	0.47581	7.6946	3.8526e^{-5}

The fifth column shows the FEM maximum stress results (MPa), and the sixth column shows the results FEM maximum strain results. Table 5.15, the test results show the set of results from the DEM and FEM simulation. The results for the 1 mm volcanic ash particles show the lesser values for the 1000 (Kgm^{-3}) density DEM pressure value as 2.1465 (Pa) for simulation that of 2000 (Kgm^{-3}) density have the DEM pressure value as 2.1465 (Pa). The highest value for this data set is the 10mm volcanic ash particles DEM pressure value of 2556.8 (MPa); apart from the 1mm volcanic ash particles sites, the rest of the DEM pressure will be high with the corresponding FEM stress values. Some impart on the roof with no wind simulation.

Table 5.15 shows the 20 degrees pitched concrete roof simulation data from Table 4.9, for the 170,000 volcanic ash particles simulation with No wind effects. The first column shows the

variable volcanic ash particles diameter for 1 mm, 5 mm, and 10 mm. The second column shows the variable Volcanic Ash Particle densities for 1000 (Kgm^{-3}), 2000 (Kgm^{-3}) and 3000 (Kgm^{-3}).

Table 5.16: Result of 20 Degrees Concrete Tile Pitched Roof for 170000 Simulations Volcanic Ash DEM and FEM Simulation with Wind Effects.

Volcanic Ash Particle Size in Diameter (mm)	Volcanic Ash Particle densities (Kgm^{-3})	Horizontal wind direction (ms^{-1})	DEM Maximum Pressure (Pa)	FEM Maximum Deformation Results (mm)	FEM Maximum von Mises stress (MPa)	FEM Maximum Strain Results (mm/mm)
5	1000	0.5	1578.66	0.38522	5.7543	2.883e^{-5}
10	1000	1.0	3472.2	0.70084	11.988	6.0047e^{-5}
5	2000	0.5	562.81	0.041757	1.0516	5.2623e^{-6}
10	2000	1.0	278.17	0.053258	0.87847	4.393e^{-6}
5	3000	0.5	541.111	0.040171	1.0121	5.0648e^{-6}
10	3000	1.0	227.56	0.043617	0.72025	3.6018e^{-6}

The third column shows a horizontal wind direction (ms^{-1}). The fourth column shows the DEM simulation result for the maximum pressure loading on the flat concrete roof (Pa). The fifth column shows the simulation results from the FEM maximum deformation results (mm). The sixth column shows the FEM maximum stress results (MPa), and the seventh column shows the results FEM maximum strain results. Table 5.16 the test results for the set of values for the DEM pressure values and the FEM stress values strain values, and deformation values will affect these results of the volcanic ash loading on the roof. The 5 mm, volcanic ash particle with the horizontal wind direction has the highest DEM pressure value of 1578.66 (Pa). That will affect the roof because of the higher stress level on the roof. Table 5.17 shows the 25 degrees pitched concrete roof simulation data for the 170,000 volcanic ash particles simulation

with No wind effects. The first column shows the variable volcanic ash particles diameter for 1 mm, 5 mm and 10 mm.

Table 5.17: Result of 25 Degrees Concrete Tile Pitched Roof for 170000 Simulations Volcanic Ash DEM and FEM Simulation with No Wind Effects.

Volcanic Ash Particle Size in Diameter (mm)	Volcanic Ash Particle densities (Kgm ⁻³)	DEM Maximum Pressure (Pa)	FEM Maximum Deformation Results (mm)	FEM Maximum von Mises stress (MPa)	FEM Maximum Strain Results (mm/mm)
1	1000	2.59892	0.00047982	0.0076547	3.8326e ⁻⁸
5	1000	2193.33	0.49444	8.155	4.0844e ⁻⁵
10	1000	2040.56	0.51486	8.0286	4.0192e ⁻⁵
1	2000	2.5989	0.00047982	0.0076547	3.826 ⁻⁸
5	2000	159.842	0.033743	0.52059	2.6061e ⁻⁶
10	2000	2970.64	0.88884	13.706e ⁻⁷	6.8614e ⁻⁵
1	3000	131.753	0.01328	0.20128	1.0075e ⁻⁶
5	3000	4060.9	0.95708	14.809	7.4143e ⁻⁵

The second column shows the variable volcanic ash particle densities for 1000 (Kgm⁻³), 2000 (Kgm⁻³) and 3000 (Kgm⁻³). The third column shows the DEM simulation result for the maximum pressure loading on the flat concrete roof (Pa). The fourth column shows the simulation results from the FEM maximum deformation results (mm). The fifth column shows the FEM maximum stress results (MPa), and the sixth column shows the results FEM maximum strain results. Table 5.17, the result shows a similar pattern as in table 5.16. The 1m volcanic ash particle size for the volcanic ash particle density for the 1000 (Kgm⁻³) recorded the same values for the DEM pressure values 2.59822 (Pa) whilst the rest of the values for 5 mm and 10 mm volcanic ash particles with volcanic ash densities for 2000 (Kgm⁻³) and 3000 (Kgm⁻³) recorded variable values for DEM and FEM simulation values for deformation stress and strain rests. Data for a set of results for 25 degrees and 30 degrees is presented for Concrete

Tile pitched roof for 170000 Simulations volcanic ash DEM and FEM Simulation with wind and No Wind Effects.

Table 5.18: Result of 25 Degrees Concrete Tile Pitched Roof for 170000 Simulations Volcanic Ash DEM and FEM Simulation with Wind Effects

Volcanic Ash Particle Size in Diameter (mm)	Volcanic Ash Particle densities (Kg/m ³)	Horizontal direction (ms ⁻¹)	DEM Maximum Pressure (Pa)	FEM Maximum Deformation Results (mm)	FEM Maximum von Mises stress (MPa)	FEM Maximum Strain Results (mm/mm)
5	1000	0.5	121.861	2.1569e ⁻⁵	3.9221e ⁻⁵	1.9633e ⁻⁵
10	1000	1.0	1339.07	0.2986	4.5403	2.2731e ⁻⁵
5	2000	0.5	70.6207	0.005336	0.11487	5.7484e ⁻⁷
10	2000	1.0	3215.44	0.80002	13.023	6.5214e ⁻⁵
5	3000	0.5	62.3963	0.0048505	0.10544	5.2765e ⁻⁷
10	3000	1.0	11141.9	3.1321	47.952	0.00024012

Table 5.18 shows the 25 degrees pitched concrete roof simulation data from chapter 4 for the 170,000 volcanic ash particles simulation with No wind effects. The first column shows the variable volcanic ash particles diameter for 1 mm, 5 mm, and 10 mm. The second column shows the variable Volcanic Ash Particle densities for 1000 (Kg/m³), 2000 (Kg/m³) and 3000 (Kg/m³). The third column shows a horizontal wind direction (ms⁻¹). The fourth column shows the DEM simulation result for the maximum pressure loading on the flat concrete roof (Pa). the fifth column shows the simulation results from the FEM maximum deformation results (mm) The sixth column shows the FEM maximum stress results (MPa), and the seventh column shows the results for FEM maximum strain results (mm/mm).

Table 5.19: Result of 30 Degrees Concrete Tile Pitched Roof for 170, 000 Simulation Volcanic Ash DEM and FEM Simulation with Wind Effects

Volcanic Ash Particle Size in Diameter (mm)	Volcanic Ash Particle identities (Kgm^{-3})	DEM Maximum Pressure (Pa)	FEM Maximum Deformation Results (mm)	FEM Maximum von Mises stress (MPa)	FEM Maximum Strain Results (mm/mm)
5	1000	12723.2	4.0687	60.477	0.00030278
5	2000	240.51	0.04513	0.70281	$3.5185e^{-6}$
10	2000	106049	0.031106	470.88	0.0023575
5	3000	110.564	0.020693	0.32017	$1.6029e^{-6}$
10	3000	35218	6.9968	121.95	0.00061038

Table 5.19 shows the results for the 30 degrees pitched concrete roof simulation data from table 4.12 for the 170,000 volcanic ash particles simulation with No wind effects. The first column shows the variable volcanic ash particles diameter for 1 mm, 5 mm, and 10 mm. The second column shows the variable Volcanic Ash Particle densities for 1000 (Kgm^{-3}), 2000 (Kgm^{-3}) and 3000 (Kgm^{-3}). The third column shows horizontal wind direction (ms^{-1}). The fourth column shows the DEM simulation result for the maximum pressure loading on the flat concrete roof (Pa). The fifth column shows the simulation results from the FEM maximum deformation results (mm). The sixth column shows the FEM maximum stress results (MPa). The seventh column shows the results FEM maximum strain results. The result for the DEM and FEM simulation test shows that 5 mm and 10 mm volcanic ash particles with the volcanic ash particles densities pf 1000 (Kgm^{-3}) for 5 mm and 2000 (Kgm^{-3}) and 3000 (Kgm^{-3}) for the 10mm particles have the highest FEM stress Deformation and the strain values. It will certainly impact the tile-pitched roof.

Table 5.20: Result of 30 Degrees Concrete Tile Pitched Roof for 170, 000 Simulation Volcanic Ash DEM and FEM Simulation with Wind No Effects

Volcanic Ash Particle Size in Diameter (mm)	Volcanic Ash Particle densities (Kgm^{-3})	Horizontal direction (ms^{-1})	DEM Maximum Pressure (Pa)	FEM Maximum Deformation Results (mm)	FEM Maximum von Mises stress (MPa)	FEM Maximum Strain Results (mm/mm)
5	1000	0.5	9971.8	2.7771	42.036	0.00021046
10	1000	1.0	43016.6	14.908	218.87	0.0010957
5	2000	0.5	302.508	0.088155	1.2864	6.4403e ⁻⁶
10	2000	1.0	189.302	0.036981	0.61631	3.0851e ⁻⁶
5	3000	0.5	123.59	2.3495e ⁻⁵	0.37836	1.8942e ⁻⁶
10	3000	1.0	4496.03	0.0010866	17.87	8.9494e ⁻⁵

Table 5.20 shows the results for the 30 degrees pitched concrete roof simulation data from table 4.13 for the 170,000 volcanic ash particles simulation with No wind effects. The first column shows the variable volcanic ash particles diameter for mm, 5 mm, and 10 mm. The second column shows the variable Volcanic Ash Particle densities for 1000 (Kgm^{-3}), 2000 (Kgm^{-3}) and 3000 (Kgm^{-3}). The third column shows horizontal wind direction (ms^{-1}). The fourth column shows the DEM simulation result for the maximum pressure loading on the flat concrete roof (Pa). The fifth column shows the simulation results from the FEM maximum deformation results (mm). The sixth column shows the FEM maximum stress results (MPa). The seventh column shows the results FEM maximum strain results. The result for the DEM and FEM simulation test shows that 5 mm and 10 mm volcanic ash particles with the volcanic ash particles densities pf 1000 (Kgm^{-3}) for 5 mm and 2000 (Kgm^{-3}) and 3000 (Kgm^{-3}) for the 10mm particles have the highest FEM stress deformation and the strain values. It will certainly impact the tile-pitched roof. The other simulation test wouldn't have much significant impact on the tile-pitched roof.

5.2.3 Structural Failures Identified from Pitched Concrete Roof simulation

The failure of structure using the stress data from the numerical modelling tool (EDEM software) for the Discrete Element Method (DEM) and structural analysis tool (ANSYS) for the Finite Element Method (FEM) simulation are discussed here. It also shows how the various decisions to determine how the allowable stress was related to the maximum stress regarding the EU and the UK regions. The tables below relate to the EN Values calculated.

Table 5.21: Result of 20 Degrees Pitched Concrete Tile Pitched Roof for 170 000 Simulation Volcanic Ash DEM and FEM Simulation with No Wind Effects.

Volcanic Ash Particles Size(mm)	Volcanic Particles Density(Kgm ⁻³)	FEM Maximum von Mises stress (MPa)	FEM Maximum Strain Results (mm/m)	≤ Allowable Stress (MPa)	Maximum stress ≤ Allowable Stress is satisfied (MPa)	Maximum stress ≤ Allowable stress' is not satisfied (MPa)
1	1000	0.14833	7.4237e ⁻⁹	1.8		
5	1000	0.14496	7.2549e ⁻⁷	1.8		
10	1000	2.6009	1.4024e ⁻⁵	1.8		
1	2000	0.14833	7.4237e ⁻⁹	1.8		
5	2000	0.289921	1.4508e ⁻⁶	1.8		
10	2000	1.7761	8.8892e ⁻⁶	1.8		
1	3000	6.6844	3.3467	1.8		
5	3000	7.6946	3.8526e ⁻⁵	1.8		

Table 5.21 shows 170,000 volcanic ash particles failure results data for 20 degrees pitched concrete tile roof structure, using maximum stress and strain values from the modelling tool (EDEM software) for the Discrete Element Method DEM and structural analysis tool (ANSYS) for the Finite Element Method (FEM) simulation in relations with the allowable stress (EU Code values). The first column shows the variable volcanic ash particles diameter for 1mm,5 mm and 10 mm. The second column shows the variable Volcanic Ash Particle densities for 1000 (kgm⁻³), 2000 (kgm⁻³) and 3000 (kgm⁻³). The third column shows the FEM maximum

stress results (MPa). The fourth column shows the FEM maximum strain results, and the fifth shows the $\sigma_{\max} \leq \sigma_a$ Allowable Stress (MPa). The sixth column shows the nature of assessing the results use for the criterion $\sigma_{\max} \leq \sigma$ allowable, and the seventh column shows $\sigma_{\max} \leq \sigma_a$ is not satisfied (MPa) for flat concrete roof structure. Table 5.21 the sets of results for the DEM and FEM simulation show that the values for 5mm 10mm volcanic ash particles with volcanic ash densities for 1000 (Kgm⁻³) 2000 (Kgm⁻³) and 3000 (Kgm⁻³) are high for horizontal direction for 0.5 (ms⁻¹), 1.0 (ms⁻¹) have high values. Two of the simulation results are low as such cannot have any impact on the roof.

Table 5.22: Result of 20 Degrees Pitched Concrete Tile Pitched Roof for 170000 Simulation Volcanic Ash DEM and FEM simulation with wind effects

Volcanic Ash Particles Size(mm)	Volcanic Particles Density (Kgm ⁻³)	Horizontal direction (ms ⁻¹)	FEM Maximum von Mises stress (MPa)	FEM Maximum Strain Results (mm/m)	≤ Allowable Stress (MPa)	Maximum stress ≤ Allowable Stress is satisfied (MPa)	Maximum stress ≤ Allowable stress' is not satisfied (MPa)
5	1000	0.5	5.7543	2.883e ⁻⁵	1.8		
10	1000	1.0	11.988	6.0047e ⁻⁵	1.8		
5	2000	0.5	1.0516	5.2623e ⁻⁶	1.8		
10	2000	1.0	0.87847	4.393e ⁻⁶	1.8		
5	3000	0.5	1.0121	5.0648e ⁻⁶	1.8		
10	3000	1.0	0.72025	3.6018e ⁻⁶	1.8		

Table 5.22 shows the 170,000 volcanic ash particles resulting from failure data for 20 degrees pitched concrete tile roof structure, using maximum stress and strain values from the modelling tool (EDEM software) for the Discrete Element Method DEM and structural analysis tool (ANSYS) for the Finite Element Method (FEM) simulation in relations with the allowable stress (EU Code values). Table 5.21, the set of the FEM simulation results shows that the 10 mm volcanic ash particles with a density of 1000 (Kgm⁻³) and 3000 (Kgm⁻³) and the 5 mm volcanic ash particles with a density of 3000 (Kgm⁻³) do not certify the criterion in column five

as indicated in column seven. The rest of the results do certify the criterion for column five, as indicated in column six.

The simulation data shows the 170,000 volcanic ash particles simulation with wind effects. The first column shows the variable volcanic ash particles diameter for 1 mm, 5 mm, and 10 mm. The second column show the variable volcanic ash particle densities for 1000 (kgm⁻³), 2000, (kgm⁻³) and 3000 (kgm⁻³). The third column shows the horizontal wind direction (ms⁻¹). The fourth column shows the FEM maximum stress results (MPa). The fifth column shows the FEM maximum strain results, from the sixth shows the $\sigma_{\max} \leq$ Allowable Stress (MPa). The seventh column shows the nature of assessing the results use for the criterion $\sigma_{\max} \leq \sigma$ allowable and the eight-column shows $\sigma_{\max} \leq \sigma$ allowable is not satisfied (MPa) for flat concrete roof structures. Table 5.22, the set for results for the FEM simulation, shows that volcanic ash particles for 5 mm and 10 mm for the volcanic ash densities of 1000 (Kgm⁻³) do not certify the criterion for column six as it is indicated in column eight. The rest of the test certifies the criterion. That means the roof will be safe under these conditions.

Table 5.23: Result of 25 Degrees Pitched Concrete Tile Pitched Roof for 170000 Simulation Volcanic Ash DEM and FEM Simulation with No Wind Effects

Volcanic Ash Particles Size(mm)	Volcanic Particles Density (Kgm ⁻³)	FEM Maximum von Mises stress (MPa)	FEM Maximum Strain Results (mm/m)	\leq Allowable Stress (MPa)	Maximum stress \leq Allowable Stress is satisfied (MPa)	Maximum stress \leq Allowable stress' is not satisfied(MPa)
1	1000	0.0076547	3.8326e ⁻⁸	1.8		
5	1000	8.155	4.0844e ⁻⁵	1.8		
10	1000	8.0286	4.0192e ⁻⁵	1.8		
1	2000	0.0076547	3.826e ⁻⁸	1.8		
5	2000	0.52059	2.6061e ⁻⁶	1.8		
10	2000	13.706e ⁻⁷	6.8614e ⁻⁵	1.8		
5	3000	0.20128	1.0075e ⁻⁶	1.8		
10	3000	14.809	7.4143e ⁻⁵	1.8		

Table 5.23 shows 170,000 volcanic ash particles data failure results for 25 degrees pitched concrete tile roof structure, using maximum stress and strain values from the modelling tool (EDEM software) for the Discrete Element Method DEM and structural analysis tool (ANSYS) for the Finite Element Method (FEM) simulation in relations with the allowable stress (EU Code values). Table 5.23 shows the simulation results in Table 4.15 for the 170,000 volcanic ash particles simulation with No wind effects. The first column shows the variable volcanic ash particles diameter for 1 mm, 5 mm and 10 mm. The second column show the variable volcanic ash particle densities for 1000 (kgm^{-3}) 2000 (kgm^{-3}) and 3000 (kgm^{-3}). The third column shows the FEM maximum stress results (MPa). The fourth column shows the FEM maximum strain results, and the fifth shows the $\sigma_{\max} \leq \text{Allowable Stress (MPa)}$. The sixth column shows the nature of assessing the results use for the criterion $\sigma_{\max} \leq \sigma_{\text{allowable}}$, and the seventh column shows $\sigma_{\max} \leq \sigma_{\text{allowable}}$ is not satisfied (MPa) for flat concrete roof structures. Table 5.23 shows that the set results for the FEM simulation with volcanic ash particles for the volcanic as densities of 1000 (Kgm^{-3}), 2000 (Kgm^{-3}) will certify the criterion in column five as indicated in column six. It means the pitched roof will be safe under these volcanic ash loadings. The rest of the test will not certify the column five criteria, as indicated in column six. These volcanic loadings will have an impact on the tile-pitched roof.

Table 5.24: Result of 25 Degrees Pitched Concrete Tile Pitched Roof for 170000 Simulation Volcanic Ash DEM and FEM Simulation with Wind Effects

Volcanic Ash Particles Size (mm)	Volcanic Particles Density (Kgm ⁻³)	Horizontal direction (ms ⁻¹)	FEM Maximum von Mises stress (MPa)	FEM Maximum Strain Results (mm/m)	≤ Allowable Stress (MPa)	Maximum stress ≤ Allowable Stress is satisfied (MPa)	Maximum stress ≤ Allowable stress' is not satisfied (MPa)
5	1000	0.5	121.861	2.1569e ⁻⁵	1.8		
10	1000	1.0	1339.07	0.2986	1.8		
5	2000	0.5	70.6207	0.005336	1.8		
10	2000	1.0	3215.44	0.80002	1.8		
5	3000	0.5	62.3963	0.0048505	1.8		
10	3000	1.0	11,141.9	3.1321	1.8		

Table 5.24 shows 170,000 volcanic ash particles failure results for 25 degrees pitched concrete tile roof structure, using maximum stress and strain values from the modelling tool (EDEM software) for the Discrete Element Method DEM and structural analysis tool (ANSYS) for the Finite Element Method (FEM) simulation in relations with the allowable stress (EU Code values). Table 5.24 shows the simulation results in Table 4. for the 170,000 volcanic ash particles simulation with wind effects. The first column shows the variable volcanic ash particles diameter for 1 mm, 5 mm, and 10 mm. The second column show the variable volcanic ash particle densities for 1000 (kgm⁻³), 2000 (kgm⁻³) and 3000 (kgm⁻³). The third column shows the horizontal wind direction (ms⁻¹). The fourth column shows the FEM maximum stress results (MPa). The fifth column shows the FEM maximum strain results from the six shows the $\sigma_{max} \leq$ Allowable Stress (MPa). The seventh column shows the nature of assessing the results use for the criterion $\sigma_{max} \leq \sigma_a$ and the eight-column shows $\sigma_{max} \leq \sigma_a$ is not satisfied (MPa) for flat concrete roof structures. Table 5.24, the set of results from the FEM simulation, shows that all the different test results did not certify the column six criterion, as indicated in column six. That means all the simulation tests will have an immense impact on the roof.

Table 5.25: Result of 30 Degrees Pitched Concrete Tile Pitched Roof for 170000 Simulation Volcanic Ash DEM and FEM Simulation with No Wind Effects

Volcanic Ash Particles Size (mm)	Volcanic Particles Density (Kgm ⁻³)	FEM Maximum von Mises stress (MPa)	FEM Maximum Strain Results (mm/m)	≤ Allowable Stress (MPa)	Maximum stress ≤ Allowable Stress is satisfied (MPa)	Maximum stress' is not satisfied (MPa)
1	2000	60.477	0.00030278	1.8		
5	2000	0.70281	3.5185e ⁻⁶	1.8		
10	2000	470.88	0.0023575	1.8		
5	3000	0.32017	1.6029e ⁻⁶	1.8		
10	3000	121.95	0.00061038	1.8		

Table 5.25 shows the 170,000 volcanic ash particles failure results for 30 degrees pitched concrete tile roof structure, using maximum stress and strain values from the modelling tool (EDEM software) for the Discrete Element Method DEM and structural analysis tool (ANSYS) for the Finite Element Method (FEM) simulation in relations with the allowable stress (EU Code values). Table 5.25 shows the simulation results in Table 4.16 for the 170,000 volcanic ash particles simulation with No wind effects. The first column shows the variable volcanic ash particles diameter for 1 mm, 5 mm, and 10 mm. The second column shows the variable volcanic ash particle densities for 1000 (kgm⁻³), 2000 (kgm⁻³) and 3000 (kgm⁻³). The third column shows the FEM maximum stress results (MPa). The fourth column shows the FEM maximum strain results, from the fifth shows the $\sigma_{max} \leq$ Allowable Stress (MPa). The sixth column shows the nature of assessing the results use for the criterion $\sigma_{max} \leq \sigma$ allowable and the seventh column shows $\sigma_{max} \leq \sigma$ allowable is not satisfied (MPa) for flat concrete roof structures). Table 5.25 shows that the three FEM simulation tests exceeded the criterion in column six. As indicated in column and three of the other simulation were within the criterion in column six indicated in column seven, all the red colours show the criterion was not certified. The column in yellow means the criterion is being certified.

Table 5.26: Result of 30 Degrees Pitched Concrete Tile Pitched Roof for 170 000 Simulation Volcanic Ash DEM and FEM Simulation with Wind Effects

Volcanic Ash Particles Size (mm)	Volcanic Particles Density (Kgm ⁻³)	Horizontal direction (ms ⁻¹)	FEM Maximum von Mises stress (MPa)	FEM Maximum Strain Results (mm/m)	≤ Allowable Stress (MPa)	Maximum stress ≤ Allowable Stress is satisfied (MPa)	Maximum stress ≤ Allowable stress' is not satisfied (MPa)
5	1000	5	42.036	0.00021046	1.8		
10	1000	10	218.87	0.0010957	1.8		
5	2000	5	1.2864	6.4403e-6	1.8		
10	2000	10	0.61631	3.0851e-6	1.8		
5	3000	5	0.37836	1.8942e-6	1.8		
10	3000	10	17.87	8.9494e-5	1.8		

Table 5.26 shows 170,000 volcanic ash particles failure results for 30 degrees pitched concrete tile roof structure, using maximum stress and strain values from the modelling tool (EDEM software) for the Discrete Element Method DEM and structural analysis tool (ANSYS) for the Finite Element Method (FEM) simulation in relations with the allowable stress (EU Code values). Table 5.26: shows the simulation results in Table 4.17 for the 170,000 volcanic ash particles simulation with wind effects. The first column shows the variable volcanic ash particles diameter for 1 mm, 5 mm and 10 mm. The second column shows the variable Volcanic Ash Particle densities for 1000 (kgm⁻³), 2000 (kgm⁻³) and 3000 (kgm⁻³). The third column shows the Horizontal wind direction (ms⁻¹). The fourth column shows the FEM maximum stress results (MPa). The fifth column shows the FEM maximum strain results from the six shows the $\sigma_{max} \leq$ Allowable Stress (MPa). The seventh column shows the nature of assessing the results use for the criterion $\sigma_{max} \leq \sigma$ allowable and the eight-column shows $\sigma_{max} \leq \sigma$ allowable is not satisfied (MPa) for flat concrete roof structures. Table 5.26 the results for the FEM simulation show that their stress test values exceeded the criterion in column six indicated

in both the column seven results are safe as the column eight results are not safe and would have an impact on the tile pitched roof.

Table 5.27: Result of 20 Degrees Pitched Concrete Tile Pitched Roof for 170 000 Simulation Volcanic Ash DEM and FEM Simulation with No Wind Effects_

Volcanic Ash Particles Size(mm)	Volcanic Particles Density(Kgm ⁻³)	FEM Maximum von Mises stress (MPa)	FEM Maximum Strain Results (mm/m)	≤ Allowable Stress (MPa)	Maximum stress ≤ Allowable Stress is satisfied (MPa)	Maximum stress ≤ Allowable stress' is not satisfied (MPa)
1	1000	0.14833	7.4237e ⁻⁹	1.8		
5	1000	0.14496	7.2549e ⁻⁷	1.8		
10	1000	2.6009	1.4024e ⁻⁵	1.8		
1	2000	0.14833	7.4237e ⁻⁹	1.8		
5	2000	0.289921	1.4508e ⁻⁶	1.8		
10	2000	1.7761	8.8892e ⁻⁶	1.8		
5	3000	6.6844	3.3467	1.8		
10	3000	7.6946	3.8526e ⁻⁵	1.8		

Table 5.27 shows 170,000 volcanic ash particles failure results data for 20 degrees pitched concrete tile roof structure, using maximum stress and strain values from the modelling tool (EDEM software) for the Discrete Element Method DEM and structural analysis tool (ANSYS) for the Finite Element Method (FEM) simulation in relations with the allowable stress (EU Code values). The first column shows the variable volcanic ash particles diameter for 1 mm, 5 mm, and 10 mm. The second column shows the variable Volcanic Ash Particle densities for 1000 (kgm⁻³), 2000 (kgm⁻³) and 3000 (kgm⁻³). The third column shows the FEM maximum stress results (MPa). The fourth column shows the FEM maximum strain results, and the fifth shows the $\sigma_{max} \leq \sigma_a$ allowable stress (MPa). The sixth column shows the nature of assessing the results use for the criterion $\sigma_{max} \leq \sigma_a$ allowable, and the seventh column shows $\sigma_{max} \leq \sigma_a$ is not satisfied (MPa) for flat concrete roof structure. Table 5.20 the sets of results for the DEM

and FEM simulation shows that the values for 5 mm 10 mm volcanic ash particles with volcanic ash densities for 1000 (Kgm⁻³) 2000 (Kgm⁻³) and 3000 (Kgm⁻³) are high for horizontal direction for 0.5 (ms⁻¹), 1.0 (ms⁻¹) have high values. Two of the simulation results are low as such cannot have any impact on the roof.

Table 5.28: Result of 20 Degrees Pitched Concrete Tile Pitched Roof for 170000 Simulation Volcanic Ash DEM and FEM simulation with wind effects

Volcanic Ash Particles Size(mm)	Volcanic Particles Density (Kgm ⁻³)	Horizontal direction (ms ⁻¹)	FEM Maximum von Mises stress (MPa)	FEM Maximum Strain Results (mm/m)	≤ Allowable Stress (MPa)	Maximum stress ≤ Allowable Stress is satisfied (MPa)	Maximum stress ≤ Allowable stress' is not satisfied (MPa)
5	1000	0.5	5.7543	2.883e-5	1.8		
10	1000	1.0	11.988	6.0047e-5	1.8		
5	2000	0.5	1.0516	5.2623e-6	1.8		
10	2000	1.0	0.87847	4.393e-6	1.8		
5	3000	0.5	1.0121	5.0648e-6	1.8		
10	3000	1.0	0.72025	3.6018e-6	1.8		

Table 5.28 shows the 170,000 volcanic ash particles results from failure data for 20 degrees pitched concrete tile roof structure, using maximum stress and strain values from the modelling tool (EDEM software) for the Discrete Element Method DEM and structural analysis tool (ANSYS) for the Finite Element Method (FEM) simulation in relations with the allowable stress (EU Code values). Table 5.21, the set of the FEM simulation results shows that the 10 mm volcanic ash particles with a density of 1000 (Kgm⁻³) and 3000 (Kgm⁻³) and the 5 mm volcanic ash particles with a density of 3000 (Kgm⁻³) do not certify the criterion in column five as indicated in column seven. The rest of the results do certify the criterion for column five, as indicated in column six.

The simulation data shows the 170,000 volcanic ash particles simulation with wind effects. The first column shows the variable volcanic ash particles diameter for 1mm, 5 mm and 10 mm. The second column show the variable volcanic ash particle densities for 1000 (kgm⁻³), 2000, (kgm⁻³) and 3000 (kgm⁻³). The third column shows the horizontal wind direction (ms⁻¹). The fourth column shows the FEM maximum stress results (MPa). The fifth column shows the FEM maximum strain results, and the sixth shows the $\sigma_{\max} \leq \sigma_a$ allowable Stress (MPa). The seventh column shows the nature of assessing the results use for the criterion $\sigma_{\max} \leq \sigma_a$ allowable and the eight-column shows $\sigma_{\max} \leq \sigma_a$ allowable is not satisfied (MPa) for flat concrete roof structure. Table 5.22, the set for results for the FEM simulation, shows that volcanic ash particles for 5 mm and 10 mm for the volcanic ash densities of 1000 (Kgm⁻³) do not certify the criterion for column six as it is indicated in column eight. The rest of the test certifies the criterion. That means the roof will be safe under these conditions.

Table 5.29: Result of 25 Degrees Pitched Concrete Tile Pitched Roof for 170000 Simulation Volcanic Ash DEM and FEM Simulation with No Wind Effects

Volcanic Ash Particles Size(mm)	Volcanic Particles Density (Kgm ⁻³)	FEM Maximum von Mises stress (MPa)	FEM Maximum Strain Results (mm/m)	\leq Allowable Stress (MPa)	Maximum stress \leq Allowable Stress is satisfied (MPa)	Maximum stress \leq Allowable stress' is not satisfied (MPa)
1	1000	0.0076547	3.8326e ⁻⁸	1.8		
5	1000	8.155	4.0844e-5	1.8		
10	1000	8.0286	4.0192e-5	1.8		
1	2000	0.0076547	3.826e-8	1.8		
5	2000	0.52059	2.6061e-6	1.8		
10	2000	13.706e7	6.8614e-5	1.8		
5	3000	0.20128	1.0075e-6	1.8		
10	3000	14.809	7.4143e-5	1.8		

Table 5.29 shows 170,000 volcanic ash particles data failure results for 25 degrees pitched concrete tile roof structure, using maximum stress and strain values from the modelling tool (EDEM software) for the Discrete Element Method DEM and structural analysis tool (ANSYS) for the Finite Element Method (FEM) simulation in relations with the allowable stress (EU Code values). Table 5.23 shows the simulation results in Table 4.15 for the 170,000 volcanic ash particles simulation with No wind effects. The first column shows the variable volcanic ash particles diameter for 1 mm, 5 mm, and 10 mm. The second column show the variable volcanic ash particle densities for 1000 (kgm^{-3}) 2000 (kgm^{-3}) and 3000 (kgm^{-3}). The third column shows the FEM maximum stress results (MPa). The fourth column shows the FEM maximum strain results, from the fifth shows the $\sigma_{\max} \leq \sigma_a$ Allowable Stress (MPa). The sixth column shows the nature of assessing the results use for the criterion $\sigma_{\max} \leq \sigma$ allowable, and the seventh column shows $\sigma_{\max} \leq \sigma_a$ allowable is not satisfied (MPa) for flat concrete roof structure. Table 5.23 shows that the set results for the FEM simulation with volcanic ash particles for the volcanic as densities of 1000 (Kgm^{-3}), 2000 (Kgm^{-3}) will certify the criterion in column five as indicated in column six. It means the pitched roof will be safe under these volcanic ash loadings. The rest of the test will not certify the column five criteria, as indicated in column six. These volcanic loadings will have an impact on the tile-pitched roof.

Table 5.30: Result of 25 Degrees Pitched Concrete Tile Pitched Roof for 170000 Simulation Volcanic Ash DEM and FEM Simulation with Wind Effects

Volcanic Ash Particles Size (mm)	Volcanic Particles Density (Kgm ⁻³)	Horizontal direction (ms ⁻¹)	FEM Maximum von Mises stress (MPa)	FEM Maximum Strain Results (mm/m)	≤ Allowable Stress (MPa)	Maximum stress ≤ Allowable Stress is satisfied (MPa)	Maximum stress ≤ Allowable stress' is not satisfied (MPa)
5	1000	0.5	121.861	2.1569e ⁻⁵	1.8		
10	1000	1.0	1339.07	0.2986	1.8		
5	2000	0.5	70.6207	0.005336	1.8		
10	2000	1.0	3215.44	0.80002	1.8		
5	3000	0.5	62.3963	0.0048505	1.8		
10	3000	1.0	11141.9	3.1321	1.8		

Table 5.30 shows 170,000 volcanic ash particles failure results for 25 degrees pitched concrete tile roof structure, using maximum stress and strain values from the modelling tool (EDEM software) for the Discrete Element Method DEM and structural analysis tool (ANSYS) for the Finite Element Method (FEM) simulation in relations with the allowable stress (EU Code values). Table 5.30 shows the simulation results in Table 4. for the 170,000 volcanic ash particles simulation with wind effects. The first column shows the variable volcanic ash particles diameter for 1mm,5 mm and 10 mm. The second column show the variable volcanic ash particle densities for 1000 (kgm⁻³), 2000 (kgm⁻³) and 3000 (kgm⁻³). The third column shows the horizontal wind direction (ms⁻¹). The fourth column shows the FEM maximum stress results (MPa). The fifth column shows the FEM maximum strain results from the six shows the $\sigma_{\max} \leq \sigma_a$ allowable stress (MPa). The seventh column shows the nature of assessing the results use for the criterion $\sigma_{\max} \leq \sigma_a$ and the eight-column shows $\sigma_{\max} \leq \sigma_a$ is not satisfied (MPa) for flat concrete roof structures. Table 5.24, the set of results from the FEM simulation, shows that all

the different test results did not certify the column six criterion, as indicated in column six. That means all the simulation tests will have an immense impact on the roof.

Table 5.31: Result of 30 Degrees Pitched Concrete Tile Pitched Roof for 170000 Simulation Volcanic Ash DEM and FEM Simulation with No Wind Effects

Volcanic Ash Particles Size(mm)	Volcanic Particles Density(Kgm ⁻³)	FEM Maximum von Mises stress (MPa)	FEM Maximum Strain Results (mm/m)	≤ Allowable Stress (MPa)	Maximum stress ≤ Allowable Stress is satisfied (MPa)	Maximum stress ≤ Allowable stress' is not satisfied (MPa)
5	1000	60.477	0.00030278	1.44		
5	2000	0.70281	3.5185e ⁻⁶	1.44		
10	2000	470.88	0.0023575	1.44		
5	3000	0.32017	1.6029e ⁻⁶	1.44		
10	3000	121.95	0.00061038	1.44		

Table 5.31: shows the 70,000 volcanic ash particles failure results for 30 degrees pitched concrete tile roof structure, using maximum stress and strain values from the modelling tool (EDEM software) for the Discrete Element Method DEM and structural analysis tool (ANSYS) for the Finite Element Method (FEM)simulation in relations with the allowable stress (UK Code values). Table 5.31 shows the results from the simulation data in Table 4.15, for the 170,000 volcanic ash particles simulation with No wind effects. The first column shows the variable volcanic ash particles diameter for 1 mm, 5 mm and 10 mm. The second column shows the variable.

Volcanic Ash Particle densities for 1000 (kgm⁻³) 2000 (kgm⁻³) and 3000 (kgm⁻³) The third column shows the FEM maximum stress results (MPa). The fourth column shows the FEM maximum strain results the shows the $\sigma_{max} \leq \sigma_a$ allowable Stress (MPa). The sixth column shows the nature of assessing the results use for the criterion $\sigma_{max} \leq \sigma_a$ allowable and the

seventh column shows $\sigma_{\max} \leq \sigma_a$ allowable is not satisfied (MPa) for flat concrete roof structure. Table 5.31 set of tests result shows four of the FEM test results exceed the criterion in column five as it is indicated in red colour in column seven. The other two results did not exceed as indicated in the sixth column. That means the volcanic ash will not affect the tiled pitched roof. Table 5.32, the test set results for the FEM simulation, indicates that three of the results were beyond the criterion for column six, as indicated in eight columns. The remaining tests show that the results did not exceed the column six criterion, as indicated in column seven. That means the import of the volcanic ash particle states for the tile pitched roof.

Table 5.32: Result of 30 Degrees Pitched Concrete Tile Pitched Roof for 170000 Simulation Volcanic Ash DEM and FEM Simulation with Wind Effects

Volcanic Ash Particles Size(mm)	Volcanic Particles Density(Kgm ⁻³)	Horizontal direction (ms ⁻¹)	FEM Maximum von Mises stress (MPa)	FEM Maximum Strain Results (mm/m)	≤ Allowable Stress (MPa)	Maximum stress ≤ Allowable Stress is satisfied (MPa)	Maximum stress ≤ Allowable stress' is not satisfied (MPa)
5	1000	5	42.036	0.00021046	1.44		
10	1000	10	218.87	0.0010957	1.44		
5	2000	5	1.2864	6.4403e ⁻⁶	1.44		
10	2000	10	0.61631	3.0851e ⁻⁶	1.44		
5	3000	5	0.37836	1.8942e ⁻⁶	1.44		
10	3000	10	17.87	8.9494e ⁻⁵	1.44		

Table 5.32 shows 170,000 volcanic ash particles failure results for 30 degrees pitched concrete tile roof structure, using maximum stress and strain values from the modelling tool (EDEM software) for the Discrete Element Method (DEM) and structural analysis tool (ANSYS) for the Finite Element Method (FEM) simulation in relations with the allowable stress (UK Code values). Table 5.32 shows the results from the simulation data in Table 4.15, for the 170,000

volcanic ash particles simulation with wind effects. The first column shows the variable volcanic ash particles diameter for 1 mm, 5 mm and 10 mm. The second column shows the variable Volcanic Ash Particle densities for 1000 (Kgm⁻³), 2000 (Kgm⁻³) and 3000 (Kgm⁻³). The third column shows the Horizontal wind direction (ms⁻¹). The fourth column shows the FEM maximum stress results (MPa). The fifth column shows the FEM maximum strain results the six shows the $\leq \sigma_a$ Allowable Stress (MPa). The seventh column shows the nature of assessing the results use for the criterion $\sigma_{max} \leq \sigma_a$ allowable and the eighth column shows $\sigma_{max} \leq \sigma_a$ allowable is not satisfied (MPa) for flat concrete roof structure. Table 5.32, the test set results for the FEM simulation, indicates that three of the results were beyond the criterion for column six, as indicated in eight columns. The remaining tests show that the results did not exceed the column six criterion, as indicated in column seven. That means the import of the volcanic ash particle states for the tile pitched roof.

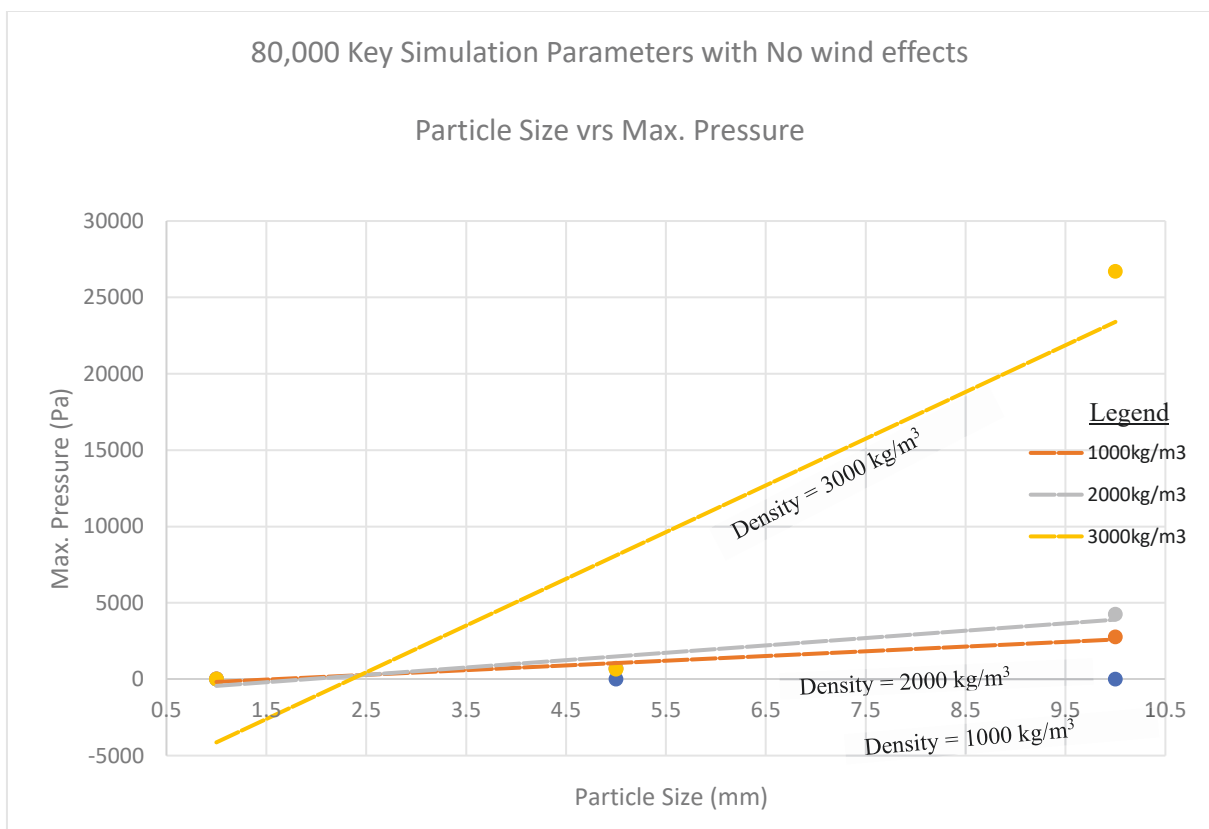


Figure 5.1: Maximum Pressure Verse Particle for 80000 Volcanic Ash Particle with No Wind Effects (extracted from Table 4.4).

Figure 5.1 shows a diagram shows the pressure changes corresponding to the range of the particle sizes for various densities involved in the results from the modelling tool (EDEM software) for the Discrete Element Method DEM and structural analysis tool (ANSYS) for the Finite Element Method (FEM) simulation parameters for the 800000 volcanic ash particles for the no wind effects.

The diagram shows that the pressure changes correspond to the range of particle sizes for various densities involved. That shows that the higher the volcanic densities, the higher the volcanic ash loading effect on the roof. As shown on the roof, the volcanic ash densities increase with the diagram's pressure values. The 1000 (kgm^{-3}) and the 2000 (kgm^{-3}) densities are very close to their corresponding pressure values. The 3000 (kgm^{-3}) volcanic ash particles' density for the 10 mm volcanic ash particle has a higher corresponding pressure value. That is very significant regarding the densities of the volcanoes that can have an immense effect on the roof.

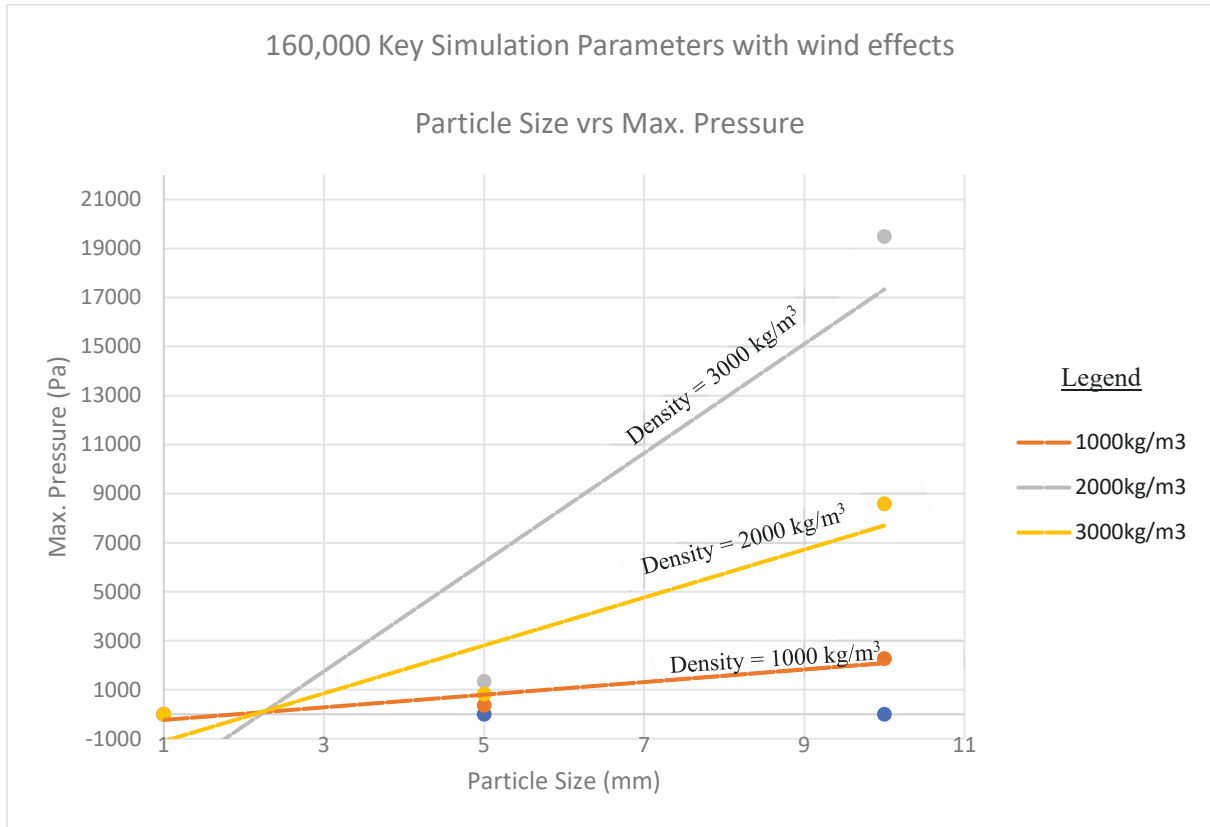


Figure 5.2: Maximum Pressure Verse Particle for 160000 Volcanic Ash Particle with No Wind Effects

Figure 5.2 shows the pressure changes corresponding to the range of the particle sizes for various densities involved in the results from Table 4.11 results from the modelling tool (EDEM software) for the Discrete Element Method (DEM) and structural analysis tool (ANSYS) for the Finite Element Method (FEM) simulation parameters for the 160000volcanic ash particle for the no wind effects.

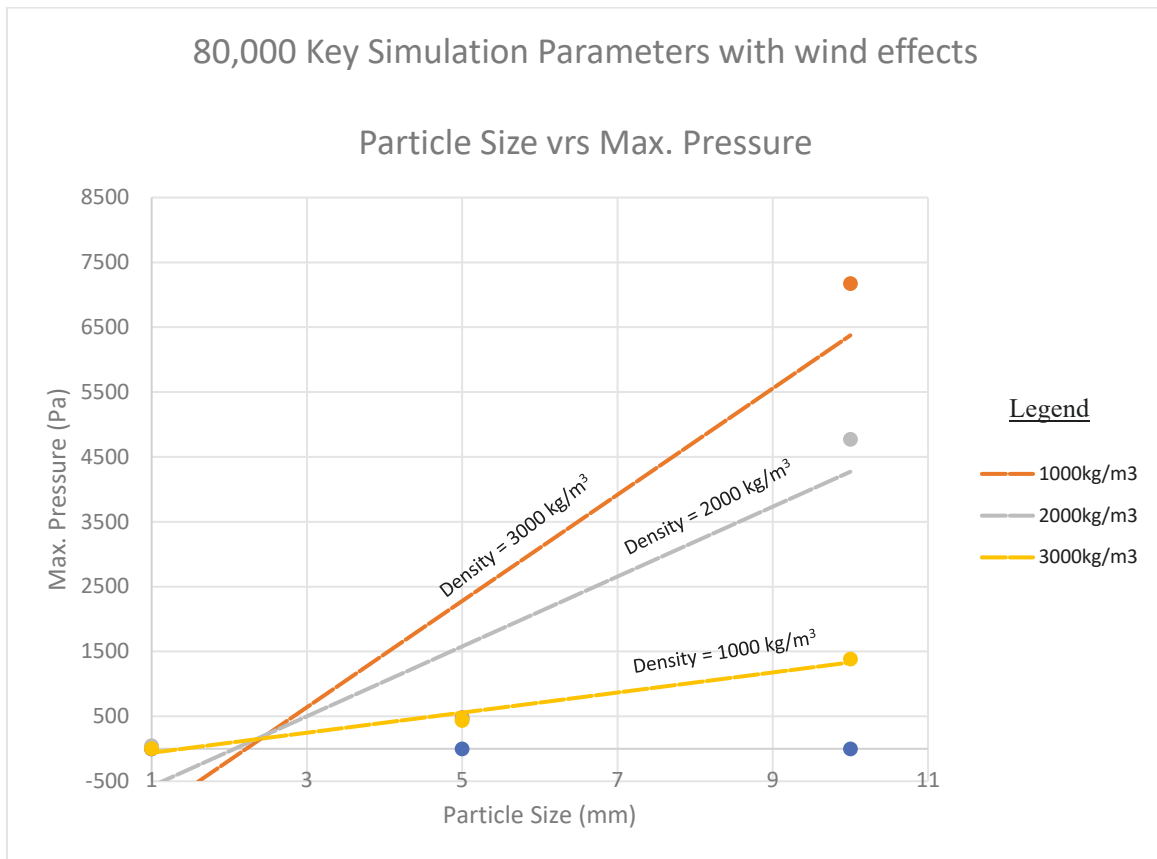


Figure 5.3: from Table 4.6 for: Maximum Pressure Verse Particle for 160000 Volcanic Ash Particle with No Wind Effects

Figure 5.3 shows the pressure changes corresponding to the range of the particle sizes for various densities involved in the results from Table 4.6 results from the modelling tool (EDEM software) for the Discrete Element Method (DEM) and structural analysis tool (ANSYS) for the Finite Element Method (FEM) simulation parameters for the 160,000 volcanic ash particle for the no wind effects.

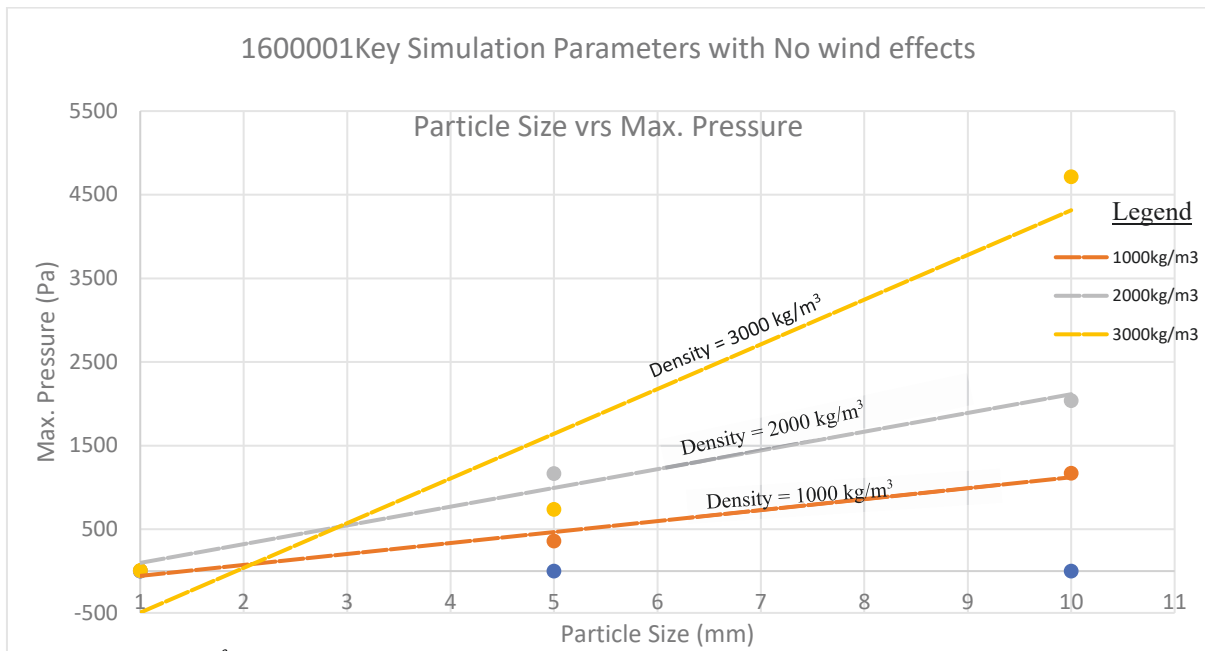


Figure 5.4: from Table 4.6 for Maximum Pressure Verse Particle for 160000 Volcanic Ash Particle with No Wind Effects

Figure 5.3 is the results from Table 4.6 results from the modelling tool (EDEM software) for the Discrete Element Method (DEM) and structural analysis tool (ANSYS) for the Finite Element Method (FEM) simulation parameters for the 160,000 volcanic ash particles for the no wind effects. The results show the 10 mm size volcanic ash particles, pressure result margins for the density results for 1000 (kgm^{-3}) and the 2000 (kgm^{-3}) is about 800 MPa. The results differ for the pressure load result between the density results for 2000 kg/m^3 and 3000 (kgm^{-3}) margins is about 2800.MPa. The 5.mm volcanic ash particle size pressure margin values for the 1,000 (kgm^{-3}) 2,000 (kgm^{-3}) and 3,000 (kgm^{-3}) is about 250 MPa, 500 MPa and 1,200 MPa. respectively from Table 5.2. pressure load margin values appear to be larger for the 10 mm volcanic ash particles than the 5 mm and 1 mm volcanic ash particles results. it can be attributed to the high possibility of the low SiO_2 composition of the particles, which makes the particles' weight very compacted, which can have a very detrimental effect on the roof's buildings within volcanic prone areas.

Figure 5.2 is the results from Table 4.5 results from the modelling tool (EDEM software) for the Discrete Element Method (DEM) and structural analysis tool (ANSYS) for the Finite Element Method (FEM) simulation parameters. for the 80,000 volcanic ash particles for the no wind effects the 10 mm volcanic ash particle size pressure margin values for the 1,000 (kgm^{-3}), 2,000 (kgm^{-3}) and 3,000 (kgm^{-3}) is about 3,500 (Pa), 0,4800 (Pa) and 2,800 (Pa) respectively. The results show the 5 mm volcanic ash pressure margins for the density results for 1,000 (kgm^{-3}), 2000 and 3,000 (kgm^{-3}) is about 1,800 (Pa), 2,300 (Pa) and 2,7000 (Pa) respectively. However, the pressure load margin value appears larger for the density volcanic ash particle of 3,000 (kgm^{-3}). This can again be attributed to the low SiO_2 composition of the volcanic ash particles, which makes the weight of the volcanic ash particles very compacted. The 1 mm pressure load margin values appear to be low and will not directly impact the roof.

Figure 5.3 is the results from Table 4.6 results from the modelling tool (EDEM software) for the Discrete Element Method (DEM) and structural analysis tool (ANSYS) for the Finite Element Method (FEM) simulation parameters. for the 160,000 volcanic ash particles for the wind effects the 10 mm volcanic ash particle size pressure margin values for the 1,000 (kgm^{-3}), 2,000 (kgm^{-3}) and 3,000 (kgm^{-3}) is about 2,500 (Pa), 8,000 (Pa) and 19,000 (Pa) respectively.

The results show, the 5 mm volcanic ash pressure margins for the density results for 1000 (kgm^{-3}), 2,000 (kgm^{-3}) and 3,000 (kgm^{-3}) is about 1,000 (Pa), 1,500 (Pa) and 2,000 (Pa) respectively. However, the pressure load margin value appears larger for the density volcanic ash particle of 3,000 (kgm^{-3}). This can again be attributed to the low SiO_2 composition of the volcanic ash particles, which makes the particles' weight very compacted. The 1 mm pressure load margin values appear to be low (negligible) and will not have a direct impact on the roof. Figure 5.4 is the results of the modelling tool (EDEM software) for the Discrete Element Method (DEM)

and structural analysis tool (ANSYS) for the Finite Element Method (FEM) simulation parameters. The 80,000 volcanic ash particles for the wind effects the 10mm volcanic ash particle size pressure margin values for the 1,000 (kgm^{-3}), 2,000 (kgm^{-3}) and 3,000 (kgm^{-3}) about 14,000 (Pa), 48,000 (Pa) and 70000 (Pa) respectively, for the Figure 5.2.4 is the results from Table 5.9 data.

The results show the 5 mm volcanic ash pressure margins for the density results for 1,000 (kgm^{-3}), 2,000 (kgm^{-3}) and 3,000 (kgm^{-3}) is about 6,000 (Pa), 1,5000 (Pa) and 24,000 (Pa) respectively. Again, the pressure load margin value appears larger than the density of volcanic ash particle 3,000 (kgm^{-3}). That can again be attributed to the low SiO_2 composition of the volcanic ash particles and can make the ash particles' weight very compacted. The 1 mm pressure load margin values appear to be low(negligible) and will not directly impact the roof. The effects of the maximum pressure on the flat concrete roof are severe, as shown in the diagrams, the higher the volcanic ash density level. The higher the maximum pressure exerted on the roof. It will have an impact on the roof, from Table 4. 4 and Table 4.5 for both the 160,000 and 80,000 volcanic ash particles. The flat concrete roof's loading data shows that the safer zone for the structure for the maximum allowable stress design is to be ≤ 1.8 with regards to the full EU code. Any results above the allowable stress will cause higher stress within the roof structure and lead to the high possibility of the collapse of the flat concrete roof and the pitched roof within the volcanic prone areas.

As shown in Table 5.2. The test results coloured yellow column indicate the lower risk related to the maximum stress from the DEM and FEM (ANSYS) FEM simulation results. BEN 1992-2004(E). The allowable stress is calculated based on the BSEN code regarding equation (2). The study has two results for the EU because of the two different coefficient values of 1 for

EU countries and 0.8 for the UK. The discussion here is based on EU values. In relation to Table 5.31, the simulation results with the red coloured indicate the higher risk simulation test results, which can have a higher possibility that leads to the collapse of the building as the 10 mm volcanic ash particles recorded the maximum stress of the 2.074 (MPa) which is higher than the EU allowable stress of 1.8. This means the building will not be resilient enough to withstand the volcanic ash deposition of the concrete roof within the volcanic prone areas within Europe.

Table 4. 3 follows the same pattern as Table 4. 2 with the same allowable stress of 1.8 MPa. The density with the 10 mm volcanic ash particles has the highest volcanic ash maximum stress of 14.30 (MPa), which is higher than the calculated Europe allowable code. That means the roof has a high risk of collapse and the hazard is the probability of killing people in such a circumstance within Europe.

Table 5.10 shows two higher risk levels as shown for maximum stress of 3.789 (MPa) and 2.4913 (MPa). The rest of the simulations are within the region of safe allowable stress zones. Based on these arguments, the researchers thought it is very important to use the allowable stress to determine the impact of volcanic ash on building in the UK as such considerations need to be done. As per the above discussion concerning volcanoes, the UK value from Table 5.11 shows that most of the simulator results were safe except for the 3000 (kgm^{-3}) density with maximum stress 2.074 (MPa) and no wind effects. Considering the data from Table 5.12, 96 simulation shows two simulation test that was more than the UK allowable stress value \leq 1.44 (MPa). These maximum stress values are 10.76 (MPa) and 4.424 (MPa). The two-roof simulation test result will not make the building resilient regarding the deposition of the volcanic ash particles for No-wind effects. Data from Table 5.13 shows that two simulations

test results were more than the UK allowable stress value of ≤ 1.44 (MPa). These maximum stress values are 1.655 (MPa) and 14.39 (MPa) for the wind effects. The rest of the simulation test was within the safe allowable stress cones.

Data from Table 5.14 shows that again two simulation test results were more than the UK allowable stress value of 1.44 (MPa). These maximum stresses values are 2.4913 (MPa) and 3.789 (MPa) for no wind effect. The rest of the simulation test results were within the safe allowable stress cone. The simulation results that were outside the allowable stress of the EU and the UK codes zone were these 10mm volcanic ash particles with 1,000 (kgm^{-3}), 2,000 (kgm^{-3}), and 3,000 (kgm^{-3}) density. The data simulation results are related to the flat concrete roof.

In contracts to the research, aim and objective 1 was to investigate building roofs' resilience against volcanic ash's weight in the volcanic prone area in Europe. The result is discrete Element Method (DEM), and structured analysis tool (ANSYS) for the Finite Element Method (FEM) simulation test for the flat concrete roof certifies the aims and object 1 for concrete, and the pitched roof to The data result shows that the condition for certifying the resilience condition of the building roof the weight of the volcanic ash proved that simulation test rest for the EU and the UK from BSEN1992-1-1-2004(E) from eq (2) the value of the design tensile strength f_{ctd} is defined as;

$$f_{ctd} = \alpha_{ct} f_{ctk,0.05} / \gamma_C \quad (2)$$

Where γ_c is the parted factor for the concrete act is the coefficient talking accounts of long-term effects on the tensile and the unfavourable effects resulting from how the load is applied.

The value of α for use in a count in its national effect. The recommended value for EU countries is 1, and for the national annexe for the UK, the α value is 0.8 (BSEN 1992-1-1-2004 (E)).

Based on these parameters, the flat concrete roof's allowable stress was determined as 1.8 MPa for the EU, and 1.44 MPa was for the UK; carried out were 36 simulation tests for the flat concrete roof for both the EU and the UK values. 6 simulation tests for the 10 mm volcanic ash particle for the 3,000 (kgm^{-3}) density exceeded the EU allowable stress value of 1.8 MPa 30 of the simulation test for the rest of the test were within the safe allowable stress zone

It can be argued by the study that the remainder of the 30-simulation test volcanic ash particles results for the density of 1,000 (kgm^{-3}) and 2,000 (kgm^{-3}) were more resilient for the roof and were more bearable on the roof; however, the roof resilience for the volcanic ash particle was not enough to be sustained by the roof for the 10 mm volcanic ash particle, and for that matter, there was the high risk of possibility that the roof will collapse under such circumstances.

Spencer et al., (2005) suggested that their field experiment shows that roofs would collapse under such pressure load in the range of (1-5 KPa), but field and other experimental works have shown that some designs can withstand pressure load up to 10 (KPa).

The study considers the logical approach for it to fit the criteria for the static and dynamic pressure load of the volcanic ash on the roof of the concrete and then the pitched roof. The strategy adopted for the methodology has been explained in chapter 3 extensively for both volcanic ash particle pressure loading for wind and no-wind effect to meet for the static and dynamic strategy for the study.

5.2.4 Pitch Roof Simulation Results Discussions

The results discussed in this section are based on their respective data from chapter 4. The 20 degrees of inclination shows the impact of the volcanic ash on the roof, more volcanic ash deposition was observed. This shows the DEM pressure recording of 2.146 Pa and the FEM maximum deformation recordings of $2.7944e^{-5}$ and the maximum stress recordings of 0.14833 MPa from Table 5.15. The 5 mm DEM maximum pressure recording of 182.73 recorded a higher FEM maximum stress value of 0.14496 MPa.

The 10 mm volcanic ash particle recorded the maximum DEM maximum pressure values of 940.33 Pa and the FEM maximum stress values of 2.6009 MPa. The same pattern pertains to the simulation for the no wind effects simulation for the 170,000 volcanic ash particles. The results for the 170,000 volcanic ash particle simulation results indicate that the same pattern for the results indicates the same pattern for the results in Table 5.15 compared to Table 5.15. The higher the DEM maximum pressure results. The higher the FEM maximum stress values for the 1 mm 5 mm particle and the 10mm size volcanic ash particles., and vice versa.

The results for Table 5.15 recorded the DEM maximum pressure value of 1,578.66 Pa with the corresponding FEM maximum stress value of 5.7543 MPa. The 10mm particle for 2000 Kg m^{-3} density recorded the DEM pressure value of 3,472.2 Pa. The corresponding stress values are 11.988, MPa, the maximum deformation values of 0.70084 mm and the maximum strain values $6.0047e^{-5}$ MPa for the effect's simulation for the 20 degrees of inclination.

The simulation for the 25 degrees pitched roof inclination from Table 5.17 No wind of 170,000 volcanic ash particles. The records indicate the $1000 (\text{kg m}^{-3})$ density recordings for the DEM maximum pressure value as 2.59892 Pa. The corresponding value for the maximum

deformation value is 0.00048 mm, the maximum stress value is 0.00766 MPa and the maximum strain value of 3.8326×10^{-5} . Again, as there is an increase in the DEM maximum pressure value, the maximum deformation values' corresponding increase increases the stress and strain values. The simulation for the wind effect for the DEM and FEM results indicates the maximum pressure values for as from Table 5.18 for volcanic ash 5 mm parts 1000 kg/m^3 density as 121.861 Pa the FEM maximum deformation 2.1569×10^{-5} mm, the maximum stress values as 3.9221×10^{-5} MPa and the maximum strain value as 1.9633×10^{-5} . It is clear from Table 5.18 shows that there is an increase in the DEM pressure value for the 5 mm 10 mm ash particles for the 1,000 (kgm^{-3}) 2,000 (kgm^{-3}) and 3,000 (kgm^{-3}) corresponding values for the FEM maximum deformation values increase in the maximum stress value and the increase in the maximum strain values. The same appears to occur for both the pitched roof with the 30 degrees of inclination. The test clearly shows Table 5.6 for the simulation of the wind effects and Table 5.7 for the simulation. The higher the DEM pressure result, the high the corresponding values for the FEM simulation test result for the maximum stress values, and maximum strain. The DEM pressure results will result in lesser FEM simulation results for the maximum deformation value and the maximum stress values. This pattern is shown in Table 5.19 to Table 5.32 simulation with the wind effects and no wind effects. It is clear from the simulation that the 10 mm diameters size volcanic ash particles have the highest recordings, followed by 5 mm diameter size particles and the 1mm diameter size volcanic ash particles.

5.2.5 FEM simulation for the maximum deformation and the maximum stress results for the tile concrete roof's pitched strength and failure.

The total number of simulations test conducted for both the wind simulation effect and no wind simulation effect was thirty-nine. The result shows a significant impact on the roofs, and this will need serious attention regarding the EN 1991 code.

Table 5.15 for the no wind effects simulation results in the 10mm for the 1,000 (kgm^{-3}) volcanic ash density and the 5 mm particle with the 2,000 (kgm^{-3}) density and the 10 mm volcanic ash particle 3,000 (kgm^{-3}) densities were at risk of serious consequence impartation of the pitched roof by the volcanic ash. The rest of the ash for the no wind effects. (Table.5.2) Table 5.16 the DEM wind effects simulation had the 5 mm and 10mm volcanic ash particles impacting more maximum pressure than the roof than the 1mm particle of 1000 (kgm^{-3}) density particle. The values were DEM maximum pressure for 5 mm particles for densities of 1000 (kgm^{-3}) as 1578.66 Pa with corresponding FEM maximum stress 5.7543 MPa. The 10 mm volcanic ash particles' maximum pressure value was 3472.2 Pa with the FEM maximum stress. These values as 11.988 MPa for the simulation with wind effects for the 20 degrees of inclination.

The result shows that the pitched concrete tiles roof will be in danger of collapsing, killing people if occupied within the volcanic prone areas. The rest of the result shows the roof was resilient to the volcanic ash loading impact; the wind direction will also impact the deposition of the volcanic ash on the roof. Suppose the wind direction of the volcanic ash particle is in the flow of the wind. In that case, the volcanic ash's lesser deposition will be deposited on the roof and vice versa. If the volcanic ash particles are against the wind particle's flow, much more of the volcanic ash particles deposition on the roof. The DEM higher maximum pressure values in Table 5.16 show that the volcanic ash particles in the wind direction flow recorded lesser

values. However, the particles that were against the wind direction flow recorded higher DEM maximum pressure values. The pattern pertains to all the simulations for the 20 degrees to the 30 degrees simulations.

Considering Table 5.17 for the 25 degrees pitched concrete roof simulation, the results show that out of the DEM simulation test result, four of the simulation tests were 5 mm volcanic ash particles which were above the allowable stress value for the EU 1.8 MPa, and the other four simulation test result were below the EU allowable stress result of 1.8 MPa. That means the pitched concrete roof was more resilient and at the same time, very vulnerable to the impact of the volcanic ash particle loadings. The simulation test result for Table 5.18 shows that all the six DEM results caused the increase of the FEM maximum stress values above the EU \leq allowable stress value of 1.8 MPa. The Dem results for the Table 5.18 simulation for the 30 degrees pitched concrete tile shows that out of the five tests results, three tests were above the EU \leq to the allowable stress 1.8 MPa two test results in less than EU \leq to the allowable stress 1.8 MPa for the no wind effect. for the 30 degrees for the wind affect DEM and FEM simulation test results, out of the six simulation test results, three of the results were above the EU \leq allowable stress 1.8 MPa. The other 3 test results were \leq the maximum allowable stress of 1.8 MPa. That means that three of the pitched concrete roofs were affected. Simultaneously, the other three tested roofs were resilient to the volcanic ash particles' impact on the pitched concrete roof what simulation. The study has been able to prove that the volcanic ash particles will impart on the roof of building in the European region for the building within volcanic prone areas. The result for the is not different from the UK regions. As a matter of fact, regarding the data results, it clearly shows that building within the UK region will have significant effects of the volcanic ash particles on the European region. The code in the region must have to be reviewed, especially in the volcanic ash-prone areas.

As it has been established in the literature review concerning the devastating effects of the volcanic ash impact on life and properties that lead to death, the study needs to be taken seriously to save people's lives. As argued in the literature, people still live near volcanic vents with all their effects come with different reasons. However, it is the view of the study, irrespective of the divergent reason given, since people always live too close to the volcanic vents with building deficiency with regards to the building roof resilience against the volcanic ash effect must be addressed within the volcanic prone areas in Europe and the rest of the world.

CHAPTER SIX

6.0. CONCLUSION AND FUTURE WORK

6.1 Summary

The study aims to propose a revision to European building code EN1991 for static and dynamic roof loading by volcanic ash. The initial puzzle that has driven the study was how the thesis could propose a European building revision regarding EN 1991 and the volcanic ash effect's impact on the volcanic prone areas in Europe. This study has argued regarding volcanic ash effects on building roofs within the volcanic prone area in chapters one and two. In establishing the gap in the thesis, it was clear that the EN 1991 building code design variable did not include the volcanic ash's impact. Some of the variables included were the snow effects, wind effects, self-weight of the building, including the live load and the loads and other considerations. However, there was not any consideration of the volcanic ash load effects on the roofs of building in the volcanic prone areas in Europe.

This study attempts to address the gaps established in the literature, it seeks to examine the impact of the volcanic ash particles on flat concrete roofs and the pitched concrete roof buildings within the volcanic prone areas within Europe and other parts of the world. The study commenced with getting a clearer understanding of the causes and effects of volcanic ash particles and their properties, and the death toll caused because of the volcanic ash particles, the impact on the roof building the took further knowledge from various investigations undertaken in the field of volcanology to validate and validate the problem in the context.

The study's aims and objectives have been reviewed as to whether it has been achieved as follows.

The first aim is to investigate the building roof's resilience against the load due to volcanic ash's weight in the code regulation within the volcanic prone areas in Europe. Simulations were carried out as shown in the DEM, and FEM structural analysis tool (ANSYS) methodology for the finite element method (FEM) simulation for the flat concrete roof and the tile pitched roof for variable angles of 20, 25, and 30 degrees. Variable volcanic ash densities and variable volcanic ash particles were utilised for the simulation. The results observed show that there is a significant impact of volcanic ash on the roofs. The region where there will be a great benefit is shown in Figure 2.1 for the summary map of the volcanoes of Europe. The research shows which building was resilient against the load due to the volcanic ash particles and those that were not resilient to the loading of volcanic ash particles.

The study investigated the existing EN (BSEN) building codes used by local building codes in member states. A proposal for the revision of the EN 1991-1-1-3 is proved through the results obtained from this research, which will help prevent volcanic ash on the roof of the building in the prone areas in Europe (Etna and Iceland). The success of this study will be beneficial to the volcanic prone countries in Europe (Iceland, Italy, Spain) as illustrated in the figure, newly found volcanic ash sports, dead volcanic sport to design building's roof should there be activation of volcanic events and the world at large.

The results show that the criterion for the $\sigma_{\max} \leq \sigma_a = 1.8 \text{ MPa}$ (EU Values) and the $\sigma_{\max} \leq \sigma_a = 1.44 \text{ MPa}$ (UK values) indicates the criterion for the simulation was not satisfied for the simulation for the flat concrete and the tiled pitched roofs. The study shows that the volcanic ash effects would have been immersed if the allowable stress of 1.8 MPa (EU values) and 1.44 MPa (UK values) were scaled to 1:10, and the volcanic ash particles for 80,000, 160,000 and 170,000 simulations. Again, the study is of the view that the original model size of 10m x 10m x 0.154

m would have an immersed impact considering the criterion for the $\sigma_{\max} \leq \sigma_a = 1.8$ MPa (EU Values) and the $\sigma_{\max} \leq \sigma_a = 1.44$ MPa (UK values) and thus, the need for the proposal for the revision by addition of the volcanic as loading for the 1991-1-1-4. Code.

The study focuses on volcanic ash loading on roofs of buildings has been deliberated on in chapter 3. EN 1991 shows that the nature of the snow deposition on a roof that occurs in many different patterns is clearly stated. That has enabled the study to adopt the static and dynamic approach of the volcanic deposition on buildings' roofs during the simulation. The EN code 1991 described the various coefficient of snow for the ash as stated in Table 2.20.

According to the BSEN 1991, the design guidance and actions for the structural design of the building are considered the following.

- densities of construction materials
- self-weight of construction works
- imposed load for buildings

This study has proved the impact of volcanic ash effects on the roof of building as other studies such as Hampton et al., (2005), Johnson (1997), just to mention a few in which the impact of the volcanic ash on the roof of buildings was of great consideration. The research shows that the volcanic ash particle is much heavy than the snow in terms of densities and loads. The simulation test has shown that the volcanic ash particles will affect the flat concrete roof and the pitched concrete tile roof.

6.2 Recommendation

The study aims to investigate the resilience of building roofs against the load due to volcanic ash weight in the volcanic prone area of Europe and propose a revision of the European building code EN1991 (in the current European code regulation) within the volcanic prone areas in Europe. These aims are directly linked to the study's objectives which focus on the gap and contribution to the research. That is the effect of the volcanic ash on the roofs of buildings within the volcanic prone areas, as this wasn't part of the European building code E1991.

The study could ascertain the effects of the volcanic ash loading using static and dynamic approaches on the roof of the building within the volcanic prone area using the DEM and FEM simulations as illustrated in objective 3. Furthermore, the results of the study have indicated in chapter 5 the effects of the variable volcanic ash densities (1000 kg/m^3 , 2000 kg/m^3 and 3000 kg/m^3) that have led to the collapse of buildings within the volcanic prone areas in Europe as indicated by the study.

This part of the recommendation relates to objective 1, and objective 2 illustrates the research's contribution regarding the geographical distribution of the regions that will benefit all volcanic-prone areas in Europe from the revision of the building regulation. However, Europe will benefit from this study, but the world at large with countries' experiencing the effect of volcanic ash loadings on the roofs of buildings.

The proposal of the revision of the EN1991 is linked led to objective 4 clearly shows that the results from the various tests indicated the impact of the volcanic ash effects on the roof within the volcanic prone area in Europe. Furthermore, it was clear that the buildings with flat concrete roofs would be more impacted than the pitched roofs within the volcanic prone.

As already indicated, the preliminary simulation test for the tile pitched roof, with the angle of inclination from 35 degrees to 45 degrees, shed most of the volcanic ash on its roof, resulting in less deformation and stress on the roofs. The study, therefore, recommended the strengthening of all those flat roofs as follows:

- 6) All existing flat roofs should be retrofit or structurally reinforced to increase the roof's resilience against the volcanic ash loading effects.
- 7) Flat roofs should not be encouraged in to the design of new buildings within the volcanic prone areas unless buildings designers can increase the strength of buildings with flat roofs within the volcanic prone areas in Europe and the world at large.
- 8) 3) All existing pitched roofs in the volcanic ash-prone areas should be retrofit or structurally reinforced to increase the roof's strength.
- 9) Existing pitched roofs within the range of 20-30 degrees are prone to roof failures. Therefore, they must not be encouraged in volcanic prone areas unless they can be retrofit or structurally reinforced to increase the roof's resilience against the volcanic ash loading effects.
- 10) Pitched roofs buildings with steep roof angles that can flash off the volcanic ash quickly must be recommended within the volcanic prone areas as that helps sheared off the deposition of the volcanic ash loading on the roofs.

This measure means cost implications for owners of buildings within the volcanic-prone areas. This approach will require government support to avert situations where buildings will collapse and kill people in volcanic-prone areas.

Existing pitched roofs with an angle of inclination between 20-30 degrees should be retrofit to increase the strength of the roofs within the volcanic-prone areas. However, this will need government and political will to undertake such a policy to avert a situation of the hazard of the collapse of the pitched roof within the angle of inclination affected during a volcanic eruption.

The study recommended that newly built buildings should be encouraged to use pitched roofs with steep a steep roofs angle that can flash off the volcanic ash quickly must be recommended within the volcanic prone areas as that will help sheared off the deposition of the volcanic ash loading on the roofs.

Though the designs approach will increase the cost of buildings within the volcanic-prone areas in Europe and the rest of the world, it will help avert the hazard of volcanic ash loading leading to the collapse of roofs of buildings in the volcanic-prone areas and save lives.

Every life matters, and people live in the volcanic prone areas in Europe and the rest of the world's lives matter.

This study approach will help make buildings within the volcanic prone areas more resilient against the volcanic ash particle loadings on the roofs and will also contribute to Knowledge.

6.2.1 Load Arrangements for Volcanic ash particles

The study proposes the volcanic ash's load arrangement concerning the exiting one for the snow load arrangement within the volcanic prone areas. The study suggests the architecture, designer, and volcanologist determine the volcanic ash particle coefficient for the volcanic ash particles for various shapes incorporated in the nation annex or the EU code.

BS EN 1991-1-3 Part 1-3 is devoted to snow loading.

A new addition to BS EN 1991-1-1-4 Part 1-4 to accommodate the effect of the volcanic ash loading within the volcanic prone areas is proposed as follows:

1. The persistent/transient design situation

$$V_{ap} = \mu_v C_e C_t V_k \quad (6-1)$$

2. The accidental design situations where exceptional volcanic ash particles loads are accidental action.

$$V_{ap} = \mu_v C_e C_t V_{AD} \quad (6-2)$$

3. For the accidental design situations where exceptional volcanic ash particles drift if the accidental action

$$V_{ap} = \mu_v \cdot V_k \quad (6-3)$$

Where

- V_{ap} is the volcanic ash loading on the roof in (Pa)
- V_K is the characteristic value of the volcanic ash particles load on the roof.
- V_{AD} is the design value of exceptional on the ground(Pa)
- C_e is the exposure coefficient.
- C_t is the thermal coefficient.

In the regions with possible deposition of volcanic ash on the roof, rainfalls, Snow on the roof, the consecutive melting and freezing, roof volcanic ash particles load on the roof snow load on

the roof, especially in the case of volcanic ash particles, snow and ice can block the drainage systems of the roof.

The proposed coefficient C_e exposure of the volcanic ash particles should be determined by the Nation annex or the EU for the volcanic ash load on the roof, and the snow load should be used where it is applicable. It has been observed from the study that when the EN1991 building is reviewed as proposed by the study, it will help reduce the volcanic ash load's impact on the buildings of roofs within the European countries within volcanic prone areas.

There is a need for further simulations on the pitched roof because the study did not complete the simulation test, on the roof's variable angle for 35 degrees, 40 degrees and 45 degrees, because of time. However, preliminary results conducted for the DEM simulation test on a pitched tiled roof indicated that the volcanic ash particles were less deposited on the roof for the 35 degrees simulation and much lesser deposition for the 40 degrees angle of inclination and a virtual no volcanic ash deposition of ash on the pitched roof for the angle of inclination for 45 degrees.

6.3 Future Work

It is recommended that further research could be carried out on the pitched roof because the study did not complete the simulation test on the roof's variable angle of inclination for 35 degrees, 40 degrees and 45 degrees due to time constraint. However, preliminary results conducted for the DEM simulation test on a pitched tiled roof indicated that the volcanic ash particles were less deposited on the roof for the 35 degrees simulation and much lesser deposition for the 40 degrees angle of inclination and a virtual no volcanic ash deposition of the pitched roof for the angle of inclination for 45 degrees.

- DEM and FEM Simulations test with wet volcanic ash particles
- DEM and FEM Mixed shapes of volcanic ash particle
- Discrete Element Method (DEM) and Computational Fluid Dynamics (CFD) co-simulation.
- The reverse DEM simulation to determines the exact volcanic ash loading that will cause the roof to fail or collapse for the 1 mm, 5 mm, and 10 mm volcanic ash loading of the roof.

REFERENCES

- Acocella, V. and Puglisi, G., 2013. How to cope with volcano flank dynamics? A conceptual model behind possible scenarios for Mt. Etna. *Journal of Volcanology and Geothermal Research*, 251, .137-148.
- Al Ibrahim, M.A., Kerimov, A., Mukerji, T. and Mavko, G., 2019. Particular: A simulator tool for computational rock physics of granular media. *Geophysics*, 84(3), pp.1-59.
- Andronico, D. and Del Carlo, P., 2015. PM10 measurements in urban settlements after lava fountain episodes at Mt Etna, Italy: pilot test to assess volcanic ash hazard on human health. *Natural Hazards and Earth System Sciences Discussions*,3, .3925-3953.
- Anon 2013. Volcanoes-are they such a bad thing? The positives and negatives of a volcanic eruption. *Astronomy and Geography*. [Online] Available from: [https://vamoswearegolden.wordpress.com /tag/volcano/](https://vamoswearegolden.wordpress.com/tag/volcano/) Accessed on 17/12/2016
- Argus, D.F., Gordon, R.G., DeMets, C. and Stein, S.,1989. Closure of the Africa-Eurasia-North America plate motion circuit and tectonics of the Gloria fault. *Journal of Geophysical Research: Solid Earth*,94(B5), .5585-5602.
- Banerjee, R., 2015. Importance of Building Code. *International Journal of Engineering Research and Applications*, 5(6). 94-95.
- Barclay, J., Haynes, K., Mitchell, T., Solana, C., Teeuw, R., Darnell, A., Crosweller, H.S., Cole, P., Pyle, D., Lowe, C. and Fearnley, C.,2008. Framing volcanic risk communication within disaster risk reduction: finding ways for the social and physical sciences to work together. *Geological Society, London, Special Publications*, 305(1), 163-177.
- Behncke, B., Neri, M. and Nagay, A., 2005. Lava flow hazard at Mount Etna (Italy): new data from a GIS-based study. *Geological Society of America Special Papers*, 396, .189-208.
- Besson, B., Bjarnason, J.Ö., Gudmundsson, A., Sólnes, J. and Steedman, S., 2012. Probabilistic earthquake damage curves for low-rise buildings based on field data. *Earthquake Spectra*, 28(4), 1353-1378.

Bilham, R., 2013. Societal and observational problems in earthquake risk assessments and their delivery to those most at risk. *Tectonophysics*, 584, pp.166-173.

Bisson, T., (2009). *Fire on the Mountain*. PM Press

Blaikie, P., Cannon, T., Davis, I. and Wisner, B., 2004. *At risk: natural hazards, people's vulnerability and disasters*. Routledge

Blong R.J., 1984 *Volcanic hazards: a sourcebook on the effects of eruptions*. Sydney: Academic Press Australia; 1984. pp. 424.

Blong, R., 2003. A review of damage intensity scales. *Natural hazards*, 29(1), .57-76

Blong, R., 2004. Residential building damage and natural perils: Australian examples and issues. *Building Research & Information*, 32(5), .379-390

Blong, R.J., Grasso, P., Jenkins, S.F., Magill, C.R., Wilson, T.M., McMullan, K. and Kandlbauer, J., 2017. Estimating building vulnerability to volcanic ash fall for insurance and other purposes. *Journal of Applied Volcanology*, 6(1), .2.

Blong, T.J., Babb, R.F., Harrison, P.J. and Percha, P.A., 2014 3M Innovative Properties Co, Multilayer film. U.S. Patent 8,835,749.

Bonaccorso, A., Calvari, S., Coltelli, M., Del Negro, C. and Falsaperla, S., 2004. Mt. Etna: volcano laboratory. Washington DC American. Geophysical Union Geophysical Monograph Series, 143.

Bonanno, G., Giudice, R.L. and Pavone, P., 2012. Trace element biomonitoring using mosses in urban areas affected by mud volcanoes around Mt. Etna. The case of the Salinelle, Italy. *Environmental monitoring and assessment*, 184(8), .5181-5188.

Branca, S. and Ferrara, V., 2013. The morph structural setting of Mount Etna sedimentary basement (Italy): Implications for the geometry and volume of the volcano and its flank instability. *Tectonophysics*, 586, .46-64.

Branca, S., Azzaro, R., De Beni, E., Chester, D. and Duncan, A., 2015. Impacts of the 1669 eruption and the 1693 earthquakes on the Etna Region (Eastern Sicily, Italy): An example of recovery and response of a small area to extreme events. *Journal of Volcanology and Geothermal Research*, 303, .25-40.

BS EN 1992-1-1:2004+A1:2014 Eurocode 2: Design of concrete structures. General rules and rules for buildings

Chester, D.K., Dibben, C.J. and Duncan, A.M., 2002. Volcanic hazard assessment in western Europe. *Journal of Volcanology and Geothermal Research*, 115(3-4), pp.411-435.

Chester, D.K., Duncan, A.M. and James, P.A., 2010. Mount Etna, Sicily: landscape evolution and hazard responses in the pre-industrial era. In *Landscapes and Societies* (. 235-253). Springer Netherlands.

Colleen M. Riley, William I. Rose Gregg J.S. Bluth 2003 Quantitative shape measurements of distal volcanic ash. *Journal of Geophysical Research: Solid Earth* Volume 108, Issue B10.

COMSOL AB (2004), "FEMLAB Quick Start";T gnergatan 23 SE-111 40 Stockholm, Sweden.

COMSOL, A., 2018. Comsol multiphysics reference manual, version 5.3. COMSOL AB

Corsaro, R.A. and Pompilio, M., 2004. Magma dynamics at Mount Etna. *Mt. Etna: Volcano Laboratory, Geophysics. Monogr. AGU, Washington DC*, .91-110.

Crowe, C.T., Sommerfeld, M. and Tsuji, Y. 1998, *Multiphase Flows with Droplets and Particles*, CRC Press, Boca Raton, Florida, USA.

Cundall, P.A. 1971, A Computer Model for Simulating Progressive, Large-Scale Movements in Block Rock Systems, *Symposium of International Society of Rock Mechanics, Vol.1(ii-b)*, 11-8

D'Orazio, M., Di Perna, C. and Di Giuseppe, E., 2010. The effects of roof covering on the thermal performance of highly insulated roofs in Mediterranean climates. *Energy and Buildings*, 42(10), .1619-1627

David M Pyle (2017). *Volcanoes. Encounters through the Ages*. Bodleian Library Broad Street, Oxford, UK.

DeMets, C., Gordon, R.G. and Argus, D.F., 2010. Geologically current plate motions. *Geophysical Journal International*, 181(1), .1-80.

Donnadieu, F., Freville, P., Hervier, C., Coltelli, M., Scollo, S., Prestifilippo, M., Valade, S., Rivet, S. and Cacault, P., 2016. Near-source Doppler radar monitoring of tephra plumes at Etna. *Journal of Volcanology and Geothermal Research*, 312, .26-39.

Donovan, A.R., Bravo, M. and Oppenheimer, C., 2012. Co-production of an institution: Montserrat Volcano Observatory and social dependence on science. *Science and Public Policy*, 40(2), .171-186.

Donovan, K., 2010. Doing social volcanology: exploring volcanic culture in Indonesia. *Area*, 42(1), .117-126.

Dougal Jerram, Alwyn Scarth and Jean-Claude Tanguy (2017). *Volcanoes of Europe*. Dunedin Academic Press, Edinburgh

EN 1991-1-3:2003/AC:2009. Eurocode 1: Actions on structures - Part 1-3: General actions - Snow loads. Brussels: CEN/TC 250

EM-DAT 2014. EM-DAT: The OFDA/CRED International Disaster Database, Université Catholique de Louvain, Brussels, Belgium

Ernst, G. G. J., M. I. Bursik, S. N. Carey, and R. R. J. Sparks, 1996. Sedimentation from turbulent jets and plumes, *J. Geophys. Res.*, 101, 5575

Etiopie, G., Fridriksson, T., Italiano, F., Winiwarter, W. and Theloke, J., 2007. Natural emissions of methane from geothermal and volcanic sources in Europe. *Journal of Volcanology and Geothermal Research*, 165(1), .76-86.

Euro control 2010. Ash-cloud of April and May 2010: Impact on Air Traffic. *Statfor*. (1), 1-137,

EUROCODES (2008, February). Common standard to improve competitiveness of construction industry. Available from <https://vamoswearegolden.wordpress.com/tag/volcano/> Accessed on 17/09/2017

Forka Leyepey and Mathew Fomine 2011. The Strange Lake Nyos CO₂ Gas Disaster: Impacts and the displacement and return of affected communities. *The Australasian Journal of Disaster and Trauma Studies*. 1174-4707 (2011-1), 1-10.

Formichi, P., 2008. February. EN 1991–Eurocode 1: Actions on structures. Part 1-3 General actions–Snow Loads. In presentation at Workshop “Eurocodes. Background and Applications (18-20)

Gino M. Crisci, Maria V. Avolio, Boris Behncke, Donato D'Ambrosio, Salvatore Di Gregorio, Valeria Lupiano, Marco Neri, Rocco Rongo, William Spataro 2010. Predicting the impact of lava flows at Mount Etna, Italy. *Journal of Geophysical Research: Solid Earth*. 115, (B4), 1-22.

Guardian 2015. Sakurajima volcano: chance of large eruption 'extremely high [Online] Available from: <https://www.theguardian.com/world/2015/aug/15/japans-sakurajima-volcano-chance-of-large-eruption-extremely-high> [Accessed on:09/10/2017]

Guy Dinmore and Giulia Segreti 2009. Italy's quake tells familiar tale of risk, *Financial Times*. [Online] Available from: <https://guydinmore.wordpress.com/tag/financial-times/page/50/> [Accessed on: 20/09/2016]

Hampton, S.J., Cole, J.W., Wilson, G., Wilson, T.M. and Broom, S.,2015. Volcanic ash fall accumulation and loading on gutters and pitched roofs from laboratory empirical experiments:

Implications for risk assessment. *Journal of Volcanology and Geothermal Research*, 304, .237-252

Hartley, M.E. and Thordarson, T., 2013. The 1874–1876 volcano-tectonic episode at Askja, North Iceland: Lateral flow revisited. *Geochemistry, Geophysics, Geosystems*, 14(7), .2286-2309

Hartley, M.E., Thordarson, T. and de Joux, A., 2016. Postglacial eruptive history of the Askja region, North Iceland. *Bulletin of Volcanology*,78(4), p.28.

Heap, M.J., Mollo, S., Vinciguerra, S., Lavallée, Y., Hess, K.U., Dingwell, D.B., Baud, P. and Iezzi, G., 2013. Thermal weakening of the carbonate basement under Mt. Etna volcano (Italy): implications for volcano instability. *Journal of volcanology and geothermal research*, 250, .42-60.

Heiken, G., (2013). *Dangerous neighbors: volcanoes and cities*. Cambridge University Press.

Horwell, C.J. and Baxter, P.J., 2006. The respiratory health hazards of volcanic ash: a review for volcanic risk mitigation. *Bulletin of Volcanology*, 69(1), .1-24.

Horwell, C.J., 2007. Grain-size analysis of volcanic ash for the rapid assessment of respiratory health hazard. *Journal of Environmental Monitoring*,9(10), pp.1107-1115.

Huiskes, R. and Chao, E.Y., 1983. A survey of finite element analysis in orthopaedic biomechanics: the first decade. *Journal of biomechanics*,16(6), pp.385-409.

Ian McIver (2014). 'Investigating the Application of Building Regulations at Lammas'. Ph.D. Thesis. Leeds. Metropolitan University.

Jenkins, S.F., Spence, R.J.S., Fonseca, J.F.B.D., Solidum, R.U. and Wilson, T.M., 2014. Volcanic risk assessment: Quantifying physical vulnerability in the built environment. *Journal of Volcanology and Geothermal Research*, 276, .105-120.

Jerram, D., Scarth, A. and Tanguy, J.C., 2017. *Volcanoes of Europe*. Dunedin Academic Press Ltd.

Jerram, D., 2021. *Introducing Volcanology: A Guide to Hot Rocks*. Dunedin Academic Press Ltd.

Johnson, K.L. and Johnson, K.L., 1987. *Contact mechanics*. Cambridge university press. Johnston, D., 2012. *The role of multidisciplinary research and collaboration for improving the resilience of communities to volcanic risk*.

Johnston, D.M., 1997. *The impact of recent falls of volcanic ash on public utilities in two communities in the United States of America*. Institute of Geological & Nuclear Sciences Limited.

Kandlbauer, J., Carey, S.N. and Sparks, R.S.J., 2013. *The 1815 Tambora ash fall: implications for transport and deposition of distal ash on land and in the deep sea*. *Bulletin of volcanology*, 75(4), p.708.

Karátson, D., Veres, D., Wulf, S., Gertisser, R., Magyari, E. and Bormann, M., 2017. *The youngest volcanic eruptions in East-Central Europe—new findings from the Ciomadul lava dome complex, East Carpathians, Romania*. *Geology Today*, 33(2), .60-65

Kereszturi, G., 2014. *Edgardo Cañón-Tapia and Alexandru Szakács (Eds.): What is a volcano?*

La Delfa, S., Negusini, M., Di Martino, S. and Patanè, G., 2012. *Geodetic techniques applied to the study of the Etna volcano area (Italy)*. *International Journal of Earth Sciences*, 101(4), .1065-1075.

Langmann, B., Folch, A., Hensch, M. and Matthias, V., 2012. *Volcanic ash over Europe during the eruption of Eyjafjallajökull on Iceland, April–May 2010*. *Atmospheric Environment*, 48, .1-8

Luckett, R., Baptie, B. and Neuberg, J., 2002. *The relationship between degassing and rock fall signals at Soufriere Hills Volcano, Montserrat*. *Geological Society, London, Memoirs*, 21(1), .595-602.

Macedonio, G. and Costa, A., 2012. *Brief Communication" Rain effect on the load of tephra deposits"*. *Natural Hazards and Earth System Sciences*, 12(4), .1229-1233.

Manual for the design of building structures to Eurocode 1 and Basis of Structural Design April 2010. © 2010 The Institution of Structural Engineers

Matuttis, H.G. and Chen, J., 2014. Understanding the discrete element method: simulation of non-spherical particles for granular and multi-body systems. John Wiley & Sons.

Mazzolani, F.M. ed., 2019. Urban Habitat Constructions Under Catastrophic Events: COST C26 Action Final Report. CRC Press.

McKenzie, D., 1972. Active tectonics of the Mediterranean region. *Geophysical Journal International*,30(2), .109-185.

Multiphysics, C.O.M.S.O.L., 2012. Effective Modelling and Simulation of Engineering Problems

Multiphysics, C.O.M.S.O.L., 2018. version 5.2. COMSOL AB, Stockholm, Sweden

Murakami, S. 2000, “Computational environment design for indoor and outdoor climates”, University of Tokyo Press, Tokyo, Japan with. *International Journal of Science and Technology*,2(10).

Muzeau, J.P., Talon, A., Thouret, J.C., Rossetto, T., Faggiano, B., De Gregorio, D., Zuccaro, G. and Indirli, M., 2010. 1.5 Actions due to volcanic eruptions. *Urban Habitat Constructions Under Catastrophic Events: COST C26 Action Final Report*, p.73.

NA+A2:2014 BS EN 1992-1-1:2004+A1:2014 UK National Annex to Eurocode 2. Design of concrete structures. General rules and rules for buildings

NEN, E., 1991. Eurocode 1: Actions on Structures-Part 1-3: General Actions-Snow loads

Newhall, C.G. and Self, S., 1982. The volcanic explosivity index (VEI) an estimate of explosive magnitude for historical volcanism. *Journal of Geophysical Research: Oceans*, 87(C2), .1231-1238.

Nguyen, D.N. and Vo, D.T., 2020. Comprehensive finite element modelling for pulsed magnet design using COMSOL and Java. *IEEE Transactions on Applied Superconductivity*, 30(4), pp.1-5.

Nicholas M. B. 1987. "Finite Element Analysis of Microcomputers", McGraw-Hill New York.

Osman.S., Mark .T., Carvers. S., and Crummy. J.,I 2021 Vulnerability of roof collapse to tephra loading: Ascension Island case study

O'Sullivan (2015) Advancing Geomechanics Using DEM, International Symposium on Geomechanics from Micro to Macro, IS-Cambridge 2014, September 1, 2014 - September 3, 2014

Perlt, J., Heinert, M. and Niemeier, W., 2008. The continental margin in Iceland—A snapshot derived from combined GPS networks. *Tectonophysics*,447(1), .155-166.

Pirnia, P., Duhaime, F., Ethier, Y. and Dubé, J.S., 2019. ICY: An interface between COMSOL multiphysics and discrete element code YADE for the modelling of porous media. *Computers & Geosciences*, 123, pp.38-46.

Polacci, M., 2012. Ash Characterization

Pomonis, A., Spence, R. and Baxter, P., 1999. Risk assessment of residential buildings for an eruption of Furnas Volcano, Sao Miguel, the Azores. *Journal of volcanology and geothermal research*, 92(1-2), .107-131.

Pyle, D., (1998). SCARPA, R. & TILLING, RI (eds) 1996. *Monitoring and Mitigation of Volcano Hazards*. xx+ 841 pp. Berlin, Heidelberg, New York, Barcelona, Budapest, Hong Kong, London, Milan, Paris, Santa Clara, Singapore, Tokyo: Springer-Verlag. Price DM 198.00, Ös 1445.40, SFr 173.00 (hard covers). ISBN 3 540 60713 7.-. *Geological Magazine*, 135(2), .287-300.

Rao, S.S., 2005. *Mechanical Vibrations Fourth Edition in SI Units*.Chapter,2, pp.146-148

Rao, S.S., 2011.*The finite element method in engineering*. Butterworth-heinemann.

Rose, W. I. & Durant, A. J. 2009. *J. Volcano. Geotherm. Res.* 186, 32-39, doi: 10.1016/j.jvolgeores.2009.01.010

Sánchez de Rojas, M.I., Marin, F.P., Frías, M. and Rivera, J., 2007. Properties and performances of concrete tiles containing waste-fired clay materials. *Journal of the American Ceramic Society*, 90(11), .3559-3565.

Sarna-Wojcicki, A. M., S. Shipley, R. B. Waitt, D. Dzurisin, and S. H. Wood, 1981 Areal distribution, thickness, mass, volume, and grain size of airfall ash from the six major eruptions of 1980, *U.S. Geol. Surv. Prof. Pap.*, 1250, 577–600,

Scalisi, L., 2013. *Per riparar lincendio. Le politiche dellemergenza dal Perù al Mediterraneo (Huaynapuyina 1600-Vesuvio 1631-Etna 1669).*

Scollo, S., Kahn, R.A., Nelson, D.L., Coltelli, M., Diner, D.J., Garay, M.J. and Realmuto, V.J., 2012. MISR observations of Etna volcanic plumes. *Journal of Geophysical Research: Atmospheres*, 117(D6).

Scollo, S., Kahn, R.A., Nelson, D.L., Coltelli, M., Diner, D.J., Garay, M.J. and Realmuto, V.J., 2012. MISR observations of Etna volcanic plumes. *Journal of Geophysical Research: Atmospheres*, 117(D6).

Self, S., Rampino, M.R., Newton, M.S. and Wolff, J.A., 1984. Volcanological study of the great Tambora eruption of 1815. *Geology*, 12(11), .659-663.

Shipley, S. & Sarna-Wojcicki, A.M. 1982. *US Geological Survey Miscellaneous Field Studies Map MF-1435*

Shipley, S. and Sarna-Wojcicki, A.M., 1982. Distribution, thickness, and mass of late Pleistocene and Holocene tephra from major volcanoes in the northwestern United States: a preliminary assessment of hazards from volcanic ejecta to nuclear reactors in the Pacific Northwest. *US Geological Survey Miscellaneous Field Studies Map MF-1435.*

Siddique, R., 2008. Volcanic Ash. In *Waste Materials and By-Products in Concrete* (pp. 323-349). Springer, Berlin, Heidelberg.

Singer, I.L., 1992. Solid lubrication processes. In *Fundamentals of friction: macroscopic and microscopic processes* (pp. 237-261). Springer, Dordrecht

Spence, R.J., Pomonis, A., Baxter, P.J. and AW, C., 1996. Building damage caused by the Mount Pinatubo eruption of June 15, 1991. *Fire and Mud: Eruptions and Lahars of Mount Pinatubo, Philippines*. University of Washington Press, Seattle, .1055-1062.

Spence, R.J.S., Kelman, I., Baxter, P.J., Zuccaro, G. and Petrazzuoli, S., 2005. Residential building and occupant vulnerability to tephra fall. *Natural Hazards and Earth System Science*, 5(4), .477-494.

Spence, R.J.S., Kelman, I., Baxter, P.J., Zuccaro, G. and Petrazzuoli, S., 2005. Residential building and occupant vulnerability to tephra fall. *Natural Hazards and Earth System Sciences*, 5(4), pp.477-494.

Structural Eurocodes, July 2003 (DAV). EN 1991-1-3 (2003) (English): Eurocode 1: Actions on structures - Part 1-3: General actions - Snow loads

Structural Eurocodes, March 2009. EN 1991-1-3:2003. Eurocode 1 - Actions on structures - Part 1-3: General actions - Snow loads. Brussels: CEN/TC 250

The European Union Per Regulation 305/2011, Directive 98/34/EC, Directive 2004/18/EC].

Thomas, M.E., 2007. Geomechanics of volcano instability and the effects of internally elevated pore fluid (gas) pressures (Doctoral dissertation, Kingston University).

Thordarson, T. and Larsen, G., 2007. Volcanism in Iceland in historical time: Volcano types, eruption styles and eruptive history. *Journal of Geodynamics*, 43(1), .118-152.

Trippanera, D., Ruch, J., Acocella, V., Thordarson, T. and Urbani, S., 2018. Interaction between central volcanoes and regional tectonics along divergent plate boundaries: Askja, Iceland. *Bulletin of Volcanology*, 80(1),.1.

Tsuchiya, M., Tomabechi, T., Hongo, T. and Ueda, H. 2002, “Wind effects on snowdrift on stepped flat roofs”, *J. Wind Eng. Ind. Aerod.*, 90(12-15), 1881-1892

Turner, M.J., Clough, R.W., Martin, H.C. and Topp, L.J., 1956. Stiffness and deflection analysis of complex structures. *Journal of the Aeronautical Sciences*, 23(9), pp.805-823.

Ucgul, M., Saunders, C. and Fielke, J.M., 2018. Comparison of the discrete element and finite element methods to model the interaction of soil and tool cutting edge. *Biosystems Engineering*, 169, pp.199-208.

Wang, W.H., Liao, H.L. and Li, M.S. 2014, “Wind tunnel test on wind-induced roof snow distribution”, *J. Build. Struct.*, 35(5), 135-141. (in Chinese)

Wang, Y., Ju, Y., Chen, J. and Song, J., 2019. Adaptive finite element–discrete element analysis for the multistage supercritical CO₂ fracturing and microseismic modelling of horizontal wells in tight reservoirs considering pre-existing fractures and thermal-hydro-mechanical coupling. *Journal of Natural Gas Science and Engineering*, 61, pp.251-269

Williams, G.T., Kennedy, B.M., Wilson, T.M., Fitzgerald, R.H., Tsunematsu, K. and Teissier, A., 2017. Buildings vs. ballistics: Quantifying the vulnerability of buildings to volcanic ballistic impacts using field studies and pneumatic cannon experiments. *Journal of Volcanology and Geothermal Research*, 343, 171-180.

Wilson, T., Cole, J., Cronin, S., Stewart, C. and Johnston, D., 2011. Impacts on agriculture following the 1991 eruption of Vulcan Hudson, Patagonia: lessons for recovery. *Natural Hazards*, 57(2), pp.185-212.

Wilson, T., Stewart, C., Cole, J., Johnston, D. and Cronin, S., 2010. Vulnerability of farm water supply systems to volcanic ashfall. *Environmental Earth Sciences*, 61(4), .675-688.

Wilson, T.M., Stewart, C., Sword-Daniels, V., Leonard, G.S., Johnston, D.M., Cole, J.W., Wardman, J., Wilson, G. and Barnard, S.T., 2012. Volcanic ash impacts on critical infrastructure. *Physics and Chemistry of the Earth, Parts A/B/C*, 45, .5-23.

Zhao, L., Yu, Z., Zhu, F., Qi, X. and Zhao, S., 2016. CFD-DEM modelling of snowdrifts on stepped flat roofs. *Wind and Structures*, 23(6), pp.523-542

Zimanowski, B., Wohletz, K., Dellino, P. and Büttner, R., 2003. The volcanic ash problem. *Journal of Volcanology and Geothermal Research*, 122(1), .1-5.

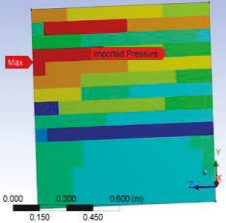
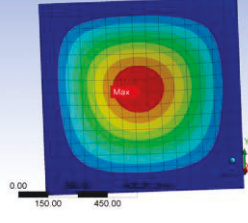
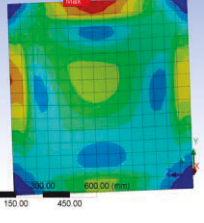
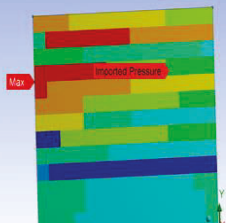
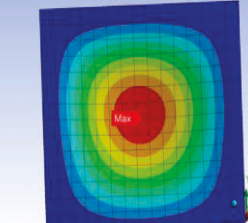
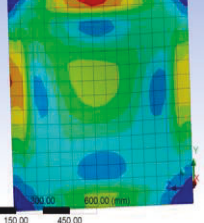
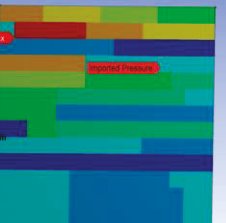
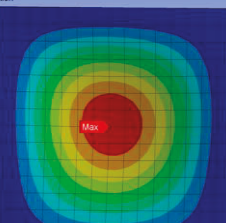
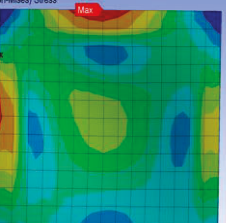
APPENDICES

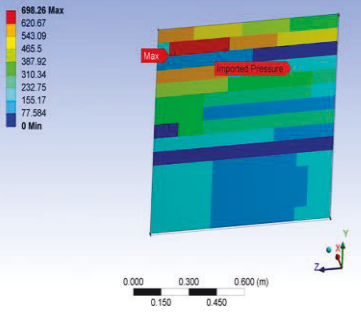
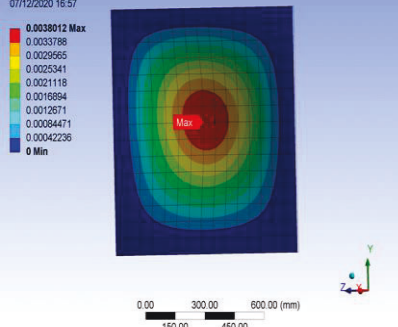
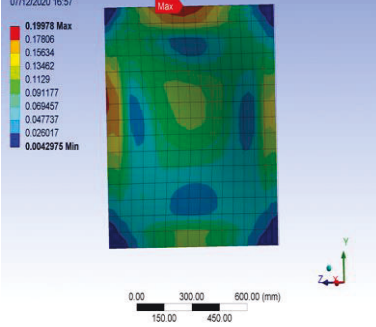
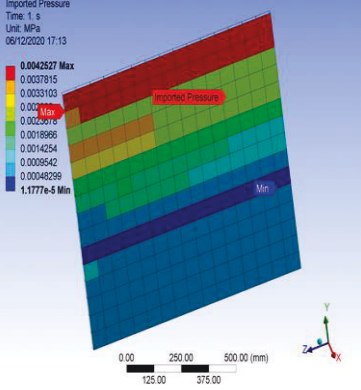
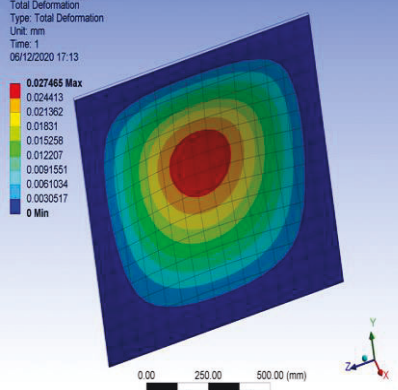
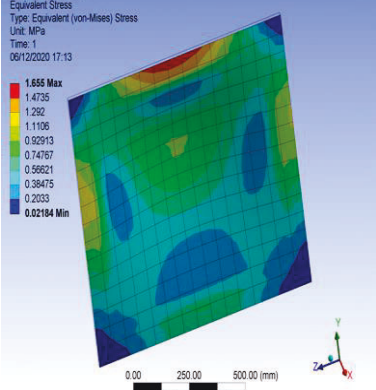
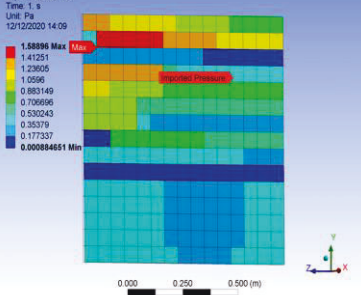
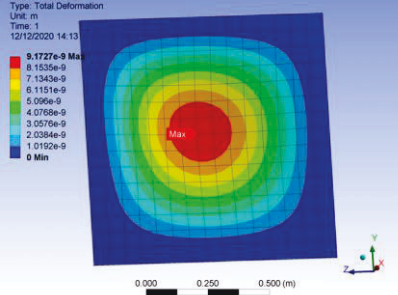
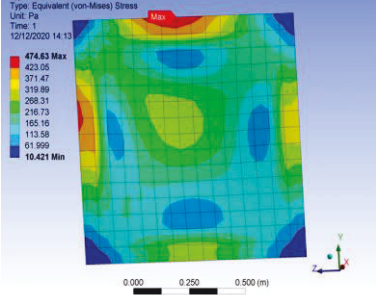
APPENDIX 1:

RELATED RESOURCES FOR CHAPTER 4

Table AP1.1: Results for 80,000 Volcanic Ash Particles Simulation with No Wind Effects

Volcanic Ash Particle Size in Diameter (mm)	Volcanic Ash Particle densities (Kg/m ³)	Maximum Pressure (Pa)	Maximum Deformation (mm)	FEM Maximum von Mises stress (MPa)	FEM Imagery Results shows the distribution of pressure load (Pa)	FEM Imagery Results shows the distribution of deformations (mm)	FEM Imagery Results shows the distribution of von Mises stress (MPa)
1	1000	17.5146	0.00016594	0.0083915			

5	1000	708.139	0.0039647	0.20675	<p>B: Static Structural Imported Pressure Time: 1 s Unit: Pa 10/12/2020 17:41</p> <p>2766.85 Max 2452.01 2147.16 1842.32 1537.48 1232.63 927.789 622.946 318.103 13.2893 Min</p> 	<p>B: Static Structural Total Deformation Type: Total Deformation Unit: mm Time: 1 10/12/2020 17:43</p> <p>0.022562 Max 0.020365 0.017548 0.015041 0.012534 0.010027 0.0075206 0.0050137 0.0025069 0 Min</p> 	<p>B: Static Structural Equivalent Stress Type: Equivalent (von-Mises) Stress Unit: MPa Time: 1 10/12/2020 17:44</p> <p>1.1983 Max 1.0331 0.90891 0.78073 0.65456 0.52838 0.40221 0.27604 0.14986 0.023987 Min</p> 
10	1000	2756.85	0.022562	1.1593	<p>B: Static Structural Imported Pressure Time: 1 s Unit: Pa 10/12/2020 17:41</p> <p>2766.85 Max 2452.01 2147.16 1842.32 1537.48 1232.63 927.789 622.946 318.103 13.2893 Min</p> 	<p>B: Static Structural Total Deformation Type: Total Deformation Unit: mm Time: 1 10/12/2020 17:43</p> <p>0.022562 Max 0.020365 0.017548 0.015041 0.012534 0.010027 0.0075206 0.0050137 0.0025069 0 Min</p> 	<p>B: Static Structural Equivalent Stress Type: Equivalent (von-Mises) Stress Unit: MPa Time: 1 10/12/2020 17:44</p> <p>1.1983 Max 1.0331 0.90891 0.78073 0.65456 0.52838 0.40221 0.27604 0.14986 0.023987 Min</p> 
1	2000	3.23877	1.7572-5	0.00092441	<p>B: Static Structural Imported Pressure Time: 1 s Unit: Pa 10/12/2020 12:57</p> <p>3.23877 Max 2.87892 2.51907 2.15921 1.79936 1.43951 1.07966 0.719812 0.359961 0.000111 Min</p> 	<p>B: Static Structural Total Deformation Type: Total Deformation Unit: mm Time: 1 10/12/2020 12:58</p> <p>1.7572e-5 Max 1.5619e-5 1.3667e-5 1.1715e-5 9.7621e-6 7.8097e-6 5.8573e-6 3.9048e-6 1.9524e-6 0 Min</p> 	<p>B: Static Structural Equivalent Stress Type: Equivalent (von-Mises) Stress Unit: MPa Time: 1 10/12/2020 12:59</p> <p>0.00092441 Max 0.00032178 0.00071916 0.00061653 0.00051329 0.00041128 0.00030865 0.00020602 0.0001034 7.8829e-7 Min</p> 

5	2000	698.26	0.00338012	0.19978	<p>B: Static Structural Imported Pressure Time: 1, s Unit: Pa 07/12/2020 16:55</p>  <p>698.26 Max 620.67 543.09 465.5 387.92 310.34 232.75 155.17 77.594 0 Min</p>	<p>B: Static Structural Total Deformation Type: Total Deformation Unit: mm Time: 1 07/12/2020 16:57</p>  <p>0.0038012 Max 0.0033788 0.0029565 0.0025341 0.0021118 0.0016984 0.0012671 0.0008471 0.0004236 0 Min</p>	<p>B: Static Structural Equivalent Stress Type: Equivalent (von-Mises) Stress Unit: MPa Time: 1 07/12/2020 16:57</p>  <p>0.19978 Max 0.17806 0.15634 0.13462 0.1129 0.091177 0.069457 0.047737 0.026017 0.0042975 Min</p>
10	2000	4252.68	0.027465	1.655	<p>B: Static Structural Imported Pressure Time: 1, s Unit: MPa 06/12/2020 17:13</p>  <p>0.044327 Max 0.0237815 0.0033103 0.0011006 0.0002076 0.0018966 0.0014254 0.0005542 0.0004929 1.1777e-6 Min</p>	<p>B: Static Structural Total Deformation Type: Total Deformation Unit: mm Time: 1 06/12/2020 17:13</p>  <p>0.027465 Max 0.0204413 0.021362 0.01831 0.015258 0.012207 0.0091551 0.0061034 0.0030517 0 Min</p>	<p>B: Static Structural Equivalent Stress Type: Equivalent (von-Mises) Stress Unit: MPa Time: 1 06/12/2020 17:13</p>  <p>1.655 Max 1.4735 1.252 1.1106 0.92913 0.74767 0.56821 0.38475 0.2033 0.02184 Min</p>
1	3000	1.58896	9.1727e-6	0.00047463	<p>B: Static Structural Imported Pressure Time: 1, s Unit: Pa 12/12/2020 14:09</p>  <p>1.58896 Max 1.41251 1.23605 1.0596 0.883149 0.706996 0.530243 0.35379 0.177337 0.00084651 Min</p>	<p>B: Static Structural Total Deformation Type: Total Deformation Unit: m Time: 1 12/12/2020 14:13</p>  <p>9.1727e-6 Max 8.1535e-9 7.1343e-9 6.1151e-9 5.096e-9 4.0768e-9 3.0576e-9 2.0384e-9 1.0192e-9 0 Min</p>	<p>B: Static Structural Equivalent Stress Type: Equivalent (von-Mises) Stress Unit: Pa Time: 1 12/12/2020 14:13</p>  <p>474.63 Max 423.05 371.47 319.89 268.31 216.73 165.16 113.58 61.999 19.421 Min</p>

5	3000	659.918	0.0039246	0.20135			
10	3000	26703	0.25235	14.39			

Table AP1.1: shows the results for 80,000 volcanic ash particles below were tabulated from the numerical modelling tool (EDEM software) for the Discrete Element Method (DEM) and structural analysis tool (ANSYS) for the Finite Element Method (FEM) simulation with No wind effects. The result in this section is like that of figure 4.5 for the 160,000 volcanic ash particles. It is clear as the density is high, the higher the pressure loading of the volcanic ash particles, the deformation and stress impact on the roof for the 1000 (Kg m^{-3}) density for the 1mm, 5mm and 10mm volcanic ash particles, there is an increase of the stress (MPa) effects from the figure 4.6 as 0.20675 (MPa) and 1.1593 (MPa) respectively. This section is linked to table 5.4 results.

Table API.2: Set of results for 80,000 Volcanic Ash Particles Simulation with Wind Effects in The Horizontal Direction

Volcanic Ash Particle Size in Diameter (mm)	Volcanic Ash Particle densities (Kg/m3)	Horizontal direction (ms-1)	DEM Maximum Pressure (Pa)	FEM maximum Deformation (mm)	FEM Maximum von Mises stress (MPa)	DEM Imagery Results shows the distribution of pressure load (Pa)	FEM Imagery Results shows the distribution of deformations (mm)	FEM Imagery Results shows the distribution of von Mises stress (MPa)
1	1000	0.1	1.1817	6.8103e-6	0.00035234			
5	1000	0.5	480.428	0.006538	0.17653			
10	1000	1.0	7174.4	0.071698	3.789			

1	2000	0.1	48.557	0.0004906	0.025401			
5	2000	0.5	452.69	0.004	0.168			
10	2000	1.0	4772.1	0.0475731	2.4913			

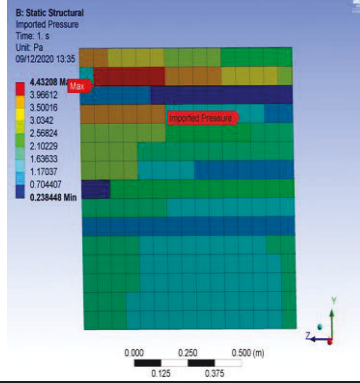
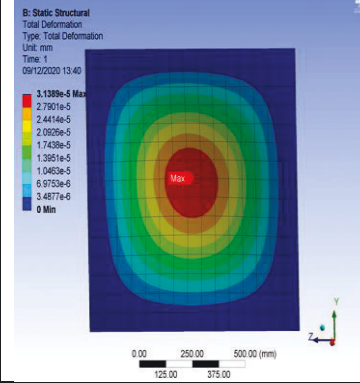
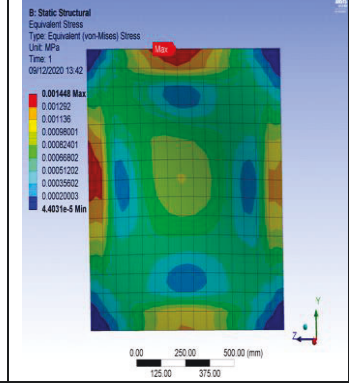
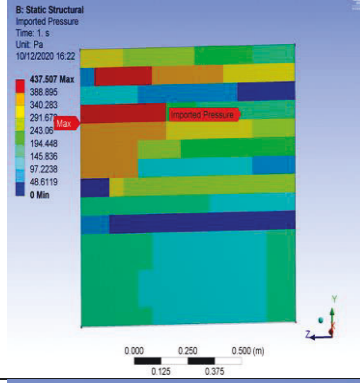
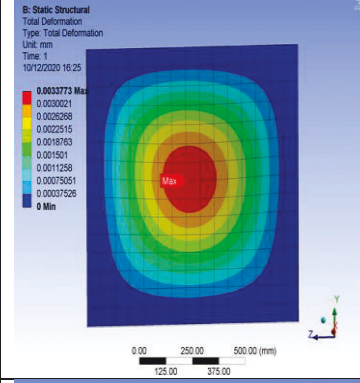
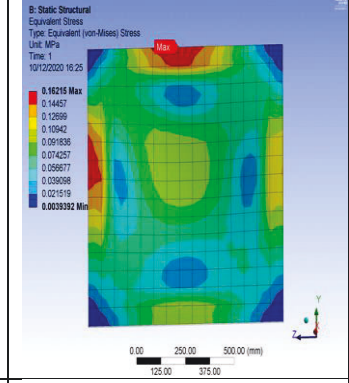
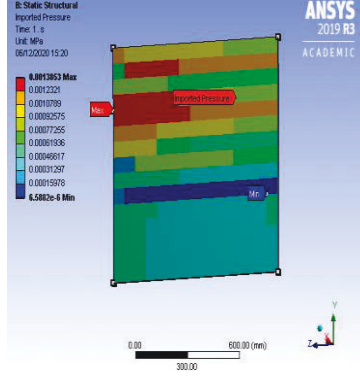
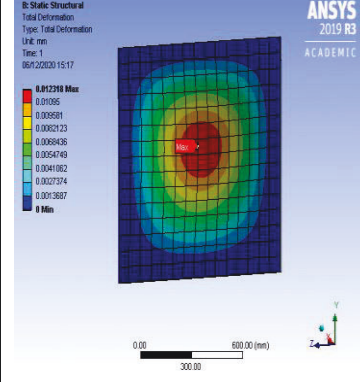
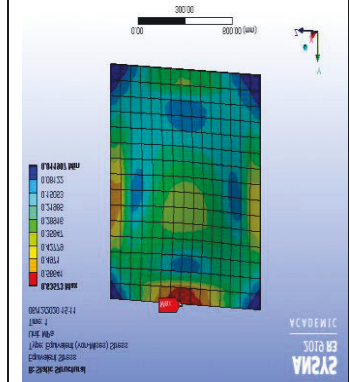
1	3000	0.1	4.43208	3.1389-5	0.001448			
5	3000	0.5	437.51	0.003	0.162			
10	3000	1.0	1385.3	0.012318	0.63573			

Table AP1.2 shows the results for 80,000 volcanic ash particles below were tabulated from the further data sorting were carried out for the various numerical results from the above data for the flat roof from the numerical modelling tool (EDEM software) for the Discrete Element Method (DEM) and structural analysis tool (ANSYS) for the Finite Element Method (FEM) simulation. This section is linked to table 5.4 results data.

Results for the Discrete Element Method (DEM) and Structural Analysis tool (ANSYS) for the Finite Element Method (FEM) Simulation. The numerical modelling tool data (EDEM software) for the Discrete Element Method (DEM) and structural analysis tool (ANSYS) for the Finite Element Method (FEM) simulation for Pitched Roof, Looking at table 4.7 the 2000 (Kgm^{-3}) density for the variable volcanic ash particles for 1m,5m,10m diameter size, it can be seen that there is an increase with the DEM pressure values that as in 48.557 (Pa), 452.60 (Pa) and 4772.1 (Pa) and these have a corresponding increase for the FEM deformation and the FEM stress values the figure also shows a set of different kinds of imagery results for the DEM distribution for the pressure loading the FEM distribution for the deformation and the FEM distribution of the stress values.

The results below were tabulated from the numerical modelling tool (EDEM software) for the Discrete Element Method (DEM) and structural analysis tool (ANSYS) for the Finite Element Method (FEM) simulation. (Pitched Roof)

Table API.3: Set of results for the 25 degrees 170,000 DEM and FEM CO- Simulation for Volcanic Ash Particles with No Wind Effects

Volcanic Ash Particle Size in Diameter (mm)	Volcanic Ash Particle densities (Kg/m ³)	DEM Maximum Pressure (Pa)	FEM Maximum Deformation Results (mm)	FEM Maximum von Mises stress (MPa)	FEM Maximum Strain Results (mm/m)	DEM Imagery Results shows the distribution of pressure load (Pa)	FEM Imagery Results shows the distribution of deformations (mm)	FEM Imagery Results shows the distribution of von Mises stress (MPa)	FEM Imagery Results shows the distribution of stress Strain (mm/mm)
1	1000	2.59892	0.00047982	0.0076547	3.8326e-8				
5	1000	2193.33	0.49444	8.155	4.0844e-5				

10	1000	2040.56	0.51486	8.0286	4.0192e-5				
1	2000	2.5989	0.00047982	0.0076547	3.826-8				
5	2000	159.842	0.033743	0.52059	2.6061e-6				

10	2000	2970.64	0.88884	13.706e7	6.8614e-5				
5	3000	131.753	0.01328	0.20128	1.0075e-6				
10	3000	4060.9	0.95708	14.809	7.4143e_5				

Table AP1.3: shows the results for 170,000 volcanic ash particles below were tabulated from the simulation data sorting were carried out for the various numerical results flat roof from the numerical modelling tool (EDEM software) for the discrete element method (DEM). The structural analysis tool (ANSYS) for the finite element method (FEM) simulation results for the variable pitch concrete tile roof for (25 degrees), this section is linked to table 5. 15. Table 4:12 shows the DEM and FEM set of results for the 170,000 volcanic ash particles. This section has 1 mm,5 mm and 10 mm volcanic ash particles. Comparing the pressure results shows that the 1 mm size particles are the least pressure loading followed by the 5mm and 10mm volcanic ash particles. The imagery distribution for the DEM and FEM simulation result is shown for the 25-degree tiled pitched roof for the no wind effects data.

Table AP1.4.: Results for the 25 Degrees 170,000 DEM and FEM CO-Simulation for Volcanic Ash Particles with Wind Effects in the Horizontal Direction.

Volcanic Ash Particle Size in Diameter (mm)	Volcanic Ash Particle densities (Kg/m3)	Horizontal direction (ms-1)	DEM Maximum Pressure (Pa)	FEM Maximum Deformation Results (mm)	FEM Maximum von Mises stress (MPa)	FEM Maximum Strain Results (mm/m)	DEM Imagery Results shows the distribution of pressure load (Pa)	FEM Imagery Results shows the distribution of deformations (mm)	FEM Imagery Results shows the distribution of von Mises stress (MPa)	FEM Imagery Results shows the distribution of stress Strain (mm/mm)
5	1000	0.5	121.861	2.1569e-5	3.9221e-5	1.9633e-65				
10	1000	1.0	1339.07	0.2986	4.5403	2.2731e-5				

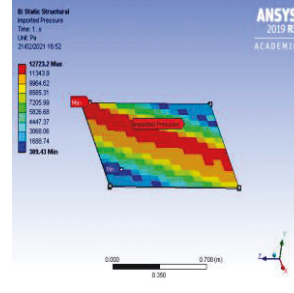
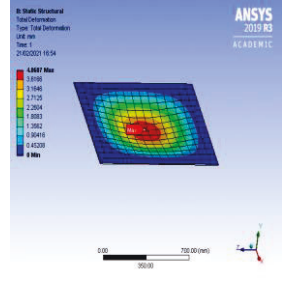
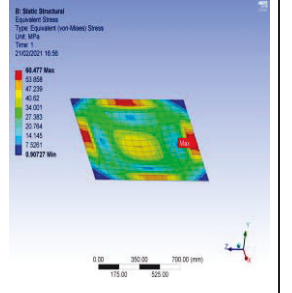
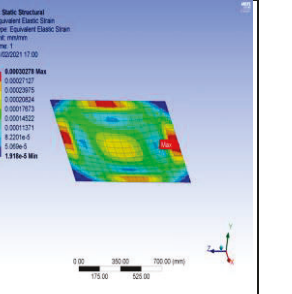
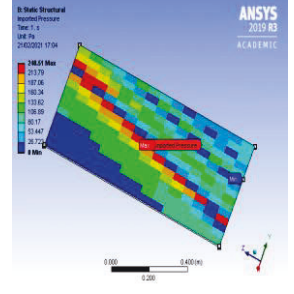
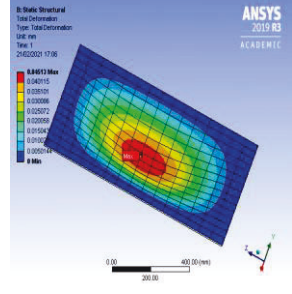
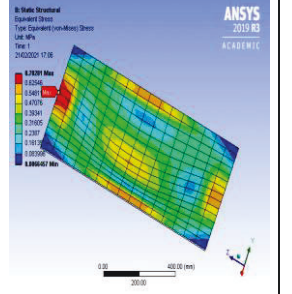
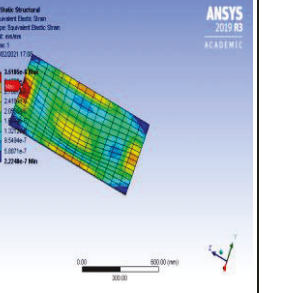
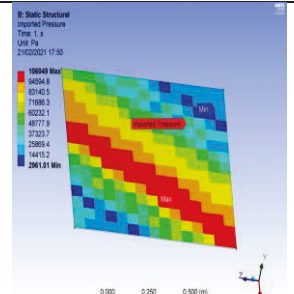
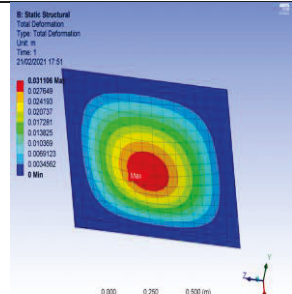
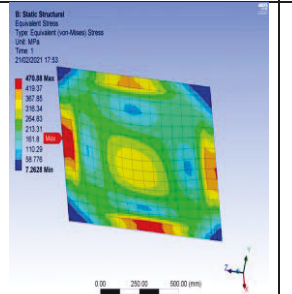
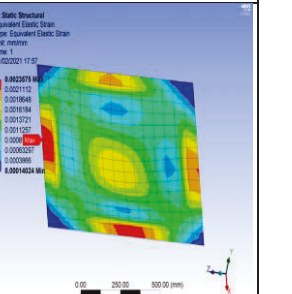
5	2000	0.5	70.6207	0.005336	0.11487	5.7484e-7				
10	2000	1.0	3215.44	0.80002	13.023	6.5214e-5				
5	3000	0.5	62.3963	0.0048505	0.10544	5.2765e-7				

10	3000	1.0	11141.9	3.1321	47.952	0.00024012	<p>B: Static Structural Equivalent Pressure Time: 1 s Unit: Pa 18/02/2021 14:47</p> <p>11142 Max 9953.9 8955.9 7957.9 6959.9 4951.9 374.4 2476 1238 0 Min</p> <p>0.00 0.250 0.500 (m) 0.125 0.375</p>	<p>B: Static Structural Total Deformation Type: Total Deformation Unit: mm Time: 1 18/02/2021 14:48</p> <p>2.1321 Max 2.734 2.435 2.089 1.74 1.392 1.044 0.69601 0.34801 0 Min</p> <p>0.00 250.00 500.00 (mm) 125.00 375.00</p>	<p>B: Static Structural Equivalent Stress Type: Equivalent von-Mises Stress Unit: MPa Time: 1 18/02/2021 14:48</p> <p>47.952 Max 42.988 37.433 32.159 26.885 21.63 16.366 11.102 5.8373 0.57268 Min</p> <p>0.00 250.00 500.00 (mm) 125.00 375.00</p>	<p>B: Static Structural Equivalent Elastic Strain Type: Equivalent Elastic Strain Unit: mm/mm Time: 1 18/02/2021 14:52</p> <p>0.00024012 Max 0.00021491 0.001897 0.001745 0.0011929 0.0011429 0.007965 0.007364 0.0045164 1.2016e-9 Min</p> <p>0.00 250.00 500.00 (mm) 125.00 375.00</p>
----	------	-----	---------	--------	--------	------------	---	--	---	---

Table AP1.4 shows the results for 170,000 volcanic ash particles below were tabulated from the simulation data sorting was carried out for the various numerical results flat roof from the numerical modelling tool (EDEM software) for the discrete element method (DEM). The structural analysis tool (ANSYS) for the finite element method (FEM) simulation results for the variable pitch concrete tile roof for 25 degrees).

Table AP1.4 shows the set of results for the 25 degrees shows the 5mm and 10mm volcanic ash diameter size produces a higher value for the DEM and FEM results, which will certainly affect the tile pitched roof wind effects. The storm values are also high and would also affect the roof. Column 8-10 shows a set of imagery set of results for the different kinds of simulations

Table API.5:: Results for the 30 Degrees 170,000 DEM and FEM co-Simulation for Volcanic Ash Particles with No Wind Effects

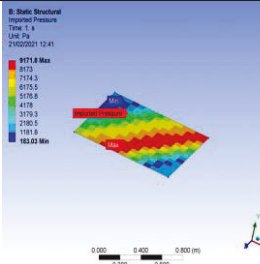
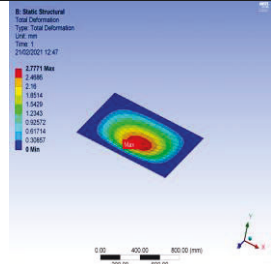
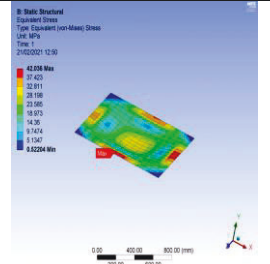
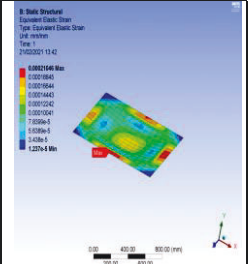
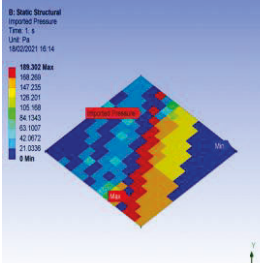
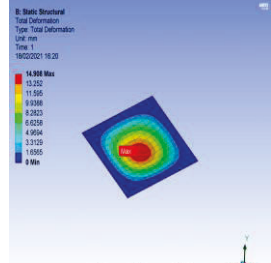
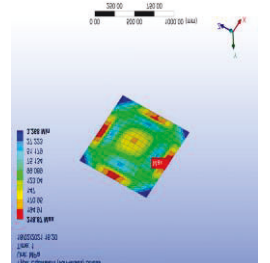
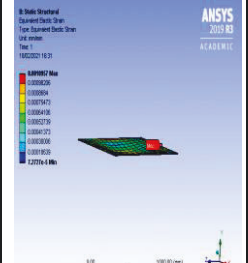
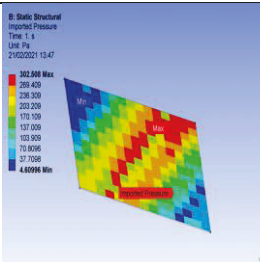
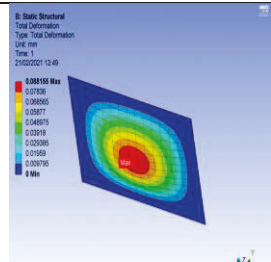
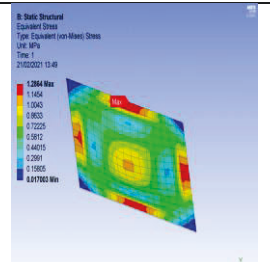
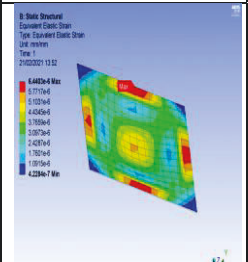
Volcanic Ash Particle Size in Diameter (mm)	Volcanic Ash Particle densities (Kg/m ³)	DEM Maximum Pressure (Pa)	FEM Maximum Deformation Results (mm)	FEM Maximum von Mises stress (MPa)	FEM Maximum Strain Results (mm/m)	DEM Imagery Results shows the distribution of pressure load (Pa)	FEM Imagery Results shows the distribution of deformations (mm)	FEM Imagery Results shows the distribution of von Mises stress (MPa)	FEM Imagery Results shows the distribution of stress Strain (mm/mm)
5	1000	12723.2	4.0687	60.477	0.00030278				
5	2000	240.51	0.04513	0.70281	3.5185e-6				
10	2000	106049	0.031106	470.88	0.0023575				

5	3000	110.564	0.020693	0.32017	1.6029e-6				
10	3000	35218	6.9968	121.95	0.00061038				

Table AP1.5 shows the results for 170,000 volcanic ash particles below were tabulated from the simulation data sorting were carried out for the various numerical results flat roof from the numerical modelling tool (EDEM software) for the discrete element method (DEM). The structural analysis tool (ANSYS) for the finite element method (FEM) simulation results for the variable pitch concrete tile roof for 30 degrees). linked to table 5. 17

Table AP1.5 shows the set of results for the 30 degrees no wind effect simulation shows that the DEM pressure values and the FEM simulation compared to table 4.15 are lesser. The wind may affect the deposition of volcanic ash particles.

Table AP1.6: Results for 30 Degrees 170,000 DEM and FEM CO - Simulation for Volcanic Ash Particles with Wind Effects in the Horizontal Direction

Volcanic Ash Particle Size in Diameter (mm)	Volcanic Ash Particle densities (Kg/m ³)	Horizontal direction (ms-1)	DEM Maximum Pressure (Pa)	FEM Maximum Deformation Results (mm)	FEM Maximum von Mises stress (MPa)	FEM Maximum Strain Results (mm/m)	DEM Imagery Results shows the distribution of pressure load (Pa)	FEM Imagery Results shows the distribution of deformations (mm)	FEM Imagery Results shows the distribution of von Mises stress (MPa)	FEM Imagery Results shows the distribution of stress Strain (mm/mm)
5	1000	0.5	9971.8	2.7771	42.036	0.00021046				
10	1000	1.0	43016.6	14.908	218.87	0.0010957				
5	2000	0.5	302.508	0.088155	1.2864	6.4403e-6				

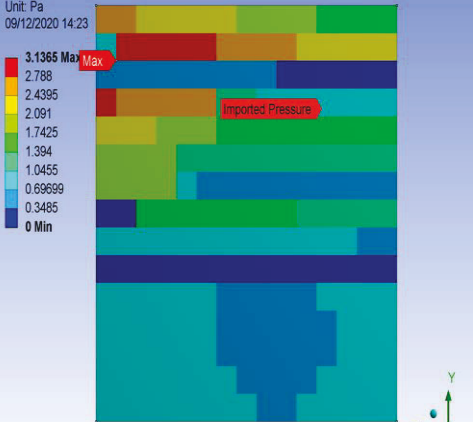
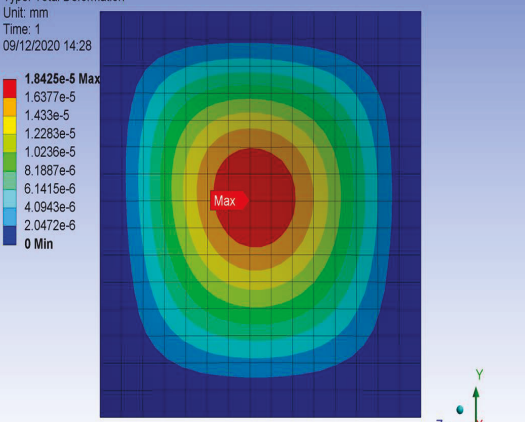
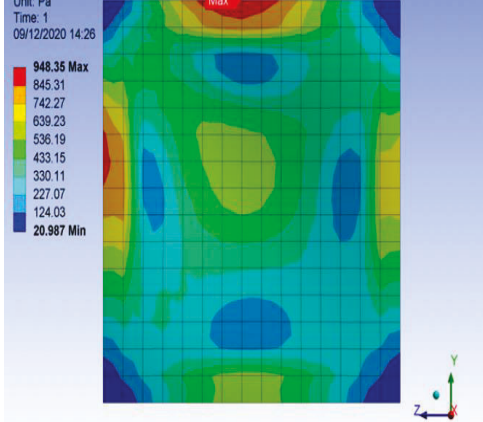
10	2000	1.0	189.302	0.036981	0.61631	3.0851e-6				
5	3000	0.5	123.59	2.3495e-5	0.37836	1.8942e-6				
10	300	1.0	4496.03	0.0010866	17.87	8.9494e-5				

Table AP1.6 shows the results for 170,000 volcanic ash particles below were tabulated from the simulation data sorting were carried out for the various numerical results flat roof from the numerical modelling tool (EDEM software) for the discrete element method (DEM). The structural analysis tool (ANSYS) for the finite element method (FEM) simulation results for the variable pitch concrete tile roof for 30 degrees). This section is linked to table 5. 18 Table 4.15 shows the 30 degrees for the DEM and FEM simulation test for the no wind effects on the tile pitched roof. The results show higher results, and the FEM results for the deformation stress and strain results. The imagery distribution test results show the level of effects on the roofs.

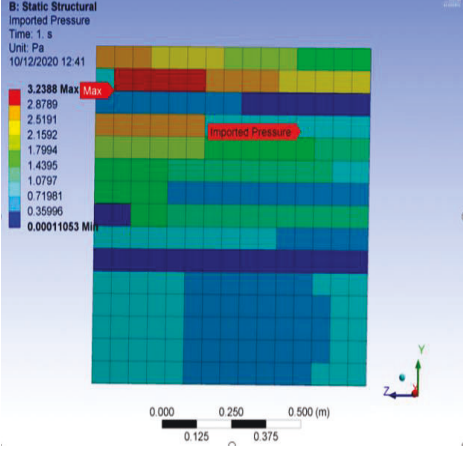
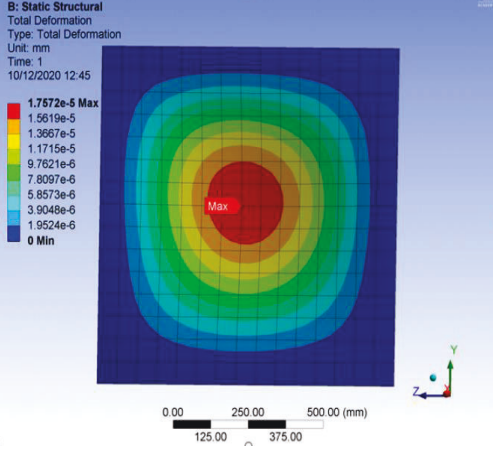
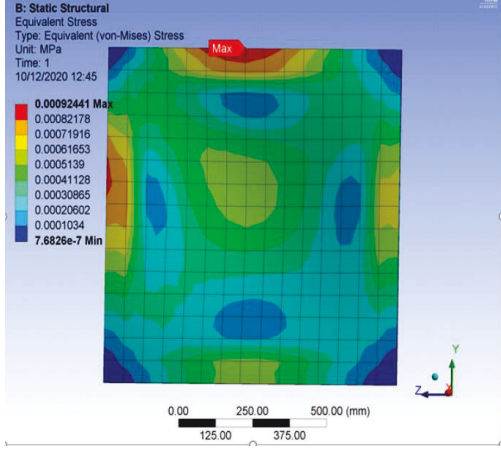
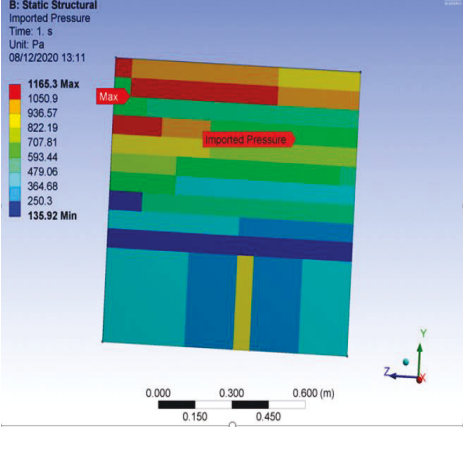
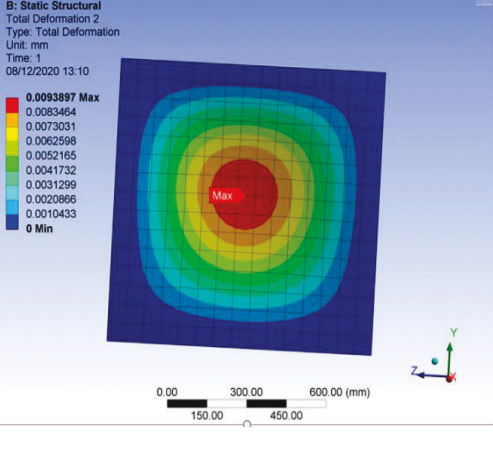
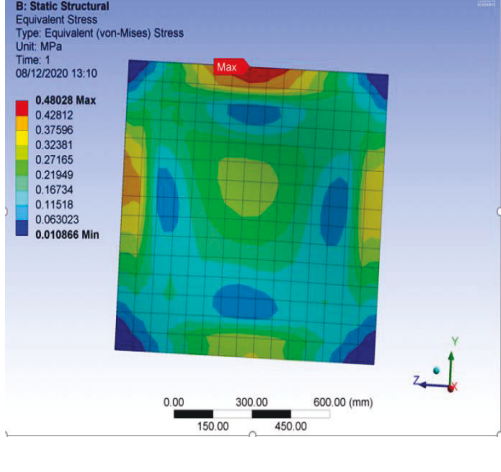
APPENDIX 2:

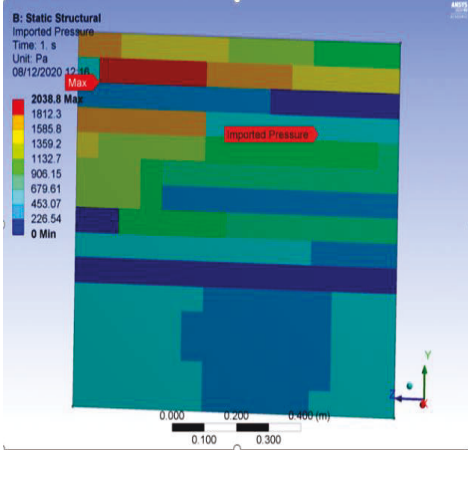
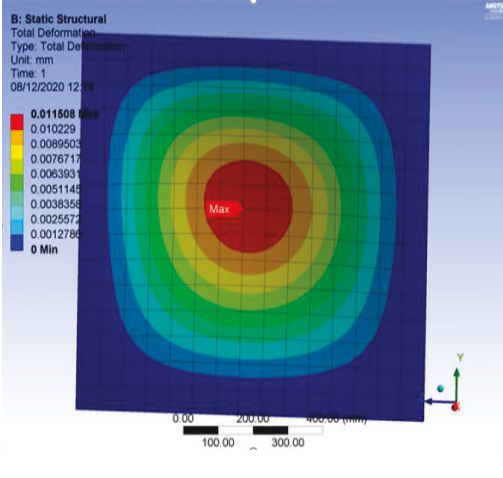
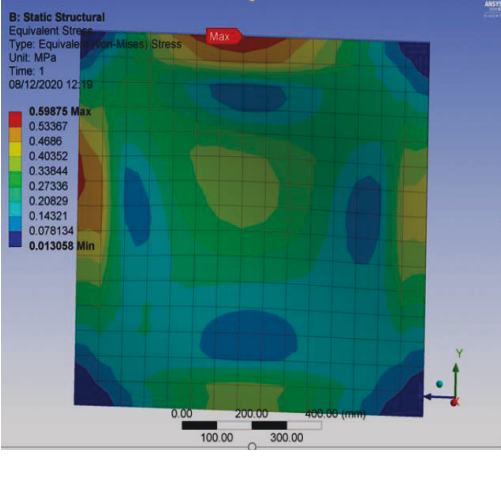
EXTRACTION AND EXPANDED TABLE OF RESULTS FROM IN CHAPTER FOUR

Table AP2.1: Extracted Table 4.4: Result of 160,000 Volcanic Ash Particles Simulation with No Wind Effects

Volcanic Ash Particle Size in Diameter (mm)	Volcanic Ash Particle densities (Kg/m ³)	FEM Imagery Results shows the distribution of pressure load (Pa)	FEM Imagery Results shows the distribution of deformations (mm)	FEM Imagery Results shows the distribution of von Mises stress (MPa)
1	1000	<p>B: Static Structural Imported Pressure Time: 1. s Unit: Pa 09/12/2020 14:23</p>  <p>3.1365 Max 2.788 2.4395 2.091 1.7425 1.394 1.0455 0.69699 0.3485 0 Min</p> <p>0.000 0.250 0.500 (m) 0.125 0.375</p>	<p>B: Static Structural Total Deformation Type: Total Deformation Unit: mm Time: 1 09/12/2020 14:28</p>  <p>1.8425e-5 Max 1.6377e-5 1.433e-5 1.2283e-5 1.0236e-5 8.1887e-6 6.1415e-6 4.0943e-6 2.0472e-6 0 Min</p> <p>0.00 250.00 500.00 (mm) 125.00 375.00</p>	<p>B: Static Structural Equivalent Stress Type: Equivalent (von-Mises) Stress Unit: Pa Time: 1 09/12/2020 14:26</p>  <p>948.35 Max 845.31 742.27 639.23 536.19 433.15 330.11 227.07 124.03 20.987 Min</p> <p>0.000 0.250 0.500 (m) 0.125 0.375</p>

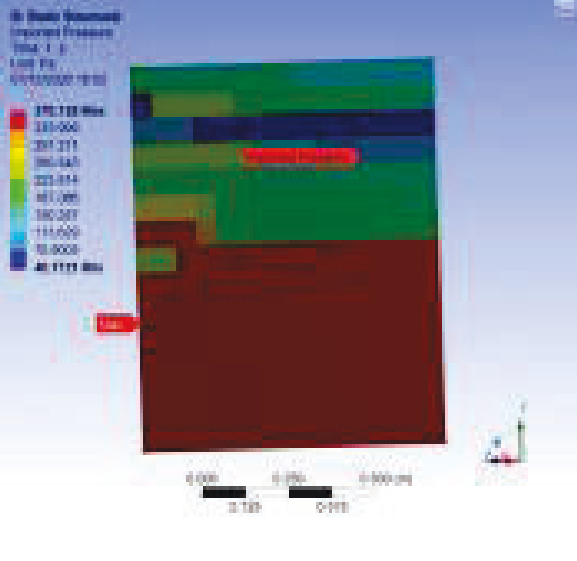
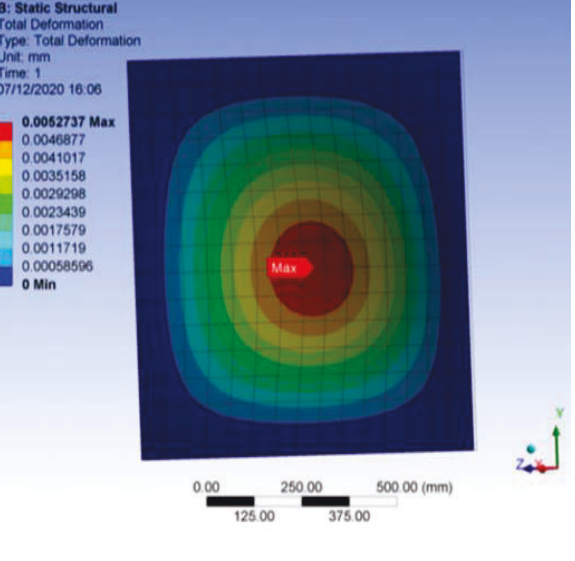
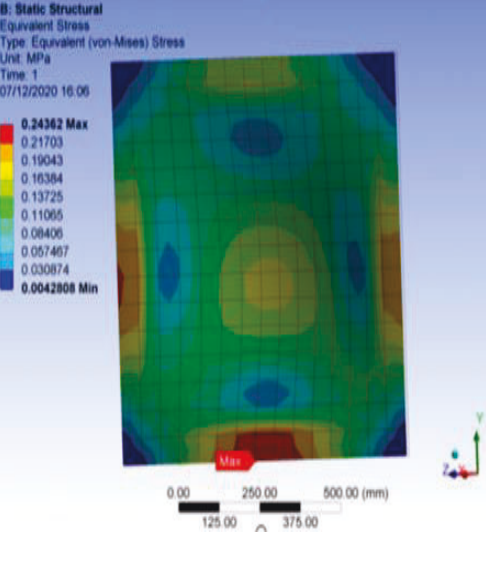
Volcanic Ash Particle Size in Diameter (mm)	Volcanic Ash Particle densities (Kg/m ³)	FEM Imagery Results shows the distribution of pressure load (Pa)	FEM Imagery Results shows the distribution of deformations (mm)	FEM Imagery Results shows the distribution of von Mises stress (MPa)
5	1000	<p>B: Static Structural Imported Pressure Time: 1 s Unit: Pa 08/12/2020 12:42</p> <p>357.558 Max 324.826 292.094 259.361 226.629 193.896 161.164 128.431 95.6988 62.9664 Min</p> <p>0.000 0.250 0.500 (m) 0.125 0.375</p>	<p>B: Static Structural Total Deformation Type: Total Deformation Unit: mm Time: 1 08/12/2020 12:43</p> <p>0.0043215 Max 0.0039414 0.0033612 0.002881 0.0024009 0.0019207 0.0014405 0.00096034 0.00048017 0 Min</p> <p>0.00 250.00 500.00 (mm) 125.00 375.00</p>	<p>B: Static Structural Equivalent Stress Type: Equivalent (von-Mises) Stress Unit: MPa Time: 1 08/12/2020 12:43</p> <p>0.1875 Max 0.16724 0.14697 0.12671 0.10645 0.086189 0.065927 0.045666 0.0254 Max 0.0051419 Min</p> <p>0.00 250.00 500.00 (mm) 125.00 375.00</p>
10	1000	<p>B: Static Structural Imported Pressure Time: 1 s Unit: Pa 08/12/2020 12:42</p> <p>357.558 Max 324.826 292.094 259.361 226.629 193.896 161.164 128.431 95.6988 62.9664 Min</p> <p>0.000 0.250 0.500 (m) 0.125 0.375</p>	<p>B: Static Structural Total Deformation Type: Total Deformation Unit: mm Time: 1 08/12/2020 11:55</p> <p>0.0066948 Max 0.005951 0.0052071 0.0044632 0.0037193 0.0029755 0.0022316 0.0014877 0.00074387 0 Min</p> <p>0.00 300.00 600.00 (mm) 150.00 450.00</p>	<p>B: Static Structural Equivalent Stress Type: Equivalent (von-Mises) Stress Unit: MPa Time: 1 08/12/2020 11:56</p> <p>0.34707 Max 0.30935 0.27163 0.23391 0.1962 0.15848 0.12076 0.083042 0.045324 0.0076066 Min</p> <p>0.00 300.00 600.00 (mm) 150.00 450.00</p>

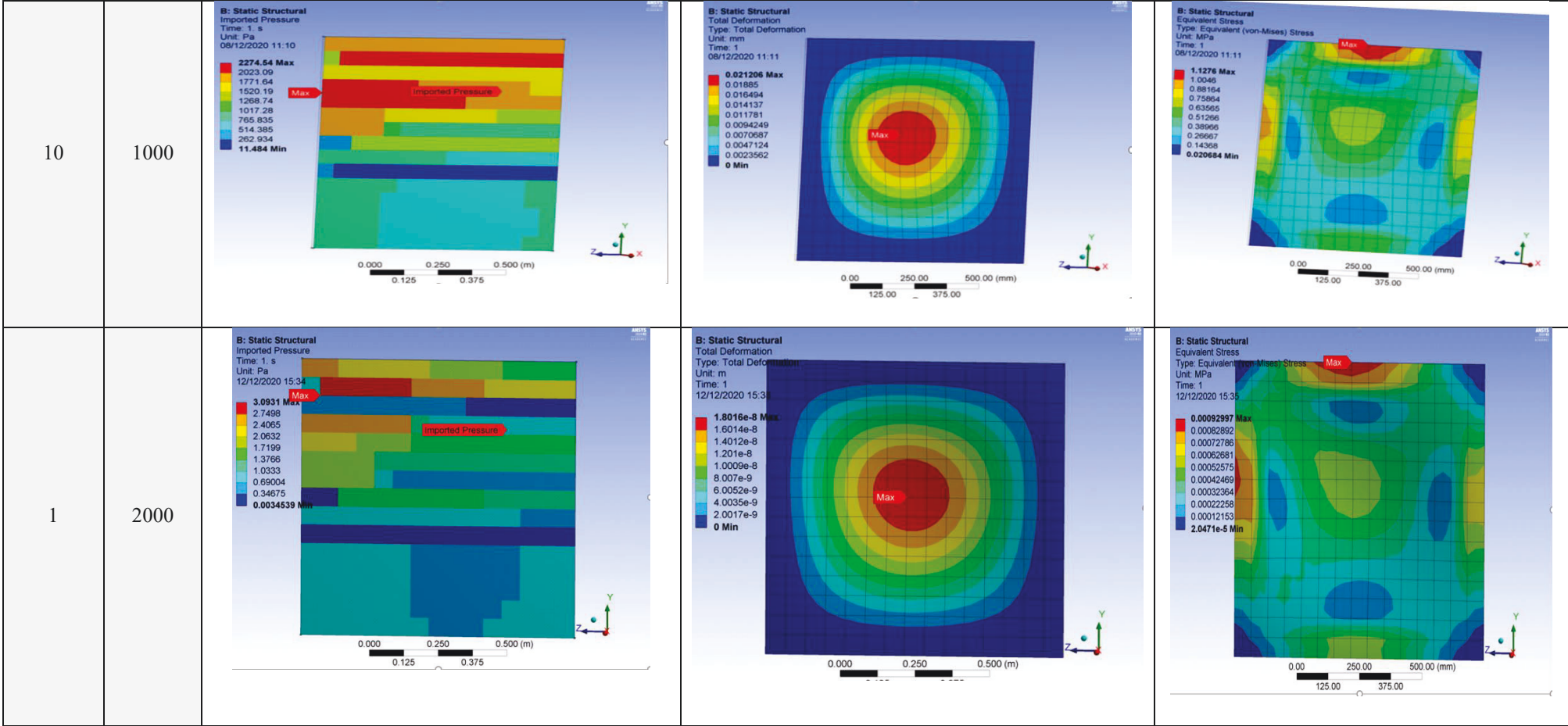
Volcanic Ash Particle Size in Diameter (mm)	Volcanic Ash Particle densities (Kg/m ³)	FEM Imagery Results shows the distribution of pressure load (Pa)	FEM Imagery Results shows the distribution of deformations (mm)	FEM Imagery Results shows the distribution of von Mises stress (MPa)
1	2000	<p>B: Static Structural Imported Pressure Time: 1 s Unit: Pa 10/12/2020 12:41</p> 	<p>B: Static Structural Total Deformation Type: Total Deformation Unit: mm Time: 1 10/12/2020 12:45</p> 	<p>B: Static Structural Equivalent Stress Type: Equivalent (von-Mises) Stress Unit: MPa Time: 1 10/12/2020 12:45</p> 
5	2000	<p>B: Static Structural Imported Pressure Time: 1 s Unit: Pa 08/12/2020 13:11</p> 	<p>B: Static Structural Total Deformation 2 Type: Total Deformation Unit: mm Time: 1 08/12/2020 13:10</p> 	<p>B: Static Structural Equivalent Stress Type: Equivalent (von-Mises) Stress Unit: MPa Time: 1 08/12/2020 13:10</p> 

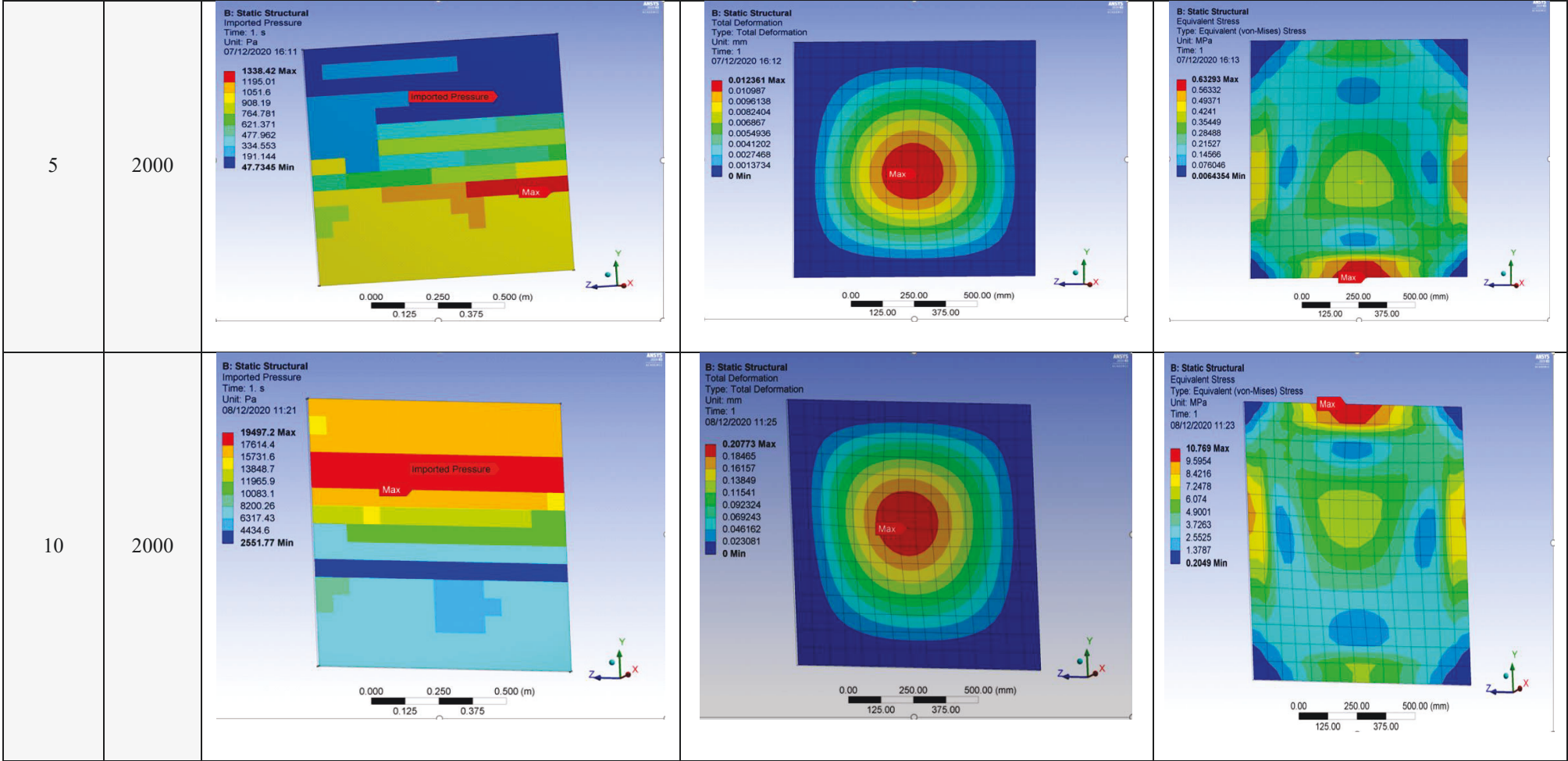
Volcanic Ash Particle Size in Diameter (mm)	Volcanic Ash Particle densities (Kg/m ³)	FEM Imagery Results shows the distribution of pressure load (Pa)	FEM Imagery Results shows the distribution of deformations (mm)	FEM Imagery Results shows the distribution of von Mises stress (MPa)
10	2000	 <p>B: Static Structural Imported Pressure Time: 1 s Unit: Pa 08/12/2020 12:19 2038.8 Max 1812.3 1585.8 1359.2 1132.7 906.15 679.61 453.07 226.54 0 Min</p>	 <p>B: Static Structural Total Deformation Type: Total Deformation Unit: mm Time: 1 08/12/2020 12:19 0.011608 Max 0.010229 0.0089503 0.0076717 0.0063931 0.0051145 0.0038358 0.0025572 0.0012786 0 Min</p>	 <p>B: Static Structural Equivalent Stress Type: Equivalent (von-Mises) Stress Unit: MPa Time: 1 08/12/2020 12:19 0.59875 Max 0.53367 0.4686 0.40352 0.33844 0.27336 0.20829 0.14321 0.078134 0.013058 Min</p>
1	3000			

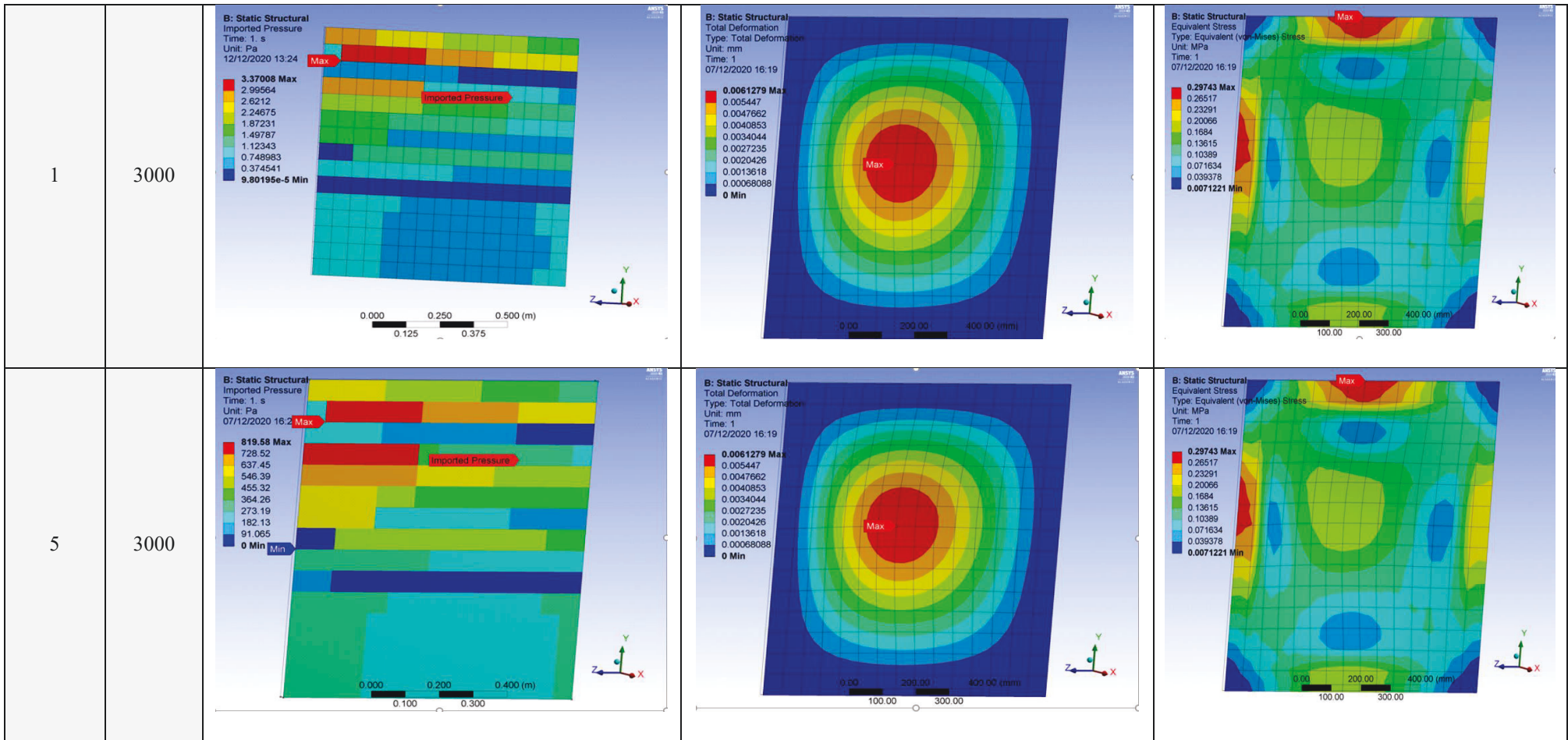
Volcanic Ash Particle Size in Diameter (mm)	Volcanic Ash Particle densities (Kg/m ³)	FEM Imagery Results shows the distribution of pressure load (Pa)	FEM Imagery Results shows the distribution of deformations (mm)	FEM Imagery Results shows the distribution of von Mises stress (MPa)
5	3000			
10	3000			

Table AP2.2: Extracted Table 4.5: Result of 160,000 Volcanic Ash Particles Simulation with Wind Effects in The Horizontal

Volcanic Ash Particle Size in Diameter (mm)	Volcanic Ash Particle densities (Kg/m ³)	FEM Imagery Results shows the distribution of pressure load (Pa)	FEM Imagery Results shows the distribution of deformations (mm)	FEM Imagery Results shows the distribution of von Mises stress (MPa)
1	1000			
5	1000			







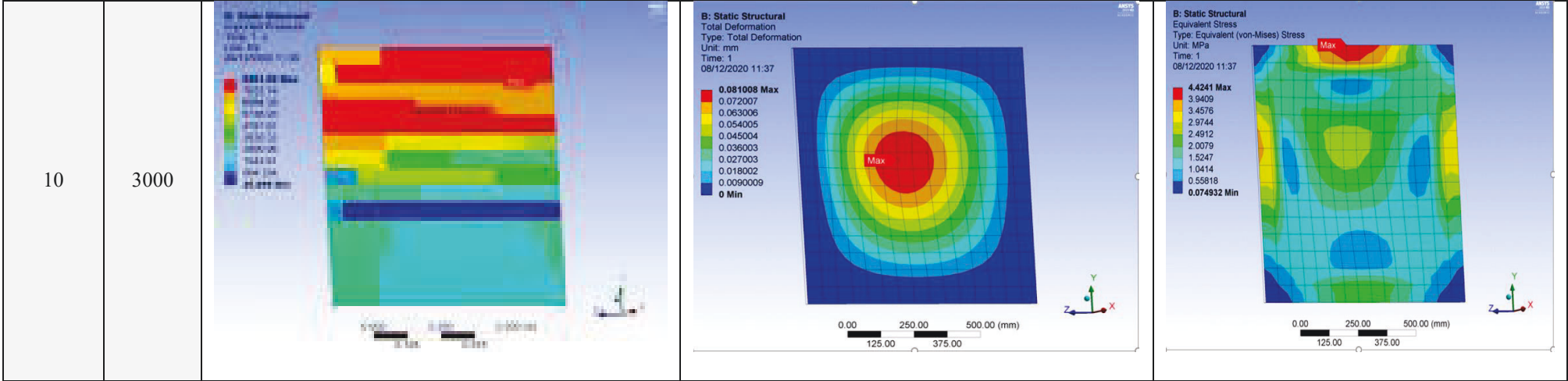
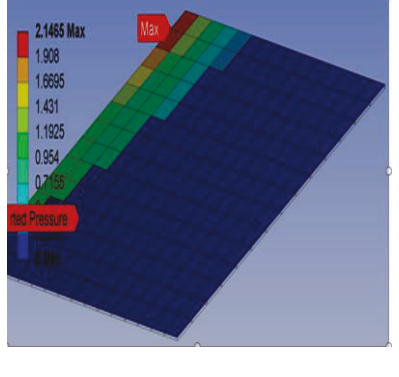
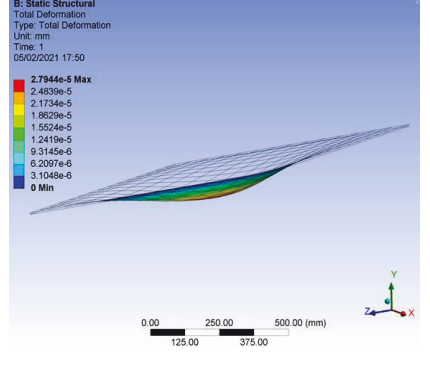
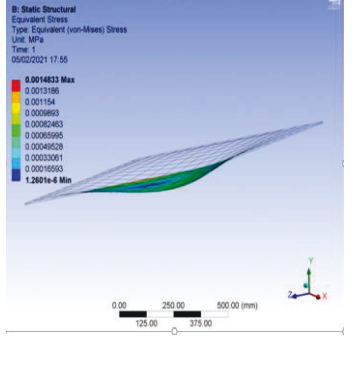
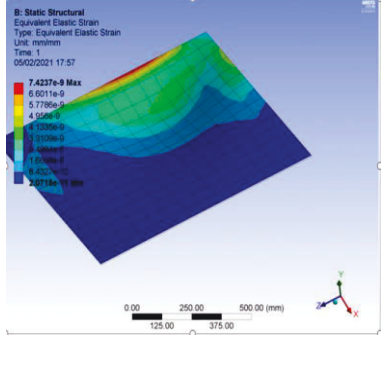
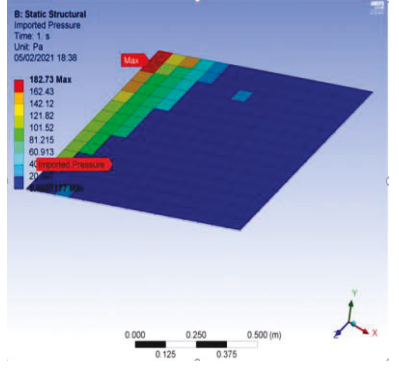
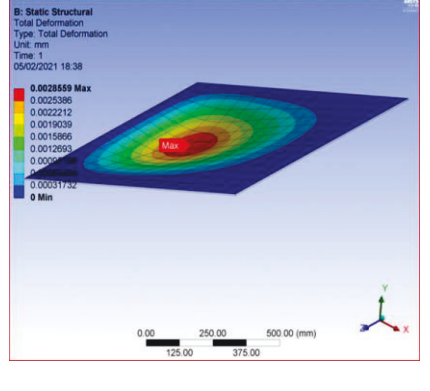


Table AP2.3: Extracted Table 4.8: Result of 20 Degrees 170,000 DEM and FEM CO-Simulation for Volcanic Ash Particles with No Wind Effects

Volcanic Ash Particle Size in Diameter (mm)	Volcanic Ash Particle densities (Kg/m ³)	DEM Imagery Results shows the distribution of pressure load (Pa)	FEM Imagery Results shows the distribution of deformations (mm)	FEM Imagery Results shows the distribution of von Mises stress (MPa)	FEM Imagery Results shows the distribution of stress Strain (mm/mm)
1	1000				
5	1000				

APPENDIX 3:

DEM AND FEM SIMULATION ANIMATION RESULTS (IMAGES AND VIDEOS)

FEM SIMULATION IMAGES

Results for the Finite Element Method (FEM)

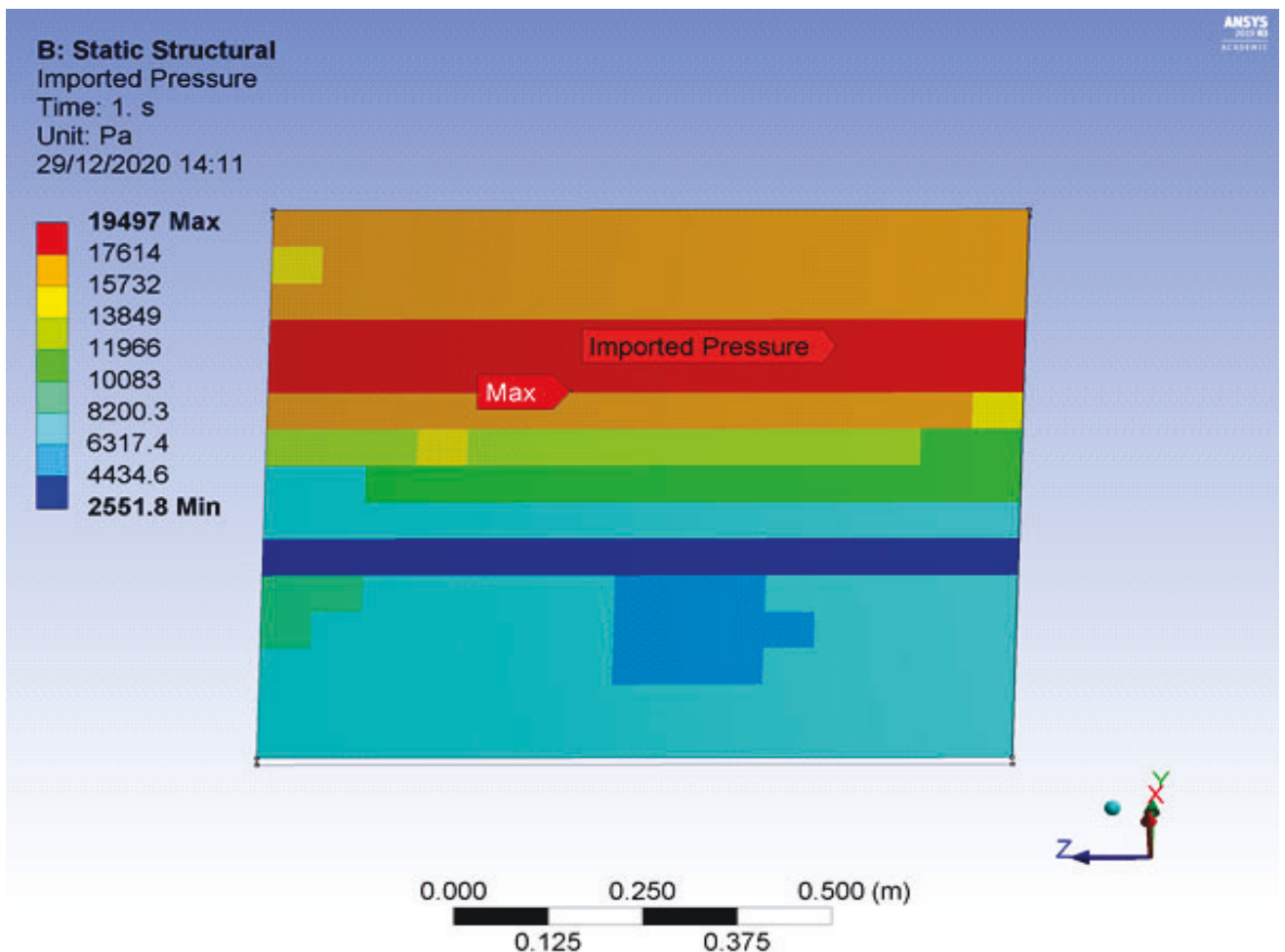


Figure AP3.1: Pressure exported from the DEM model to the FEM model for the wind effects reading for the maximum pressure as 19497.2 (Pa)

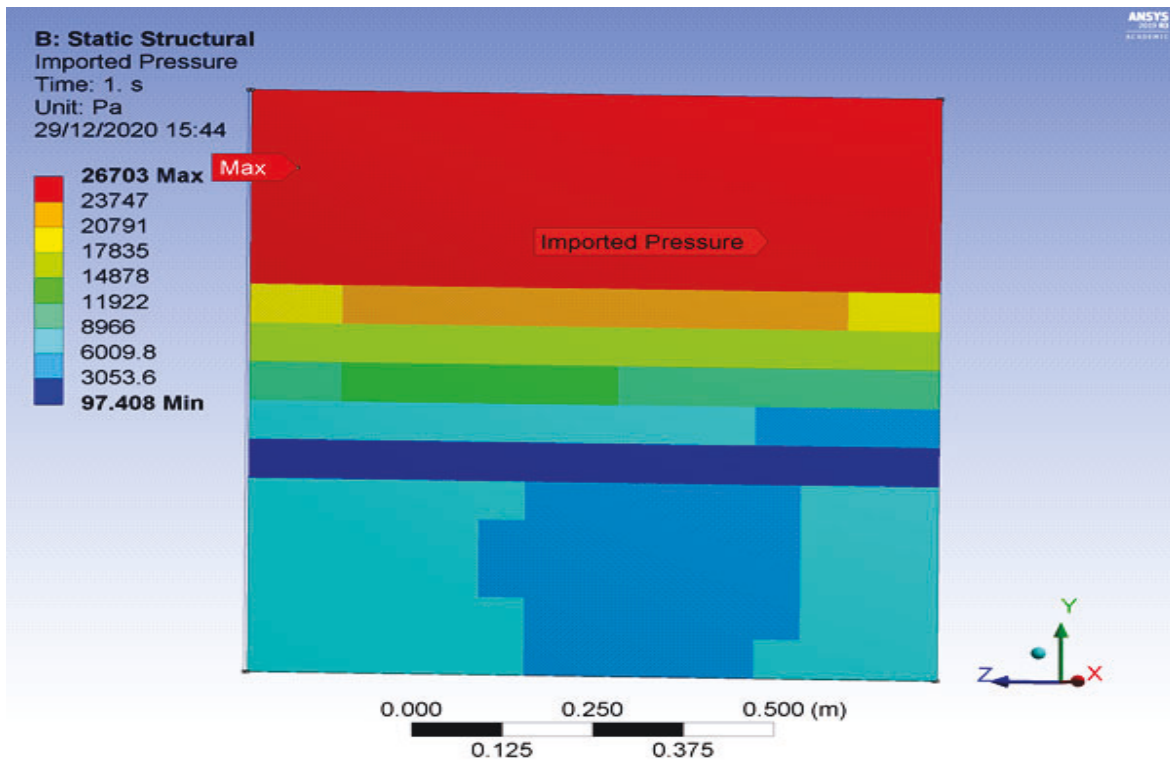


Figure AP3.2: Pressure exported from the DEM model to the FEM model for maximum pressure for the No wind effects reading as 26703 (Pa)

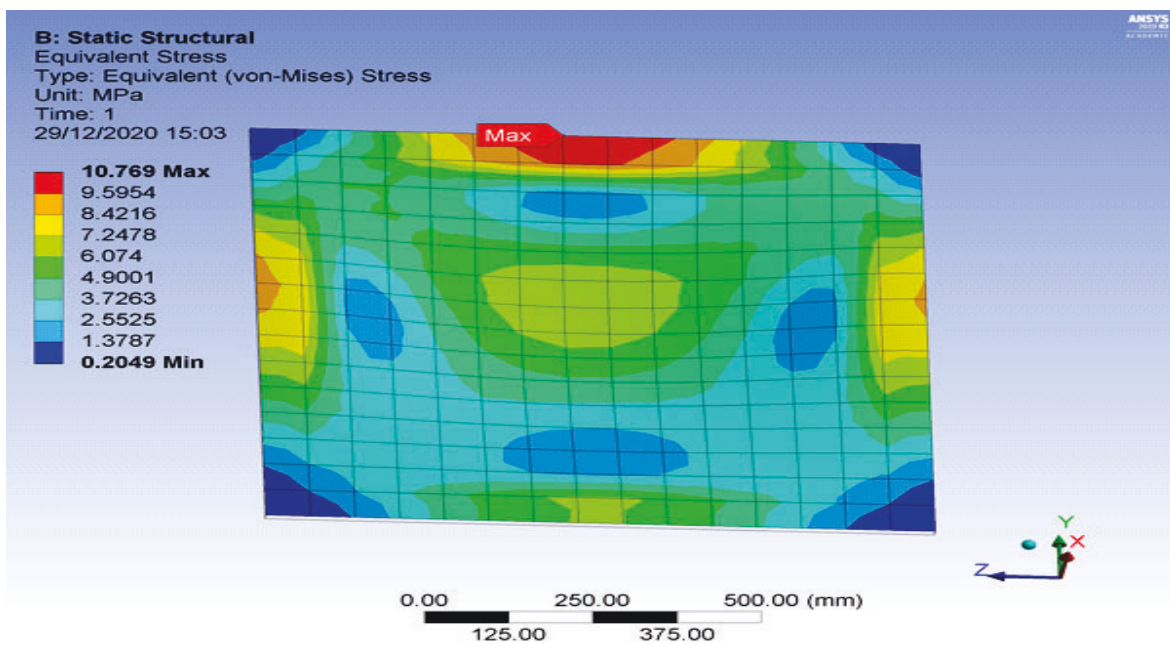


Figure AP3.3: Maximum Stress for wind effects reading as 10.769 (MPa)

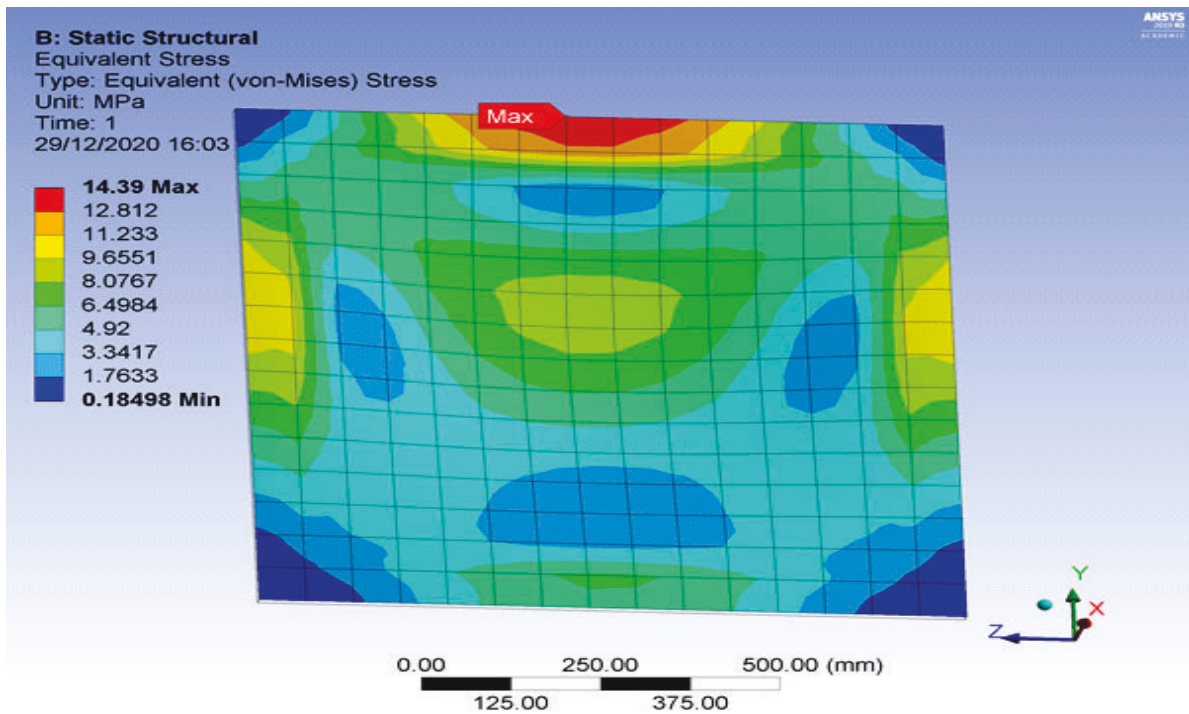


Figure AP3.4: Maximum Stress for No wind effects reading as 14.39

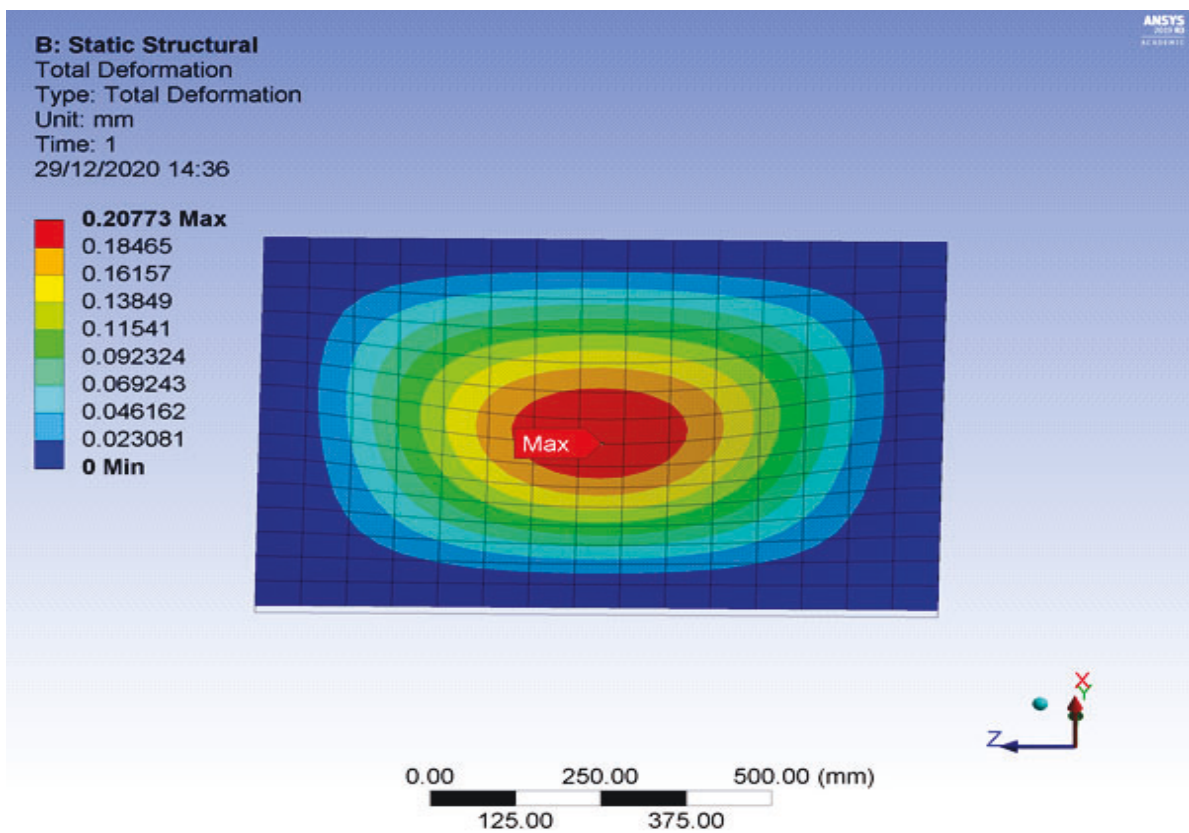


Figure AP3.5: Maximum deformation for wind effects reading as 0.208 (mm)

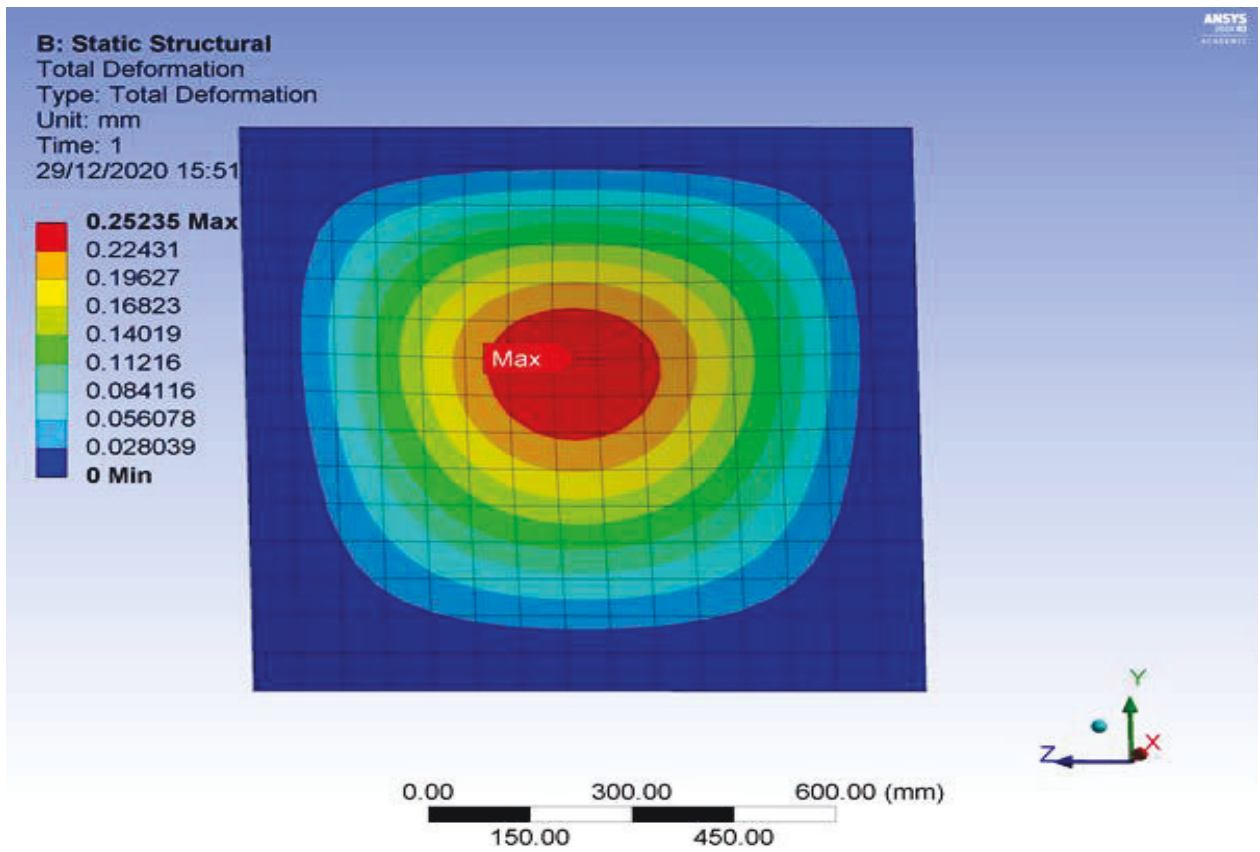


Figure AP3.6: Maximum deformation for No wind effects reading as 0.253(mm)

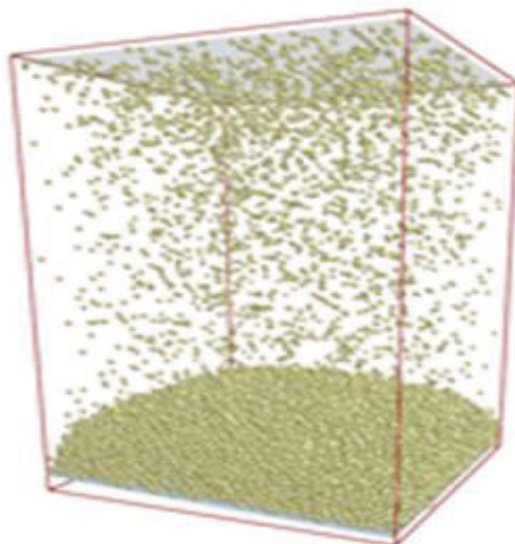


Figure AP3.7: Model showing DEM simulation of volcanic ash on the concrete roof plate

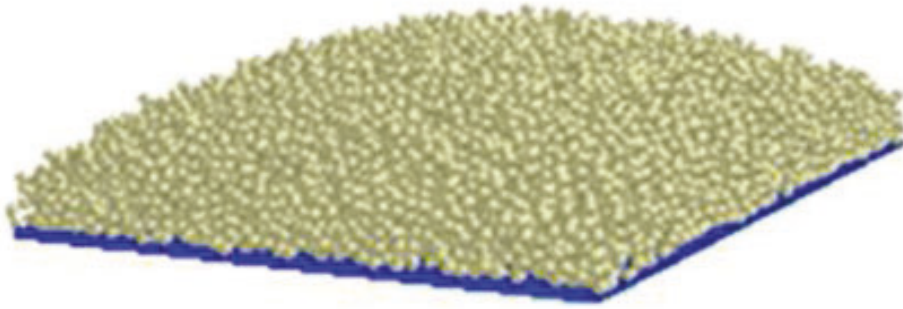


Figure AP3.8: Model without wind effect volcanic ash deposition

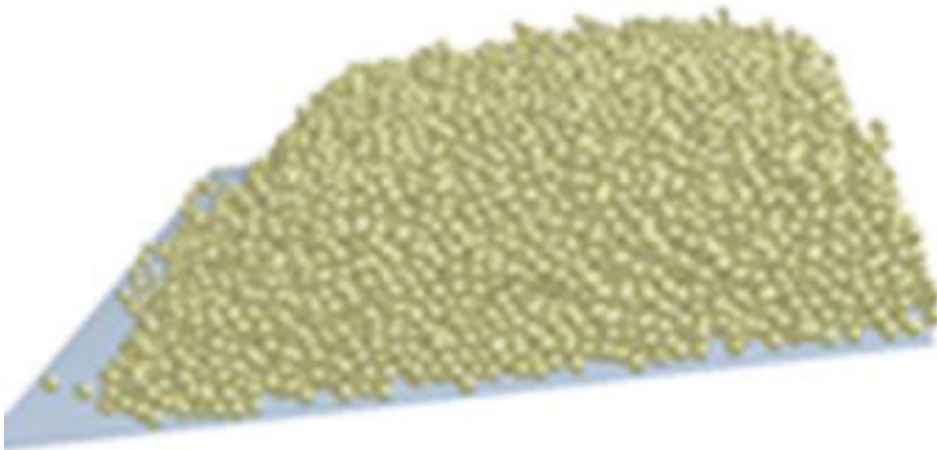


Figure AP3.9: Model with 1 ms^{-1} wind effects volcanic ash deposition.

Time: 0.990014 s
EDEM™
Academic

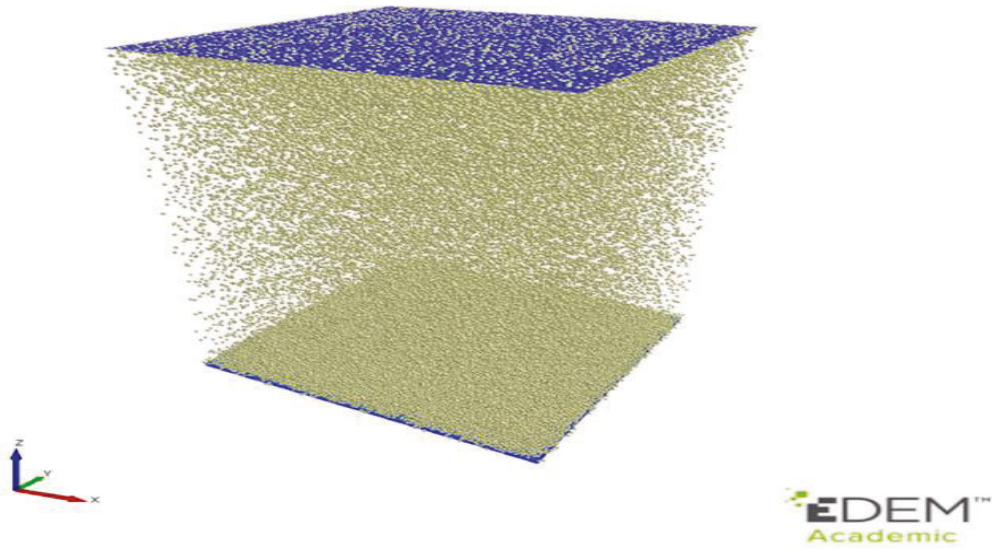


Figure AP3.10: Volcanic Ash Particles Generated from the EDEM

Time: 0.990014 s
EDEM™
Academic

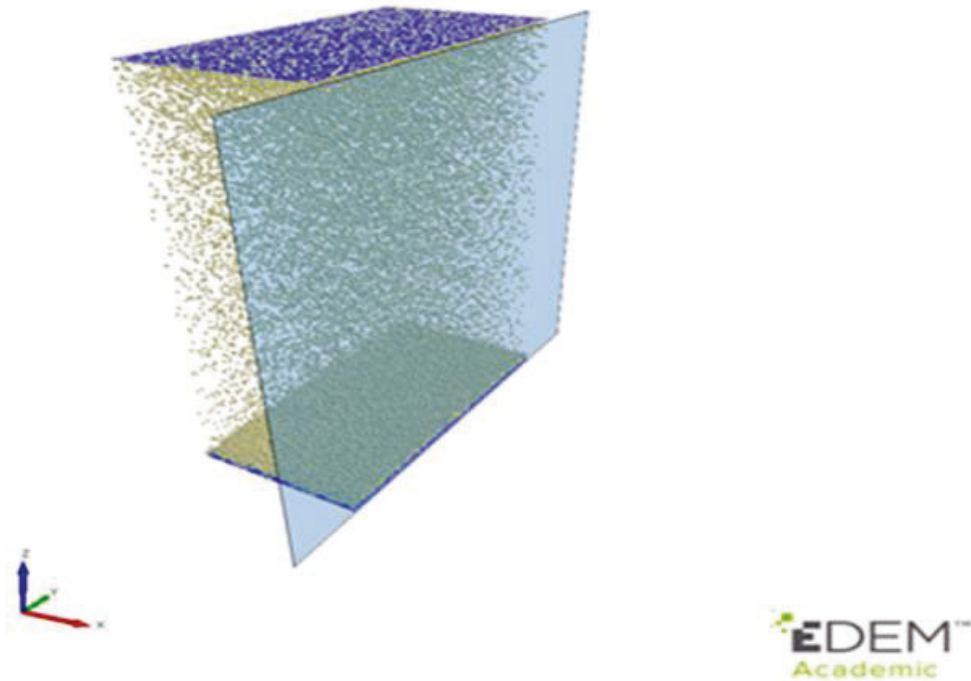


Figure AP3.11: Sliced Section of the Volcanic Ash Particles' Internal Structure Falling and Settling on the Concrete Roof.

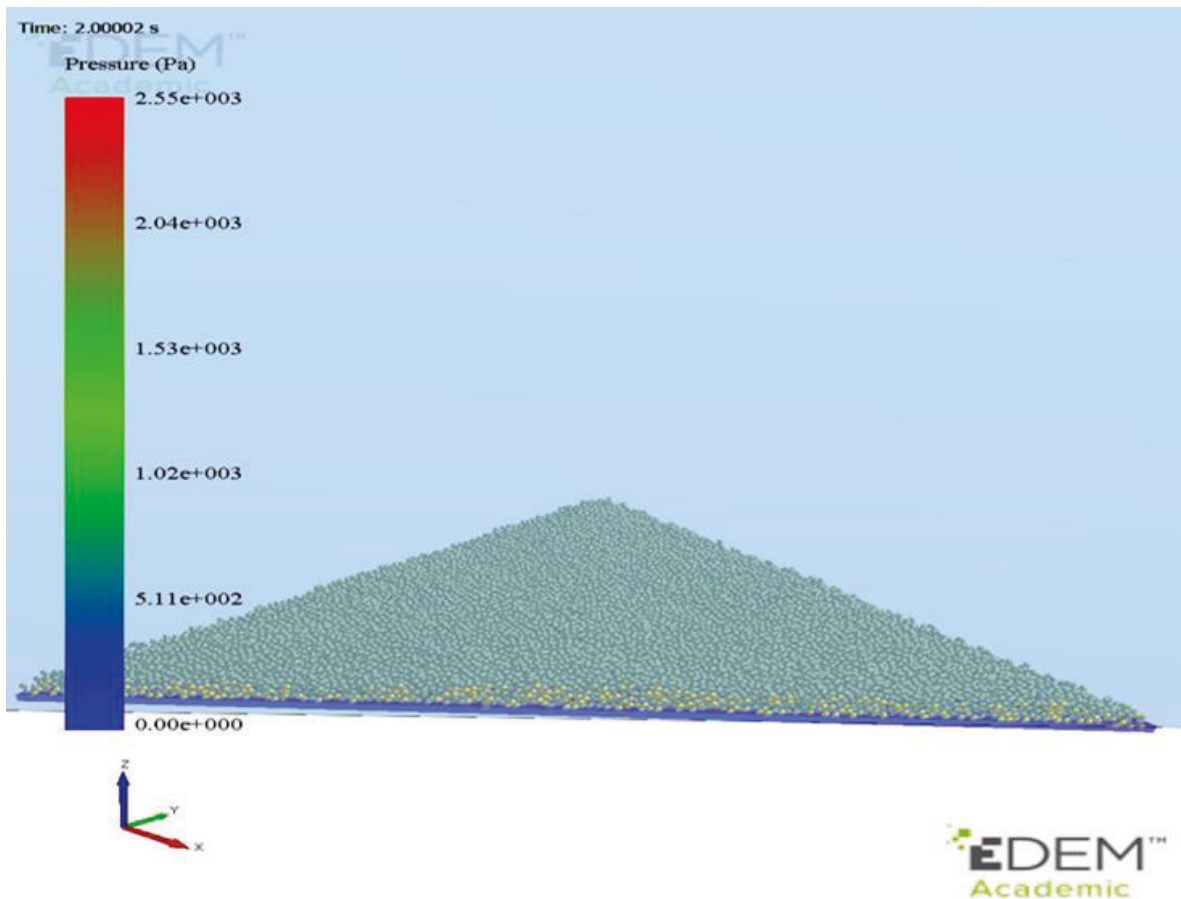


Figure AP3.12: Volcanic Ash Particles Deposition on the Concrete Roof Plate with the Pressure Load

Results for the Finite Element Method (FEM) modelling tool.

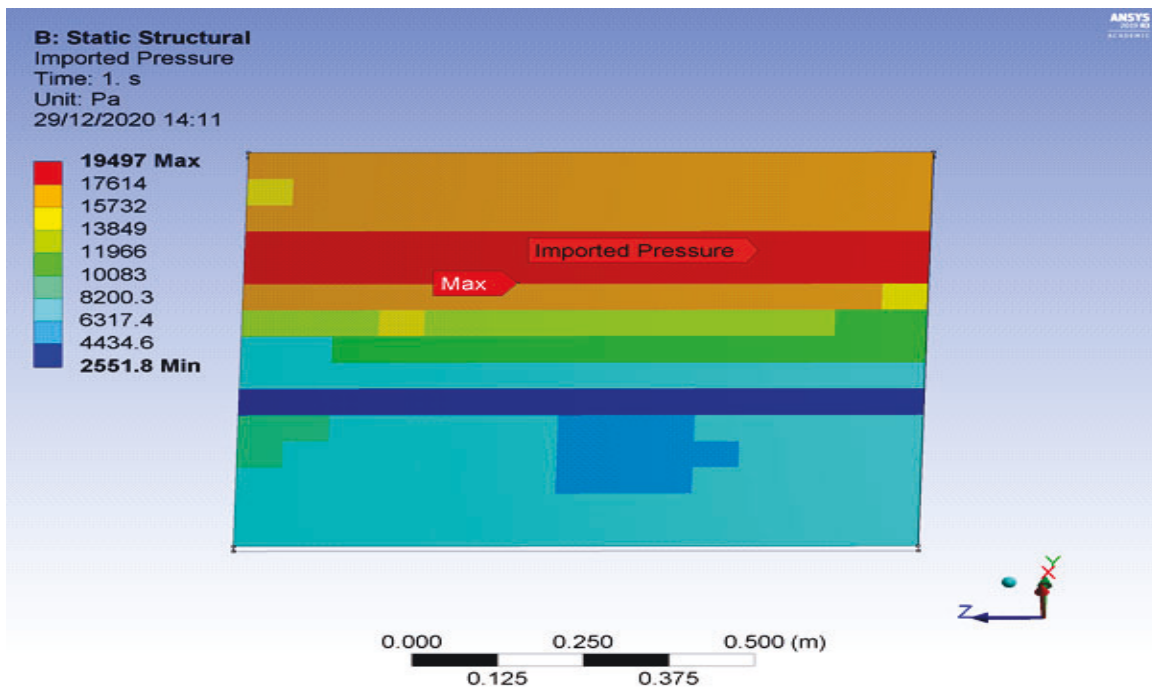


Figure AP3.13: Pressure exported from the DEM model to the FEM model for the wind effects reading for the maximum pressure as 19497.2 (Pa)

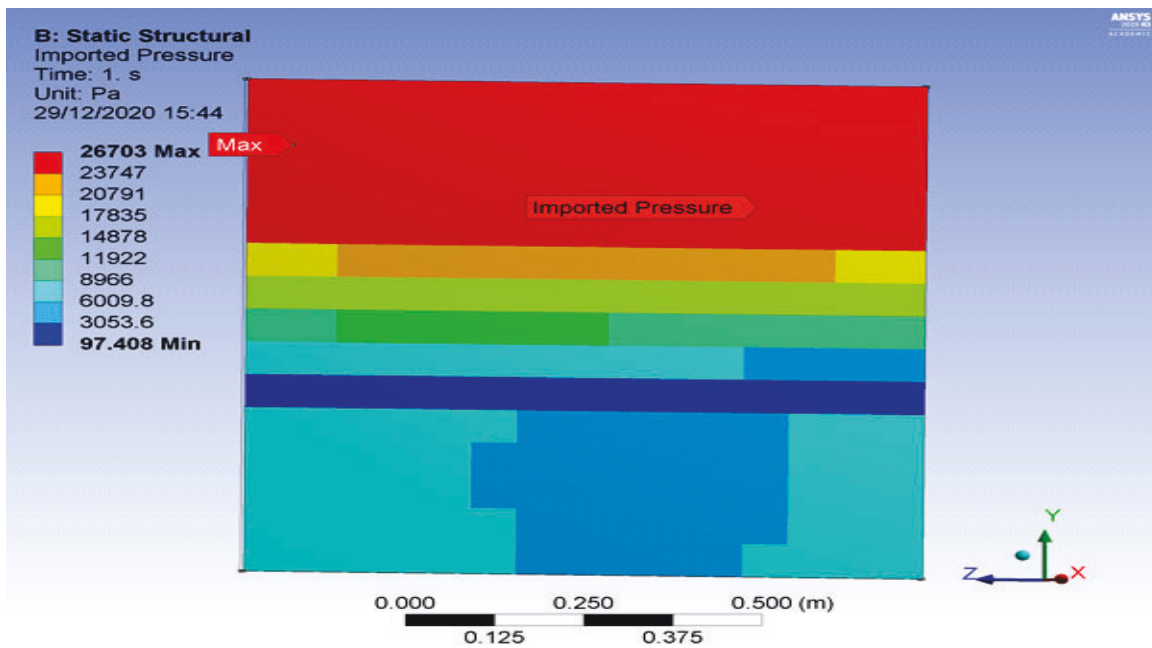


Figure AP3.14: Pressure exported from the DEM model to the FEM model for maximum pressure for the No wind effects reading as 26703 (Pa)

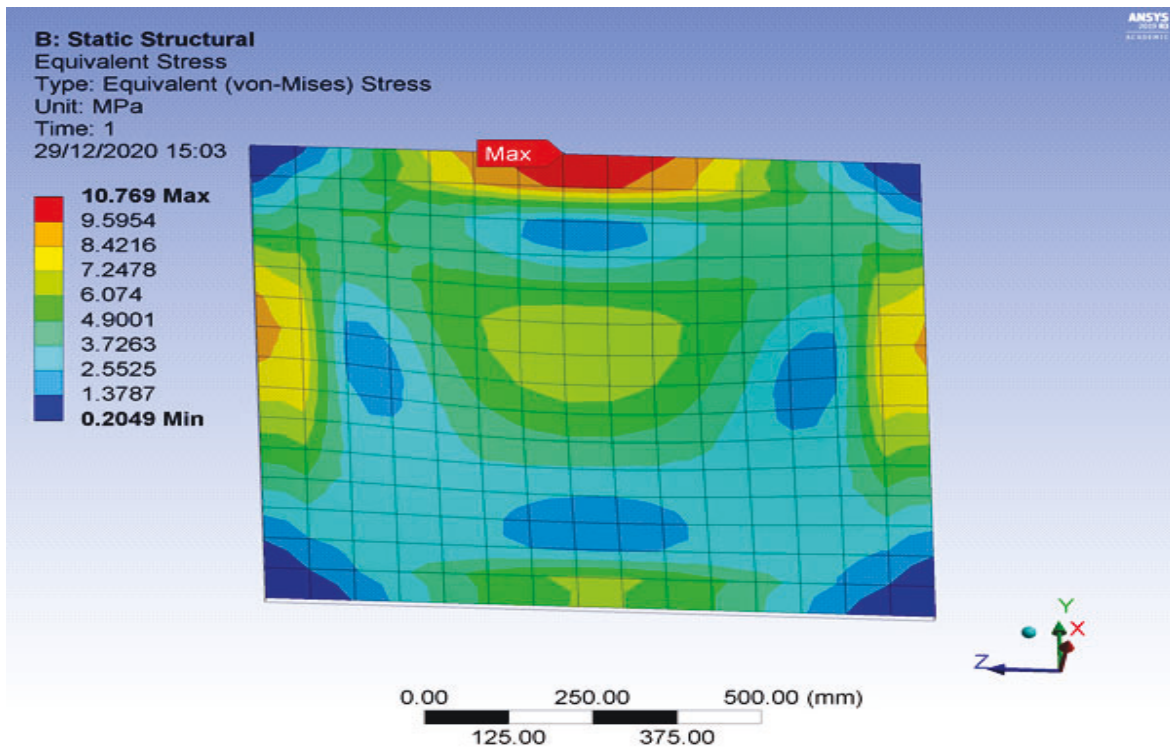


Figure AP3.15: Maximum Stress for wind effects reading as 10.769 (MPa)

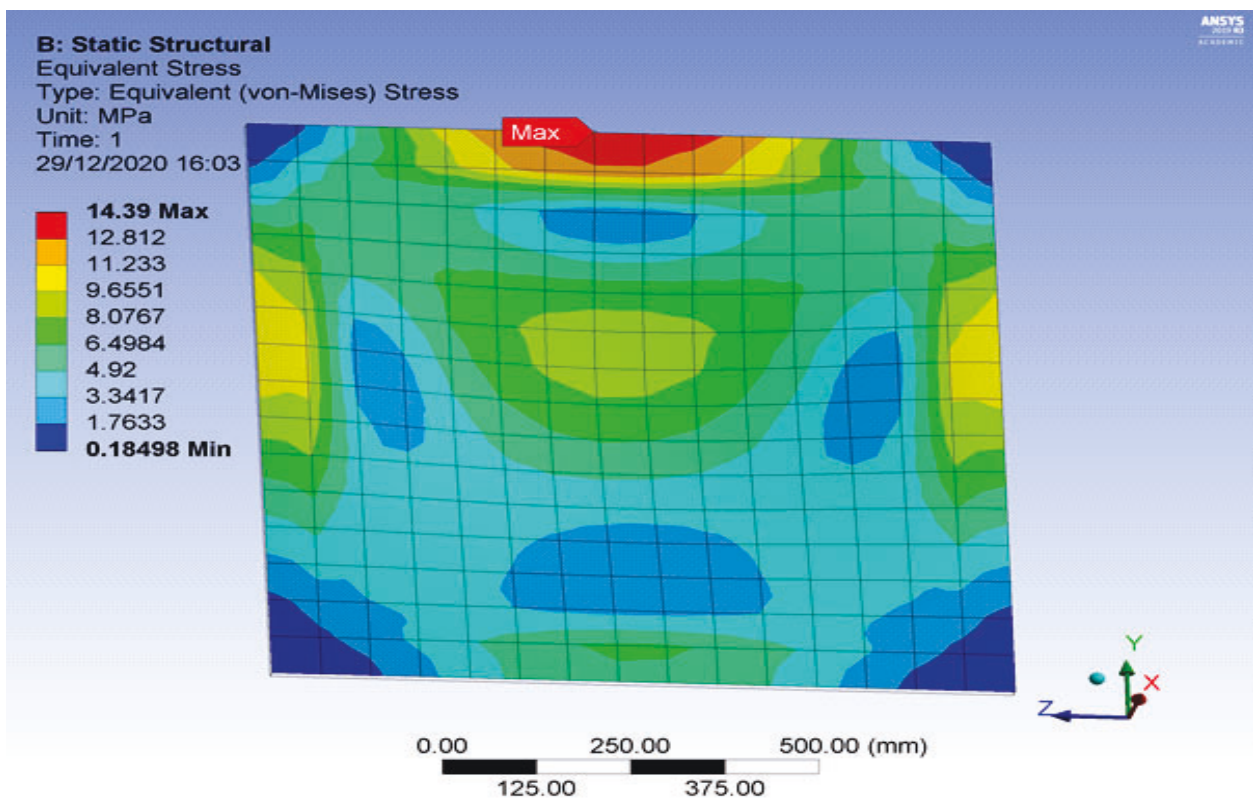


Figure AP3.16: Maximum Stress for No wind effects reading as 14.39

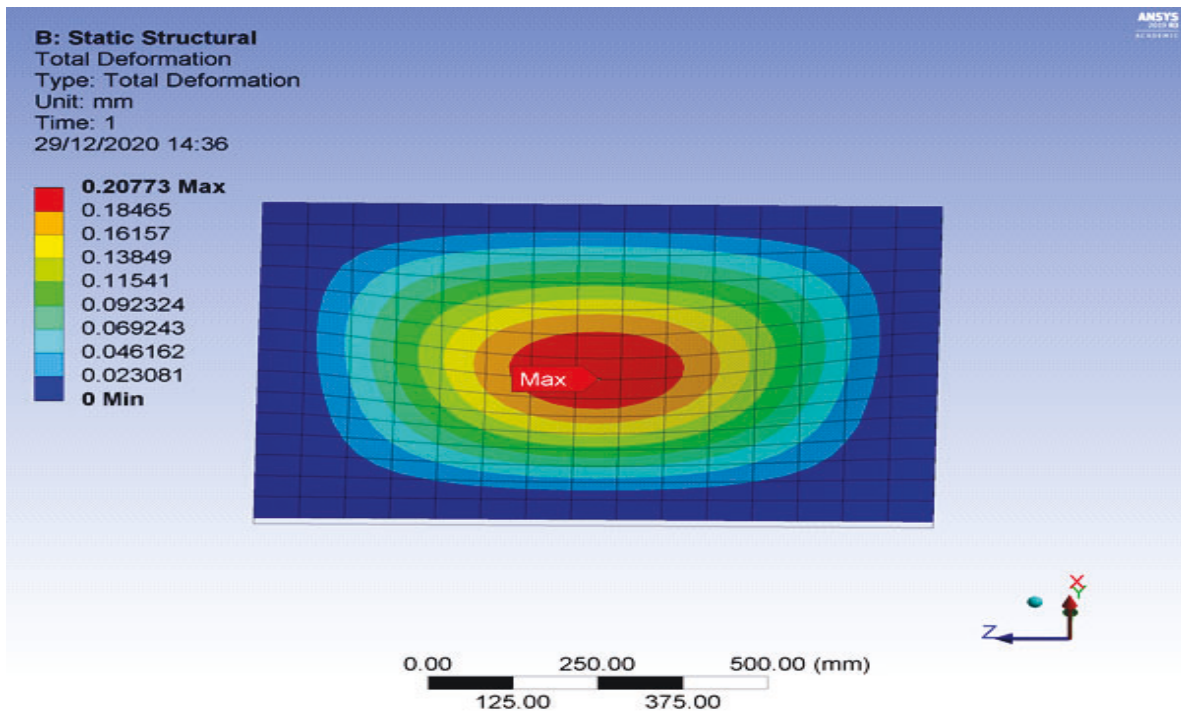


Figure AP3.17: Maximum deformation for wind effects reading as 0.208 (mm)

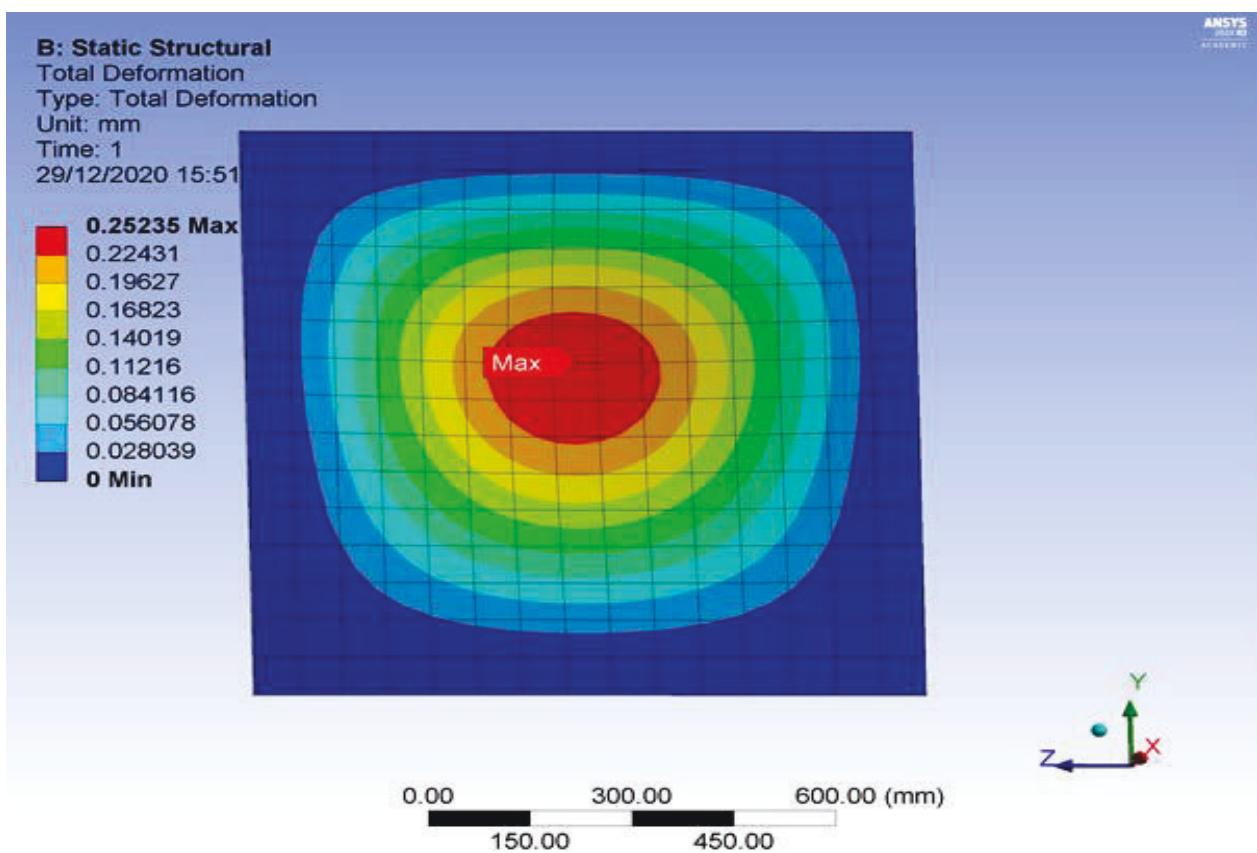


Figure AP3.17: Maximum deformation for No wind effects reading as 0.253(mm)

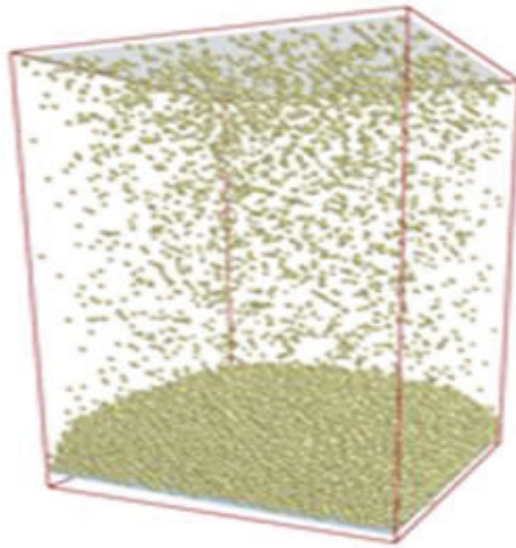


Figure AP3.19: Model showing DEM simulation of volcanic ash on the concrete roof plate

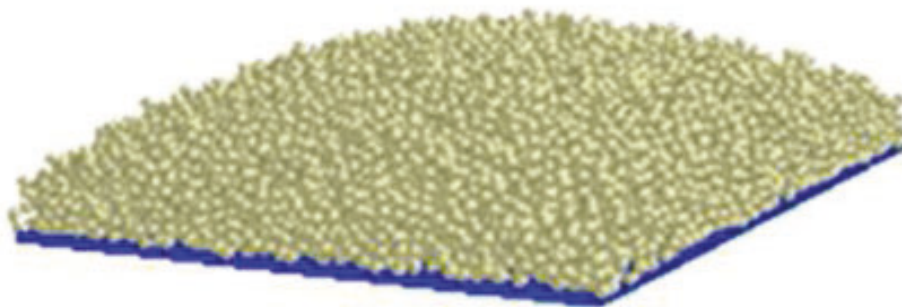


Figure AP3.20: Model without wind effect volcanic ash deposition

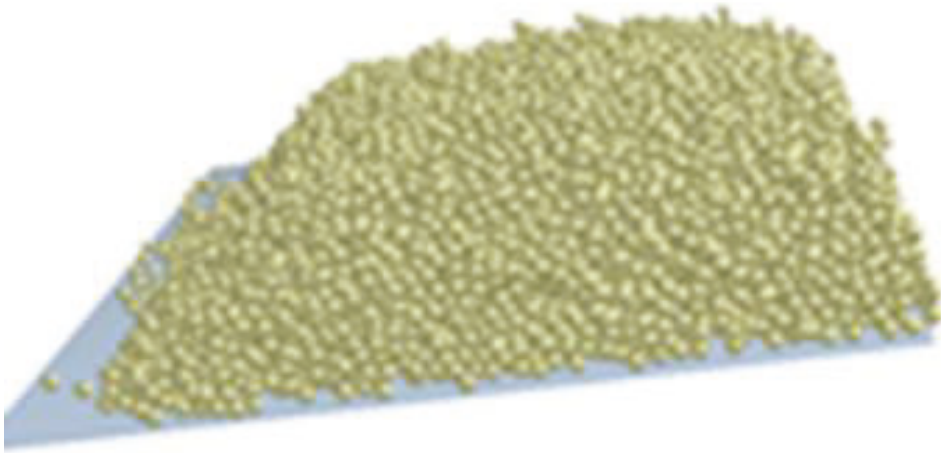


Figure AP3.21: Model with 1 ms^{-1} wind effects volcanic ash deposition.

Time: 0.990014 s
EDEM™
Academic

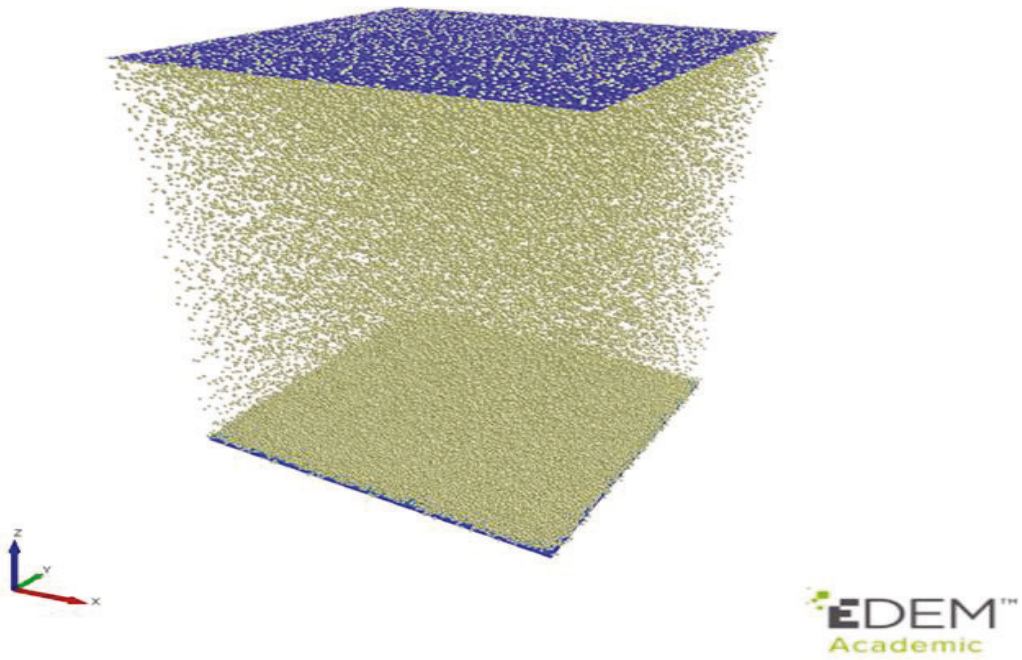


Figure AP3.22: Volcanic Ash Particles Generated from the EDEM

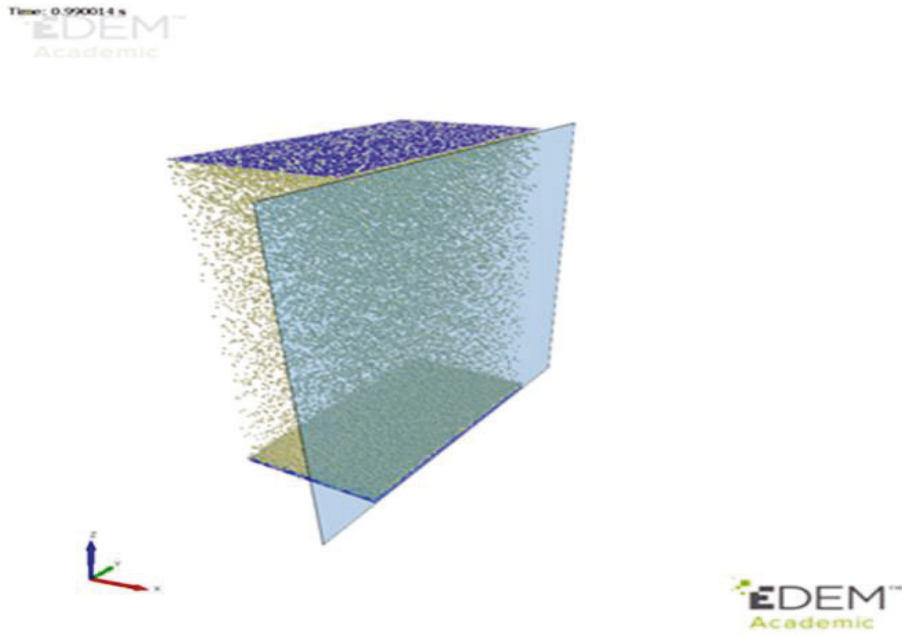


Figure AP3.23: Sliced Section of the Volcanic Ash Particles' Internal Structure Falling and Settling on the Concrete Roof.

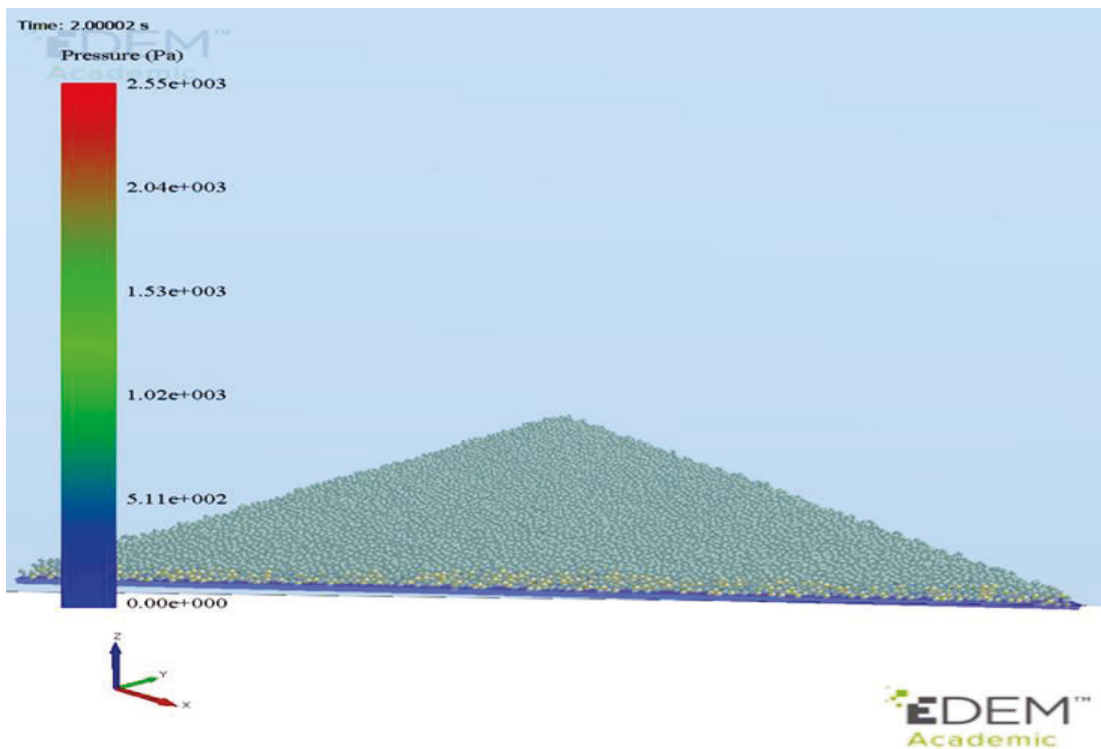


Figure AP3.24: Volcanic Ash Particles Deposition on the Concrete Roof Plate with the Pressure Load

Results for the Finite Element Method (FEM) modelling tool.

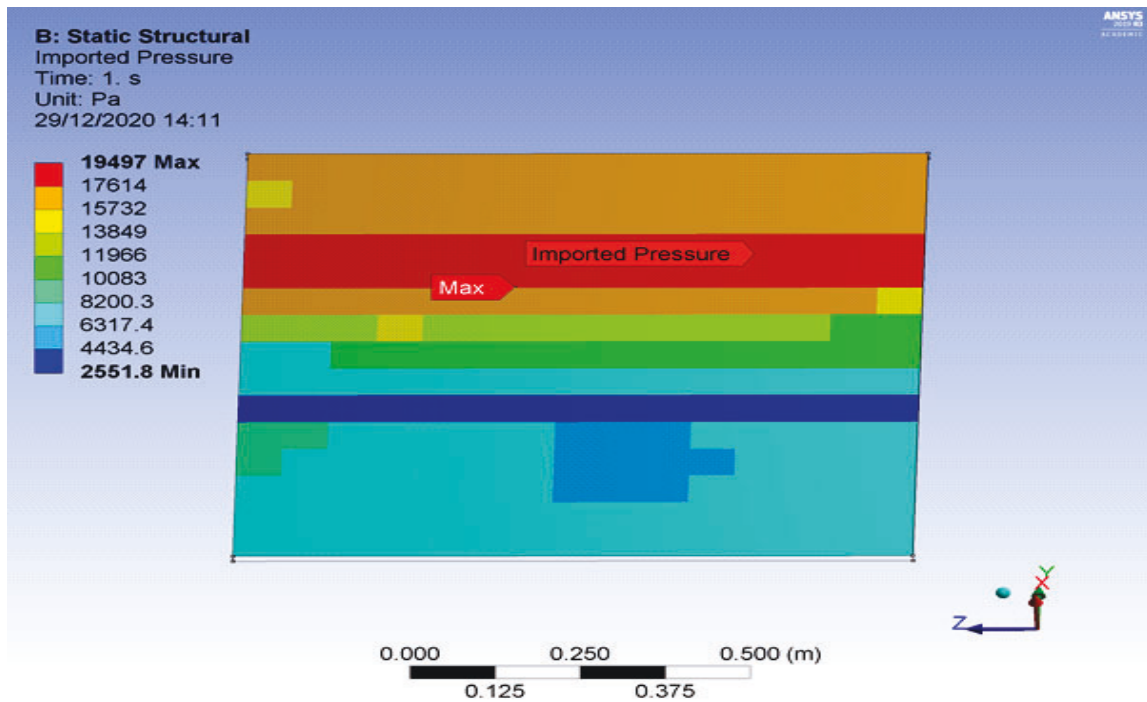


Figure AP3.25: Pressure exported from the DEM model to the FEM model for the wind effects reading for the maximum pressure as 19497.2 (Pa)

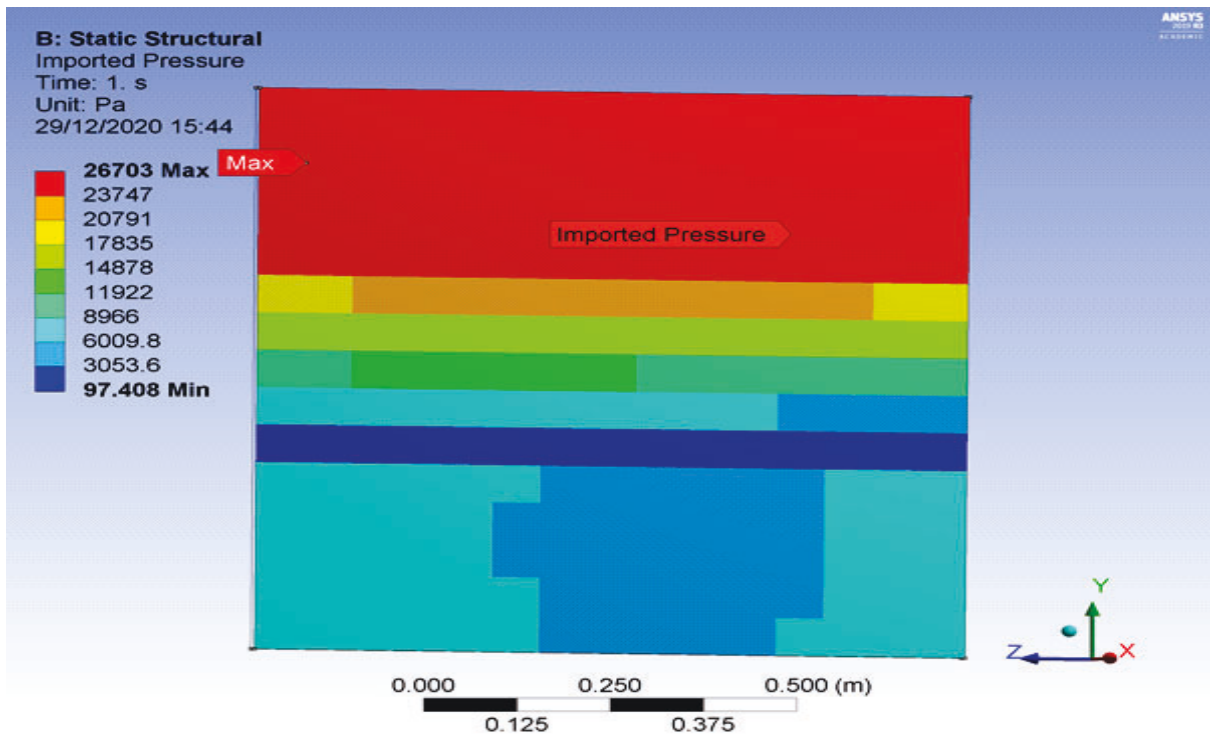


Figure AP3.26: Pressure exported from the DEM model to the FEM model for maximum pressure for the No wind effects reading as 26703 (Pa)

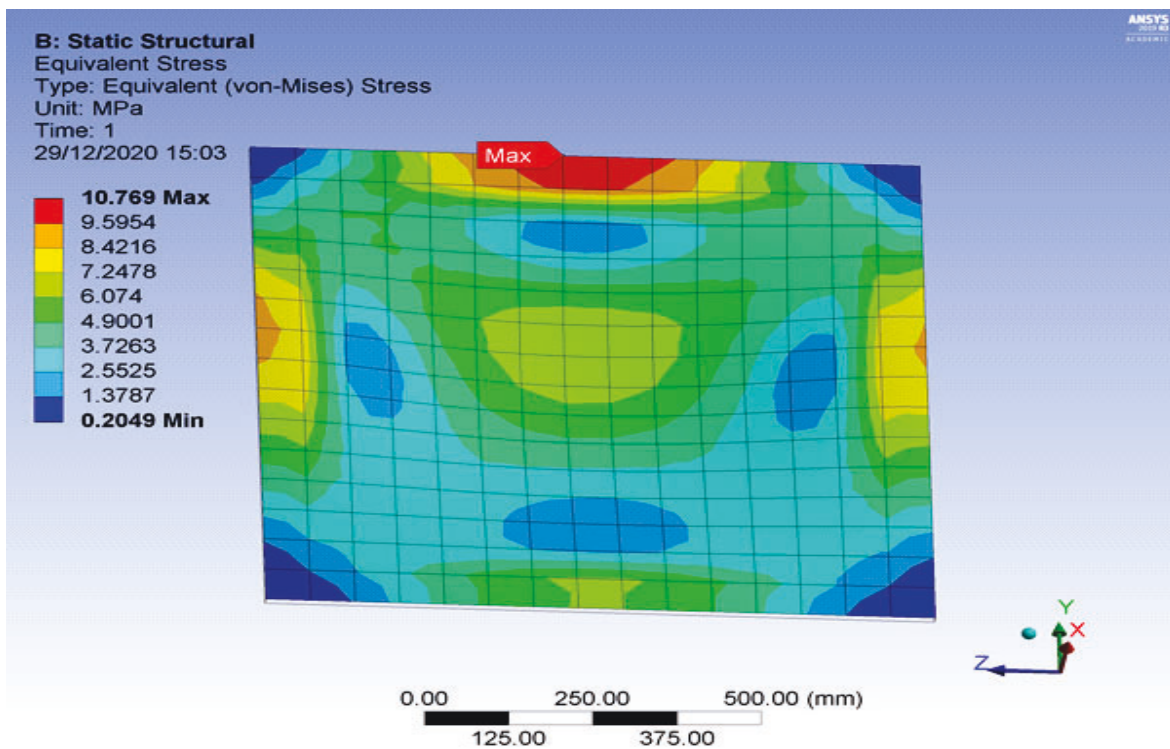


Figure AP3.27: Maximum Stress for wind effects reading as 10.769 (MPa)

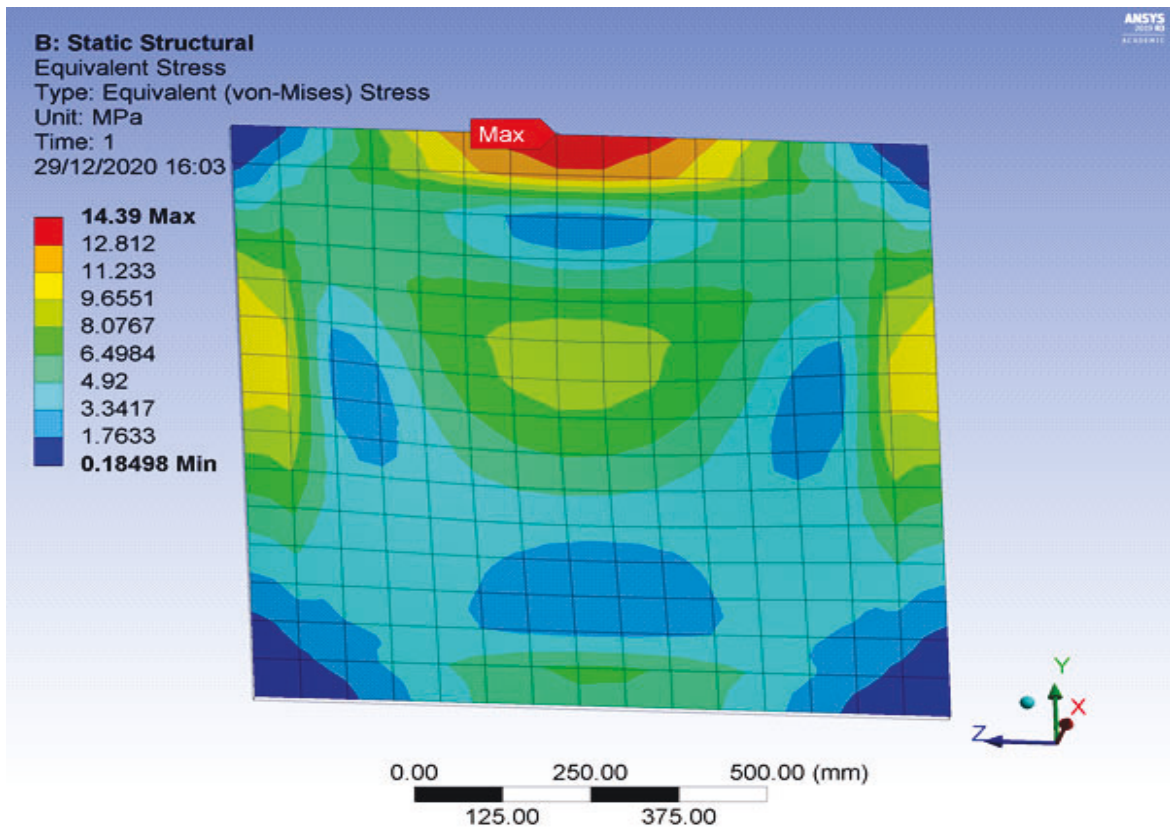


Figure AP3.28: Maximum Stress for No wind effects reading as 14.39

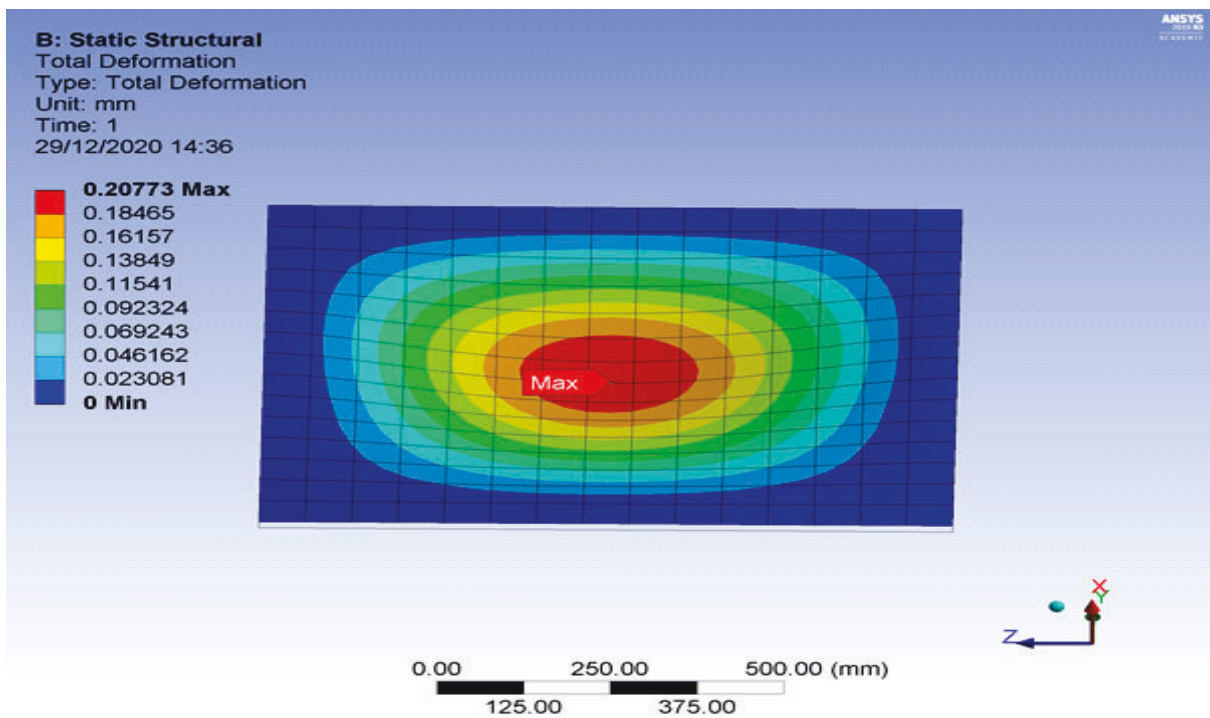


Figure AP3.29: Maximum deformation for wind effects reading as 0.208 (mm)

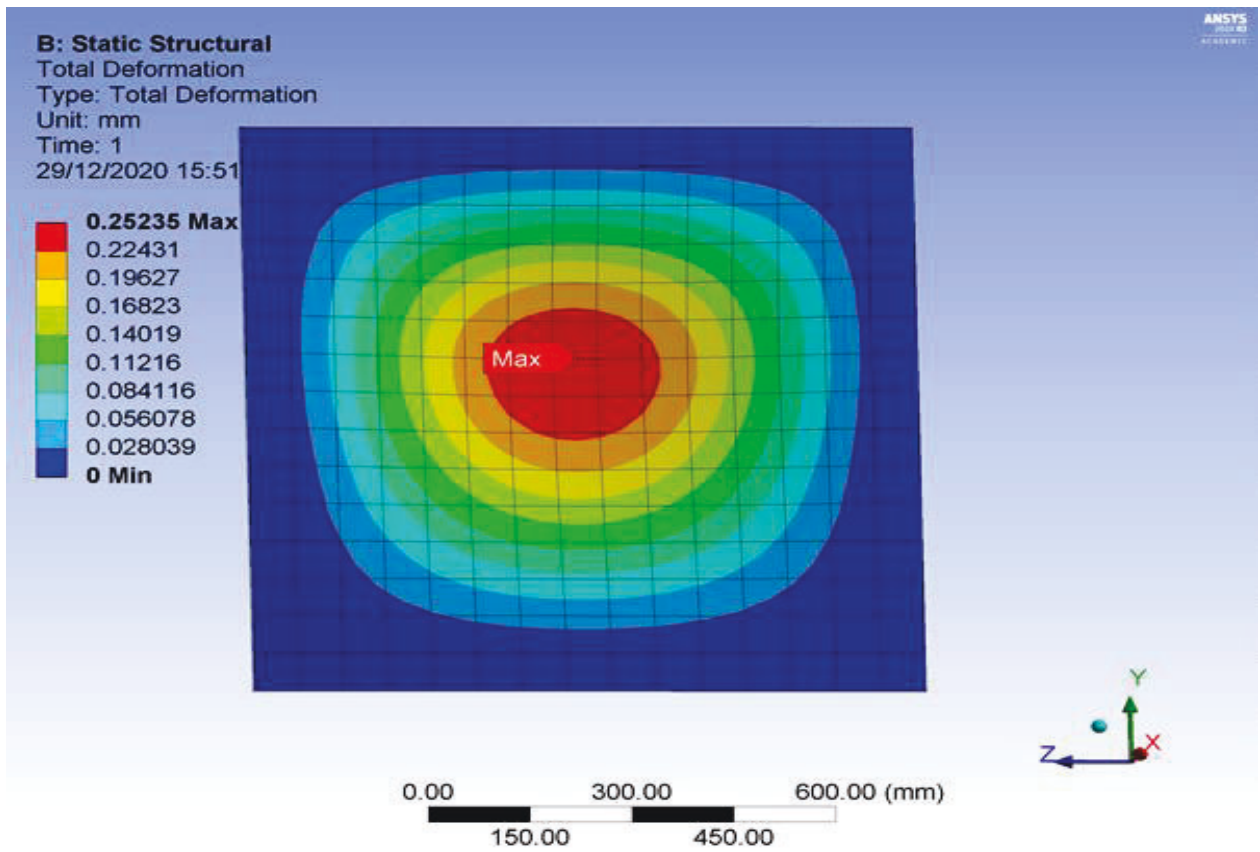


Figure AP3.30: Maximum deformation for No wind effects reading as 0.253(mm)

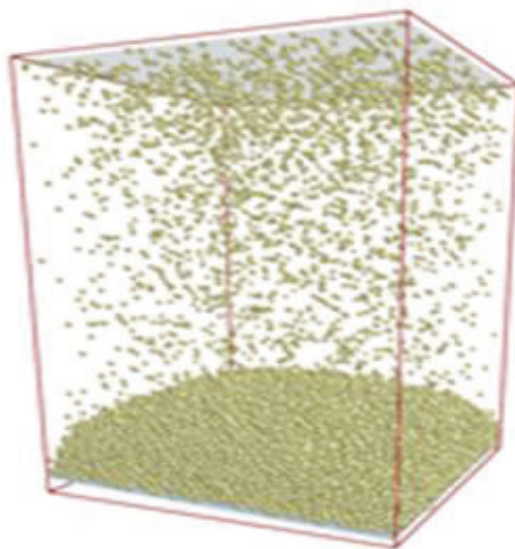


Figure AP3.31: Model showing DEM simulation of volcanic ash on the concrete roof plate

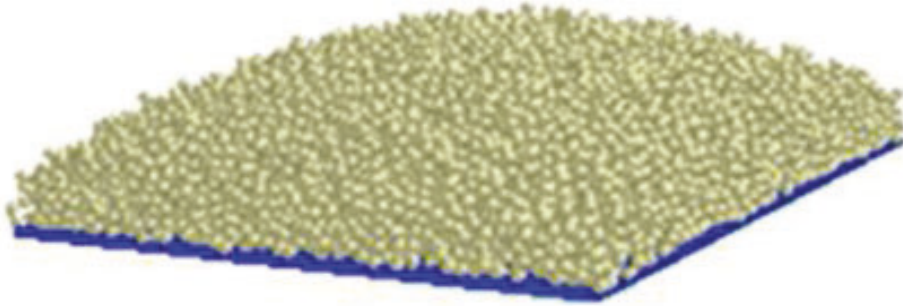


Figure AP3.32: Model without wind effect volcanic ash deposition

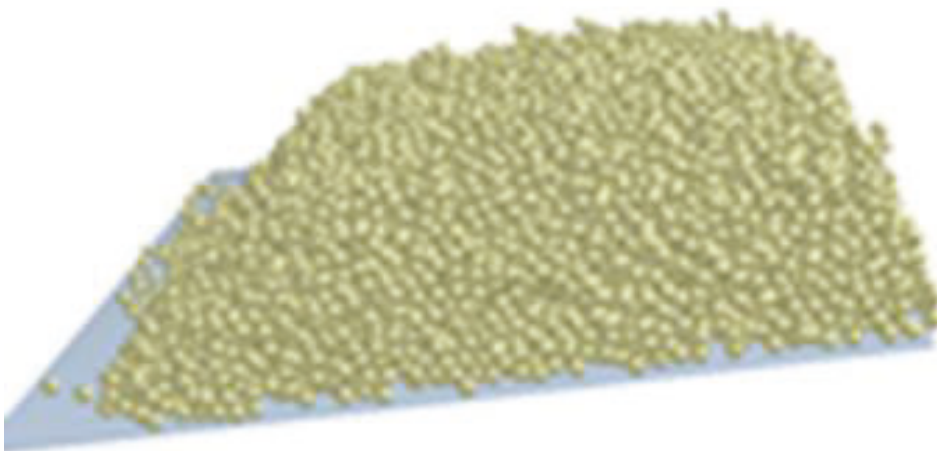


Figure AP3.33: Model with 1 ms⁻¹ wind effects volcanic ash deposition.

Time: 0.990014 s
EDEM™
Academic

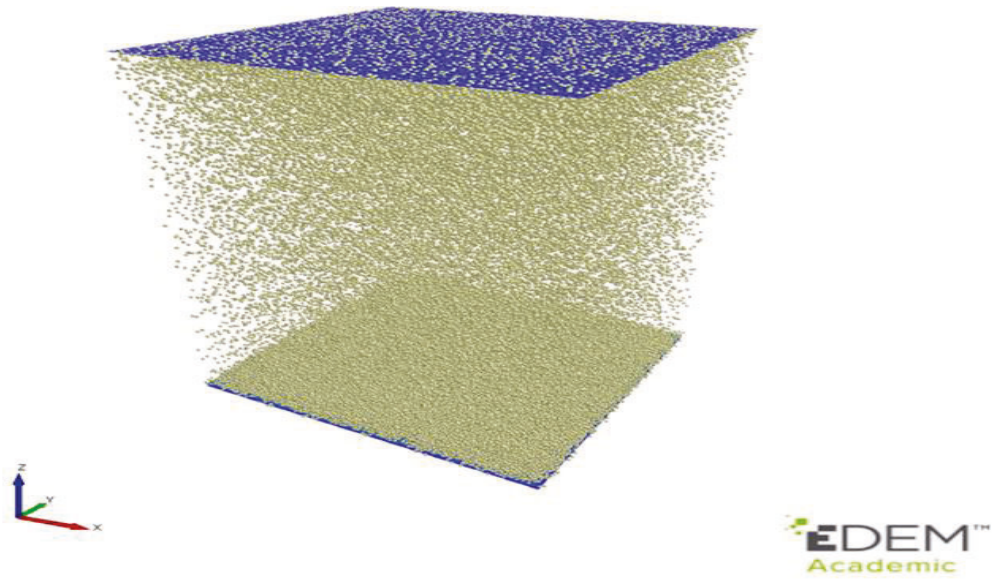


Figure AP3.34: Volcanic Ash Particles Generated from the EDEM

Time: 0.990014 s
EDEM™
Academic

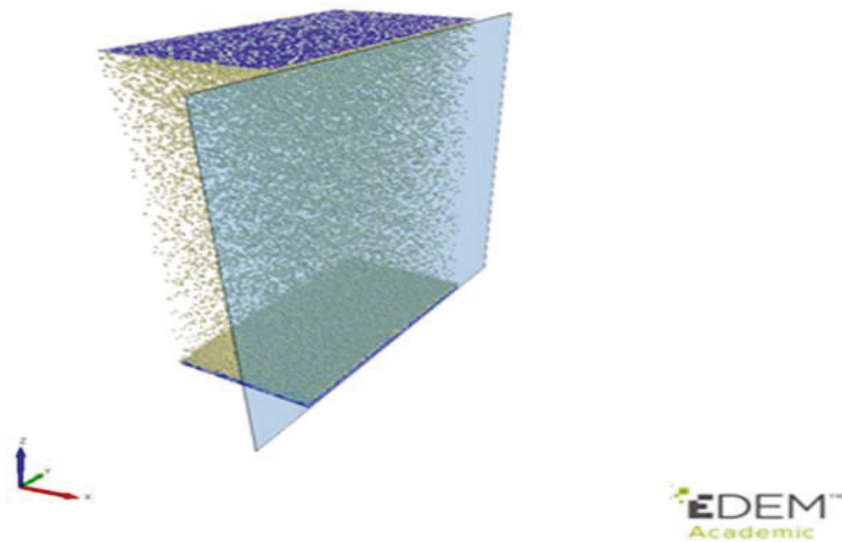


Figure AP3.35: Sliced Section of the Volcanic Ash Particles' Internal Structure Falling and Settling on the Concrete Roof.

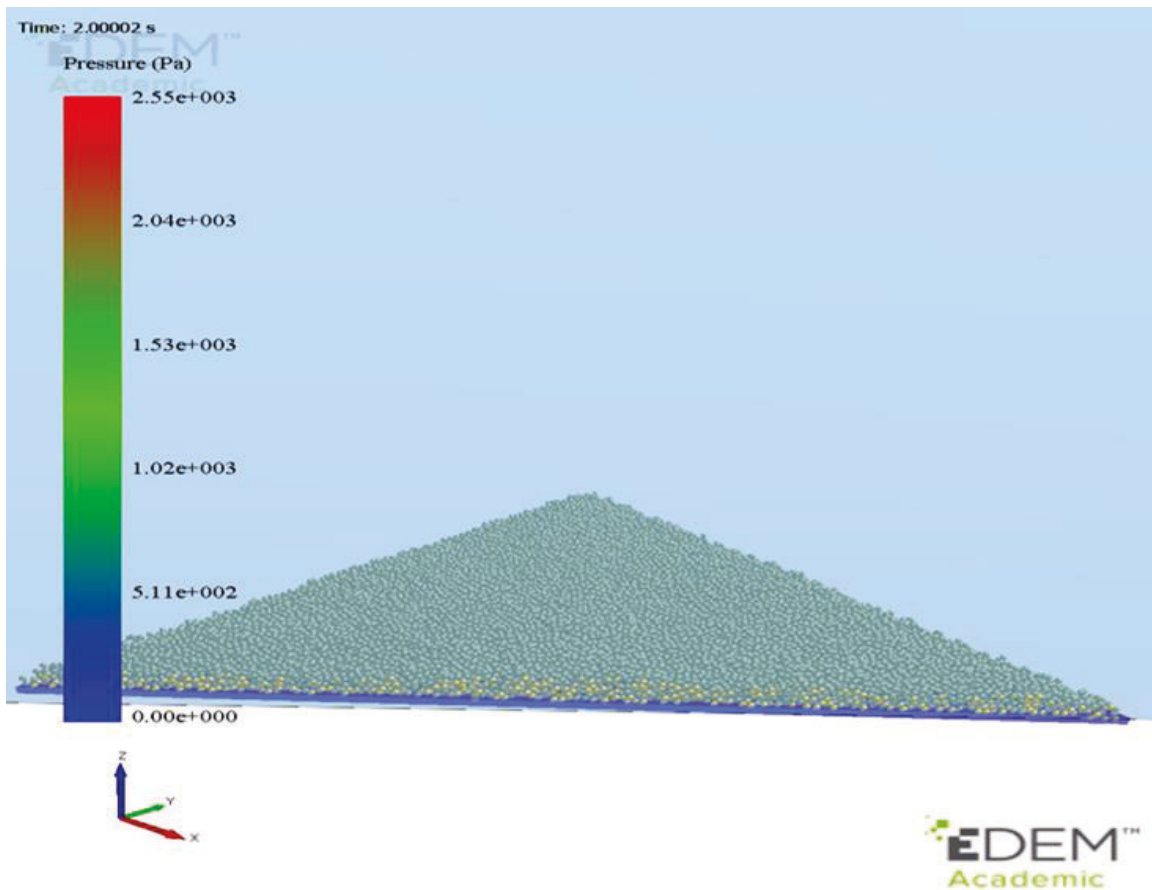


Figure AP3.36: Volcanic Ash Particles Deposition on the Concrete Roof Plate with the Pressure Load

Results for the Finite Element Method (FEM) modelling tool.

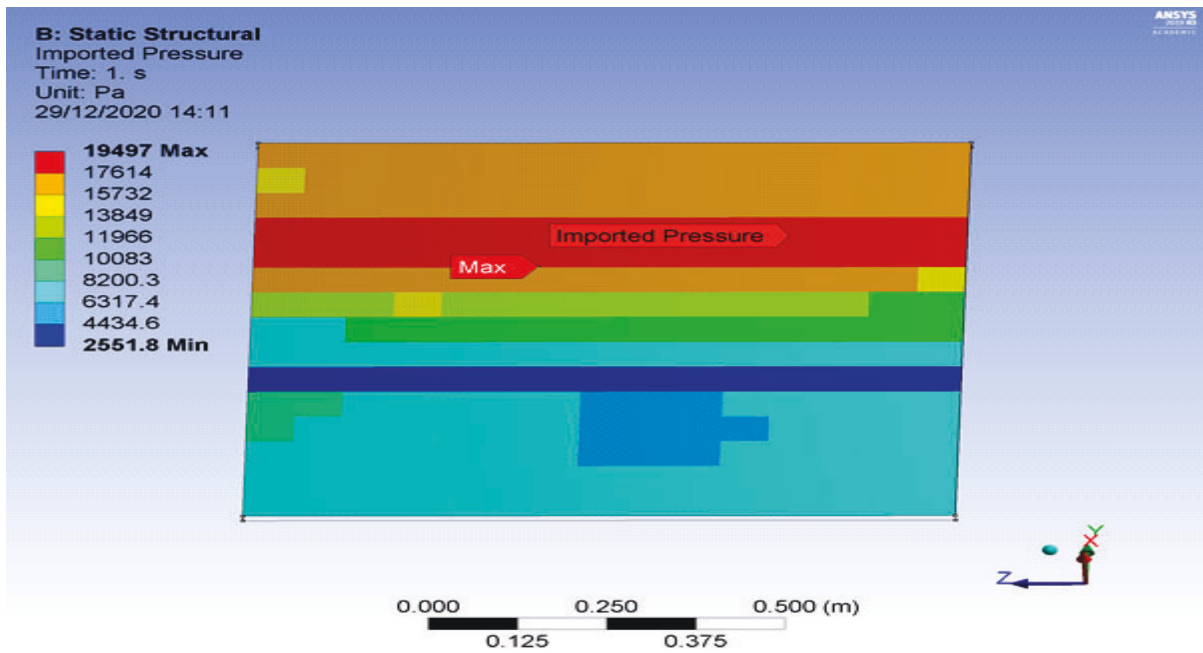


Figure AP3.37: Pressure exported from the DEM model to the FEM model for the wind effects reading for the maximum pressure as 19497.2 (Pa)

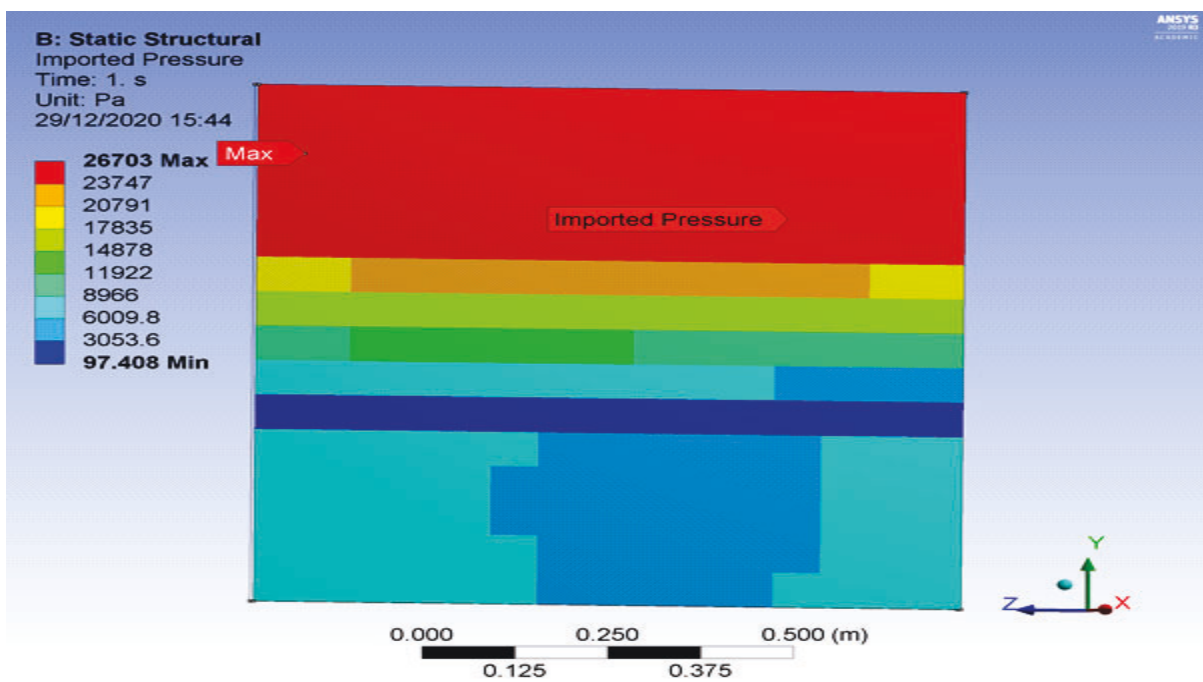


Figure AP3.38: Pressure exported from the DEM model to the FEM model for maximum pressure for the No wind effects reading as 26703 (Pa)

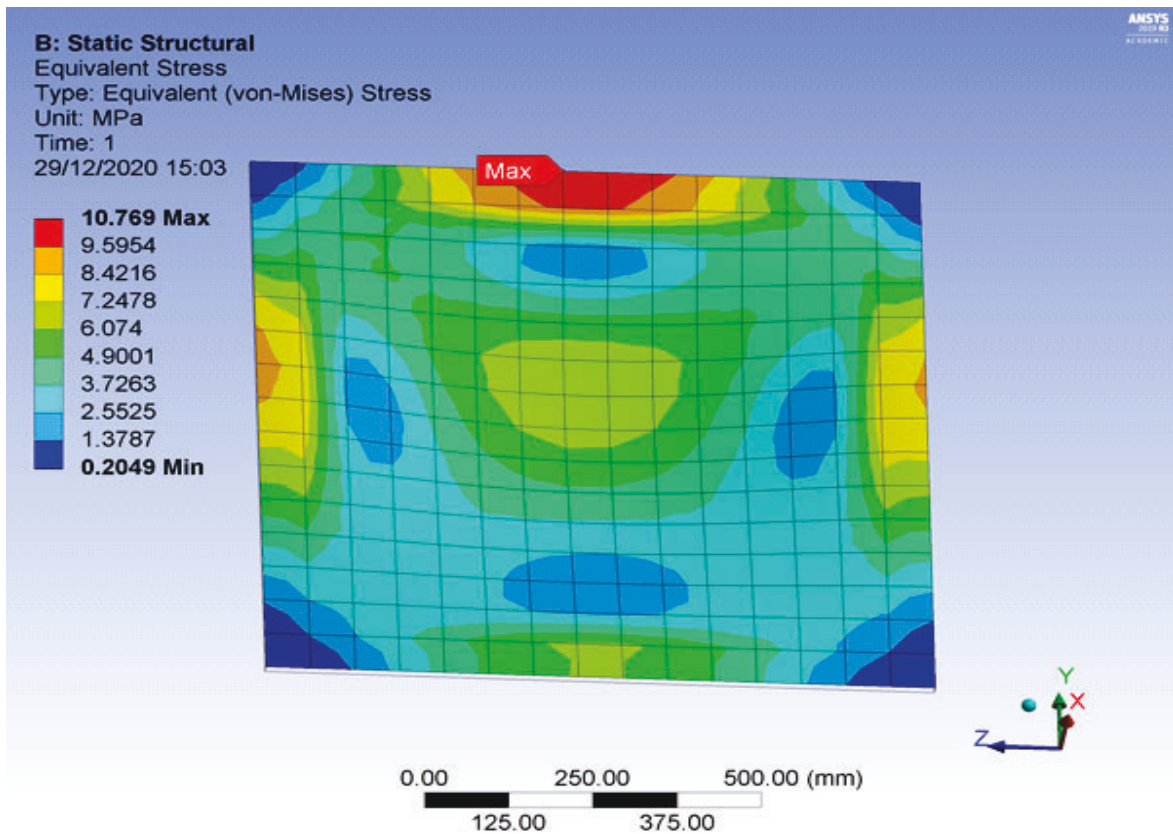


Figure AP3.39: Maximum Stress for wind effects reading as 10.769 (MPa)

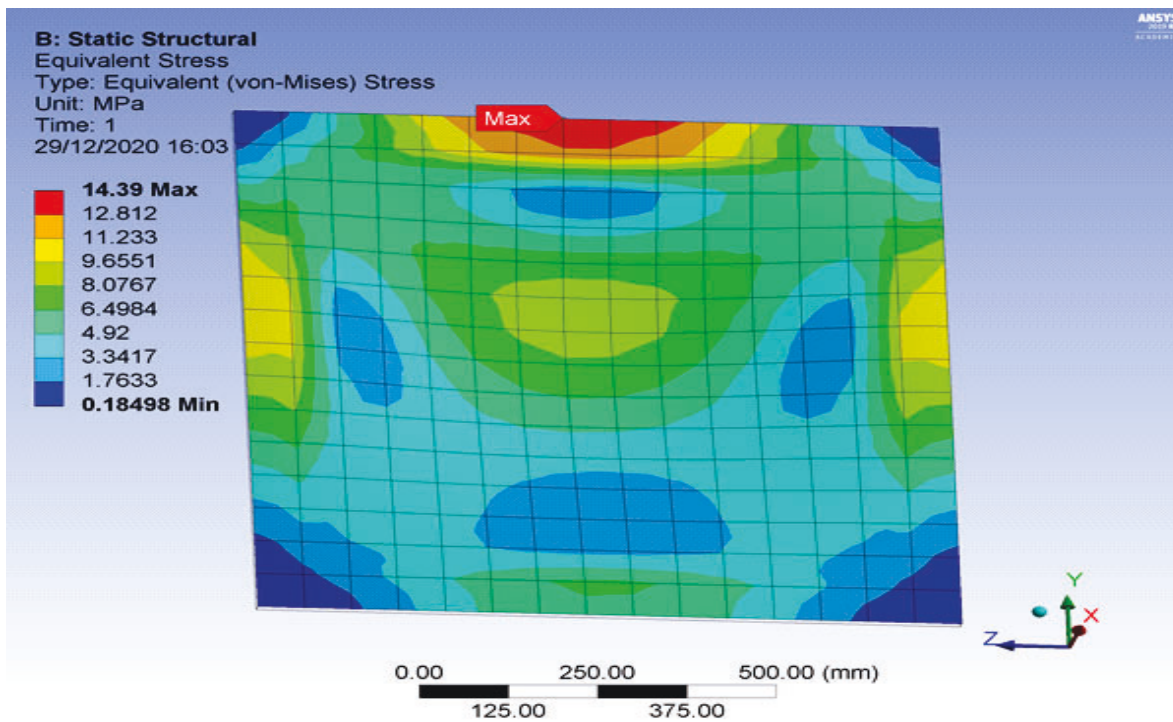


Figure AP3.40: Maximum Stress for No wind effects reading as 14.39

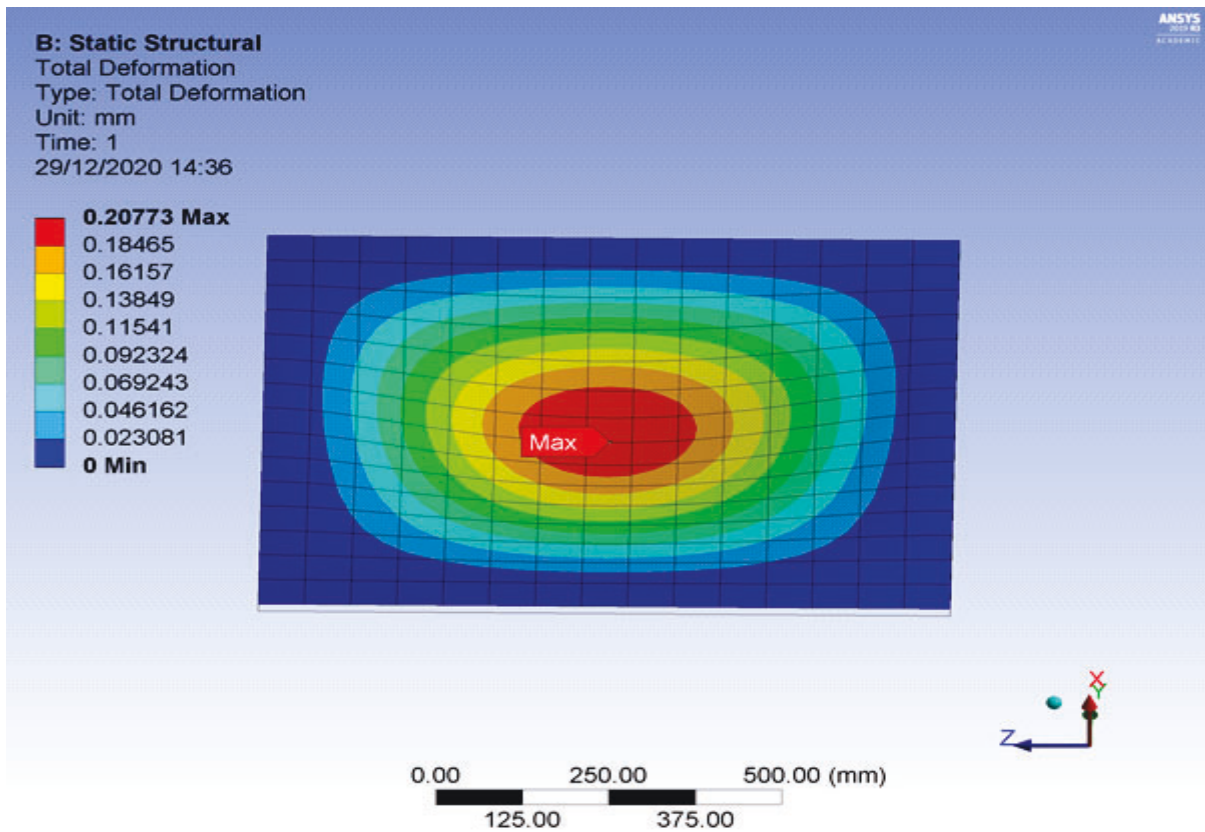


Figure AP3.41: Maximum deformation for wind effects reading as 0.208 (mm)

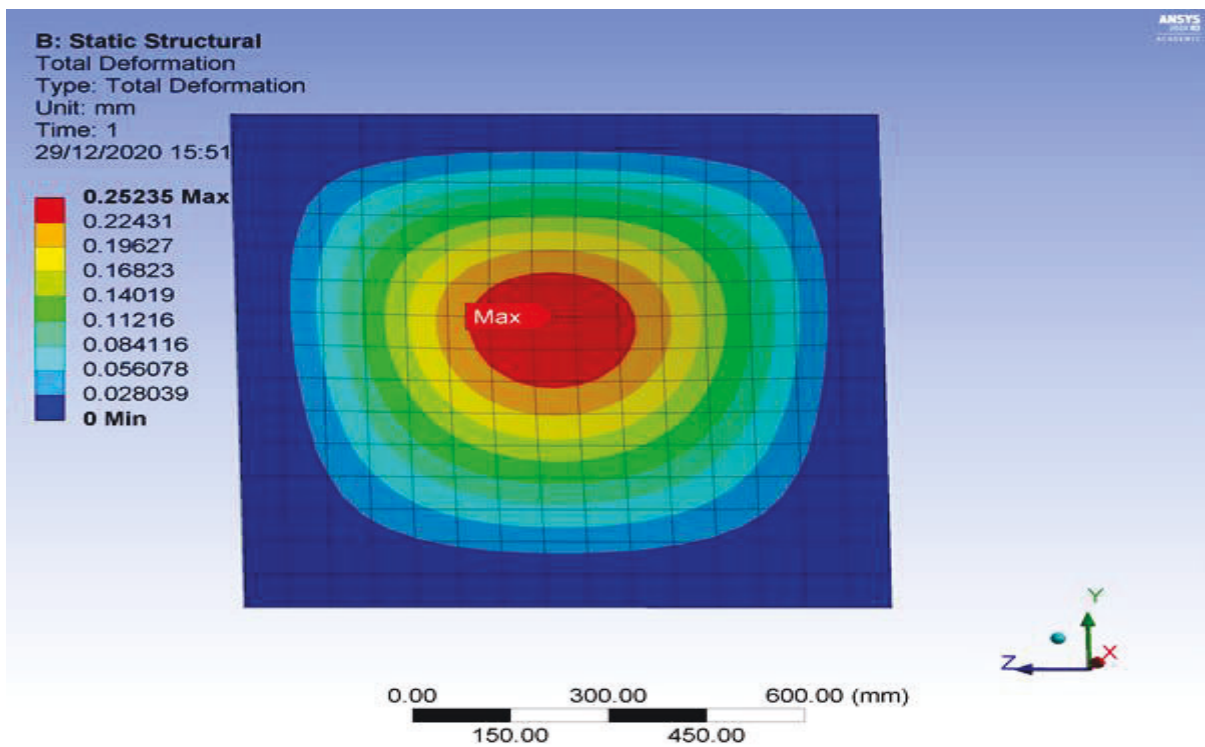


Figure AP3.41: Maximum deformation for No wind effects reading as 0.253(mm)

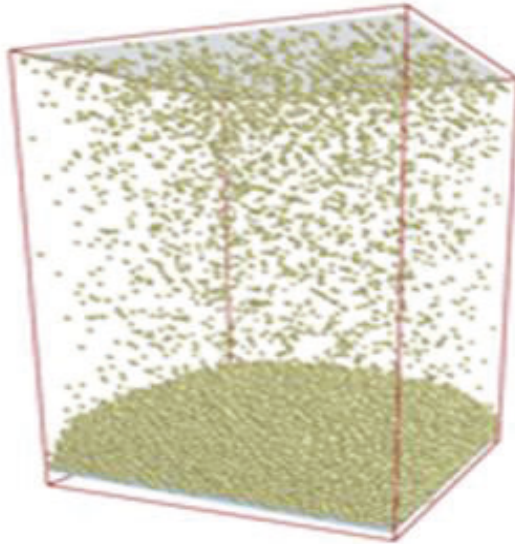


Figure AP3.42: Model showing DEM simulation of volcanic ash on the concrete roof plate

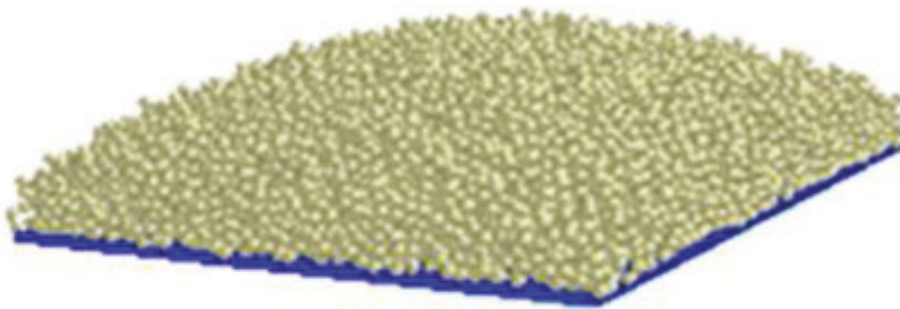


Figure AP3.43: Model without wind effect volcanic ash deposition

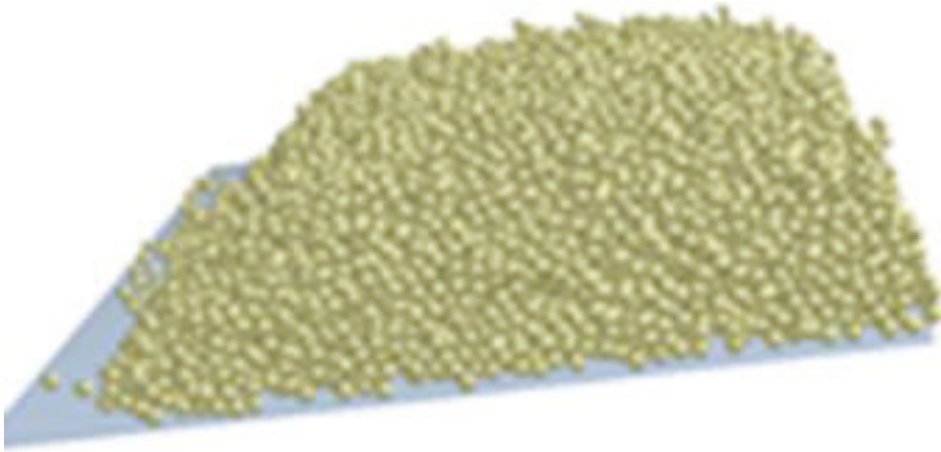


Figure AP3.44: Model with 1 ms^{-1} wind effects volcanic ash deposition.

Time: 0.990014 s
EDEM™
Academic

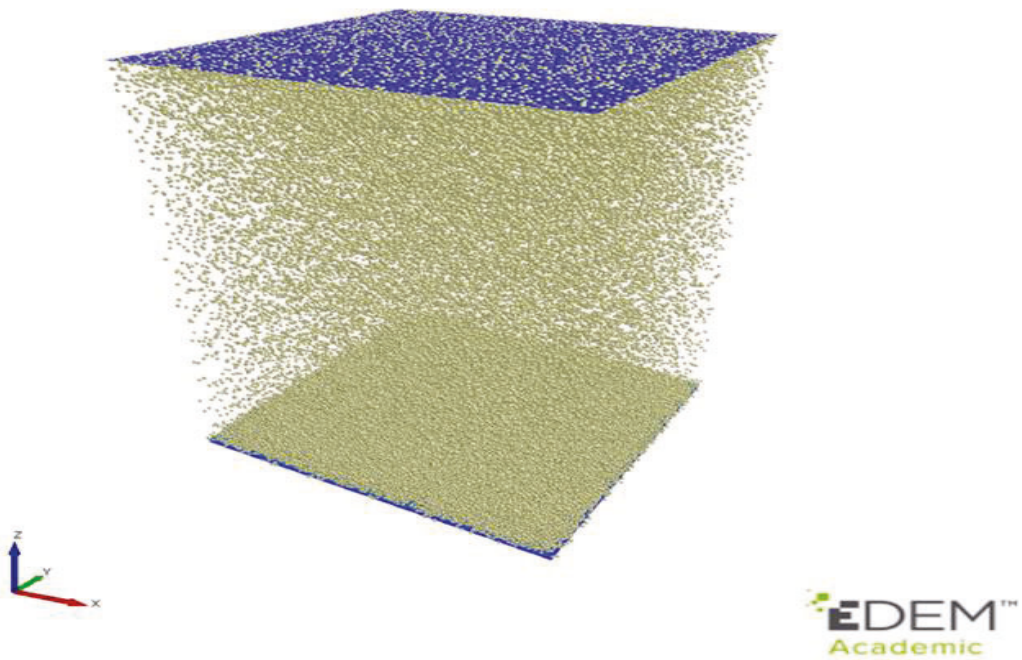
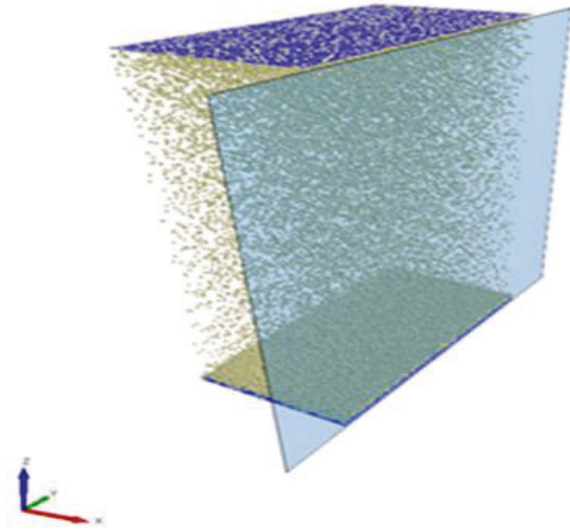


Figure AP3.45: Volcanic Ash Particles Generated from the EDEM

Time: 0.990014 s
EDEM™
Academic



EDEM™
Academic

Figure AP3.46: Sliced Section of the Volcanic Ash Particles' Internal Structure Falling and Settling on the Concrete Roof.

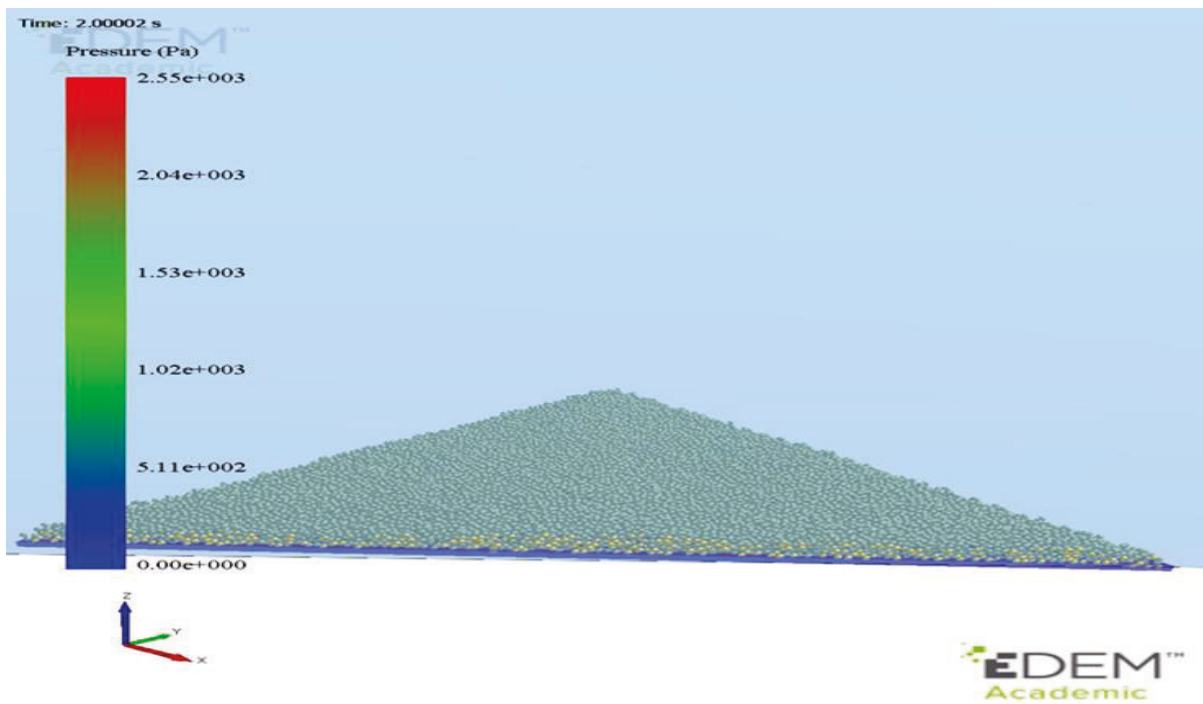


Figure AP3.47: Volcanic Ash Particles Deposition on the Concrete Roof Plate with the Pressure Load

DEM AND FEM SIMULATION VIDEOS LINKS

<https://mynorthamptonac->

my.sharepoint.com/:v:/g/personal/philip_quainoo_northampton_ac_uk/EecQ64cfCHxLgz_7P1488OoBT9dICRGe63wYv1AFJWZy4A?e=yc6L96

<https://mynorthamptonac->

my.sharepoint.com/:v:/g/personal/philip_quainoo_northampton_ac_uk/ESiaR1eLrOROpbmQP HQiiaUBYmtj4eKcihMuZZlimt0iYA?e=6zSrTr

<https://mynorthamptonac->

my.sharepoint.com/:v:/g/personal/philip_quainoo_northampton_ac_uk/ERbkKhdRG9hAiLMxwOUYrLcBo0LnKB-yFZBdf6VCvmP6rw?e=vtUjll

<https://mynorthamptonac->

my.sharepoint.com/:v:/g/personal/philip_quainoo_northampton_ac_uk/ESiaR1eLrOROpbmQP HQiiaUBYmtj4eKcihMuZZlimt0iYA?e=ydLF2F

<https://mynorthamptonac->

my.sharepoint.com/:v:/g/personal/philip_quainoo_northampton_ac_uk/ES3-1m2qYldCn4rUwiBgg4cBG0tMEKsNWfN0pC5iiykbXQ?e=s7ptzR

<https://mynorthamptonac->

my.sharepoint.com/:v:/g/personal/philip_quainoo_northampton_ac_uk/EdSb2OeCKsBNtd6rkyZy96lBCjXmsDbwY9355mUrMrfa_Q?e=FPiZVa

https://mynorthamptonac-my.sharepoint.com/:v:/g/personal/philip_quainoo_northampton_ac_uk/EanRn6AU4tdMvOcEglc0eSUBNrQZzOwxnGE0JD0tg1YU4w?e=wmZWWe

https://mynorthamptonac-my.sharepoint.com/:v:/g/personal/philip_quainoo_northampton_ac_uk/ERbkKhdRG9hAiLMxwOUYrLcBo0LnKB-yFZBdf6VCvmP6rw?e=KXF6Ag

https://mynorthamptonac-my.sharepoint.com/:v:/g/personal/philip_quainoo_northampton_ac_uk/EbbB5GA1VelChtwXjCCR7JIBAejxVaL244_UqpoICVUDTQ?e=bvAwmX

https://mynorthamptonac-my.sharepoint.com/:v:/g/personal/philip_quainoo_northampton_ac_uk/EanRn6AU4tdMvOcEglc0eSUBNrQZzOwxnGE0JD0tg1YU4w?e=UaXayc